

Design and Synthetic Studies on Plant Based Bioactives Against Metabolic Disorders

By

Renjitha J.

10CC16J39001

A thesis submitted to the
Academy of Scientific and Innovative Research
for the award of the degree of
DOCTOR OF PHILOSOPHY
in
SCIENCE

Under the combined supervision of
Dr. Sasidhar B. S. and Dr. Mangalam S. Nair



**CSIR-National Institute for Interdisciplinary
Science and Technology (CSIR-NIIST),
Thiruvananthapuram-695019**



Academy of Scientific and Innovative Research
AcSIR Headquarters, CSIR-HRDC Campus
Sector 19, Kamla Nehru Nagar,
Ghaziabad, U.P.-201 002, India

January 2022

CSIR-NATIONAL INSTITUTE FOR INTERDISCIPLINARY SCIENCE AND
TECHNOLOGY




Council of Scientific & Industrial Research (CSIR)
Industrial Estate (P.O), Thiruvananthapuram-695019, Kerala, India

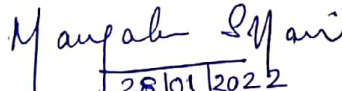
AcSIR

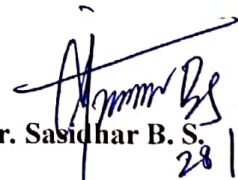
January, 2022

Certificate

This is to certify that the work incorporated in this Ph.D. thesis entitled, "*Design and Synthetic Studies on Plant Based Bioactives Against Metabolic Disorders*", submitted by *Mrs. Renjitha J.*, to the Academy of Scientific and Innovative Research (AcSIR) in fulfillment of the requirements for the award of the *Degree of Doctor of Philosophy in Sciences*, embodies original research work carried out by the student. We, further certify that this work has not been submitted to any other University or Institution in part or full for the award of any degree or diploma. Research materials obtained from other sources and used in this research work have been duly acknowledged in the thesis. Images, illustrations, figures, tables etc., used in the thesis from other sources, have also been duly cited and acknowledged.


Renjitha J. 28/01/2022


28/01/2022
Dr. Mangalam S. Nair
(Thesis Co-Supervisor)


28/01/2022
Dr. Sasidhar B. S.
(Thesis Supervisor)

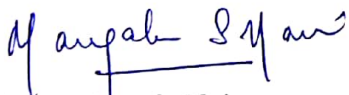
STATEMENTS OF ACADEMIC INTEGRITY

I Renjitha J., a Ph.D. student of the Academy of Scientific and Innovative Research (AcSIR) with Registration No. 10CC16J39001 hereby undertake that, the thesis entitled "**Design and Synthetic Studies on Plant Based Bioactives Against Metabolic Disorders**" has been prepared by me and that the document reports original work carried out by me and is free of any plagiarism in compliance with the UGC Regulations on "*Promotion of Academic Integrity and Prevention of Plagiarism in Higher Educational Institutions (2018)*" and the CSIR Guidelines for "*Ethics in Research and in Governance (2020)*".


Renjitha J.

28 January 2022
Thiruvananthapuram

It is hereby certified that the work done by the student under our supervision, is plagiarism-free in accordance with the UGC Regulations on "*Promotion of Academic Integrity and Prevention of Plagiarism in Higher Educational Institutions (2018)*" and the CSIR Guidelines for "*Ethics in Research and in Governance (2020)*".



Dr. Mangalam S. Nair

28 January 2022

Thiruvananthapuram


Dr. Sasidhar B. S.


28 January 2022

Thiruvananthapuram

DECLARATION

I, **Renjitha J.**, bearing AcSIR Registration No. 10CC16J39001 declare: that my thesis entitled, “**Design and Synthetic Studies on Plant Based Bioactives Against Metabolic Disorders**” is plagiarism free in accordance with the UGC Regulations on “*Promotion of Academic Integrity and Prevention of Plagiarism in Higher Educational Institutions (2018)*” and the CSIR Guidelines for “*Ethics in Research and in Governance (2020)*”.

I would be solely held responsible if any plagiarised content in my thesis is detected, which is violative of the UGC regulations 2018.


Renjitha J.
28/01/2022

Thiruvananthapuram

28 January 2022

ACKNOWLEDGEMENTS

I have received a great deal of support and help throughout my career.

*With immense pleasure and gratitude I am extremely grateful to my research supervisor, **Dr. Sasidhar B. S.**, for suggesting the fascinating research area and for his immense advice, patience, encouragement and support throughout my research time that led to the successful completion of this work.*

*With great respect and delightful happiness, I would like to convey my sincere thanks to my co-supervisor **Dr. Mangalam S. Nair**, for introducing me in the area of natural products and her insightful help, support and encouragement given to me and as former AcSIR programme co-ordinator at CSIR-NIIST, which helped to the successful completion of my research work.*

*I am deeply grateful to **Dr. A. Ajayaghosh**, Director, CSIR-National Institute for Interdisciplinary Science and Technology (CSIR-NIIST), Thiruvananthapuram, for providing the infrastructure facilities to carry out the research work.*

I would like to express a deep sense of thanks to Dr. Raghu K. G., Dr. Shyni G. L. and Dr. Priya S., Agro-Processing and Technology Division (APTD), CSIR-NIIST, for collaborating with all the biology work carried out, which was influential in shaping my thesis.

My sincere gratitude is also due to

- ✓ *Dr. G. Vijay Nair, emeritus scientist, for his inspiration.*
- ✓ *Dr. V. Karunakaran, Dr. C. H. Suresh and Dr. R. Luxmi Varma, present and former AcSIR co-ordinators.*
- ✓ *Dr. R. Luxmi Varma, Dr. K.V. Radhakrishnan and Dr. P. Jayamurthy., Doctoral Advisory Committee (DAC) members.*
- ✓ *Dr. Joshy Joseph and and the whole AcSIR faculty members for the successful completion of the course work.*
- ✓ *Dr. P. Sujatha Devi, Dr. R. Luxmi Varma and Dr. K. R. Gopidas, present and former Head of the Division, Chemical Sciences and Technology Division (CSTD).*
- ✓ *Dr. A. Kumaran, Dr. Kaustabh Kumar Maiti, Dr. L. Ravi Shankar, Dr. Sunil Varughese, Dr. Jubi John and Dr. Shridevi. D, Scientists of Organic Chemistry Section, for their encouragement.*

- ✓ *Dr. K. P. Prathish, Dr. Joshy George and Ms. Geethu B. V., for their kind help and support to complete CSIR-800 project work.*
- ✓ *Mrs. Saumini Matthew, Mr. Saran P. Raveendran and Mr. Rakesh Gokul for NMR, Mrs. Viji S. and Ms. Athira for mass spectral analyses.*
- ✓ *Dr. Venkata Rao D. Krishna Rao, CSIR - Central Institute of Medicinal and Aromatic Plants (CSIR-CIMAP), Research Centre, Bangalore, for molecular docking studies.*
- ✓ *Dr. Mathew Dan, identified the plant materials and ICAR-Central Tuber Crops Research Institute (ICAR-CTRI), Thiruvananthapuram and ICAR-Indian Institute of Spices Research, Kozhikode, for providing plant materials.*
- ✓ *My seniors Dr. Sajin K. Francis and Dr. Dhanya S. R., for their continuous help, support and encouragement throughout my work.*
- ✓ *My lab mates Dr. Fathimath Salfeena C. T., Dr. Jagadeesh K., Ms. Ashitha K. T., Mr. V. Praveen Kumar, Mr. Basavaraj, Ms. Sangeetha Mohan, Ms. Athira C. S., Mr. Ajay Krishna, Mr. Mohan B., Ms. Geethu V. Ms. Nithya Madhu for their kind help, support and love, that made my research life smooth and a cherished time spent together in the lab and institute.*
- ✓ *Mr. Vishnu K. O., Mr. Shibir M., Ms. Eunika K. Sunny, Ms. Anju V., Ms. Gayathri R. S., Ms. Shadiya S., Ms. Shubhada Gore, Ms. Sushmitha, Ms. Jwala Joy and Ms. Devi Priya for their help and support to complete some of my work.*
- ✓ *Mr. Merin Santhosh and Mrs. Gayathri for their timely help and support regarding AcSIR programme and fellowship.*
- ✓ *Mr. Madhu Krishnan, for GC-MS analysis*
- ✓ *Dr. Manu M. Joseph, Dr. Maniganda S., Dr. Parvathy Rathnam, Dr. Varsha Karunakaran, Dr. Nisha N., Dr. Jyothi B Nair Dr. Saranya Giridharan, Dr. Sujai P.T., Ms. Arya J.S., Ms. Sreedevi P., Ms. Nitha P. R., Dr. Sarathna P., Mr. Shamjith S, Dr. Maya R. J., Dr. Rajeev K. K., Dr. Mayadevi T. S., Dr. Greeshma Gopalan, Dr. Veena K. S., Dr. Sasikumar P. for their love, encouragement and friendship.*
- ✓ *Former and present members of CSTD for their love, help and support.*
- ✓ *Ms. Indhu L. G., Dr. P. K. Viswanathan, Prof. T. N. Manoharan, Prof. Sumam Ramachandran, Dr. R. Revamma, Dr. I. G. Shibi, Dr. Suma Sudharsan, Dr. K. P. Jayasree, Dr. Vijayakumar, Dr. V. Bhagavathy, Dr. Neela Kumari, Dr. Suresh,*

and all my teachers in GGHSS Kannyakulangara, GHSS Neduveli, Sree Narayana College Chempazhanthy, Govt. University College Thiruvananthapuram for their help, inspiration and encouragement during different stages of my academic career.

- ✓ *Ms. Meera Sebastian, Ms. Amala Varugese, Dr. Swetha S., Ms. Sumitha Paul, Ms. Anjali K. Sajeev, Ms. Shijina and all friends at CSIR-NIIST, for their love, support and friendship.*
- ✓ *Ms. Jisha George, Dr. Saumya Krishnan and all my friends for their friendship and love.*
- ✓ *Council of Scientific and Industrial Research (CSIR), Government of India, for funding Research fellowship.*

I am deeply and forever indebted to my parents Mr. Rajan A., Mrs. Jalaja S., my husband Prasanth G. K., and my brother Ranjith R., for their blessings, unconditional love, support, encouragement and sympathetic ear throughout my life who made it possible for me to reach up to here. You are always there for me. I also offer special thanks to Mr. Anandhu S. S., sister-in-law Mrs. Anuja A. S., grandparents Mr. Balakrishnan (Late), Sarasamma (Late), Mother-in-law Ms. Kanchana C., Mr. Praveen G. K and Mrs. Jiji Sreekumar and all family members for their love, support and encouragement.

Above all, I thank almighty for giving blessings showered upon me during all the good and tough time to the successful achievement of my goal.



Renjitha J.

CONTENTS

	Page No.
Certificate	i
Statement of Academic Integrity	ii
Declaration	iii
Acknowledgements	iv
Contents	vii
List of Figures	xvii
List of Schemes	xxi
List of Tables	xxi
Abbreviations	xxiii
Preface	xxvii
Chapter 1 The Role of Natural Products in Drug Discovery: Special Focus on Metabolic Disorders	1-52
1.1. Abstract	1
1.2. Introduction	1
1.3. Natural products derived drugs from plant source	8
1.3.1. Quinine	8
1.3.2. Artemisinin	9
1.3.3. Pilocarpine	10
1.3.4. Colchicine	10
1.3.5. Vincristine and Vinblastine	11
1.3.6. Paclitaxel (Taxol)	12
1.3.7. Digitoxin	13
1.3.8. Ingenol mebutate	14
1.4. Natural products derived drugs and drug candidates from microbial source	14
1.5. Natural products derived drugs and drug candidates from marine source	16
1.6. Natural products derived drugs and drug candidates from animal source	17
1.7. Natural products derived drugs and drug candidates for metabolic	20

	disorders	
1.7.1.	Obesity	20
1.7.1.1.	Orlistat	21
1.7.2.	Diabetes	22
1.7.2.1.	Metformin	24
1.7.2.2.	Berberine	25
1.7.2.3.	Exenatide	25
1.7.2.4.	Acarbose	26
1.7.2.5.	Miglitol	26
1.7.2.6.	Voglibose	27
1.7.2.7.	Phlorizin and its analogues	27
1.7.3.	Non-alcoholic fatty liver disease and Hyperlipidemia	29
1.7.3.1.	Mevastatin	30
1.7.3.2.	Lovastatin	31
1.7.3.3.	Simvastatin	31
1.7.4.	Hypertension	32
1.7.4.1.	Reserpine	33
1.7.4.2.	Captopril	33
1.8.	Importance of structural modifications of natural products	34
1.9.	Drug discovery and development	35
1.9.1.	High-throughput screening (HTS)	37
1.9.2.	Computer-aided drug design (CADD)	38
1.9.3.	Biotherapeutics	39
1.9.4.	Drug repurposing (Drug repositioning)	40
1.10.	Conclusion and outline of the thesis	40
1.11.	References	41
Chapter 2	Isolation of Bioactives from Selected Medicinally Important Plants from <i>Zingiberaceae</i> Family and their Biological Evaluations	53-126
2.1.	Abstract	53
2.2.	Introduction	53
2.3.	<i>Zingiberaceae</i> family	54
2.4.	The genus <i>Curcuma</i> L.	56
2.5.	A brief review on different plant species under present study	57

2.5.1.	<i>Curcuma amada</i> Roxb.	57
2.5.2.	<i>Curcuma malabarica</i>	61
2.5.3.	<i>Curcuma aromatica</i> Salisb.	63
2.6.	Aim and scope of the present work	65
2.7.	Gas Chromatography Mass Spectrometry (GC-MS) analysis of <i>C. amada</i>	65
2.7.1.	Isolation of essential oil of <i>C. amada</i>	66
2.7.2.	GC-MS analysis of essential oil of <i>C. amada</i>	66
2.8.	Isolation and characterization of phytochemicals from <i>C. amada</i> rhizomes	68
2.8.1.	Collection of plant material and extraction	68
2.8.2.	Isolation and characterization of phytochemicals from chloroform extract	68
2.9.	Isolation and characterization of phytochemicals from <i>C. malabarica</i> rhizomes	79
2.9.1.	Collection and extraction of plant material	79
2.9.2.	Isolation and characterization of phytochemicals from methanol extract	80
2.10.	Isolation and characterization of phytochemicals from <i>C. aromatica</i> rhizomes	91
2.10.1.	Collection and extraction of plant material	91
2.10.2.	Isolation of compounds from hexane extract	92
2.10.3.	Isolation of compounds from chloroform extract	99
2.11.	Pancreatic lipase inhibition studies of isolated phytochemicals	104
2.11.1.	Cytotoxicity studies by MTT assay	104
2.11.2.	Inhibition studies of bioactives against porcine pancreatic lipase	105
2.12.	Conclusion	106
2.13.	Experimental Section	107
2.13.1.	General Experimental Details	107
2.13.1.1.	GC-MS profiling	107
2.13.2.	Spectral data of the isolated compounds from <i>C. amada</i> rhizomes	108
2.13.2.1.	Compound 1 ((<i>E</i>)-15,15-Diethoxy λ -8(17),12-diene-16-al)	108
2.13.2.2.	Compound 2 ((<i>E</i>)- λ -8(17),12-diene-15,16-dial)	109
2.13.2.3.	Compound 3 (Aframodial)	110

2.13.2.4.	Compound 4 (Coronarin D)	110
2.13.2.5.	Compound 5 (Zerumin A)	111
2.13.3.	Spectral data of the isolated compounds from <i>C. malabarica</i> rhizomes	112
2.13.3.1.	Compound 6 (Furanodienone)	112
2.13.3.2.	Compound 7 (Zederone)	113
2.13.3.3.	Compound 8 (Procurcumenol)	114
2.13.3.4.	Compound 9 (Curcumenone)	114
2.13.3.5.	Compound 10 (Zedoarondiol)	115
2.13.4.	Spectral data of the isolated compounds from hexane extract of <i>C. aromatica</i> rhizomes	116
2.13.4.1.	Compound 11 (Coronarin E)	116
2.13.4.2.	Compound 12 (Germacrone)	117
2.13.4.3.	Compound 13 (Curdione)	117
2.13.5.	Spectral data of the isolated compounds from chloroform extract of <i>C. aromatica</i> rhizomes	118
2.13.5.1.	Compound 14 (Villosin)	118
2.13.5.2.	Compound 15 (1-epihydroxy-zedoalactone D)	119
2.14.	References	120
Chapter 3	Design and Synthesis Labdane Appended Triazoles as Potent Pancreatic Lipase Inhibitors	127-169
3.1.	Abstract	127
3.2.	Introduction	128
3.3.	Review of literature	128
3.3.1.	Anti-obesity properties of <i>Curcuma amada</i>	128
3.3.2.	Anti-obesity properties of triazole	129
3.4.	Aim and scope of the present study	130
3.5.	Design strategy for the synthesis of labdane appended Triazoles	131
3.6.	Results and discussion	132
3.6.1.	Diversity of triazole appended labdane molecules	136
3.6.2.	Cytotoxicity studies by MTT assay	136
3.6.3.	Inhibition studies of compounds against porcine pancreatic lipase (Method A)	137
3.6.4.	Inhibition studies of compounds against Human pancreatic lipase	138

	(Method B)	
3.6.5.	Structure-activity relationships (SAR) studies	140
3.6.6.	Molecular docking studies	141
3.7.	Conclusion	141
3.8.	Experimental section	142
3.8.1.	Chemistry	142
3.8.1.1.	Isolation of (<i>E</i>)-labda-8(17),12-diene-15,16-dial (1)	143
3.8.1.2.	Procedure for the synthesis of zerumin A (2)	143
3.8.1.3.	Procedure for the synthesis of (<i>E</i>)-prop-2-yn-1-yl 3-formyl-5-(5,5,8a-trimethyl-2-methylenedecahydronaphthalen-1-yl)pent-3-enoate (3)	143
3.8.1.4.	General procedure for the synthesis of azides (5a-5q)	143
3.8.1.5.	General procedure for the synthesis of triazole analogues (6a-6q)	144
3.8.2.	Spectral data	144
3.8.2.1.	(<i>E</i>)-Labda-8(17),12-diene-15,16-dial (1)	144
3.8.2.2.	Zerumin A (2)	144
3.8.2.3.	(<i>E</i>)-prop-2-yn-1-yl-3-formyl-5-(5,5,8a-trimethyl-2-methylenedecahydronaphthalen-1-yl)pent-3-enoate (3)	144
3.8.2.4.	Synthesis of (<i>E</i>)-(1-benzyl-1 <i>H</i> -1,2,3-triazol-4-yl) methyl 3-formyl-5-(5,5,8a-trimethyl-2-methylenedecahydronaphthalen-1-yl)pent-3-enoate (6a)	145
3.8.2.5.	Synthesis of (<i>E</i>)-(1-(4-fluorobenzyl)-1 <i>H</i> -1,2,3-triazol-4-yl)methyl 3-formyl-5-(5,5,8a-trimethyl-2-methylenedecahydronaphthalen-1-yl)pent-3-enoate (6b)	145
3.8.2.6.	Synthesis of (<i>E</i>)-(1-(4-nitrobenzyl)-1 <i>H</i> -1,2,3-triazol-4-yl)methyl 3-formyl-5-(5,5,8a-trimethyl-2-methylenedecahydronaphthalen-1-yl)pent-3-enoate (6c)	146
3.8.2.7.	Synthesis of (<i>E</i>)-(1-(2-chlorobenzyl)-1 <i>H</i> -1,2,3-triazol-4-yl)methyl 3-formyl-5-(5,5,8a-trimethyl-2-methylenedecahydronaphthalen-1-yl)pent-3-enoate (6d)	147
3.8.2.8.	Synthesis of (<i>E</i>)-(1-(4-(methylthio) benzyl)-1 <i>H</i> -1,2,3-triazol-4-yl) methyl 3-formyl-5-(5,5,8a-trimethyl-2-methylenedecahydronaphthalen-1-yl)pent-3-enoate (6e)	147
3.8.2.9.	Synthesis of (<i>E</i>)-(1-(4-chlorobenzyl)-1 <i>H</i> -1,2,3-triazol-4-yl)methyl 3-	148

	formyl-5-(5,5,8a-trimethyl-2-methylenedecahydronaphthalen-1-yl)pent-3-enoate (6f)	
3.8.2.10.	Synthesis of (<i>E</i>)-(1-(4-(tert-butyl)benzyl)-1 <i>H</i> -1,2,3-triazol-4-yl)methyl 3-formyl-5-(5,5,8a-trimethyl-2-methylenedecahydronaphthalen-1-yl)pent-3-enoate (6g)	149
3.8.2.11.	(<i>E</i>)-(1-(2-bromo-5-fluorobenzyl)-1 <i>H</i> -1,2,3-triazol-4-yl)methyl 3-formyl-5-((1 <i>S</i> ,4 <i>aS</i> ,8 <i>aS</i>)-5,5,8a-trimethyl-2-methylenedecahydronaphthalen-1-yl)pent-3-enoate (6h)	150
3.8.2.12.	Synthesis of (<i>E</i>)-(1-(2-hydroxy-5-nitrobenzyl)-1 <i>H</i> -1,2,3-triazol-4-yl)methyl 3-formyl-5-(5,5,8a-trimethyl-2-methylenedecahydronaphthalen-1-yl)pent-3-enoate (6i)	150
3.8.2.13.	Synthesis of (<i>E</i>)-(1-(4-methoxybenzyl)-1 <i>H</i> -1,2,3-triazol-4-yl)methyl 3-formyl-5-(5,5,8a-trimethyl-2-methylenedecahydronaphthalen-1-yl)pent-3-enoate (6j)	151
3.8.2.14.	Synthesis of (<i>E</i>)-(1-(2-bromo-5-methoxybenzyl)-1 <i>H</i> -1,2,3-triazol-4-yl)methyl 3-formyl-5-(5,5,8a-trimethyl-2-methylenedecahydronaphthalen-1-yl)pent-3-enoate (6k)	152
3.8.2.15.	Synthesis of (<i>E</i>)-(1-([1,1'-biphenyl]-2-ylmethyl)-1 <i>H</i> -1,2,3-triazol-4-yl)methyl 3-formyl-5-(5,5,8a-trimethyl-2-methylenedecahydronaphthalen-1-yl)pent-3-enoate (6l)	153
3.8.2.16.	Synthesis of (<i>E</i>)-(1-(2-oxo-2-phenylethyl)-1 <i>H</i> -1,2,3-triazol-4-yl)methyl 3-formyl-5-(5,5,8a-trimethyl-2-methylenedecahydronaphthalen-1-yl)pent-3-enoate (6m)	153
3.8.2.17.	Synthesis of (<i>E</i>)-(1-(2-(4-bromophenyl)-2-oxoethyl)-1 <i>H</i> -1,2,3-triazol-4-yl)methyl 3-formyl-5-(5,5,8a-trimethyl-2-methylenedecahydronaphthalen-1-yl)pent-3-enoate (6n)	154
3.8.2.18.	Synthesis of (<i>E</i>)-(1-(2-(4-chlorophenyl)-2-oxoethyl)-1 <i>H</i> -1,2,3-triazol-4-yl)methyl 3-formyl-5-(5,5,8a-trimethyl-2-methylenedecahydronaphthalen-1-yl)pent-3-enoate (6o)	155
3.8.2.19.	Synthesis of (<i>E</i>)-(1-(2-(4-fluorophenyl)-2-oxoethyl)-1 <i>H</i> -1,2,3-triazol-4-yl)methyl 3-formyl-5-(5,5,8a-trimethyl-2-methylenedecahydronaphthalen-1-yl)pent-3-enoate (6p)	156
3.6.2.20.	Synthesis of (<i>E</i>)-(1-(2-(4-cyanophenyl)-2-oxoethyl)-1 <i>H</i> -1,2,3-triazol-	157

	4-yl)methyl-3-formyl-5-(5,5,8a-trimethyl-2-methylenedecahydronaphthalene-1-yl)pent-3-enoate (6q)	
3.8.3.	Biology	157
3.8.3.1.	<i>In vitro</i> cytotoxic evaluation of compounds by MTT assay	157
3.8.3.2.	Pancreatic lipase inhibitory activity assay	158
3.8.3.2..	Method A	158
3.8.3.2.2	Method B	159
3.8.4.	Molecular docking studies of various triazole derivatives and intermediates	160
3.9.	References	164
Chapter 4	Anti-hyperlipidemic Potential of Labdane-Pyrroles via Inhibition of Cholesterol and Triglycerides Synthesis	170-214
4.1.	Abstract	170
4.2.	Introduction	170
4.3.	Review of Literature	172
4.3.1.	Anti-hyperlipidemic properties of <i>Curcuma amada</i>	172
4.3.2.	Anti-hyperlipidemic properties of pyrrole and pyrazole	172
4.4.	Aim and scope of the present study	174
4.5.	Design strategy for the synthesis of labdane appended pyrroles and pyrazoles	175
4.6.	Results and discussion	175
4.6.1.	Optimization of the reaction	178
4.6.2.	MTT assay	182
4.6.3.	Effect of compounds on lipid droplet accumulation in HFA treated HepG2 cells	183
4.6.4.	Effect of compounds on the inhibition of triglyceride synthesis in HepG2 cells	185
4.6.5.	Evaluation of effect of compounds on the inhibition of cholesterol synthesis in HepG2 cells	186
4.6.6.	Evaluation of effect of compounds on the inhibition of HMG CoA reductase enzyme	188
4.6.7.	Structure activity relationship (SAR) studies	189

4.7.	Conclusion	189
4.8.	Experimental section	190
4.8.1.	Isolation of (<i>E</i>)-labda 8(17),12-diene -15,16-dial (1)	191
4.8.2.	General procedure for the synthesis of (<i>E</i>)-labda-8(17),12-diene-15,16-dial-pyrrole analogues (3a-3r)	191
4.8.3.	Spectral Details	191
4.8.3.1.	Synthesis of 1-(<i>p</i> -tolyl)-2-((5,5,8a-trimethyl-2-methylene decahydronaphthalen-1-yl) methyl)-1H-pyrrole-3-carbaldehyde (3a)	191
4.8.3.2.	Synthesis of 1-(4-methoxyphenyl)-2-((5,5,8a-trimethyl-2-methylene decahydronaphthalen-1-yl)methyl)-1H-pyrrole-3-carbaldehyde (3b)	192
4.8.3.3.	Synthesis of 1-(3-methoxyphenyl)-2-((5,5,8a-trimethyl-2-methylene decahydronaphthalene-1-yl)methyl)-1H-pyrrole-3-carbaldehyde (3c)	193
4.8.3.4.	Synthesis of 1-(4-ethylphenyl)-2-((5,5,8a-trimethyl-2-methylenedecahydronaphthalene-1-yl)methyl)-1H-pyrrole-3-carbaldehyde (3d)	193
4.8.3.5.	Synthesis of 1-(4-bromophenyl)-2-((5,5,8a-trimethyl-2-methylenedecahydronaphthalen-1-yl)methyl)-1H-pyrrole-3-carbaldehyde (3e)	194
4.8.3.6.	Synthesis of 1-(4-iodophenyl)-2-((5,5,8a-trimethyl-2-methylenedecahydro naphthalene-1-yl)methyl)-1H-pyrrole-3-carbaldehyde (3f)	195
4.8.3.7.	Synthesis of 1-(4-chlorophenyl)-2-((5,5,8a-trimethyl-2-methylenedecahydronaphthalen-1-yl)methyl)-1H-pyrrole-3-carbaldehyde (3g)	195
4.8.3.8.	Synthesis of 1-(3-chlorophenyl)-2-((5,5,8a-trimethyl-2-methylenedecahydronaphthalen-1-yl)methyl)-1H-pyrrole-3-carbaldehyde (3h)	196
4.8.3.9.	Synthesis of 1-(4-hydroxyphenyl)-2-((5,5,8a-trimethyl-2-methylenedecahydronaphthalene-1-yl)methyl)-1H-pyrrole-3-carbaldehyde (3i)	197
4.8.3.10.	Synthesis of 1-(2-hydroxyphenyl)-2-((5,5,8a-trimethyl-2-methylenedecahydronaphthalen-1-yl)methyl)-1H-pyrrole-3-carbaldehyde (3j)	198
4.8.3.11.	Synthesis of 1-(3,4-dimethylphenyl)-2-((5,5,8a-trimethyl-2-methylenedecahydronaphthalen-1-yl)methyl)-1H-pyrrole-3-carbaldehyde (3k)	198
4.8.3.12.	Synthesis of 1-(3,4-dimethoxyphenyl)-2-((5,5,8a-trimethyl-2-methylenedecahydronaphthalen-1-yl)methyl)-1H-pyrrole-3-carbaldehyde (3l)	199
4.8.3.13.	Synthesis of 1-(3,4-dichlorophenyl)-2-((5,5,8a-trimethyl-2-methylenedecahydronaphthalene-1-yl)methyl)-1H-pyrrole-3-carbaldehyde (3m)	200
4.8.3.14.	Synthesis of 1-(3-chloro-4-fluorophenyl)-2-((5,5,8a-trimethyl-2-meth-	201

	ylenedecahydronaphthalen-1-yl)methyl)-1H-pyrrole-3-carbaldehyde (3n)	
4.8.3.15.	Synthesis of 1-(4-bromo-2-methylphenyl)-2-((5,5,8a-trimethyl-2-methylenedecahydronaphthalen-1-yl)methyl)-1H-pyrrole-3-carbaldehyde (3o)	201
4.8.3.16.	Synthesis of 1-(4-nitrophenyl)-2-((5,5,8a-trimethyl-2-methylenedecahydronaphthalen-1-yl)methyl)-1H-pyrrole-3-carbaldehyde (3p)	202
4.8.3.17.	Synthesis of 1-(2-nitrophenyl)-2-((5,5,8a-trimethyl-2-methylenedecahydronaphthalen-1-yl)methyl)-1H-pyrrole-3-carbaldehyde (3q)	203
4.8.3.18.	Synthesis of 1-phenyl-2-((5,5,8a-trimethyl-2-methylenedecahydronaphthalen-1-yl)methyl)-1H-pyrrole-3-carbaldehyde (3r)	203
4.8.4.	General procedure for synthesis of (<i>E</i>)-labda-8(17),12-diene-15,16-dial-pyrazole analogues (5a-5d)	204
4.8.4.1.	Synthesis of dibenzyl 4-(2-oxoethyl)-3-((5,5,8a-trimethyl-2-methylenedecahydronaphthalen-1-yl)methyl)-1H-pyrazole-1,2(3H)-dicarboxylate (5a)	204
4.8.4.2.	Synthesis of diethyl 4-(2-oxoethyl)-3-((5,5,8a-trimethyl-2-methylenedecahydronaphthalen-1-yl)methyl)-1H-pyrazole-1,2(3H)-dicarboxylate (5b)	205
4.8.4.3.	Synthesis of diisopropyl 4-(2-oxoethyl)-3-((5,5,8a-trimethyl-2-methylenedecahydronaphthalen-1-yl)methyl)-1H-pyrazole-1,2(3H)-dicarboxylate (5c)	206
4.8.4.4.	Synthesis of di- <i>tert</i> -butyl 4-(2-oxoethyl)-3-((5,5,8a-trimethyl-2-methylenedecahydronaphthalen-1-yl)methyl)-1H-pyrazole-1,2(3H)-dicarboxylate (5d)	206
4.8.5.	Biological screening	207
4.8.5.1.	Cell cultures	207
4.8.5.2.	Cytotoxic evaluation of compounds by MTT assay	207
4.8.5.3.	HepG2 cell culture for the assessment of lipid synthesis and secretion	208
4.8.5.4.	Oil red-O staining	208
4.8.5.5.	Triglycerides assay	208
4.8.5.6.	Total cholesterol assay	209
4.8.5.7.	HMG CoA reductase activity assay	209

4.8.5.8.	Statistical analysis	210
4.9.	References	210

List of Figures

Sl. No.		Page No.
1	Figure 1.1. Morphine	2
2	Figure 1.2. Penicillin, clavulanic acid and amoxicillin	3
3	Figure 1.3. New drugs approved in between 1981-2019	4
4	Figure 1.4. <i>Cinchona officinalis</i> and quinine	9
5	Figure 1.5. <i>Artemisia annua</i> and artemisinin	10
6	Figure 1.6. Structure of pilocarpine	10
7	Figure 1.7. <i>Colchicum autumnale</i> and colchicine	11
8	Figure 1.8. <i>Catharanthus roseus</i> , vinblastine and vincristine	12
9	Figure 1.9. <i>Taxus brevifolia</i> and paclitaxel	13
10	Figure 1.10. Digitoxin and digoxin	14
11	Figure 1.11. <i>Euphorbia peplus</i> and ingenol mebutate	14
12	Figure 1.12. Microbial derived drugs and drug candidates	16
13	Figure 1.13. Marine derived drugs and drug candidates	17
14	Figure 1.14. Animal derived drugs and drug candidates	19
15	Figure 1.15. Natural products having anti-obesity properties	21
16	Figure 1.16. Lipstatin and orlistat	22
17	Figure 1.17. <i>Galanga officinalis</i> , guanidine, biguanide, proguanil and metformin	24
18	Figure 1.18. <i>Berberis vulgaris</i> and berberine	25
19	Figure 1.19. Acarbose	26
20	Figure 1.20. Miglitol	27
21	Figure 1.21. Voglibose	27
22	Figure 1.22. Phlorizin and its analogues	29
23	Figure 1.23. Structure of tatin	31
24	Figure 1.24. <i>Rauwolfia serpentine</i> and reserpine	33
25	Figure 1.25. Teprotide and captopril	34
26	Figure 1.26. Paclitaxel and docetaxel	35
27	Figure 1.27. Drug discovery cycle	37
28	Figure 1.28. Diagrammatic representation of CADD	39
29	Figure 2.1. <i>C. amada</i> plant and rhizomes	57
30	Figure 2.2. Volatile constituents from <i>C. amada</i>	58

31	Figure 2.3.	Labdane diterpenes isolated from <i>C. amada</i>	59
32	Figure 2.4.	Terpenoids from <i>C. amada</i>	59
33	Figure 2.5.	Curcuminoids from <i>C. amada</i>	60
34	Figure 2.6.	Phenolic acids from <i>C. amada</i>	60
35	Figure 2.7.	Modification of labda-8(17),12-dien-15,16-dial	61
36	Figure 2.8.	<i>C. malabarica</i> plant and rhizomes	62
37	Figure 2.9.	Chemical constituents of <i>C. malabarica</i>	62
38	Figure 2.10.	<i>C. aromatica</i> plant and rhizomes	63
39	Figure 2.11.	Structure of diarylheptanoids	64
40	Figure 2.12.	Structure of sesqui and diterpenes	65
41	Figure 2.13.	Pictorial representation for the isolation of phytochemicals from <i>C. amada</i> rhizomes	69
42	Figure 2.14.	¹ H NMR spectrum of (<i>E</i>)-15,15-Diethoxylabda-8(17),12-diene-16-al in CDCl ₃	70
43	Figure 2.15.	¹³ C NMR spectrum of (<i>E</i>)-15,15-Diethoxylabda-8(17),12-diene-16-al in CDCl ₃	71
44	Figure 2.16.	¹ H NMR spectrum of (<i>E</i>)-labda-8(17),12-diene-15,16-dial in CDCl ₃	72
45	Figure 2.17.	¹³ C NMR spectrum of (<i>E</i>)-labda-8(17),12-diene-15,16-dial in CDCl ₃	73
46	Figure 2.18.	¹ H NMR spectrum of aframodial in CDCl ₃	74
47	Figure 2.19.	¹³ C NMR spectrum of aframodial in CDCl ₃	75
48	Figure 2.20.	¹ H NMR spectrum of coronarin D in CDCl ₃	76
49	Figure 2.21.	¹³ C NMR spectrum of coronarin D in CDCl ₃	77
50	Figure 2.22.	¹ H NMR spectrum of zerumin A in CDCl ₃	78
51	Figure 2.23.	¹³ C NMR spectrum of zerumin A in CDCl ₃	79
52	Figure 2.24.	Pictorial representation for the isolation of phytochemicals from <i>C. malabarica</i> rhizomes	80
53	Figure 2.25.	¹ H NMR spectrum of furanodienone in CDCl ₃	82
54	Figure 2.26.	¹³ C NMR spectrum of furanodienone in CDCl ₃	82
55	Figure 2.27.	¹ H NMR spectrum of zederone in CDCl ₃	84
56	Figure 2.28.	¹³ C NMR spectrum of zederone in CDCl ₃	84
57	Figure 2.29.	¹ H NMR spectrum of procurcumenol in CDCl ₃	86

58	Figure 2.30.	^{13}C NMR spectrum of procurcumenol in CDCl_3	86
59	Figure 2.31.	^1H NMR spectrum of curcumenone in CDCl_3	88
60	Figure 2.32.	^{13}C NMR spectrum of curcumenone in CDCl_3	88
61	Figure 2.33.	^1H NMR spectrum of zedoarondiol in CDCl_3	90
62	Figure 2.34.	^{13}C NMR spectrum of zedoarondiol in CDCl_3	90
63	Figure 2.35.	Pictorial representation for the extraction with various solvents of <i>C. aromatica</i> rhizomes	91
64	Figure 2.36.	Pictorial representation for the isolation of phytochemicals from hexane extract of <i>C. aromatica</i> rhizomes	92
65	Figure 2.37.	^1H NMR spectrum of coronarin E in CDCl_3	94
66	Figure 2.38.	^{13}C NMR spectrum of coronarin E in CDCl_3	94
67	Figure 2.39.	^1H NMR spectrum of germacrone in CDCl_3	96
68	Figure 2.40.	^{13}C NMR spectrum of germacrone in CDCl_3	96
69	Figure 2.41.	^1H NMR spectrum of curdione in CDCl_3	98
70	Figure 2.42.	^{13}C NMR spectrum of curdione in CDCl_3	98
71	Figure 2.43.	Pictorial representation for the isolation of phytochemicals from chloroform extract of <i>C. aromatica</i> rhizomes	99
72	Figure 2.44.	^1H NMR spectrum of villosin in CDCl_3	101
73	Figure 2.45.	^{13}C NMR spectrum of villosin in CDCl_3	101
74	Figure 2.46.	ORTEP diagram of 1-epihydroxy-zedoalactone D	102
75	Figure 2.47.	^1H NMR spectrum of zedoalactone B in DMSO-d_6	103
76	Figure 2.48.	^{13}C NMR spectrum of zedoalactone B in DMSO-d_6	104
77	Figure 2.49.	Cytotoxic study of phytochemicals by MTT assay	105
78	Figure 2.50.	The percentage inhibition of phytochemicals against pancreatic lipase in various concentrations	106
79	Figure 3.1.	Pancreatic lipase inhibitory activity	127
80	Figure 3.2.	Triazoles having anti-obesity properties	130
81	Figure 3.3.	Rationale for the synthesis of labdane appended triazoles	131
82	Figure 3.4.	Compound 6j	134
83	Figure 3.5.	^1H NMR spectrum of compound 6j in CDCl_3	135

84	Figure 3.6.	^{13}C NMR spectrum of compound 6j in CDCl_3	135
85	Figure 3.7.	Diversity of the reaction	136
86	Figure 3.8.	Cytotoxic study of isolates and selected semi-synthetic derivatives by MTT assay	137
87	Figure 3.9.	The percentage inhibition of isolates and synthetic derivatives against pancreatic lipase in various concentrations	138
88	Figure 3.10.	The percentage of isolates and synthetic derivatives against Human pancreatic lipase in various concentrations	139
89	Figure 3.11.	The representative molecular docking studies of compound 6e	141
90	Figure 3.12	The percentage inhibition of orlistat against porcine pancreatic lipase in various concentrations	160
91	Figure 3.13.	The percentage inhibition of orlistat against Human pancreatic lipase in various concentrations	160
92	Figure 3.14.	The representative molecular docking studies of isolates and semi-synthetic derivatives	163
93	Figure 4.1.	Atorvastatin	173
94	Figure 4.2.	Anti-obesity agents having pyrazole core	174
95	Figure 4.3.	Molecular hybridization approach led to the discovery of novel (<i>E</i>)-labda-8(17),12-diene-15,16-dial hybrids	175
96	Figure 4.4.	Compound 3k	177
97	Figure 4.5.	^1H NMR spectrum of compound 3k in CDCl_3	177
98	Figure 4.6.	^{13}C NMR spectrum of compound 3k in CDCl_3	178
99	Figure 4.7.	Scope of the reaction	180
100	Figure 4.8.	Compound 5d	181
101	Figure 4.9.	^1H NMR spectrum of compound 5d in CDCl_3	181
102	Figure 4.10.	^{13}C NMR spectrum of compound 5d in CDCl_3	182
103	Figure 4.11	Scope of the reaction	182
104	Figure 4.12.	Cytotoxic study of isolates and selected semi-synthetic derivatives by MTT assay	183

105	Figure 4.13.	The effect of compounds and standard drug FF (Fenofibrate) on lipid droplet accumulation in HepG2 cells by oil red O staining: Representative microscopic images of oil red O stained HepG2 cells	184
106	Figure 4.14.	The effect of compounds and standard drug FF (Fenofibrate) on lipid droplet accumulation in HepG2 cells by oil red O staining	185
107	Figure 4.15.	The effect of compounds on the inhibition of HMG CoA reductase enzyme	188

List of Schemes

Sl. No.			Page No.
1	Scheme 3.1.	Synthesis of propargylated labdane, substituted benzyl and phenacyl azides and labdane appended triazoles	133
2	Scheme 4.1.	One-pot synthetic strategy for the (<i>E</i>)-labda-8(17),12-diene-15,16-dial appended pyrroles	176
3	Scheme 4.2.	One-pot access for the (<i>E</i>)-labda-8(17),12-diene-15,16-dial appended pyrazoles	180

List of Tables

Sl. No.			Page No.
1	Table 1.1.	The list of FDA approved unaltered NP derived drugs launched in between 2000-2019	5
2	Table 1.1.	The list of FDA approved NP derived/inspired drugs launched in between 2005-2019	6
3	Table 2.1.	List of important genus in <i>Zingiberaceae</i> family with important medicinal plants	55
4	Table 2.2.	GC MS profile of essential oil of <i>C. amada</i>	67
5	Table 3.1.	50% Inhibitory concentration (IC ₅₀) evaluation of labdane appended Triazoles	140
6	Table 3.2.	List of compounds used in docking study and the estimated free energy of binding	164
7	Table 4.1.	Optimization of the reaction	179

8	Table 4.2.	The effect of compounds on percentage inhibition of TG synthesis in high fatty acid treated HepG2 cells	186
9	Table 4.3.	The effect of compounds on inhibition of cholesterol synthesis in high fatty acid treated HepG2 cells	187

ABBREVIATIONS

Abs	:	Absorption
AcOH	:	Acetic acid
AgNPs	:	Silver nanoparticles
AMI	:	Acute myocardial ischemia
ANOVA	:	Analysis of variance
AS	:	Atorvastatin
AGI	:	α -Glucosidase inhibitor
ADMET	:	absorption, distribution, metabolism, excretion and toxicity
ACE	:	Angiotensin-converting enzyme
ACT	:	Artemisinin combination therapy
AK	:	Actinic keratosis
ATCC	:	American Type Cell Culture
ATP	:	Adenosine triphosphate
ATZ	:	3-Amino-1,2,4-triazole
BF ₃ OEt ₂	:	Boron trifluoride diethyl etherate
BPPs	:	Bradykinin-potentiating peptides
BSA	:	Bovine serum albumin
BSAAs	:	Broad-spectrum antiviral agents
^t BuOH	:	tertiary-Butanol
CC	:	Column chromatography
CB1	:	Cannabinoid
CNS	:	Central nervous system
CO ₂	:	Carbondioxide
CVD	:	Cardiovascular disease
CG	:	Cardiac glycoside
°C	:	Degree Celsius
CADD	:	Computer-aided drug design
CDCl ₃	:	Deuterated chloroform
CHD	:	Coronary heart disease
cm	:	Centimetre
CrO ₃	:	Chromium trioxide
CuSO ₄ .5H ₂ O	:	Copper sulfate penta hydrate

d	:	Doublet
dd	:	Doublet of doublet
DCM (CH ₂ Cl ₂)	:	Dichloromethane
DEPT	:	Distortionless enhancement by polarization transfer
DM	:	Diabetes Mellitus
DMEM	:	Dulbecco's Modified Eagle's Medium
DMF	:	Dimethylformamide
DMSO	:	Dimethyl sulfoxide
DMSO-d ₆	:	Deuterated dimethyl sulfoxide
EPO	:	Erythropoietin
EA	:	Ethyl acetate
EtOAc	:	Ethyl acetate
EtOH	:	Ethanol
Equiv.	:	Equivalent
FBS	:	Fetal bovine serum
FF	:	Fenofibrate
FDA	:	Food and drug administration
FT-IR	:	Fourier-transform Infrared
g	:	Gram
GC-MS	:	Gas chromatography-mass spectrometry
Hex	:	Hexane
HCl	:	Hydrochloric acid
HeLa	:	Human cervical cancer cell lines
Hz	:	Hertz
HMG CoA	:	3-Hydroxy-3-methylglutaryl-coenzyme
HepG2	:	Human liver cell lines
HFD	:	High fat diet
H ₂ SO ₄	:	Sulfuric acid
HTS	:	High-throughput screening
HBP	:	High blood pressure
HRMS	:	High Resolution Mass Spectrometry
hrs	:	Hours
HDL	:	High density lipoprotein

HFA	:	high fatty acid
HFHS	:	High-fat high-sugar
HTN or HT	:	Hypertension
H9c2	:	cardiomyocytes cell line
IC ₅₀	:	Inhibitory concentration
J	:	Coupling constant
K ₂ CO ₃	:	Potassium carbonate
kcal	:	Kilo calorie
L	:	Litre
LDL	:	Low density lipoprotein
m	:	multiplet
MeOH	:	Methanol
min	:	Minute
mg	:	Milligram
ml	:	Millilitre
mAbs	:	Monoclonal antibodies
MHz	:	Mega hertz
m.p.	:	Melting point
MTT	:	3-[4,5-dimethylthiazol-2-yl]-2,5-diphenyl tetrazolium bromide
μM	:	Micro molar
NaCl	:	Sodium chloride
NaN ₃	:	Sodium azide
NADPH	:	Nicotinamide adenine dinucleotide phosphate
NC	:	Normal control
nm	:	Nanometer
NME	:	New molecular entity
NP	:	Natural product
NAFLD	:	Non-alcoholic fatty liver disease
NMR	:	Nuclear Magnetic Resonance
NaBH ₄	:	Sodium borohydride
Na ₂ SO ₄	:	Sodium sulphate
OD	:	Optical density
ORTEP	:	Oak Ridge Thermal Ellipsoid Plot

pTSA	:	para-Toluenesulfonic acid
PPh ₃	:	Triphenyl phosphine
PL	:	Pancreatic lipase
PS	:	Pravastatin
PNPB	:	p-Nitrophenyl butyrate
RT	:	Room temperature
SAR	:	Structure-activity relationships
SD	:	Standard deviation
t	:	Triplet
TFA	:	Trifluoroacetic acid
T2DM	:	Type 2 diabetes mellitus
TC	:	Total cholesterol
TGs	:	Triglycerides
TLC	:	Thin layer chromatography
TMS	:	Tetramethylsilane
THF	:	Tetrahydrofuran
2D	:	Two dimensional
WHO	:	World Health Organization
v _{max}	:	Maximum frequency
UV	:	Ultraviolet
VLDL	:	Very low density lipoprotein
VC	:	Vehicle control

PREFACE

Naturally occurring compounds have played a remarkable role in the discovery of drugs for various human ailments. Through experience, from time immemorial, people have identified the therapeutic potency of medicinal plants for various illnesses and conveyed their knowledge to successive generations. Historically crude extracts of the plant materials were used for curing various diseases. Ancient herbal lore/literature provides a rich source of information for the development of new drugs. The various indigenous systems such as Ayurveda, Siddha, Unani and Chinese use many plant species to treat several diseases. India has a large repository of medicinal plants and the therapeutic importance of plants lies in the presence of some phytoconstituents. After various technological developments, the isolation of pure compounds was started in accordance with bioassay-guided isolation. The first plant derived new molecular entity (NME) was morphine, isolated from the seed of *Papaver somniferum*. Even though currently most of the drugs derived from natural products are used for cancer therapy, there is remarkable contribution to infectious disease, metabolic disorders and associated diseases. Semi-synthesis is a versatile technique for developing bioactives via modification of isolated compounds from natural products. Nowadays, many modified natural products have been fruitfully developed for clinical applications. The examples include penicillin, morphine, artemisinin and paclitaxel. In view of this promising significance of natural products, in the present work we have carried out the identification of phytochemicals from medicinally relevant plants and carried out synthetic transformations of one of the abundant constituent to novel bioactives and carried out their biological evaluations to establish efficacy.

Chapter 1 gives a brief introduction about natural products and their importance in drug discovery with special emphasis on natural products derived drugs and drug candidates for metabolic disorders. Natural products play an inevitable role and inspiration for the development of new therapeutics. This is highlighted with examples from literature. This chapter also gives a brief idea about the semi-synthesis of natural products and the drug discovery process.

The *Zingiberaceae* or the ginger family is a family of flowering plants well known for their medicinal and nutritional properties. *Zingiberaceae* provides many useful products for food, spices, dyes, perfumes, cosmetics, medicine etc. It consists of a rich repository of medicinal plants. Therefore, **Chapter 2** after a brief literature survey of the two most

important *Zingiberaceae* plants, viz. *Curcuma longa* and *Zingiber officinale*, focuses on the phytochemical investigation of three medicinally important plants, *Curcuma amada*, *Curcuma malabarica* and *Curcuma aromatica* from the *Zingiberaceae* family. The isolated compounds include diterpenes and sesquiterpenes. All the isolates were characterized using various spectroscopic techniques and by comparison with the reported literature. Interestingly, some of the phytochemicals are being reported for the first time from these plants. All the phytochemicals were tested against obesity via inhibition of the pancreatic lipase enzyme.

In **Chapter 3**, we have isolated the molecule (*E*)-labda-8(17),12-diene-15,16-dial from the rhizomes of *Curcuma amada* and synthetically modified to novel labdane appended triazole analogues. The semi-synthetic analogues have been then tested against pancreatic lipase for obesity studies. Among these hybrids, two compounds exhibited excellent inhibitory activity (IC_{50} $0.75 \pm 0.02 \mu\text{M}$ and $0.77 \pm 0.01 \mu\text{M}$), slightly better than that of the positive control orlistat (IC_{50} $0.8 \pm 0.03 \mu\text{M}$). Cytotoxicity of the molecules was assessed by MTT assay and none of the compounds showed cytotoxicity (H9c2) in the concentration ranging from $1\mu\text{M}$ - $100\mu\text{M}$.

Hyperlipidemia is a clinical condition where blood has an increased level of lipids, such as cholesterol and triglycerides. Therefore controlling hyperlipidemia is considered a protective strategy to treat many associated diseases. The plants from the *Zingiberaceae* family are reported for their anti-hyperlipidemic potential. Therefore in **Chapter 4**, we deal with the anti-hyperlipidemic potential of natural product based labdane-pyrroles via inhibition of cholesterol and triglycerides synthesis. Inhibition of HMG-CoA reductase and MTT assay was also performed in this chapter. We have synthetically modified (*E*)-labda-8(17),12-diene-15,16-dial to the novel natural product derived pyrrole and pyrazole-(*E*)-labda-8(17),12-diene-15,16-dial conjugates.

The Role of Natural Products in Drug Discovery: Special Focus on Metabolic Disorders

1.1. Abstract

Herein, we discuss some important milestones in the discovery and use of natural products since ancient times to current era in drug discovery followed by the portrayal of natural product derived drugs and drug candidates, with special emphasis on metabolic disorders. In addition, a brief introduction to the drug discovery process is also incorporated.

1.2. Introduction

Since time immemorial, humans have relied on nature to satisfy their various needs. Nature is itself an art of science and through its own high-throughput (HTS) screening paradigm made natural products (NPs) with admirable specificity and potency compared to synthetic molecules.^{1,2} For millennia, various areas of NP research have been and continue to be an endless source and inspiration for human therapeutics through the discovery of drugs and drug leads.³ NP research advances have been made by tackling difficulties in different complicated and fascinating research areas, including isolation, structural elucidation, biological screening, chemical synthesis and biosynthesis.⁴

Plants possess many therapeutic properties and plant derived medicines have alleviated many pathological conditions. Plants produce different varieties of NPs with different chemical diversity. These are termed as “secondary metabolites”, in contrast to “primary metabolites” which are directly involved in plant growth, development and reproduction. Secondary metabolites do not have any physiological function on the plant.⁵ They are produced either as a result of adapting mechanisms to their environment or to defense against herbivores or other predators for their survival.⁶ These secondary metabolites are an important and inevitable source of potential drug leads. One of the important strategies for selecting a plant for pharmacological studies is the careful analysis and observations of such resources in traditional uses of various cultures, known as ethnopharmacology.⁷ Historically, traditional medical practitioners utilized crude plant extracts to produce

therapeutically active formulations for various diseases. The therapeutic efficacy of plant extract is mainly due to the synergistic effect of several secondary metabolites. Later, isolated compounds and synthetically modified chemical entities were explored for distinct therapeutic areas by pharmaceutical companies.³

The first plant derived new molecular entity (NME) was morphine (**Figure 1.1**). Friedrich Wilhelm Serturmer was the first to successfully isolate the alkaloid morphine as crystals from the seed of *Papaver somniferum* L. (Opium poppy, which belongs to the family *Papaveraceae*) in 18th century (in between 1803-1817) through diligent research. It was in use since 1827 prior to FDA approval garnered in 1938 as an analgesic.⁸

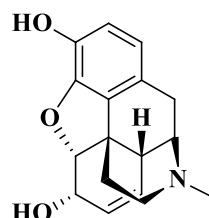


Figure 1.1. Morphine

Eventhough, the major contribution to the drug discovery is from plant source, there is considerable share from microbial, marine and animal sources too. Streptomycin (1946) and phenoxymethyl penicillin (1953) are the first FDA approved bacterial and fungal NMEs. Since the year 2000, about 77% of the FDA approved antibiotics are natural products and 100% of them are derived from microbes.⁸

The revolution of drug discovery research started after the serendipitous discovery of penicillin (**Figure 1.2**) by Alexander Fleming in 1928 from the fungus *Penicillium notatum*. The identification of its broad medicinal use and large scale production during the Second World War paved a pivotal way for drug discovery.^{2,9,10} One of the important advances in the drug discovery programme was the mechanism-based screening for bioassay-guided isolation. The mechanism-based approach has become the backbone of high-throughput screening (HTS) by considering the various screening techniques and targets. β -lactamase inhibitor clavulanic acid (**Figure 1.2**) from *Streptomyces clavuligerus*, HMG CoA reductase inhibitor mevastatin from *Penicillium citrium* etc., are some of the first compounds identified

based on mechanism based screening methods in the early 1970s. Augmentin [a combination of clavulanic acid and amoxicillin (**Figure 1.2**)] is a first line antibiotic used still today.¹⁰

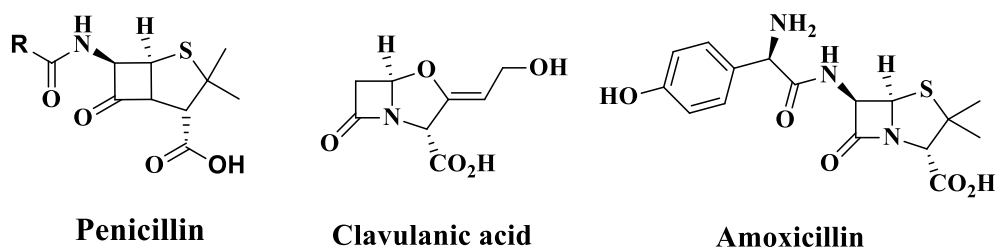


Figure 1.2.

The pursuit of isolation and identification of new bioactive molecules is often a difficult task due to their structural complexity and requires enormous effort, patience and intensive investments in resources. For this reason, there is a decline of interest in natural product chemistry and therefore, the pharmaceutical industries have embraced combinatorial chemistry in favor of producing large libraries of compounds and progressively moved from NPs to diversity oriented synthetic compounds. Over time, the traditional system of medicine has been overshadowed by the ready availability of semi-synthetic and synthetic analogues of NPs.^{1,8} The rapid development of synthetic organic chemistry methodologies have also led to more attention being given to synthetic compounds than natural products for pharmacological applications.^{7,8}

Despite these difficulties, NPs are still contributing their considerable share to the discovery of new clinical candidates and drugs. This was recently portrayed by Newman and Cragg. They have reviewed the total number of natural product derived drugs out of the total drugs marketed in the last four decades, viz., 1981-2019. A total of 1881 drugs were approved and marketed during the last four decades. Approximately 24.6% (463) drugs were Synthetic (S), 18.9% (356) were derived from natural products (ND), 18.4% (346) were vaccines where as 11.5% (217) and 11% (207) drugs were made either synthetic or total synthesis which are natural product mimics. Among all these 1881 drugs, 3.8%, that is a total of 71 drugs were unaltered NPs.¹¹ A statistical data given in the review has been redrawn in **Figure 1.3**.

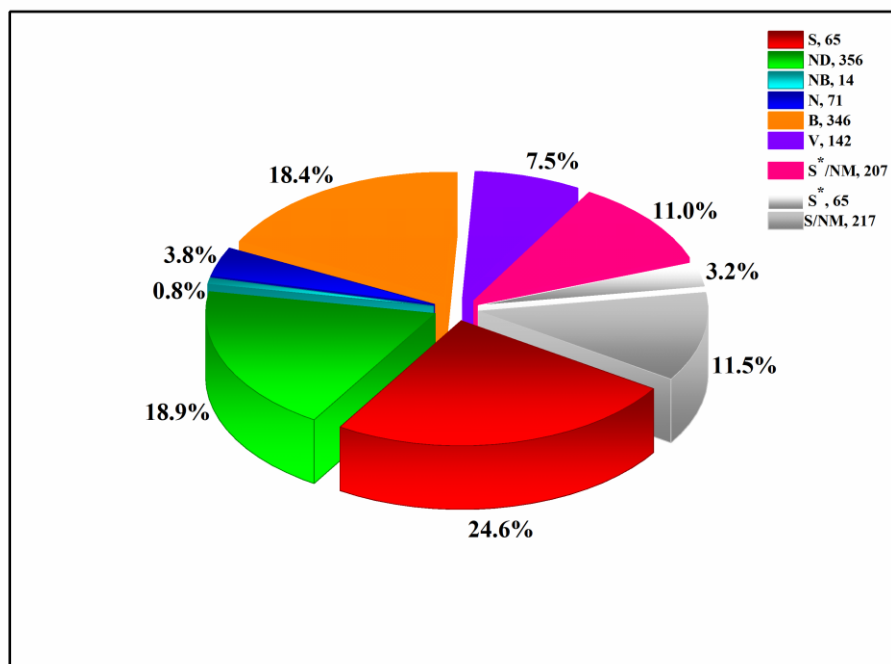


Figure 1.3. New drugs approved in between 1981-2019

Abbreviations:, **B:** Biological; usually a large (>50 residues) peptide or protein either isolated from an organism/cell line or produced by biotechnological means in a surrogate host, **N:** Natural product, **NB:** Natural product “Botanical” (in general these have been recently approved), **ND:** Derived from a natural product and is usually a semi-synthetic modification, **NM:** Mimic of natural products, **S:** Totally synthetic drug, often found by random screening/modification of an existing agent, **S*:** Made by total synthesis, but the pharmacophore is/was from a natural product, **V:** Vaccine.

Some of the important FDA approved unaltered natural products drugs which were launched in between 2000-2019 along with their disease area where they are used are given in **Table 1.1.**¹¹⁻¹⁴

Table 1.1. The list of FDA approved unaltered NP drugs launched in between 2000-2019

Sl. No:	Year Intro.	Generic Name	Trade Name	Disease
1	2000	Aminolevulinic acid	Levulan	Cancer
2	2003	Daptomycin	Cubicin	Bacterial
3	2005	Dronabinol /Cannabidiol	Sativex	Pain
4	2005	Fumagillin	Flisin	Antiparasitic
5	2005	Ziconotide	Prialt	Pain
6	2006	Exenatide	Byetta	Diabetes
7	2007	Trabectedin	Yondelis	Cancer
8	2009	Colchicine	Colcrys	Acute gout
9	2010	Romidepsin	Istodax	Cancer
10	2010	Capsaicin	Qutenza	Pain
11	2011	Spinosad(Spinosyn)	Natroba	Antiparasitic
12	2011	Fidaxomicin	Dificid	Bacterial
13	2012	Omacetaxine mepesuccinate	Synribo	Oncology
14	2012	Homoharringtonine	Ceflatonin	Cancer
15	2012	Ingenol mebutate	Picato	Cancer
16	2014	Trastuzumab	PICN	Cancer
17	2018	Aplidine	Aplidin	Cancer

As mentioned by Newman and Cragg, large number of NP inspired and NP derived drugs have been approved in recent years. Some of the NP derived/inspired drugs which are launched in between 2005-2019 along with disease area in which they are used are listed in **Table 1.2.**^{11,12}

Table 1.2. The list of FDA approved NP derived/inspired drugs launched in between 2005-2019.

Sl. No:	Year Intro.	Generic Name	Trade name	Disease
1	2005	Doripenem	Finibax/Doribax	Antibacterial
2	2005	Tigecycline	Tygacil	Antibacterial
3	2005	Zotarolimus	Endeavor stent	Cardiovascular surgery
4	2006	Anidulafungin	Eraxis/Ecalta	Antifungal
5	2006	Varenicline	Chantix/Champix	Nicotine dependence
6	2007	Lisdexamfetamine	Vyvanse	ADHD
7	2007	Retapamulin	Altabax/Altargo	Antibacterial
8	2007	Temsirolimus	Torisel	Oncology
9	2007	Ixabepilone	Ixempra	Oncology
10	2008	Ceftobiprole medocaril	Zeftera/ Zevter	Antibacterial
11	2008	Methylnaltrexone	Relistor	Opioid-induced onstipation
12	2008	Umirolimus	Biomatrix	Cardiovascular surgery
13	2008	Tafluprost	Taflotan	Antiglaucoma
14	2009	Everolimus	Afinitor	Oncology
15	2009	pralatrexate	Folotyn	Cancer
16	2009	Tebipenem pivoxil	Orapenem	Antibacterial
17	2009	Telavancin	Orapenem	Antibacterial
18	2009	Vinflunine	Javlor	Cancer
19	2009	Nalfurafine	Remitch	Pruritus
20	2010	Cabazitaxel	Jevtana	Cancer
21	2010	Fingolimod	Gilenya	Multiple sclerosis
22	2010	Monobactam aztreonam	Cayston	Antibacterial
23	2010	Ceftaroline fosamil	Teflaro	Antibacterial
24	2010	Eribulin	Halaven	Cancer
25	2010	Mifamurtide	Mepact	Cancer
26	2010	Vinflunine	Javlor	Cancer

27	2010	Zucapsaicin	Zuacta	Pain
28	2010	Laninamivir octanoate	Inavir	Antiviral
29	2011	Abiraterone acetate	Zytiga	Anticancer
30	2011	Brentuximab vedotin	Adcetris	Anticancer
31	2012	Dapagliflozin	Forxiga	Type 2 diabetes
32	2012	Carfilzomib	Kyprolis	Oncology
33	2012	Arterolane/ piperazine	Synriam	Antiparasitic
34	2013	Canagliflozin	Invokana	Type 2 diabetes
35	2013	Trastuzumab emtansine	Kadcyla	Cancer
36	2014	Dalbavancin	Dalvance	Antibacterial
37	2014	Oritavancin	Orbactiv	Antibacterial
38	2014	Cetolozane/tazobactam	Zerbaxa	Antibacterial
39	2015	Padeliporfin potassium	Stakel	Cancer
40	2017	Latanoprostene bunod	Vyzulta	Antiglaucoma
41	2017	Inotuzumab ozogamicin	Besponsa	Anticancer
42	2017	Midostaurin	Rydapt	Anticancer
43	2017	Meropenem/vaborbactam	Vabomere	Antibacterial
44	2017	Tenofovir disoproxilrotate	Viread	Antiviral
45	2018	Moxidectin		Antiparasitic
46	2018	Tafenoquine succinate	Etaquine	Antiparasitic
47	2018	Plazomicin	Zemdri	Antibacterial
48	2018	Omadacycline	Nuzyra	Antibacterial
49	2018	Eravacycline	Xerava	Antibacterial
50	2018	Sarecycline	Seysara	Antibacterial
51	2019	Lefamulin	Xenlita	Antibacterial
52	2019	Imicilast-relebactam		Antibacterial
53	2019	Polatuzumab vedotin	Polivy	Cancer

From the above table it is clear that NPs still hold out the best strategy for finding novel therapeutic agents. This will need a team work of chemists (to tailor functionalized structures from nature) and biologist to the discovery of potential drugs for various diseases.

Therefore, in the coming section we briefly discuss about natural products drugs and leads from plant, microbial, marine and animal sources.

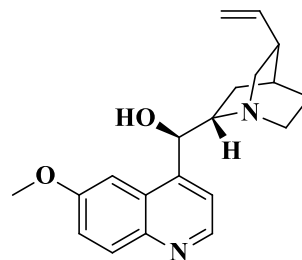
1.3. Natural products derived drugs from plant source

1.3.1. Quinine

Quinine (**Figure 1.4**) is an antimalarial drug isolated from the bark of *Cinchona officinalis* (Quina-Quina, belonging to the *Rubiaceae* family) in 1820 by Pierre Joseph Pelletier and Joseph Caventou. It belongs to the aryl amino alcohol groups of drugs. *Cinchona officinalis* is a rich source of medicinal alkaloids. Its bark had been used for centuries by the indigenous population in the Amazon region to combat shivering and fever associated with malaria. In the early 1600s, it was introduced into Europe for malaria treatment. The discovery of quinine in the 17th century was serendipitous and was the first chemical compound used successfully for infectious diseases. The isolation of the pure alkaloid was quickly appreciated compared to the use of tree bark. Before the invention of more potent synthetic antimalarial drugs (eg: chloroquine), quinine was used as a mainstay for malarial treatment until 1920s. Quinine and other cinchona alkaloids such as quinidine, cinchonine and cinchonidine are very active against malaria. Later with the emergence of resistance of *P. falciparum* to chloroquine, use of quinine again started particularly in the treatment of severe malaria. In 2010 WHO recommended that if the first-line drug fails or is not available, a combination of quinine with clindamycin, doxycycline or tetracycline can use as a second line treatment for uncomplicated malaria. Quinine with clindamycin is recommended for malaria in the first trimester of pregnancy. Therefore till now, quinine has played a significant role in the treatment of malaria. Eventhough its use as an over the counter drug has banned in 1990's, it has been reapproved by US FDA in 2004.^{6,15}



Cinchona officinalis



Quinine

Figure 1.4

1.3.2. Artemisinin

Another significant breakthrough is the discovery of the antimalarial drug artemisinin (**Figure 1.5**), which was isolated in 1972 from the plant *Artemisia annua*, known as sweet wormwood belonging to the *Asteraceae* family. The plant has been used in traditional Chinese medicine for many centuries to treat chill and fever associated with malaria. It is a sesquiterpene lactone bearing endoperoxide bridge. The mechanism of action involves interaction of artemisinin with intraparasitic heme (iron) that will result in the cleavage of endoperoxide bridges by iron, producing toxic free radicals. The malaria parasite is rich in iron, derived from the proteolysis of host cell hemoglobin. The free radical generated will damage the specific targets via alkylation, causing oxidative stress in the cells of the parasite. Artemisinin and its semi-synthetic analogues such as artefenomel, artemether etc., (collectively known as ARTs) also exhibit excellent efficacy against chloroquine-resistant *P. falciparum* and cerebral malaria. Today, artemisinin combination therapy (ACT) constitutes the standard treatment for patients with uncomplicated *falciparum* malaria. Artemisinin was discovered by Prof. You-you Tu and she was awarded the Nobel Prize in the year 2015 (for Physiology).¹⁶⁻¹⁹

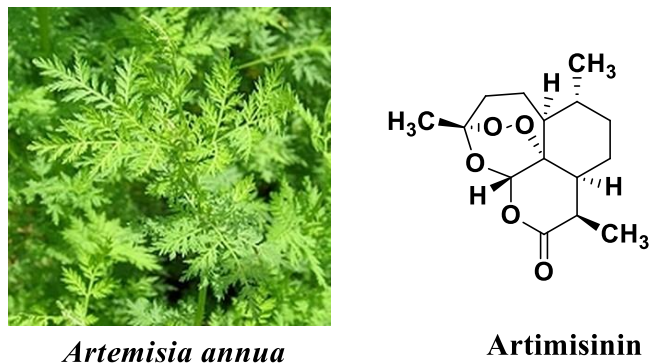


Figure 1.5

1.3.3. Pilocarpine

Pilocarpine (**Figure 1.6**) is an L-histidine-derived alkaloid isolated from the leaves of *Pilocarpus jaborandi* (belongs to *Rutaceae* family) in 1874. This has been reputed to be one of the mainstays of glaucoma therapy for over 100 years. Both pilocarpine monohydrochloride and pilocarpine nitrate are used as ophthalmic cholinergic agonists. It lowers intraocular pressure significantly in almost all patients and its side effects are comparatively few, which are the main advantages of pilocarpine. Oral administration of pilocarpine to treat dry mouth (xerostomia) resulting from radiation therapy for head and neck region or salivary gland dysfunction was also approved by FDA in 1994.^{6,26,27}

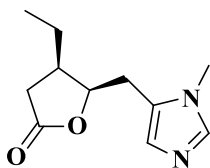


Figure 1.6. Pilocarpine

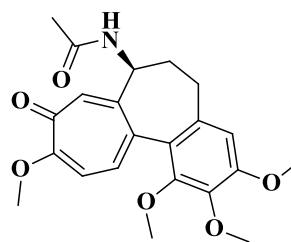
1.3.4. Colchicine

Colchicine (**Figure 1.7**) is a tricyclic alkaloid isolated from the roots of *Colchicum autumnale*, belonging to the *Colchicaceae* family. It was used since antiquity (A.D. 6th century) for the treatment of gout and also used as an anti-inflammatory, laxative etc.²⁸ Its use for the treatment of pain and swelling has been mentioned in the oldest medicinal text book, “the *Ebers papyrus*”. Colchicine was isolated in pure form by French chemists, P. J.

Pelletier and J. Caventou in 1820. The structure of colchicines was proposed in 1924 and exact structural formula was identified in 1945. Although colchicines belongs to the oldest drugs, still there is a chance to explore its therapeutic efficacy as a lead molecule. Eventhough it has been used for the treatment of acute gout from AD 560, it was approved by FDA only in 2009.²⁹⁻³¹



Colchicum autumnale



Colchicine

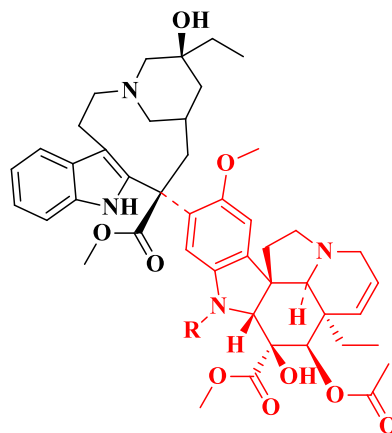
Figure 1.7

1.3.5. Vincristine and Vinblastine

Vincristine and vinblastine (**Figure 1.8**) were isolated from the periwinkle plant, *Catharanthus roseus* (L.) G. Don belonging to *Apocynaceae* family. Since the plant is native to the island of Madagascar, it is commonly known as Madagascar periwinkle. The leaf extracts of this plant were reputed for treating diabetes in the early traditional system of medicine. Later it was found that the alkaloids, vincristine and vinblastine from the leaf extract exhibit potent antileukemic activity. The discovery of the anticancer potency of vinca alkaloids was a milestone in the development of cancer therapy. Oxidation of methyl group of vinblastine led to vincristine. Vincristine and vinblastine are dimeric indole-based alkaloids in which a vindoline ring is connected with catharanthine system. These two drugs are collectively known as vinca alkaloids and are wonder drugs for cancer therapy. Vincristine got FDA approval in 1963 and vinblastine in 1965. The semi-synthetic derivative vinorelbine and its fluorinated analogue vinflunine also play an important role in chemotherapeutic treatment.²⁰⁻²²



Catharanthus roseus

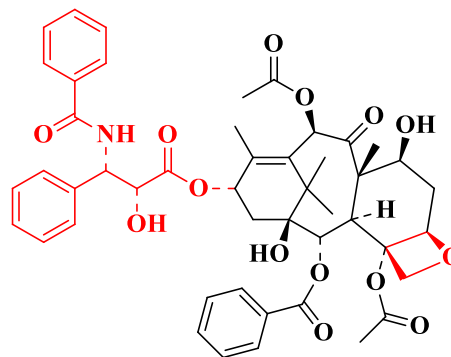


Vinblastine; R = CH₃
Vincristine; R = CHO

Figure 1.8

1.3.6. Paclitaxel (Taxol)

In the early 1960s, during the search for a potential source of anticancer drugs, Dr. Jonathan L. Hartwell of the US National Cancer Institute (NCI) collected many plants from USA. One of the plants collected was *Taxus brevifolia* (Pacific yew tree), which provided a critical milestone in the discovery of a novel anticancer drug. Historically, humans have made use of the yew tree for various purposes. Taxol (**Figure 1.9**) was isolated and characterized as the active constituent in 1969 by M. C. Wani and coworkers from *T. brevifolia*. Its discovery and development took around 30 years. The structural characterization of taxol was a daunting task in the late 1960s and its isolation and structural elucidation report was published in 1971. It is a diterpenoid molecule which consists of taxane moiety as well as a oxetane ring and an ester side chain, the latter being important for biological activity. Taxol is reputed for the treatment of different types of cancers. It was approved by the FDA in 1992 and 1994 for the treatment of ovarian cancer and breast cancer. Taxol and its analogues are well known for their efficacy and is the most successful anticancer agent from plant sources.^{6,23-25}

*Taxus brevifolia*

Paclitaxel

Figure 1.9

1.3.7. Digitoxin

Digitoxin (**Figure 1.10**), a cardiac glycoside (CG) was isolated from *Digitalis purpurea* L. (foxglove) belonging to the *Plantaginaceae* family. In the 18th century, English physician and scientist William Withering found that administering foxglove extract resulted in a dramatic change in patients with congestive heart failure. Based on this knowledge, Digitoxin and its analogues have been used to treat congestive heart failure, cardiac arrhythmias and atrial fibrillation. As a cardiotonic drug, digitoxin possesses a narrow therapeutic window. However, now it is one of the most auspicious anticancer CGs against several types of cancers, such as lung cancer, pancreatic cancer, leukemia and breast cancer. The discovery of anticancer activity of digitoxin was a breakthrough in cancer research.^{6,32,33}

Another CG is digoxin (**Figure 1.10**), isolated from *Digitalis lanata* by Dr. Sydney Smith in the year of 1930. It is one of the oldest medications for the treatment of cardiac disorders, including congestive heart failure, atrial fibrillation and certain cardiac arrhythmias. It was approved by FDA in 1998 for heart failure. Digoxin remains a useful agent to control atrial fibrillation, when it is combined with β -blockers. Both digitoxin and digoxin belongs to digitalis glycosides. Both of them have a steroidal nucleus, sugar moiety and lactone ring. The steroidal skeleton is considered to be the active pharmacophoric group.^{32,34}

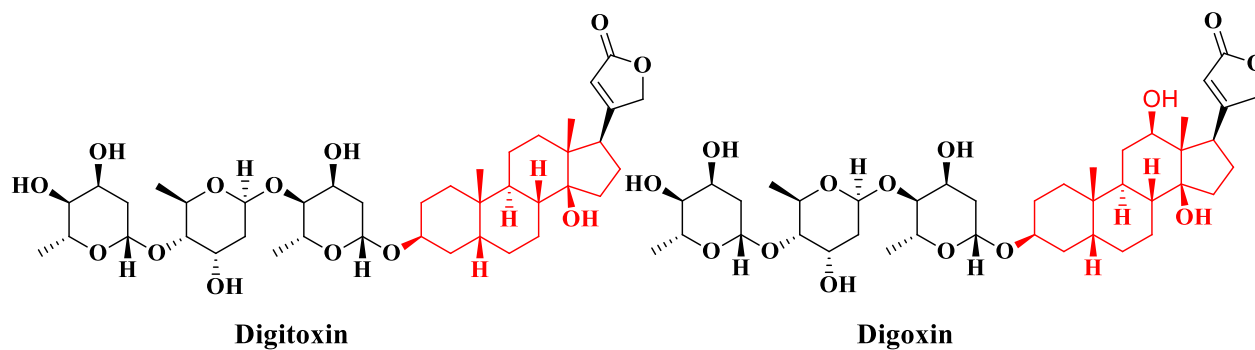
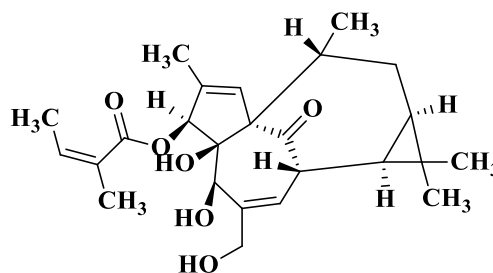


Figure 1.10

1.3.8. Ingenol mebutate

Ingenol mebutate (Picato, **Figure 1.11**) is an ingenane type macrocyclic diterpenoid, isolated from the aerial part of the plant *Euphorbia peplus*, belonging to *Euphorbiaceae* family. This plant has long been used in traditional folk medicine for the treatment of skin cancers. It was approved by FDA in 2012 and is used to treat actinic keratosis (AK), considered to be an epidermal dysplasia.^{35,36}

*Euphorbia peplus*

Ingenol mebutate

Figure 1.11

1.4. Natural products derived drugs and drug candidates from microbial source

Microorganisms such as bacteria and fungi have played a vital role as a source in the development of novel drugs and lead for various diseases. The discovery of drugs from microorganisms became popular after the discovery of the antibacterial drug penicillin. It is the most widely used antibiotic globally and was found to inhibit the growth of gram-

negative bacteria. Microorganisms have paved the way for the large scale production of food ingredients, antibiotics, agriculture procedures, natural colours etc. Microorganisms have proven to be the most productive and prolific in drug discovery process, particularly for infectious diseases, cancer, atherosclerosis, obesity, diabetes etc. Currently pharmaceutical companies rely largely on microbial sources for novel entities.³⁷ There are ample evidences for the contribution of microbes in the discovery of antibiotics. The important antibacterial drugs are streptomycin (**Figure 1.12**), discovered in 1944 from *Streptomyces griseus* and erythromycin (**Figure 1.12**), which is a broad spectrum antibiotic isolated from the species *Saccharopolyspora erythraea* in the year 1952. Other important antibiotics are vancomycin and its semi-synthetic derivative telavancin (TD-6424), a group of antibacterial drugs tetracyclines (*Streptomyces auerofaciens*, **Figure 1.12**), chloramphenicol (*Streptomyces venezuelae*, **Figure 1.12**) etc. Likewise, antifungal drugs amphotericin B (*Streptomyces nodosus*), a traditional antifungal agent and microbial derived synthetic compound PLD-118 (**Figure 1.12**) etc., are also well known. Viramidine (ribamidine) is an important anti-viral drug for the treatment of HCV (hepatitis B and C). Some important anticancer agents are also from microbial metabolites. Discovery of actinomycin in 1940 from the specie *Streptomyces parvulus* led to the first antibiotic shown to have anticancer activity. Another most widely used anticancer drug is doxorubicin (**Figure 1.12**), which was isolated from *Streptomyces peucetius* and FDA approved it in 1966.³⁷⁻³⁹ Some of the microbial derived therapeutic products are shown below.

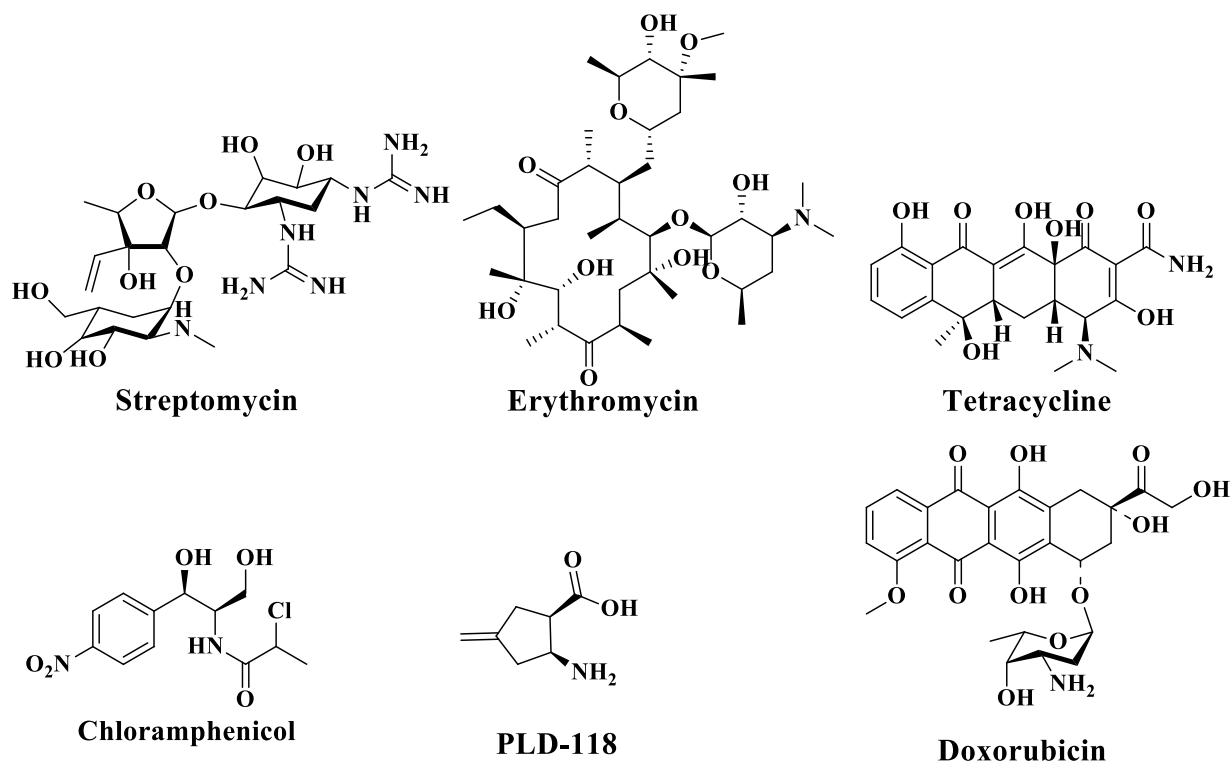


Figure 1.12. Microbial derived drugs and drug candidates

1.5. Natural products derived drugs and drug candidates from marine source

Oceans are a rich source of a variety of organisms, particularly enriched with microbes associated with marine plants and animals.^{40,41} Even though the major contribution of drugs are from terrestrial sources, there is a substantial share of drugs and drug candidates from marine sources too, marketed in recent years.⁴² Zhang *et al.* has reviewed marine derived macrolides from 1990 to 2020 and found that there are 505 macrolides reported from marine organisms.⁴³ Marine drug development programs gained momentum after the invention of spongothymidine (**Figure 1.13**) and spongouridine (**Figure 1.13**) in 1950 for cancer treatment.

As we mentioned earlier various potent anticancer agents are reported from plants and terrestrial microorganisms, however there is also a considerable contribution of anticancer agents from marine sources too. The discovery of C-nucleosides from the *Cryptotheca crypta*, a Caribbean sponge, led to the basis for the synthesis of cytarabine (**Figure 1.13**,

FDA approval in 1969), which is the first marine derived anticancer agent. It is currently used in patients with leukemia and lymphoma. Gemcitabine (**Figure 1.13**), a fluorinated derivative of cytarabine, has shown considerable activity in the treatment of patients with solid tumours such as pancreatic, breast, bladder and non-small-cell lung cancer.^{41,44} Ecteinascidin-743 (ET-743) (**Figure 1.13**), a potent and fascinating marine tetrahydroisoquinoline alkaloid isolated from the Caribbean tunicate extract *Ecteinascidia turbinata*, which exhibited potent anticancer activity in different tumour cell lines.⁴⁴⁻⁴⁶ Vidarabine (**Figure 1.13**) is an important antiviral drug isolated from the sponge nucleoside in 1950. Ziconotide, a synthetic peptide formulated on the toxin of the poisonous marine cone snail, *Conus magus* used as an analgesic drug. Some of the important marine derived drugs and molecules under clinical trials are given below.⁴¹

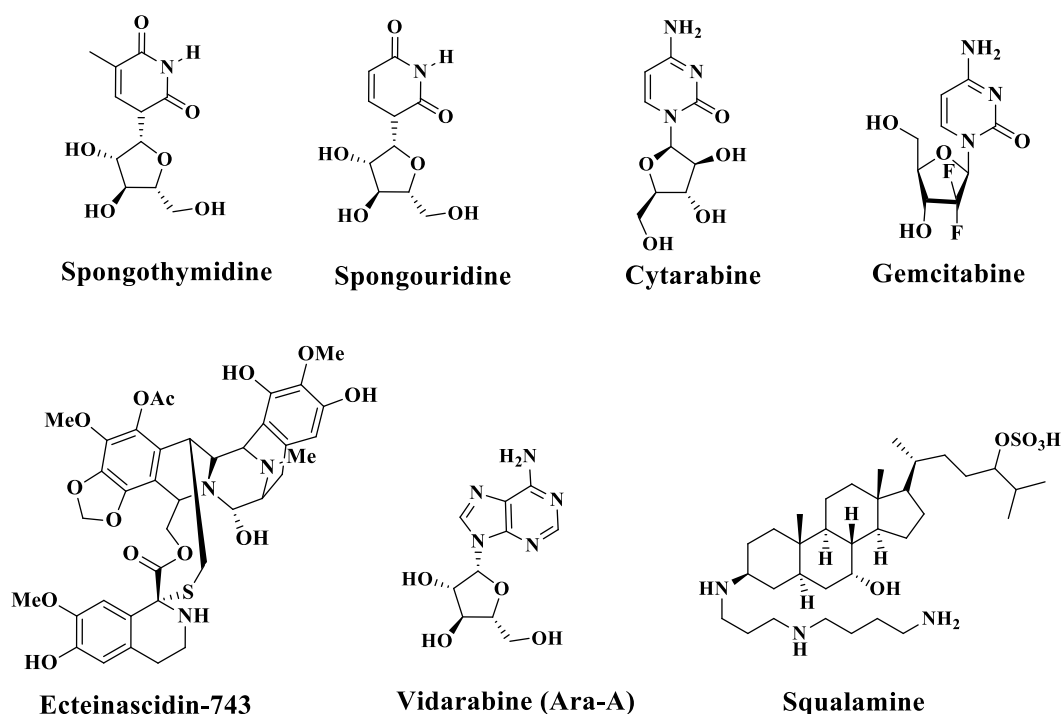


Figure 1.13. Marine derived drugs and drug candidates

1.6. Natural products derived drugs and drug candidates from animal source

Animals are also an important source of chemically diverse and promising bioactives. There are different medicines, vaccines and specific formulations such as tablets, capsules, creams

or mixtures containing animal products or are derived from animal sources. For example, gelatin used to make capsule shells, is a partially hydrolyzed collagen usually originated from bovine. Heparin, insulin and pituitary hormones are some of the oldest medications from animal sources. Heparin (**Figure 1.14**), was isolated from canine liver cells in 1916 and it is one of the oldest and most extensively used drugs for the treatment of hematologic disorders. Nevertheless, animal derived bioactives are still largely unexplored. Since animal toxins have high selectivity and specificity for the molecular targets, they have been used as a prototype for developing new therapeutic agents. Captopril is such an example of an antihypertensive drug developed from the knowledge garnered from animal venoms. Chlorotoxin, isolated from the scorpion *Leiurus quinquestriatus*, is an anticancer drug known as “tumor paint”, as it specifically binds to tumor cells without affecting normal cells.⁴⁷ Eptifibatide (**Figure 1.14**), a cyclic peptide isolated from the venom of the southeastern pygmy rattlesnake (*Sistrurns miliarius barbouri*), is used for the treatment of the acute coronary syndrome. TM-601, a chlorotoxin derived from the venom of the deathstalker scorpion (*Leiurus quinquestriatus*), is under phase II clinical trials for cancer therapy. Trabectedin (**Figure 1.14**) which is isolated from the sea squirts *Ecteinascidia turbinata* and aplidine (**Figure 1.14**) derived from the sea squirts *Aplidium albicans* are also used as anticancer agents for different malignancies. Epibatidine (**Figure 1.14**) is a toxic alkaloid isolated from a South American poison dart frog (*Epipedobates tricolor*). It is used as an analgesic agent, which is 200 times stronger than morphine and 30 times stronger than nicotine.⁴⁸ Tebanicline (ABT-594, **Figure 1.14**), a less toxic synthetic derivative of epibatidine, is a potent analgesic drug under clinical trial. ATryn is an anticoagulant produced from goat milk and was approved by the FDA in 2009.^{47,49-51}

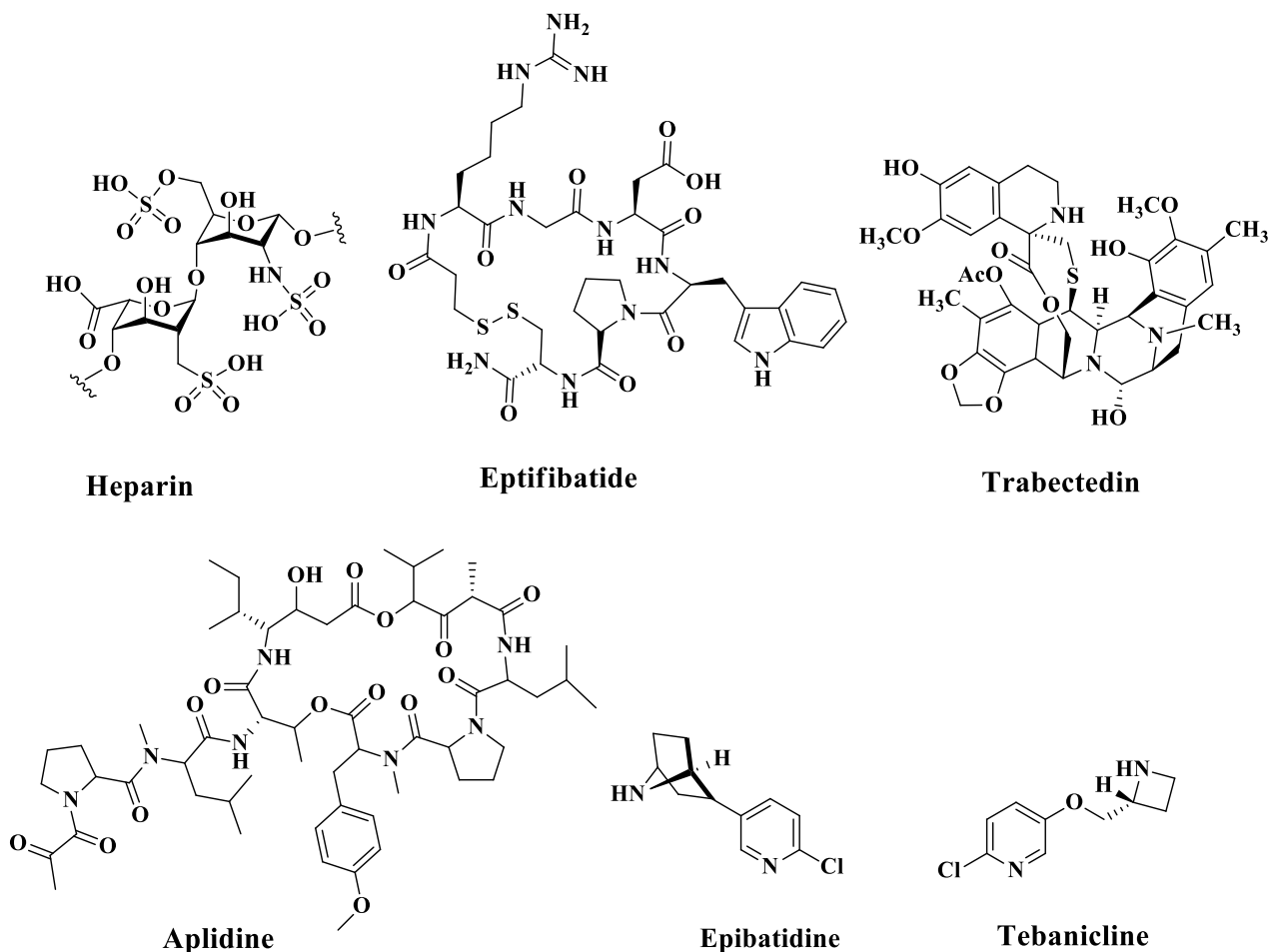


Figure 1.14. Animal derived drugs and drug candidates

From the above discussions it is clear that NPs always provide a valuable source for drugs and drug candidates for various ailments. There are large number of therapeutic agents available either as NP or inspired/derived from NPs in various disease areas such as cancer, bacterial, infectious, analgesics etc. In recent decades NPs have undisputedly gained greater attention in the area of metabolic disorders. In light of this idea, our aim is to explore the use of NPs and their derivatives against metabolic disorders. For this, we have surveyed the current status of NPs derived drugs and leads against metabolic disorders which is discussed below.

1.7. Natural products derived drugs and drug candidates for metabolic disorders

Metabolic disorders are complex conditions that disrupt the normal metabolism in our body and is a major risk factor for illness and death globally. Metabolism is the process by which the body makes energy by chemically breaking proteins, carbohydrates and fats in the digestive system towards glucose, which constitute energy for normal functioning of the body or for storage in body muscles, liver and also stored as body fat. Metabolic disorders are characterized by insulin resistance, abdominal obesity, dyslipidemia, hypertension and hyperglycemia. It is the risk factor for CVDs, Type 2 diabetes, stroke, chronic kidney disease and cancers. It may arise because of genetic factors, diet changes, lack of exercise, ageing and the disease or abnormal functions of certain organs like liver or pancreas. Many studies are reported which indicate that the main reason for metabolic disorders are heredity and other environmental factors that will contribute to the sudden increase in the risk.⁵²⁻⁵⁴

1.7.1. Obesity

Obesity is a chronic metabolic disorder that results from the imbalance between energy intake and expenditure and it is now a common disorder found in our society. The excess food taken is converted into lipid components, primarily triglycerides, and is stored in the liver, adipose and other tissues. If the positive energy balance extends for a longer period, it leads to overweight and obesity.⁵⁵ It is caused by the association between multiple factors such as excess food intake, lack of exercise, genetic problems, abnormality in metabolism and environmental problems.⁵⁶ Obesity contributes to many metabolic disorders, including metabolic syndrome, coronary heart disease (CHD), fatty liver, hypertension, certain cancers, stroke and diabetes.⁵⁷ Since obesity and related metabolic disorders continue to increase globally, there is an urgent need to identify safe and efficient therapies to combat the problem.⁵⁸ According to World Health Organization (WHO), obesity is a global epidemic. In 2018, WHO reported that global obesity has almost tripled since 1975.⁵⁹ Therefore, controlling obesity is the major challenge worldwide. Due to the increasing rate of obesity worldwide, medicinal chemists are giving more attention to the development of new therapeutic agents. Among the various treatments, pharmacotherapy is most desirable.^{60,61}

The most prescribed FDA approved drugs for obesity are orlistat, sibutramine and rimonabant, which act via different mechanisms of action. However, the latter two drugs are withdrawn from the market due to severe side effects such as cardiovascular and psychiatric complications.^{62,63} Many reports describe the importance of natural products in treating obesity. Various extracts and secondary metabolites from plants, microbial sources and marine sponges have attracted much attention for their anti-obesity properties. Caffeine (**Figure 1.15**) from tea leaves increases energy expenditure and fat oxidation. Curcumin (**Figure 1.15**) from turmeric can lower lipids and prevent obesity-related complications. Capsaicin (**Figure 1.15**), an alkaloid from *Capsicum annuum* reduces obesity. Celastrol (**Figure 1.15**) triterpene from roots of *Tripterygium wilfordii* has potent anti-obesity property as evident from animal studies. Gingerol (**Figure 1.15**) and shogaol (**Figure 1.15**) from *Zingiber officinale* have been shown to increase metabolic rate and thus help to “burn off” excessive fat.^{64,65}

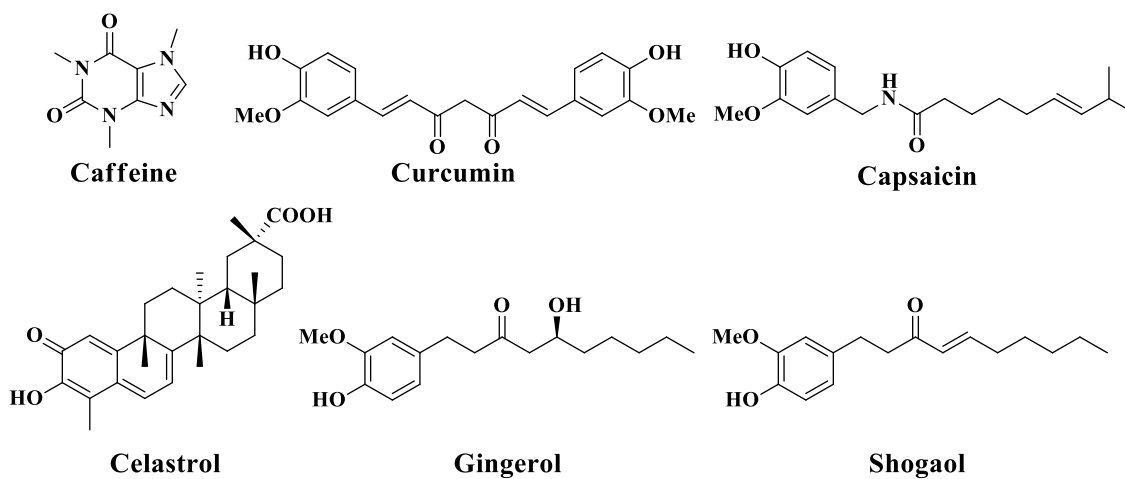


Figure 1.15. Natural products having anti-obesity properties

1.7.1.1. Orlistat

Orlistat (Xenical, **Figure 1.16**), a tetrahydrolipstatin is the most widely prescribed FDA approved (1998) anti-obesity drug in the market today. It is a partially hydrated derivative of endogenous lipstatin isolated from *Streptomyces toxytricin* and its mechanism of action is via

the inhibition of an enzyme, viz., pancreatic lipase.⁶³ It also reduces total cholesterol and low density lipoprotein (LDL) cholesterol.

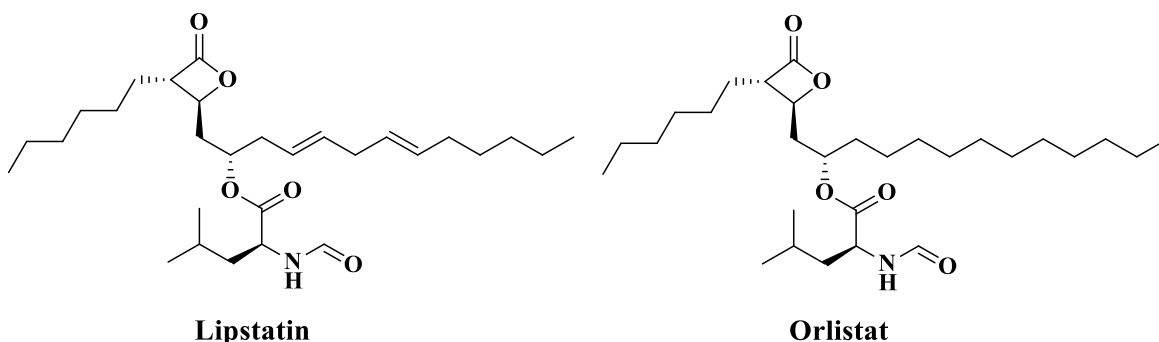


Figure 1.16

1.7.2. Diabetes

Diabetes Mellitus (DM) is commonly known as diabetes. It is one of the most common endocrine disorders caused by the deficiency in insulin production, insulin action or both in combination. Diabetes will affect at any age and the prevalence is equal for both males and females. DM is associated with a high cardiovascular morbidity/mortality and is the leading cause of chronic kidney disease (CKD). It also damages the body systems, such as the liver, eyes, blood vessels and nerves.⁶⁶⁻⁶⁸ The main types of DM is Type-I diabetes, which is associated with insulin deficiency resulted from the autoimmune destruction of the pancreatic β -cell, and Type-II diabetes, which is characterized by insulin resistance and accounts for the 90% of all reported cases. The natural hormone insulin called “key” produced from the β -cell present in the pancreas helps to transport glucose to the cells for use as energy. When sugar enters the cells, the blood sugar level is lowered. But in the absence of insulin, the sugar cannot get into the body’s cells for use as energy. This leads to an increase in the blood sugar level and the condition as called “hyperglycemia” (high blood sugar). DM is characterized by hyperglycemia. In 1988, Type 2 diabetes mellitus (T2DM) was declared as a metabolic syndrome.⁶⁹⁻⁷¹

Over the past many years, the number of diabetes cases and prevalence rate has been dramatically increasing globally and its prevalence rate in 2019 is reported to be 9.3% (463 million people), rising to 10.2% (578 million) by 2030 and 10.9% (700 million) by 2045.

About 50.1% of people living with diabetes are not aware of it.⁷² According to WHO, diabetes is a major risk factor for blindness, kidney failure, heart attack, stroke and lower limb amputation. Worldwide, more than 422 million people have diabetes and around 1.6 million deaths were caused by it in 2016, and hence diabetes is considered the seventh leading cause of death globally.⁷³

The major risk factors for getting T2DM are genetic susceptibility and environmental factors. Life style modifications such as diet, exercise etc., are the best solutions to control diabetes. Pharmacological interventions are recommended upon failure of lifestyle modifications. There are many classes of drugs available for the treatment of diabetes and the selection depends on the nature of diabetes, age and other factors. The conventional pharmacological agents used in the treatment of DM, including insulin and oral antidiabetic medications such as sulfonyl ureas, biguanides, acarbose, metformin, rosiglitazone, glibenclamide or combination of these drugs etc.^{68,74} Prolonged use of these drugs leads to many adverse effects on our health. Therefore, novel and safe therapeutic agents are necessary for diabetic treatment. Here the role of natural products arises because of their fewer side effects, easy availability and increased potency compared to synthetic drugs.⁷⁵ Many plant extracts and their active principles have been shown to exhibit potent antidiabetic efficacy, which may be helpful for the innovation of novel drug candidates and drug discovery.^{76,77}

In 2012, Hung *et al.* reviewed the recent discovery of plant derived antidiabetic natural products during 2005-2010. Many plant extracts from various families such as *Amaranthaceae*, *Apocyanaceae*, *Asteraceae*, *Cucurbitaceae*, *Fabaceae*, *Lamiaceae*, *Liliaceae*, *Malvaceae*, *Myrtaceae*, *Rubiaceae* etc., have shown promising activity. Various isolated compounds of the type lignans such as vanilic acid derivatives and cinnamaldehyde, flavonoids including daidzein, capillarisin, kaempferol, quercetin, apigenin and its derivatives, as well as terpenoids such as arjunolic acid, oleanolic acid, masilinic acid, withanolides and steroids such as cucurbitaceae glycosides and stigmasterol have shown to exhibit excellent therapeutic efficacy in type 2 diabetes mellitus.^{78,79} Some of the approved antidiabetic drugs and drug candidates synthetic as well as natural are discussed below.

1.7.2.1. Metformin

Metformin (Dimethyl biguanide, **Figure 1.17**), today is a first-line oral blood glucose-lowering agent used to alleviate type 2 diabetes. In European folklore medicine, the plant *Galega officinalis* (commonly known as French lilac, false indigo, Spanish santonin, gout's rue etc.), which belongs to *Fabaceae* family was used for relief of frequent urination, which today is established as a symptom of diabetes. However, the plant extract was found to be too toxic for continual usage. In the late 1800s, the phytochemical investigation of the plant extract was found to be rich in guanidine (**Figure 1.17**) and galegine. In 1918, guanidine was reported to reduce blood glucose in animals. The fusion of two guanidine molecules to form biguanide (**Figure 1.17**) provided the background for the synthesis of metformin. Later it was unappreciated and biguanide was not developed for the treatment of diabetes as high doses are required for lowering the glucose level. In the mid of 1940s, during the search of guanidine based antimalarial agent proguanil (**Figure 1.17**), metformin was discovered. Metformin is a wonder drug because of its numerous biological actions. It reduces insulin resistance, lowers glucogenesis and also has strong cardioprotective effect, anti-inflammatory effect etc. Metformin was first synthesized in 1922 and was approved by Europe in the 1950s and by FDA in 1994. It has been used since 1957 in the treatment of DM either as monotherapy or combination therapy with sulfonylureas such as, glimeperide. It is also used for the treatment of obesity and tumor.^{67,80-82}



Galega officinalis

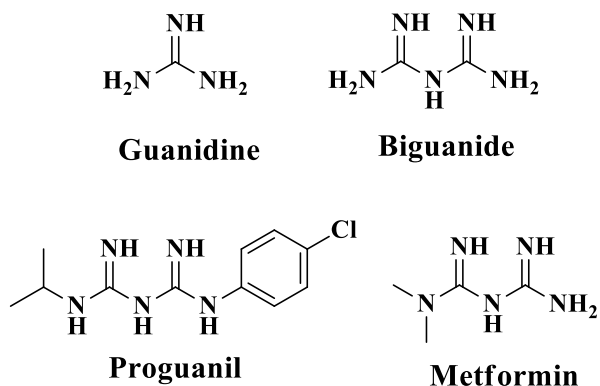


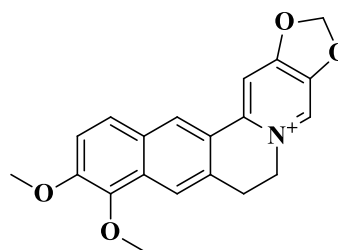
Figure 1.17

1.7.2.2. Berberine

Berberine (**Figure 1.18**) is the most important isoquinoline alkaloid from the traditional medicinal plant *Berberis vulgaris* (barberry). This plant was used as a herbal medicine to treat diarrhea and dysentery. Berberine is also found in many other plant species. Later many researchers have unraveled that berberine shows hypoglycemic actions similar to metformin. Its antidiabetic potential was first reported in 1986. Studies showed that berberine is an AMP-activated protein kinase (AMPK) activator and it also stimulates glycolysis. Therefore, berberine is a drug candidate for the treatment of type 2 diabetes.⁸²⁻⁸⁴ Other therapeutic aspects of berberine include potential use especially in lipid metabolism, anti-inflammatory, antihypertensive, antiviral, cancer etc. Berberine undergoes extensive metabolism after oral administration. Therefore many researchers are interested on doing their active research on the metabolites of berberine and many studies found that the metabolites of berberine play a significant role in the treatment of various diseases. However additional well-designed clinical trials are required before it become a drug of choice.⁸⁵⁻⁸⁷



Berberis vulgaris



Berberine

Figure 1.18

1.7.2.3. Exenatide

Exenatide (Byetta) is an FDA approved (2005) drug for treating type 2 diabetes and is used along with diet and exercise. It is a synthetic analog of exenadin-4, isolated from the saliva of the Gila monster (*Heloderma suspectum*) as a 39 amino acid peptide. It increases insulin

production, suppresses glucagon secretion, prolongs gastric emptying and reduces food intake. It is a safe and effective drug as either monotherapy or in combination with metformin.⁸⁸ A systematic review and meta-analysis study showed that other than blood glucose lowering effect, exenatide also showed beneficial effects on blood pressure and lipid profile of diabetes patients.⁸⁹ It belongs to a relatively new class of antidiabetic drugs known as glucagon-like peptide-1 (GLP-1) receptor agonists. Structurally simpler GLP-1 receptor agonists are awaited.⁴⁹

1.7.2.4. Acarbose

Acarbose (Precose, **Figure 1.19**) is the first α -glucosidase inhibitor in the treatment of T2DM. Acarbose is a pseudo tetrasaccharide isolated from the microorganism *Actinoplanes utahensis* during fermentation. FDA approved it in 1999 as an adjunct with monotherapy or in combination with sulfonylureas. Its mechanism of action is via inhibition of pancreatic α -amylase and membrane-bound alpha-glucosidase hydrolase enzymes in the intestine. This will cause delayed glucose absorption and a lowering of postprandial hyperglycemia.^{90,91}

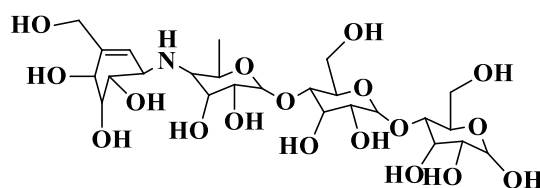


Figure 1.19. Acarbose

1.7.2.5. Miglitol

Miglitol (glyset, **Figure 1.20**) is a semi-synthetic α -glucosidase inhibitor derived from 1-desoxynojirimycin used in the treatment of T2DM and it was approved in 1996 as antidiabetic drug. Nojirimycin (desoxynojirimycin) was isolated from various *Bacillus* and *Streptomyces* microbial strains. These microbial metabolites on semi-synthetic transformation led to the discovery of miglitol. Its mode of action is similar to that of acarbose, that is, it reduces postprandial hyperglycemia by inhibiting intestinal α -glucosidase and thereby delays carbohydrate absorption. It is safe and ideal tool for mono and combination therapy. It is also reported for anti-obesity potential.^{92,93}

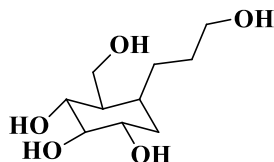


Figure 1.20. Miglitol

1.7.2.6. Voglibose

Voglibose (**Figure 1.21**) is an important α -glucosidase inhibitor (AGI) used in diabetic treatment. It was discovered by Japanese scientists in 1981 and it became commercially available since 1994. It is effective against hyperglycemia and associated disorders. Its mode of action is by delaying the digestion and absorption of carbohydrates, and hence it maintains lower blood glucose levels after meal. Voglibose is the most effective and tolerant α -glucosidase inhibitor than acarbose and miglitol. It is also reported for its anti-obesity potential.^{94,95}

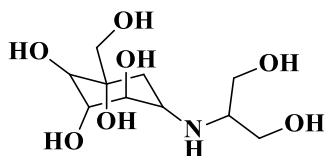


Figure 1.21. Voglibose

1.7.2.7. Phlorizin and its analogues

Phlorizin (**Figure 1.22**) was first isolated from the bark of the apple tree in 1835 and is a member of the chalcone group of organic compounds. It was used in antidiabetic therapy, which inhibits specifically and competitively both sodium glucose co-transporters (SGLT1 and SGLT2), thereby inhibiting renal glucose re-absorption in patients with type 2 diabetes. Since phlorizin possesses poor oral bioavailability and poor selectivity towards SGLT2 vs SGLT1, it was withdrawn for further development as an antidiabetic agent.^{12,96,97}

Even though phlorizin is not developed as an antidiabetic agent, it served as a lead molecule for the invention of a new class of antihyperglycemic drug, viz., SGLT 2 inhibitors and it provide multiple benefits, including decreased HbA_{1c}, body weight and blood pressure. The SGLT2 inhibitors are classified into three types, O-glucosides, C-glycosides and O-

spiroketal C-arylglucosides. The important C-glycosides phlorizin analogues such as canagliflozin (**Figure 1.22**), dapagliflozin (**Figure 1.22**) and empagliflozin (**Figure 1.22**)⁹⁸⁻¹⁰¹ were approved by the US FDA in 2012, 2013 and 2014 respectively as potent SGLT2 inhibitors in patients with type 2 diabetes as adjunct to diet and exercise.^{12,102} Ipragliflozin (C-glycoside, **Figure 1.22**) and Luseogliflozin (**Figure 1.22**) are also highly specific SGLT2 inhibitors and got first global approval in Japan and in 2014 got FDA approval. Also, tofogliflozin (**Figure 1.22**) containing O-spiroketal C-arylglucoside provides good efficacy and bioavailability, and got FDA approval in 2014. The SGLT2 inhibitors such as ertugliflozin (**Figure 1.22**) and remogliflozin etaborate (**Figure 1.22**), both containing C-glycosides, got FDA approval in 2017 and 2019 respectively. Stagliflozin is also an SGLT2 inhibitor and it was approved by FDA in 2019.^{11,103-105}

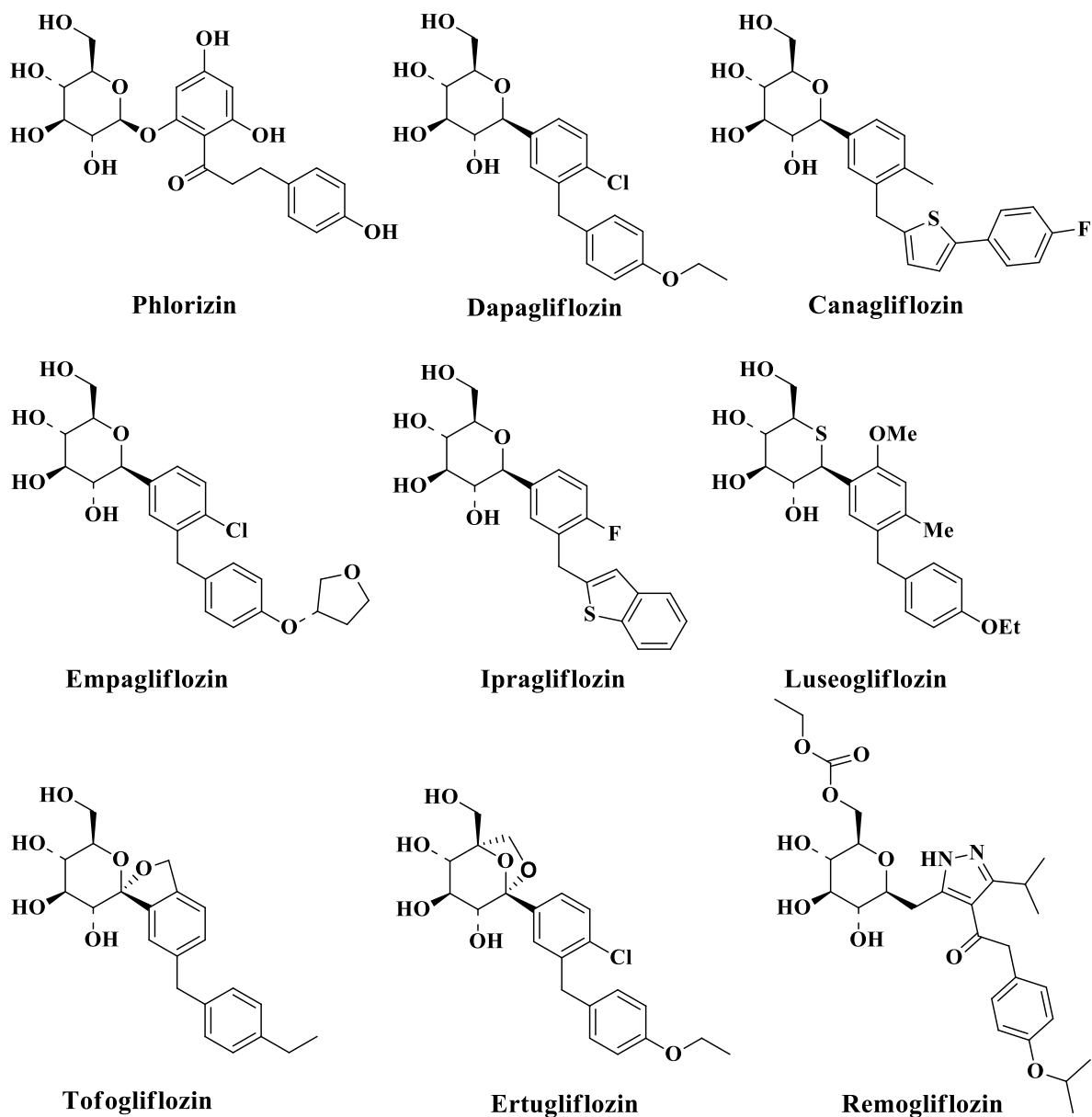


Figure 1.22. Structure of phlorizin and its analogues

1.7.3. Non-alcoholic fatty liver disease and Hyperlipidemia

Non-alcoholic fatty liver disease (NAFLD) is a clinical diagnosis characterized by excess triglyceride accumulation within hepatocytes or steatosis. It is the most leading chronic liver disease. It affects 25% of the world population and almost 8% of adolescents. Majority of patients with NAFLD are having metabolic comorbidities, which increase the risk of CVD. Liver is the main organ for lipid metabolism. NAFLD and hyperlipidemia are closely

associated. Hyperlipidemia is a condition in which there is an increase in triglycerides, cholesterol, phospholipids, or a combination of these factors in blood.^{52,106,107} Cholesterol plays a vital role in the functioning of human organs and it is formed in the liver. If the synthesized cholesterol in the body and that absorbed from diet exceeds above required level, leads to high cholesterol level in blood leading to cardiovascular problems.^{108,109} It has long been considered as elevated levels of plasma cholesterol (hypercholesterolemia) was the primary cause of atherosclerosis and coronary heart diseases. Therefore the treatment for hyperlipidemia remains the main strategy for preventing CVD and related disorders. Continuous search for the cholesterol lowering agents led to the discovery of statins, now used to control cholesterol synthesis. The word 'statin' refers to the generic name of all β -Hydroxy β -methylglutaryl-coenzyme A (HMG-CoA) reductase inhibitors, the enzyme which catalyses the rate-limiting step in the biosynthesis of cholesterol (HMG-CoA to cholesterol). Statins are used as adjuncts to healthy lifestyle interventions. It became apparent that statins will effectively reduce cardiovascular related morbidity and mortality.¹¹⁰ Many natural, semi-synthetic and synthetic statins are available to treat high level of cholesterol. The natural product and semi-synthetic derived statins are discussed below.

1.7.3.1. Mevastatin

Endo A., in 1970 isolated the first statin, namely mevastatin (formerly known as compactin or ML-236B, **Figure 1.23**), from broths of blue green mold *Penicillium citrinum*. It is a substituted hexahydronaphthalene lactone and shows the structural similarity to HMG CoA. Milestone in the discovery of HMG CoA reductase inhibitor was the invention of the first HMG CoA reductase inhibitor mevastatin, and it has paved the way for the development of various statin analogues. It produces a profound decrease in serum cholesterol and thereby decreases CVD incidences of and frequency of heart attack. It is potent in lowering serum total and LDL cholesterol in experimental animals and patients suffering from hypercholesterolemia. Apart from being the precursor for many other statins, it also shows other medicinal properties.^{108,109-113} Pravastatin (**Figure 1.23**) is another important statin derived from the biotransformation of mevastatin. It was launched in 1989 and is present in open chain β -hydroxy form.¹¹⁴

1.7.3.2. Lovastatin

Lovastatin (**Figure 1.23**) was isolated in 1978 from the fermentation broths of *Aspergillus terreus* and it was the first FDA approved HMG CoA reductase inhibitor. It was originally isolated as inactive lactone and hydrolyzed to active β -hydroxy acid, lovastatin acid. Lovastatin has been used for treating patients with hypercholesterolemia. It shows potent efficacy to lower total cholesterol and LDL cholesterol. The main skeleton of compactin and lovastatin is a polyketide of acetate origin.¹¹⁴⁻¹¹⁶

1.7.3.3. Simvastatin

Simvastatin (**Figure 1.23**), a semi-synthetic derivative of lovastatin, was first introduced in 1988 as an HMG CoA reductase inhibitor with a profound reduction in LDL cholesterol by 25-50% and increase in the level of HDL-cholesterol by approximately 8%. This will in turn reduce the risk of coronary heart disease by 35%. The structural difference of simvastatin from lovastatin is in the extra side chain methyl group in simvastatin.^{117,118} Mevastatin, lovastatin and simvastatin are present in the inactive lactone form and is hydrolysed to active β -hydroxy acid during digestion.

Today, statins represent the first line therapeutic interventions for dyslipidemia when the treatment with diet and exercise failed. These drugs selectively and competitively bind to and inhibit the enzyme HMG CoA reductase.¹¹⁹

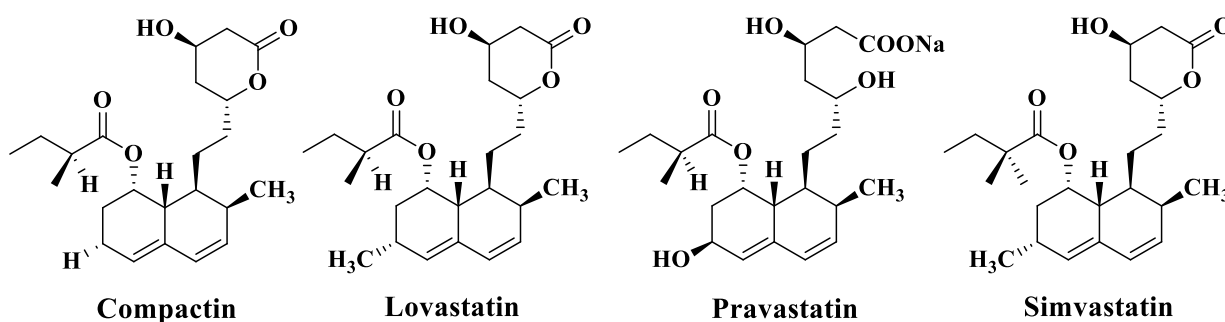


Figure 1.23. Structure of statins

1.7.4. Hypertension

Hypertension (HTN or HT), also known as high blood pressure (HBP), is a medical condition in which the blood pressure in the arteries is persistently raised to an unhealthy level. Blood pressure (BP) is the force that a person's blood exerts against the walls of blood vessels. This pressure depends on the resistance of the blood vessels and how hard the heart has to work. HT leads to severe health complications and it is responsible for around 12.8% of death annually (WHO). It is indeed a major risk factor for morbidity and mortality associated with CVD. It also damages the brain, eyes and kidneys. Treatment of hypertension includes lifestyle changes and medication. Hypertension is also called a "silent killer". It is generally a silent condition and many people won't experience any symptoms. It may take years to identify the condition, by which time it may have caused severe problems. Headache, shortness of breath, nosebleeds, flushing, dizziness, chest pain, visual changes and blood in the urine are the symptoms of high blood pressure. The persistently high BP will cause different pathological conditions such as organ (heart and kidney) failure, thrombosis events (heart attack and stroke) and eye damage.^{120,121}

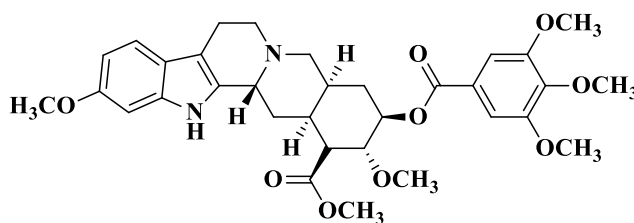
Even though many conventional antihypertensive drugs are available to manage hypertension, many of them are usually associated with various side effects. Natural products or their derivatives are the best alternatives to synthetic antihypertensive drugs with improved medicinal efficacy and reduced side effects. It is used along with the change in lifestyle and exercise. Many medicinal plants contain a boundry of phytochemicals used for hundreds of years to alleviate hypertension and related complications with minimum side effects. *Hibiscus sabdarifa*, *Allium sativum*, *Andrographis paniculata*, *Apium graveolens*, *Bidens pilosa*, *Camellia sinensis*, *Coptis chinensis*, *Coriandrum sativum*, *Crataegus spp.*, *Crocus sativus*, *Cymbopogon citrates*, *Ephedra sinica*, *Nigella sativa*, *Panax ginseng*, *Salviae miltiorrhizae*, *Salix alba*, *Zingiber officinale*, *Tribulus terrestris*, *Rauwolfia serpentina*, *Terminalia arjuna* etc., are known to possess excellent antihypertensive potential.¹²²⁻¹²⁴

1.7.4.1. Reserpine

Reserpine (**Figure 1.24**) is an indole alkaloid isolated from the roots of *Rauwolfia serpentine* (Indian snakeroot) in 1952, belonging to the *Apocyanaceae* family. It was used as a primary anti-hypertensive agent to treat mild to moderate hypertension. FDA has approved it since 1995. In India *R. serpentine* was traditionally used for snake bite, insomnia, hypochondria, insanity and as a tranquilizer. However, the compound possesses adverse effects and hence its use has declined.¹²⁵⁻¹²⁷



Rauwolfia serpentine



Reserpine

Figure 1.24

1.7.4.2. Captopril

It has been reported that some snake venoms drastically lower blood pressure. Bradykinin was reported from the venom of *Bothrops jararaca* in 1949. Bradykinin is an endogenous molecule which inhibits the angiotensin converting enzyme (ACE) through vasodilation and increase in capillary permeability. A series of bradykinin-potentiating peptides (BPPs) analogues were studied for their structure-activity relationship (SAR) and eventually one of the peptides termed as teprotide (**Figure 1.25**), emerged as a lead candidate for antihypertensive therapy.⁵¹

In addition, a large number of studies were carried out on new peptides by assaying their pharmacological activity. This led to the discovery of captopril, a small peptide molecule. Captopril (**Figure 1.25**) is the first active-site directed oral ACE inhibitor used for the treatment of hypertension and some types of congestive heart failures. It is one of the most potent competitive inhibitor. Its development became a paradigm for “rational drug design”. Captopril is isolated from the Brazilian viper *Bothrops jararaca* venom. It was

approved by FDA in the early 1980s. Nowadays, captopril and its similar compounds are extensively used as first line antihypertensive drugs. It also possesses the properties to protect post-myocardial infarction and prevent diabetic nephropathy.^{51,128-131}

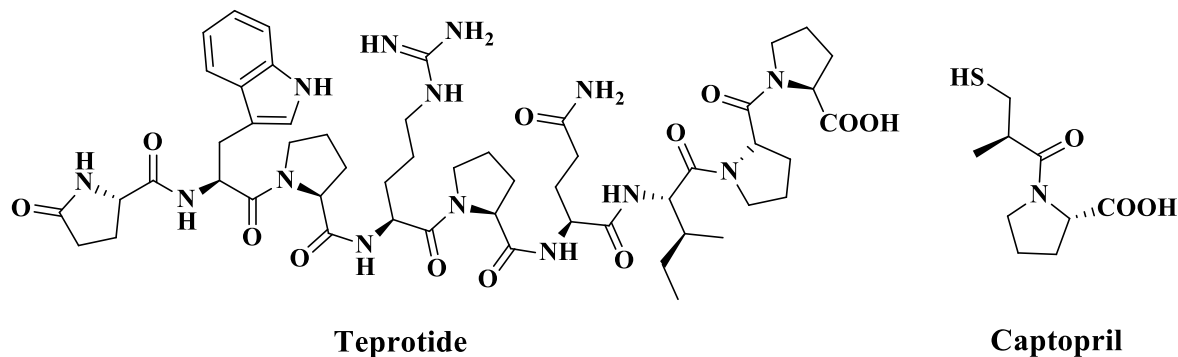


Figure 1.25

1.8. Importance of structural modifications of natural products

Natural products play a remarkable role in drug discovery due to their structural diversity, complexity and biochemical specificity. Semi-synthesis is the way of preparing novel bioactives via modification of molecules isolated from natural sources, which always stands a golden mark for drug discovery. The water solubility of natural products can be increased through structural modifications, including double bond modifications, functional group modifications etc. Even a single atom alteration can lead to a dramatical change in drug development. Nowadays, many modified natural products have been fruitfully developed for clinical applications. The examples include penicillin, morphine, artemisinin and paclitaxel. The isolation of morphine was the major breakthrough in the discovery of many semi-synthetic and synthetic compounds. Pharmacological activity and druggability are the two important criteria for drug innovation. Even though regarding the drug discovery point of view natural products possess certain disadvantages on the physio-chemical, pharmacokinetic and biopharmaceutical properties, it will play a vital role in the development of new drugs and leads. Most of the natural products contain atoms such as Carbon (C), Hydrogen (H), Oxygen (O) and are limited in Nitrogen (N) due to the poor N fixing capability of microorganisms in plants (except leguminosae plants), nitrogen is a versatile atom and having more nucleophilicity than C and O. In such scenario modifications of natural products

have great attraction via the introduction of N atom in the natural products, increasing the activity, solubility, metabolic and chemical stability. It also helps to improve pharmacokinetic parameters (ADME), removes toxicity, reduces adverse effects and improves ligand efficacy.^{132,133}

Docetaxel (**Figure 1.26**), a semi-synthetic derivative of paclitaxel, shows excellent clinical results than paclitaxel and was approved in 1994 by the FDA to treat breast cancer.¹³⁴ Synthetic modifications of natural products is a rapid method for obtaining large arrays of chemically diverse compounds and has inspired medicinal chemists as such modifications provided valuable leads in drug discovery. Mutual working between organic and medicinal chemists have paved the way for modifying natural products for industrial use through drug research and development.

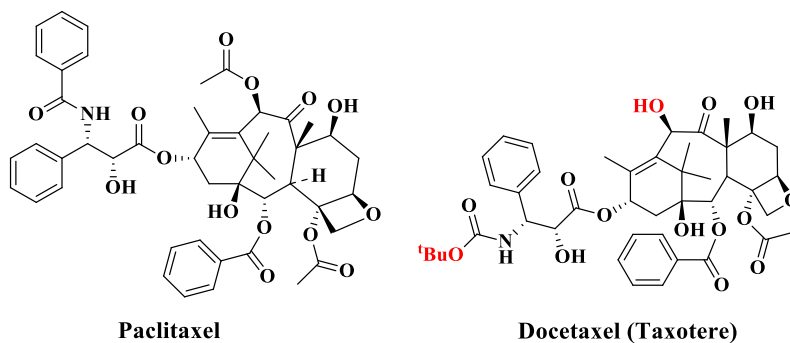


Figure 1.26

1.9. Drug discovery and development

Drug discovery is the process of developing therapeutic agents that have the potential to defend against target diseases. Such drugs need approval for use and marketing by the regulatory authorities. Drug discovery is a tedious and costly process, that takes an average of more than a decade from discovery to approval with a high failure rate, especially during phase trials. Costs are often approximately 800 million US dollars. Starting from phase I to drug marketing, the clinical failure rate is more than 90%. Depending upon the drug to be developed and the target disease, the cost and time differ. Pharmaceutical development of a drug includes the laboratory screening of approximately 5000-10,000 molecules, from which

around 250 molecules are entered into the preclinical testing and only five molecules will eventually enter into the clinical trial.

Drug discovery based on the traditional system starts with whole plant extract or concoctions without the isolation of active compounds. Historically the scientific evidence on the therapeutic efficacy of natural products have led to the development of blockbuster medications for various ailments. Drug discovery process involves the identification of drug targets. Once the target is identified and then screened against the biological system by various technology-based approaches from a library of compounds to discover a “hit”, a chemical or complex mixture with desired activity in a screening assay and whose action is confirmed upon retesting. Over many years different technological innovations have been employed to enhance the rate and efficacy of hit identification process. HTS and other methods involve screening of whole compound library against particular drug target. Hit molecules usually have the potency range of 100nM - 5 μ M at the drug target. The hits developed after the screening processes are optimized for clinical candidates. Hit-to-lead identification is a crucial phase in drug discovery and this lead identification is assisted by structure activity relationship (SAR) studies. After the lead identification, pharmaceutical parameters are evaluated for further *in vitro* and *in vivo* testing and to clarify the lead compound optimization.¹³⁵⁻¹³⁸ However, identifying robust drug from hit molecules remains a challenge that the global pharmaceutical companies have been trying to overcome for many years.

In the late 1980s, and 1990s the development of biotechnology and informatics made a revolutionary change in drug discovery in multiple ways. Clinical candidates are then subjected to different phases of clinical testing and hopefully developed to the market. Mainly four phases are associated in clinical trials and phase to phase transition is a critical milestone that may affect the overall potential of the outcome. Most of the drugs that succeeded in preclinical testing never advanced to human testing. In clinical trials many parameters are tested and many drugs are failed during these testing due to many reasons such as safety, lack of specificity, efficacy etc. Hence only a few drugs are marketed eventually.¹³⁵⁻¹³⁷

Combinatorial chemistry is a useful tool that involves the discovery of drug leads and optimization. This method is developed to reduce the time and cost associated to produce

potent new drugs. New chemical approaches and technologies are the basis for synthesizing combinatorial libraries. Combinatorial screening can be divided into two, virtual screening and experimental real screening. Virtual screening involves the use of computational methods to predict the way of interaction of particular molecule with a target protein. Real screening approaches like HTS can experimentally test the activity of thousands of compounds, providing real results. The screening of drug using small molecule libraries (compounds <500 in molecular weight) are widely used in the pharmaceutical industry. Launching a novel drug into the market is a costly process in terms of money, manpower and time, and can be made cost effective by developing new technologies.^{135,139}

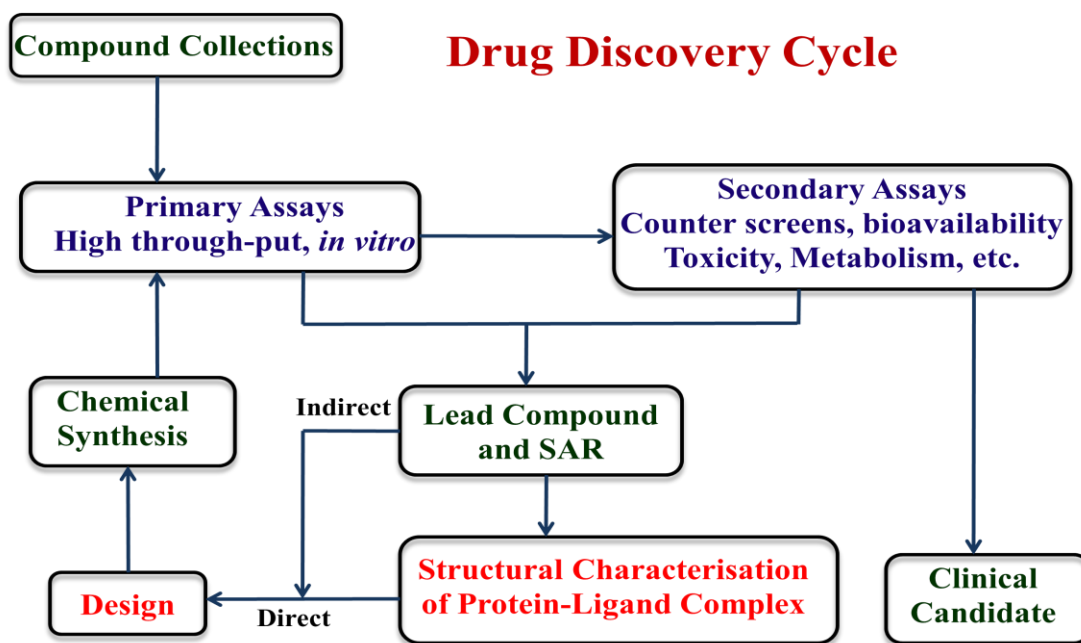


Figure 1.27. Drug discovery cycle

1.9.1. High-throughput screening (HTS)

High-throughput screening is a key strategy used in the primary stages of the drug discovery process to identify potential hits from compound libraries. It is designed to systematically screen thousands of small molecules across hundreds of selected biological targets. The prime goal of HTS is to identify defined biologically active molecules that can be developed into drug leads. In HTS screening methods, compounds are assayed (cell culture based

methods) against a variety of well characterized targets and give remarkable biological information during drug design and development. Once the compounds with the desired activities are identified, they are modified using parallel chemistry approaches to optimize their efficacy and other pharmacological properties. Ultra HTS (uHTS) is an advanced technique of HTS, which performs greater than 100,000 assays per day against one specific target. This can reduce the time required and the number of samples investigated has been greatly increased. HTS have contributed a profound role in the remarkable development of the drug discovery paradigm and thereby helps the pharmaceutical industry to produce large scale molecules at low cost.¹³⁹⁻¹⁴²

1.9.2. Computer-aided drug design (CADD)

Computer-aided drug design is based on two approaches, structure and ligand based methods. CADD plays an important role in the identification of new molecular entities and can be used prior to HTS to filter therapeutically active molecules from large libraries, thereby reducing the number of compounds to be synthesized and screened, reduce time, efforts, experimental use of animals for *in vivo* screening and associated cost. CADD helps to understand the basis of drug-receptor interactions and guides the medicinal chemist in designing new therapeutic agents. The structure-based approach, analyses the structure of biological targets and identifies active sites that are important for desired biological function. Then the computer will help in developing the molecule capable of interacting with particular biological targets. In ligand-based approaches, it analyzes the physiochemical parameters and activities of known ligands and then gives different designs of novel compounds with desired efficacy. This method is vital, especially if the information of a biological target is limited or absent. The main reason of drug withdrawals after clinical trials, around 40-60% was due to poor ADMET (absorption, distribution, metabolism, excretion and toxicity), safety and efficacy. CADD provide a significant role for pharmaceutical development, particularly in predicting 3D structure, designing of compounds with potent activity and readily synthesizable, prediction of druggability and reducing the undesirable ADMET properties. Nevertheless, the computer aided drug design needs to be integrated with experimental validation for the successful discovery and development of the drug.^{139,143-146}

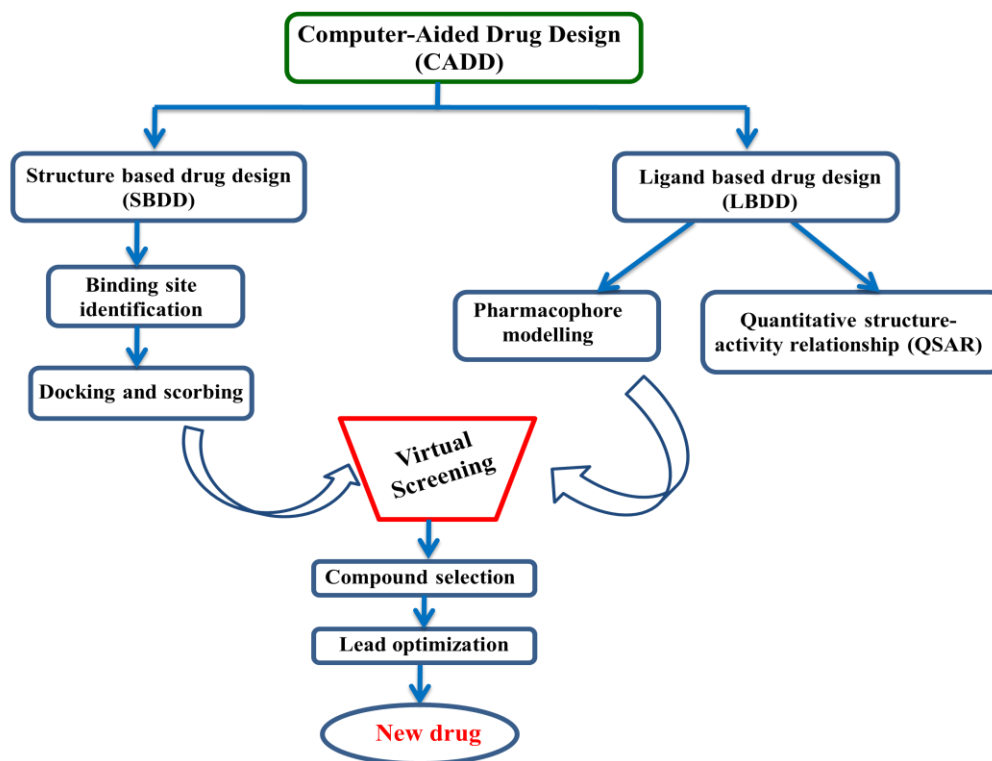


Figure 1.28. Diagrammatic representation of CADD

1.9.3. Biotherapeutics

Biological therapies account for about one third of newly marketed drugs today, making them the fastest growing sector in the global pharmaceutical market. Biological agents have the highest potential to reach the target sites that are considered as “undruggable”. Recently biotherapeutics are providing a significant role in combating cancer, diabetes and autoimmune diseases. The introduction of cellular and gene therapy products has opened the door for biologics to discover the solutions for genetic disorders, regenerative therapy and personalized medicine. Taka-diastase is the first biologic therapy used for the treatment of dyspepsia as a digestive acid and Dr. Jokichi Takamine discovered it in 1894. The discovery of insulin in 1921 from the human pancreatic extract is another excellent biological therapy. Monoclonal antibodies (mAbs) are the growing trend for biological therapies. Muromonab-CD3 (Murine antibodies) is the first approved antibodies and were launched in 1986. Nevertheless, there may be associated with several limitations including their structural complexity as well as high price. Increase in the knowledge of genetics and cell processes make substantial growth in biological therapies. In the future the novel biological

therapeutics will make a revolutionary change in medical research for developing therapeutic agents for serious diseases.^{135-137, 139,147}

1.9.4. Drug repurposing (Drug repositioning)

Despite the prodigious development of advanced technology and knowledge of human pathology, the attainability of these benefits in the development of novel drugs has always been and still slower than expected. Thus, pharmaceutical companies faces many challenges such as time consuming, high cost and high investment process due to high attrition rate to market a novel drug. In such scenario, the developments of drug repurposing of old drug have greater attention in the pharma industry. It aims to discover new uses of existing approved drugs or the molecules under clinical trial beyond the scope of the original medical indication. It is an emerging strategy to overcome certain parameters such as time, cost and attrition rate associated with other drug discovery methods.^{148,149} COVID-19 has been a pandemic situation now and needs urgent treatment. The development of new drugs for COVID-19 is a tedious, costly process and a global challenge. Drug repurposing can have a significant role in the development of drugs for COVID-19. Broad-spectrum antiviral agents (BSAAs) are identified as ‘safe-in-man’ through testing in the early stages of clinical trials and have been considered as good drug repurposing candidates. For example remdesivir (veklury), a viral RNA-dependent RNA polymerase inhibitor is currently used for mild and moderate SARS-CoV-2.^{148,150,151}

1.10. Conclusion and outline of the thesis

From the above discussions, it is apparent that natural products play an important role in developing new drugs and leads. Ancient herbal medicine and traditional knowledge provide a rich source for developing new drugs. Almost 70% of modern drugs are developed on the basis of natural resources. Approximately 100 novel drugs marketed during 1950-1970 in USA drug industry including, deserpidine, reserpine, vincristine, vinblastine etc. are plant derived. Even though most of the drugs derived from natural products are used for cancer therapy, there is a remarkable contribution towards infectious disease, metabolic disorders and associated diseases also. We have huge biodiversity and less than 10% of biodiversity has been utilized for biological activity. Therefore, many more resources have been awaiting

for the pursuit of new molecules. Owing to this, our work is focused on the isolation of various phytochemicals from selected medicinally important plants from one of the largest family *Zingiberaceae*. *Zingiberaceae* is one of the richest sources for medicinal plants. Therefore, isolation of phytochemicals from *Zingiberaceae* will provide useful insight to develop biologically active molecules. In this context, isolation of phytochemicals from selected plants are the highlights of second chapter. The isolated compounds are diterpenes and sesquiterpenes of the type. In third chapter, we have synthetically transformed one of the marker compound (*E*)-labda-8(17),12-diene-15,16-dial isolated from *C. amada*, leading to labdane appended triazole derivatives and explored its pancreatic lipase inhibition potential. Further, the semi-synthesis of (*E*)-labda-8(17),12-diene-15,16-dial to labdane-pyrroles and its anti-hyperlipidemic efficacy are the subject matter of the fourth chapter.

1.11. References

- (1) Paterson, I.; Anderson, E. A. The Renaissance of Natural Products as Drug Candidates. *Science* **2005**, *310*, 451-453.
- (2) Cragg, G. M.; Newman, D. J. Natural Products: A Continuing Source of Novel Drug Leads. *Biochim. Biophys. Acta* **2013**, *1830*, 3670-3695.
- (3) Thomford, N. E.; Senthebane, D. A.; Rowe, A.; Munro, D.; Seele, P.; Maroyi, A.; Dzobo, K. Natural Products for Drug Discovery in the 21st Century: Innovations for Novel Drug Discovery. *Int. J. Mol. Sci.* **2018**, *19*, 1-29.
- (4) La Clair, J. J. Natural Product Mode of Action (MOA) Studies: A Link between Natural and Synthetic Worlds. *Nat. Prod. Rep.* **2010**, *27*, 969-995.
- (5) Osbourn, A. E.; Lanzotti, V. *Plant-Derived Natural Products: Synthesis, Function, and Application*; Springer. **2009**, 1-588.
- (6) Dias, D. A.; Urban, S.; Roessner, U. A Historical Overview of Natural Products in Drug Discovery. *Metabolites* **2012**, *2*, 303-336.
- (7) Rates, S. M. K. Plants as Source of Drugs. *Toxicon* **2001**, *39*, 603-613.
- (8) Patridge, E.; Gareiss, P.; Kinch, M. S.; Hoyer, D. An Analysis of FDA-Approved Drugs: Natural Products and Their Derivatives. *Drug Discov. Today* **2016**, *21*, 204-207.
- (9) Baker, D. D.; Chu, M.; Oza, U.; Rajgarhia, V. The Value of Natural Products to Future

- Pharmaceutical Discovery. *Nat. Prod. Rep.* **2007**, *24*, 1225-1244.
- (10) Butler, M. S. The Role of Natural Product Chemistry in Drug Discovery. *J. Nat. Prod.* **2004**, *67*, 2141-2153.
- (11) Newman, D. J.; Cragg, G. M. Natural Products as Sources of New Drugs over the Nearly Four Decades from 01/1981 to 09/2019. *J. Nat. Prod.* **2020**, *83*, 770-803.
- (12) Butler, M. S.; Robertson, A. A. B.; Cooper, M. A. Natural Product and Natural Product Derived Drugs in Clinical Trials. *Nat. Prod. Rep.* **2014**, *31*, 1612-1661.
- (13) Mishra, B. B.; Tiwari, V. K. Natural Products: An Evolving Role in Future Drug Discovery. *Eur. J. Med. Chem.* **2011**, *46*, 4769-4807.
- (14) Kinghorn, A. D.; Pan, L.; Fletcher, J. N.; Chai, H. The Relevance of Higher Plants in Lead Compound Discovery Programs. *J. Nat. Prod.* **2011**, *74*, 1539-1555.
- (15) Renslo, A. R. Antimalarial Drug Discovery: From Quinine to the Dream of Eradication. *ACS Med. Chem. Lett.* **2013**, *4*, 1126-1128.
- (16) Liu, C. Discovery and Development of Artemisinin and Related Compounds. *Chinese Herb. Med.* **2017**, *9*, 101-114.
- (17) Bridgford, J. L.; Xie, S. C.; Cobbold, S. A.; Pasaje, C. F. A.; Herrmann, S.; Yang, T.; Gillett, D. L.; Dick, L. R.; Ralph, S. A.; Dogovski, C.; Spillman, N. J.; Tilley, L. Artemisinin Kills Malaria Parasites by Damaging Proteins and Inhibiting the Proteasome. *Nat. Commun.* **2018**, *9*, 1-9.
- (18) Klayman, D. L.; Lin, A. J.; Acton, N.; Scoviu, J. P.; Hoch, J. M.; Milhous, W. K.; Theoharides, A. D.; Dobek, A. S. Isolation of Artemisinin (Qinghaosu) From *Artemisia annua* Growing in the United States. *J. Nat. Prod.* **1984**, *47*, 715-717.
- (19) Meshnick, S. R. Artemisinin: Mechanisms of Action, Resistance and Toxicity. *Int. J. Parasitol.* **2002**, *32*, 1655-1660.
- (20) Kumar, A. Vincristine and Vinblastine: A Review. *Int. J. Med. Pharm. Sci.* **2016**, *6*, 22-30.
- (21) Silvestri, R. New Prospects for Vinblastine Analogues as Anticancer Agents. *J. Med. Chem.* **2013**, *56*, 625-627.
- (22) Cragg, G. M.; Newman, D. J. Plants as a Source of Anti-Cancer Agents. *J. Ethnopharmacol.* **2005**, *100*, 72-79.
- (23) Wani, M. C.; Taylor, H. L.; Wall, M. E.; Coggon, P.; Mcphail, A. T. Plant Antitumor

- Agents. VI. The Isolation and Structure of Taxol, a Novel Antileukemic and Antitumor Agent from *Taxus brevifolia*. *J. Am. Chem. Soc.* **1971**, *93*, 2325-2327.
- (24) Wani, M. C.; Horwitz, S. B. Nature as a Remarkable Chemist: A Personal Story of the Discovery and Development of Taxol. *Anticancer Drugs* **2014**, *25*, 482-487.
- (25) Cragg, G. M. Paclitaxel (Taxol®): A Success Story with Valuable Lessons for Natural Product Drug Discovery and Development. *Med. Res. Rev.* **1998**, *18*, 315-331.
- (26) Wiseman, L. R.; Faulds, D. Oral Pilocarpine: A Review of Its Pharmacological Properties and Clinical Potential in Xerostomia. *Drugs* **1995**, *49*, 143-155.
- (27) Zimmerman, T. J. 4. Pilocarpine. *Ophthalmology* **1981**, *88*, 85-88.
- (28) Karamanou, M.; Tsoucalas, G.; Pantos, K.; Androustos, G. Isolating Colchicine in 19th Century: An Old Drug Revisited. *Curr. Pharm. Des.* **2018**, *24*, 654-658.
- (29) Wallace, S. L. Colchicine. *Semin. Arthritis Rheum.* **1974**, *3*, 369-381.
- (30) Robinson, K. P.; Chan, J. J. Colchicine in Dermatology: A Review. *Australas. J. Dermatol.* **2018**, *59*, 278-285.
- (31) Gracheva, I. A.; Shchegravina, E. S.; Schmalz, H. G.; Beletskaya, I. P.; Fedorov, A. Y. Colchicine Alkaloids and Synthetic Analogues: Current Progress and Perspectives. *J. Med. Chem.* **2020**, *63*, 10618-10651.
- (32) Elbaz, H. A.; Stueckle, T. A.; Tse, W.; Rojanasakul, Y.; Dinu, C. Digitoxin and Its Analogs as Novel Cancer Therapeutics. *Exp. Hematol. Oncol.* **2012**, *1*, 1-10.
- (33) Haux, J. Digitoxin Is a Potential Anticancer Agent for Several Types of Cancer. *Med. Hypotheses* **1999**, *53*, 543-548.
- (34) Patocka, J.; Nepovimova, E.; Wu, W.; Kuca, K. Digoxin: Pharmacology and Toxicology-A Review. *Environ. Toxicol. Pharmacol.* **2020**, *79*, 1-6.
- (35) Hammadi, R.; Kúsz, N.; Dávid, C. Z.; Behány, Z.; Papp, L.; Kemény, L.; Hohmann, J.; Lakatos, L.; Vasas, A. Ingol and Ingenol-Type Diterpenes from *Euphorbia trigona* Miller with Keratinocyte Inhibitory Activity. *Plants* **2021**, *10*, 3-12.
- (36) Keating, G. M. Ingenol Mebutate Gel 0.015% and 0.05%: In Actinic Keratosis. *Drugs* **2012**, *72*, 2397-2405.
- (37) Gupta, C. Natural Useful Therapeutic Products from Microbes. *J. Microbiol. Exp.* **2014**, *1*, 30-37.
- (38) Amedei, A.; D'Elis, M. M. New Therapeutic Approaches by Using Microorganism-

- Derived Compounds. *Curr. Med. Chem.* **2012**, *19*, 3822-3840.
- (39) Pham, J. V.; Yilma, M. A.; Feliz, A.; Majid, M. T.; Maffetone, N.; Walker, J. R.; Kim, E.; Cho, H. J.; Reynolds, J. M.; Song, M. C.; Park, S. R.; Yoon, Y. J. A Review of the Microbial Production of Bioactive Natural Products and Biologics. *Front. Microbiol.* **2019**, *10*, 1-27.
- (40) Penesyan, A.; Kjelleberg, S.; Egan, S. Development of Novel Drugs from Marine Surface Associated Microorganism. *Mar. Drugs* **2010**, *8*, 438-459.
- (41) Newman, D. J.; Cragg, G. M.; Branch, N. P. Drugs and Drug Candidates from Marine Sources : An Assessment of the Current “ State of Play .” *Planta Med.* **2016**, *82*, 775-789.
- (42) Lindequist, U. Marine-Derived Pharmaceuticals-Challenges and Opportunities. *Biomol. Ther.* **2016**, *24*, 561-571.
- (43) Zhang, H.; Zou, J.; Yan, X.; Chen, J.; Cao, X.; Wu, J.; Liu, Y.; Wang, T. Marine-Derived Macrolides 1990- 2020 : An Overview of Chemical and Biological Diversity. *Mar. Drugs* **2021**, *19*, 1-67.
- (44) Schwartzmann, G.; Brondani, A.; Berlinck, R. G. S.; Jimeno, J. Marine Organisms as a Source of New Anticancer Agents. *Lancet oncol.* **2001**, *2*, 221-225.
- (45) Erba, E.; Bergamaschi, D.; Bassano, L.; Damia, G.; Ronzoni, S. Ecteinascidin-743 (ET-743), a Natural Marine Compound, with a Unique Mechanism of Action. *Eur. J. Cancer* **2001**, *37*, 97-105.
- (46) Le, V. H.; Inai, M.; Williams, R. M.; Kan, T. Ecteinascidins. A Review of the Chemistry, Biology and Clinical Utility of Potent Tetrahydroisoquinoline Antitumor Antibiotics. *Nat. Prod. Rep.* **2015**, *32*, 328-347.
- (47) Zambelli, V. O.; Pasqualoto, K. F. M.; Picolo, G.; Chudzinski-Tavassi, A. M.; Cury, Y. Harnessing the Knowledge of Animal Toxins to Generate Drugs. *Pharmacol. Res.* **2016**, *112*, 30-36.
- (48) Salehi, B.; Sestito, S.; Rapposelli, S.; Peron, G.; Calina, D.; Sharifi-Rad, M.; Sharopov, F.; Martins, N.; Sharifi-Rad, J. Epibatidine: A Promising Natural Alkaloid in Health. *Biomolecules* **2019**, *9*, 1-10.
- (49) Bozoghlanian, V.; Butteri, M. The Diverse and Promising World of Animal Derived Medications. *Pharos Alpha Omega Alpha Honor. Med. Soc.* **2015**, *78*, 16-22.

- (50) Mamelak, A. N.; Jacoby, D. B. Targeted Delivery of Antitumoral Therapy to Glioma and Other Malignancies with Synthetic Chlorotoxin (TM-601). *Expert Opin. Drug Deliv.* **2007**, *4*, 175-186.
- (51) Koh, C. Y.; Kini, R. M. From Snake Venom Toxins to Therapeutics-Cardiovascular Examples. *Toxicon* **2012**, *59*, 497-506.
- (52) Heindel, J. J.; Blumberg, B.; Cave, M.; Machtinger, R.; Mantovani, A.; Mendez, M. A.; Nadal, A.; Palanza, P.; Panzica, G.; Sargis, R.; Vandenberg, L. N.; vom Saal, F. Metabolism Disrupting Chemicals and Metabolic Disorders. *Reprod. Toxicol.* **2017**, *68*, 3-33.
- (53) Fenichel, G. M. Metabolic Disorders. *Neonatal Neurol.* **2007**, *15*, 143-165.
- (54) Scotti, L.; Scotti, M. T. Multi-Target Drugs Against Metabolic Disorders. *Endocrine, Metab. Immune Disord. Drug Targets* **2019**, *19*, 389-390.
- (55) Balaji, M.; Ganjayi, M. S.; Hanuma Kumar, G. E. N.; Parim, B. N.; Mopuri, R.; Dasari, S. A Review on Possible Therapeutic Targets to Contain Obesity: The Role of Phytochemicals. *Obes. Res. Clin. Pract.* **2016**, *10*, 363-380.
- (56) Landrier, J. F.; Derghal, A.; Mounien, L. MicroRNAs in Obesity and Related Metabolic Disorders. *Cells* **2019**, *8*, 1-13.
- (57) Donahue, R. P.; Bloom, E.; Abbott, R. D.; Reed, D.; Yano, K. Central Obesity and Coronary Heart Disease in Men. *Lancet* **1987**, *329*, 821-824.
- (58) Alonso, M.; Serrano, A.; Vida, M.; Crespillo, A.; Hernandez-Folgado, L.; Jagerovic, N.; Goya, P.; Reyes-Cabello, C.; Perez-Valero, V.; Decara, J.; Macías-González, M.; Bermúdez-Silva, F. J.; Suárez, J.; Rodríguez De Fonseca, F.; Pavón, F. J. Anti-Obesity Efficacy of LH-21, a Cannabinoid CB 1 Receptor Antagonist with Poor Brain Penetration, in Diet-Induced Obese Rats. *Br. J. Pharmacol.* **2012**, *165*, 2274-2291.
- (59) <https://www.who.int/news-room/fact-sheets/detail/obesity-and-overweight>
- (60) Fu, C.; Jiang, Y.; Guo, J.; Su, Z. Natural Products with Anti-obesity Effects and Different Mechanisms of Action. *J. Agric. Food Chem.* **2016**, *64*, 9571-9585.
- (61) Cosentino, G.; Conrad, A. O.; Uwaifo, G. I. Phentermine and Topiramate for the Management of Obesity: A Review. *Drug Des. Devel. Ther.* **2013**, *7*, 267-278.
- (62) Cardullo, N.; Muccilli, V.; Pulvirenti, L.; Tringali, C. Natural Isoflavones and Semisynthetic Derivatives as Pancreatic Lipase Inhibitors. *J. Nat. Prod.* **2021**, *84*, 654-

- 665.
- (63) Padwal, R. S.; Majumdar, S. R. Drug Treatments for Obesity: Orlistat, Sibutramine, and Rimonabant. *Lancet* **2007**, *369*, 71-77.
- (64) Arya, A.; Nahar, L.; Khan, H. U.; Sarker, S. D. *Anti-Obesity Natural Products*, 1st ed.; Elsevier Inc., Annual Reports in Medicinal Chemistry **2020**, *55*, 1-23.
- (65) Birari, R. B.; Bhutani, K. K. Pancreatic Lipase Inhibitors from Natural Sources: Unexplored Potential. *Drug Discov. Today* **2007**, *12*, 879-889.
- (66) Wu, Y.; Ding, Y.; Tanaka, Y.; Zhang, W. Risk Factors Contributing to Type 2 Diabetes and Recent Advances in the Treatment and Prevention. *Int. J. Med. Sci.* **2014**, *11*, 1185-1200.
- (67) Scherthaner, G.; Scherthaner, G. H. The Right Place for Metformin Today. *Diabetes Res. Clin. Pract.* **2020**, *159*, 1-23.
- (68) Nanjan, M. J.; Mohammed, M.; Prashantha Kumar, B. R.; Chandrasekar, M. J. N. Thiazolidinediones as Antidiabetic Agents: A Critical Review. *Bioorg. Chem.* **2018**, *77*, 548-567.
- (69) Kaul, K.; Tarr, J. M.; Ahmad, S.; Kohner, E. M.; Chibber, R. Chapter 1 Introduction To Diabetes Mellitus. *Diabetes An Old Dis. a New Insight* **2012**, 1-11.
- (70) Lima, A. L.; Illing, T.; Schliemann, S.; Elsner, P. Cutaneous Manifestations of Diabetes Mellitus: A Review. *Am. J. Clin. Dermatol.* **2017**, *18*, 541-553.
- (71) Palanisamy, S.; Yien, E.; Shi, L.; Si, L.; Qi, S.; Ling, L.; Lun, T.; Chen, Y. Systematic Review of Efficacy and Safety of Newer Antidiabetic Drugs Approved from 2013 to 2017 in Controlling HbA1c in Diabetes Patients. *Pharmacy* **2018**, *6*, 1-24.
- (72) Saeedi, P.; Petersohn, I.; Salpea, P.; Malanda, B.; Karuranga, S.; Unwin, N.; Colagiuri, S.; Guariguata, L.; Motala, A. A.; Ogurtsova, K.; Shaw, J. E.; Bright, D.; Williams, R. Global and Regional Diabetes Prevalence Estimates for 2019 and Projections for 2030 and 2045: Results from the International Diabetes Federation Diabetes Atlas, 9th Edition. *Diabetes Res. Clin. Pract.* **2019**, *157*, 107843-107852.
- (73) <https://www.who.int/health-topics/diabetes#tab=tab-1>
- (74) Chang, W.; Chen, L.; Hatch, G. M. Berberine as a Therapy for Type 2 Diabetes and Its Complications: From Mechanism of Action to Clinical Studies1. *Biochem. Cell Biol.* **2015**, *93*, 479-486.

- (75) Li, S.; Qin, C.; Cui, S.; Xu, H.; Wu, F.; Wang, J.; Su, M.; Fang, X.; Li, D.; Jiao, Q.; Zhang, M.; Xia, C.; Zhu, L.; Wang, R.; Li, J.; Jiang, H.; Zhao, Z.; Li, J.; Li, H. Discovery of a Natural-Product-Derived Preclinical Candidate for Once-Weekly Treatment of Type 2 Diabetes. *J. Med. Chem.* **2019**, *62*, 2348-2361.
- (76) Xu, L.; Li, Y.; Dai, Y.; Peng, J. Natural Products for the Treatment of Type 2 Diabetes Mellitus: Pharmacology and Mechanisms. *Pharmacol. Res.* **2018**, *130*, 451-465.
- (77) Waltenberger, B.; Mocan, A.; Šmejkal, K.; Heiss, E. H.; Atanasov, A. G. Natural Products to Counteract the Epidemic of Cardiovascular and Metabolic Disorders. *Molecules* **2016**, *21*, 1-24.
- (78) Hung, H. Y.; Qian, K.; Morris-Natschke, S. L.; Hsu, C. S.; Lee, K. H. Recent Discovery of Plant-Derived Anti-diabetic Natural Products. *Nat. Prod. Rep.* **2012**, *29*, 580-606.
- (79) Osadebe, P.; Odoh, E.; Uzor, P. Natural Products as Potential Sources of Antidiabetic Drugs. *Br. J. Pharm. Res.* **2014**, *4*, 2075-2095.
- (80) Bailey, C. J. Metformin: Historical Overview. *Diabetologia* **2017**, *60*, 1566-1576.
- (81) Marita, A. R.; Patade, G. Metformin: A Journey from Countryside to the Bedside. *J. Obes. Metab. Res.* **2014**, *1*, 127-130.
- (82) Wang, H.; Zhu, C.; Ying, Y.; Luo, L.; Huang, D.; Luo, Z. Metformin and Berberine, Two Versatile Drugs in Treatment of Common Metabolic Diseases. *Oncotarget* **2018**, *9*, 10135-10146.
- (83) Yin, J.; Xing, H.; Ye, J. Efficacy of Berberine in Patients with Type 2 Diabetes Mellitus. *Metabolism.* **2008**, *57*, 712-717.
- (84) Yin, J.; Ye, J.; Jia, W. Effects and Mechanisms of Berberine in Diabetes Treatment. *Acta Pharm. Sin. B* **2012**, *2*, 327-334.
- (85) Imenshahidi, M.; Hosseinzadeh, H. Berberine and Barberry (*Berberis vulgaris*): A Clinical Review. *Phytother. Res.* **2019**, *33*, 504-523.
- (86) Wang, K.; Feng, X.; Chai, L.; Cao, S.; Qiu, F. The Metabolism of Berberine and Its Contribution to the Pharmacological Effects. *Drug Metab. Rev.* **2017**, *49*, 139-157.
- (87) Warowicka, A.; Nawrot, R.; Goździcka-Józefiak, A. Antiviral Activity of Berberine. *Arch. Virol.* **2020**, *165*, 1935-1945.
- (88) Chin, Y.-W.; Balunas, M. J.; Chai, H. B.; Kinghorn, A. D. Drug Discovery from

- Natural Sources. *AAPS J.* **2006**, *8*, 239-253.
- (89) Nikfar, S.; Abdollahi, M.; Salari, P. The Efficacy and Tolerability of Exenatide in Comparison to Placebo; a Systematic Review and Meta-Analysis of Randomized Clinical Trials. *J. Pharm. Pharm. Sci.* **2011**, *15*, 1-30.
- (90) Chiasson, J. L.; Josse, R. G.; Gomis, R.; Hanefeld, M.; Karasik, A.; Laakso, M. Acarbose for Prevention of Type 2 Diabetes Mellitus: The STOP-NIDDM Randomised Trial. *Lancet* **2002**, *359*, 2072-2077.
- (91) Hanefeld, M.; Schaper, F. Acarbose: Oral Antidiabetes Drug with Additional Cardiovascular Benefits. *Expert Rev. Cardiovasc. Ther.* **2008**, *6*, 153-163.
- (92) Sugimoto, S.; Nakajima, H.; Kosaka, K.; Hosoi, H. Review: Miglitol Has Potential as a Therapeutic Drug against Obesity. *Nutr. Metab.* **2015**, *12*, 1-7.
- (93) Scott, L. J.; Spencer, C. M. Miglitol: A Review of Its Therapeutic Potential in Type 2 Diabetes Mellitus. *Drugs* **2000**, *59*, 521-549.
- (94) Dabhi, A. S.; Bhatt, N. R.; Shah, M. J. Voglibose: An Alpha Glucosidase Inhibitor. *J. Clin. Diagnostic Res.* **2013**, *7*, 3023-3027.
- (95) Chen, X.; Zheng, Y.; Shen, Y. Voglibose (Basen[®] , AO-128), One of the Most Important α -Glucosidase Inhibitors. *Curr. Med. Chem.* **2006**, *13*, 109-116.
- (96) Ehrenkranz, J. R. L.; Lewis, N. G.; Kahn, C. R.; Roth, J. Phlorizin: A Review. *Diabetes. Metab. Res. Rev.* **2005**, *21*, 31-38.
- (97) Chao, E. C.; Henry, R. R. SGLT2 Inhibition-A Novel Strategy for Diabetes Treatment. *Nat. Rev. Drug Discov.* **2010**, *9*, 551-559.
- (98) Anderson, S. L. Dapagliflozin Efficacy and Safety: A Perspective Review. *Ther. Adv. Drug Saf.* **2014**, *5*, 242-254.
- (99) Vivian, E. M. Dapagliflozin: A New Sodium-Glucose Cotransporter 2 Inhibitor for Treatment of Type 2 Diabetes. *Am. J. Heal. Pharm.* **2015**, *72*, 361-372.
- (100) Tahrani, A. A.; Barnett, A. H.; Bailey, C. J. SGLT Inhibitors in Management of Diabetes. *Lancet Diabetes Endocrinol.* **2013**, *1*, 140-151.
- (101) Beitelshes, A. L.; Leslie, B. R.; Taylor, S. I. Sodium-Glucose Cotransporter 2 Inhibitors : A Case Study in Translational Research. *Diabetes* **2019**, *68*, 1109-1120.
- (102) Fala, L. Jardiance (Empagliflozin), an SGLT2 Inhibitor, Receives FDA Approval for the Treatment of Patients with Type 2 Diabetes. *Am. Heal. drug benefits* **2015**, *8*, 92-

- 95.
- (103) Poole, R. M.; Dunto, R. T. Ipragliflozin: First Global Approval. *Drugs* **2014**, *74*, 611-617.
- (104) Markham, A.; Elkinson, S. Luseogliflozin: First Global Approval. *Drugs* **2014**, *74*, 945-950.
- (105) Wang, Y.; Lou, Y.; Wang, J.; Li, D.; Chen, H.; Zheng, T.; Xia, C.; Song, X.; Dong, T.; Li, J.; Li, J.; Liu, H. Design, Synthesis and Biological Evaluation of 6-Deoxy O-Spiroketal C-Arylglucosides as Novel Renal Sodium-Dependent Glucose Cotransporter 2 (SGLT2) Inhibitors for the Treatment of Type 2 Diabetes. *Eur. J. Med. Chem.* **2019**, *180*, 398-416.
- (106) Younossi, Z. M.; Koenig, A. B.; Abdelatif, D.; Fazel, Y.; Henry, L.; Wymer, M. Global Epidemiology of Non-alcoholic Fatty Liver Disease - Meta-analytic Assessment of Prevalence, Incidence, and Outcomes. *Hepatology* **2016**, *64*, 73-84.
- (107) Zhou, J.; Zhou, F.; Wang, W.; Zhang, X. J.; Ji, Y. X.; Zhang, P.; She, Z. G.; Zhu, L.; Cai, J.; Li, H. Epidemiological Features of NAFLD From 1999 to 2018 in China. *Hepatology* **2020**, *71*, 1851-1864.
- (108) Endo, A. A Historical Perspective on the Discovery of Statins. *Proc. Japan Acad. Ser. B Phys. Biol. Sci.* **2010**, *86*, 484-493.
- (109) Chakravarti, R.; Sahai, V. Compactin - A Review. *Appl. Microbiol. Biotechnol.* **2004**, *64*, 618-624.
- (110) Lamb, Y. N. Rosuvastatin/Ezetimibe: A Review in Hypercholesterolemia. *Am. J. Cardiovasc. Drugs* **2020**, *20*, 381-392.
- (111) Endo, A., Compactin (ML-236B) and related compounds as potential cholesterol-lowering agents that inhibit HMG-CoA reductase. *J. Med. Chem.* **1985**, *28*, 401-405.
- (112) Toth, P. P.; Banach, M. Statins: Then and Now. *Methodist Debaquey Cardiovasc. J.* **2019**, *15*, 23-31.
- (113) Endo, A. The Origin of the Statins. *Int. Congr. Ser.* **2004**, *1262*, 3-8.
- (114) Tobert, J. A. Lovastatin and beyond: The History of the HMG-CoA Reductase Inhibitors. *Nat. Rev. Drug Discov.* **2003**, *2*, 517-526.
- (115) Curran, M. P.; Goa, K. L. Lovastatin Extended Release. *Drugs* **2003**, *63*, 685-699.
- (116) Zeller, F. P.; Uvodich, K. C. Lovastatin for Hypercholesterolemia. *Drug Intell. Clin.*

- Pharm.* **1988**, 22, 542-545.
- (117) Pedersen, T. R.; Tobert, J. A. Simvastatin: A Review. *Expert Opin. Pharmacother.* **2004**, 5, 2583-2596.
- (118) Robinson, J. G. Simvastatin: Present and Future Perspectives. *Expert Opin. Pharmacother.* **2007**, 8, 2159-2172.
- (119) Rodrigues, T.; Reker, D.; Schneider, P.; Schneider, G. Counting on Natural Products for Drug Design. *Nat. Chem.* **2016**, 8, 531-541.
- (120) Kalehoff, J. P.; Oparil, S. The Story of the Silent Killer. *Current Hypertension Reports* **2020**, 22, 1-14.
- (121) O'Shea, P. M.; Griffin, T. P.; Fitzgibbon, M. Hypertension: The Role of Biochemistry in the diagnosis and Management *Clin. Chim. Acta* **2016**, 465, 131-143.
- (122) Verma, T.; Sinha, M.; Bansal, N.; Yadav, S. R.; Shah, K.; Chauhan, N. S. Plants Used as Antihypertensive. *Nat. Products Bioprospect.* **2021**, 11, 155-184.
- (123) Al Disi, S. S.; Anwar, M. A.; Eid, A. H. Anti-hypertensive Herbs and Their Mechanisms of Action: Part I. *Front. Pharmacol.* **2016**, 6, 1-24.
- (124) Kim, D. W.; Yokozawa, T.; Hattori, M.; Kadota, S.; Namba, T. Effects of Aqueous Extracts of Apocynum Venetum Leaves on Spontaneously Hypertensive, Renal Hypertensive and NaCl-Fed-Hypertensive Rats. *J. Ethnopharmacol.* **2000**, 72, 53-59.
- (125) Peri, R.; Mangipudy, R. S. Reserpine. *Encycl. Toxicol. Third Ed.* **2014**, 3, 94-96.
- (126) Glynn, J. D. *Rauwolfia serpentina* (Serpasil) in Psychiatry. *J. Neurol. Neurosurg. Psychiatry* **1955**, 18, 225-227.
- (127) Gawade, B.; Fegade, S. Rauwolfia (Reserpine) as a Potential Antihypertensive Agent: A Review. *Int. J. Pharma. Phytopharm. Res.* **2012**, 2, 46-49.
- (128) Erdös, E. G. The Discovery of Captopril: Reply. *FASEB J.* **2004**, 18, 788-789.
- (129) Narender, T. Recent Advances in the Natural Products Drug Discovery. *J. Pharmacogn. ISSN* **2012**, 3, 108-112.
- (130) Ferreira, S. H.; Bartelt, D. C.; Greene, L. J. Isolation of Bradykinin-Potentiating Peptides From *Bothrops jararaca* venom. *Biochemistry* **1970**, 9, 2583-2593.
- (131) Cushman, D. W.; Ondetti, M. A. History of the Design of Captopril and Related Inhibitors of Angiotensin Converting Enzyme. *Hypertension* **1991**, 17, 589-592.
- (132) Guo, Z. The Modification of Natural Products for Medical Use. *Acta Pharm. Sin. B*

- 2017**, 7, 119-136.
- (133) Yao, H.; Liu, J.; Xu, S.; Zhu, Z.; Xu, J. The Structural Modification of Natural Products for Novel Drug Discovery. *Expert Opin. Drug Discov.* **2017**, 12, 121-140.
- (134) Safavy, A.; Raisch, K. P.; Khazaeli, M. B.; Buchsbaum, D. J.; Bonner, J. A. Paclitaxel Derivatives for Targeted Therapy of Cancer: Toward the Development of Smart Taxanes. *J. Med. Chem.* **1999**, 42, 4919-4924.
- (135) Salazar, D. E.; Gormley, G. Modern Drug Discovery and Development. *Clin. Transl. Sci.* **2017**, 26, 719-743.
- (136) Goodnow, R. A. Hit and Lead Identification: Integrated Technology-Based Approaches. *Drug Discov. Today Technol.* **2006**, 3, 367-375.
- (137) Hughes, J. P.; Rees, S. S.; Kalindjian, S. B.; Philpott, K. L. Principles of Early Drug Discovery. *Br. J. Pharmacol.* **2011**, 162, 1239-1249.
- (138) Cai, C.; Wang, S.; Xu, Y.; Zhang, W.; Tang, K.; Ouyang, Q.; Lai, L.; Pei, J. Transfer Learning for Drug Discovery. *J. Med. Chem.* **2020**, 63, 8683-8694.
- (139) Berdigaliyev, N.; Aljofan, M. An Overview of Drug Discovery and Development. *Future Med. Chem.* **2020**, 12, 939-947.
- (140) Entzeroth, M.; Flotow, H.; Condron, P. Overview of High-Throughput Screening. *Curr. Protoc. Pharmacol.* **2009**, 44, 1-27.
- (141) Shinn, P.; Chen, L.; Ferrer, M.; Itkin, Z.; Klumpp-Thomas, C.; McKnight, C.; Michael, S.; Mierzwa, T.; Thomas, C.; Wilson, K.; Guha, R. High-Throughput Screening for Drug Combinations. *Methods Mol. Biol.* **2019**, 1939, 11-35.
- (142) Borrel, A.; Huang, R.; Sakamuru, S.; Xia, M.; Simeonov, A.; Mansouri, K.; Houck, K. A.; Judson, R. S.; Kleinstreuer, N. C. High-Throughput Screening to Predict Chemical-Assay Interference. *Sci. Rep.* **2020**, 10, 1-20.
- (143) Macalino, S. J. Y.; Gosu, V.; Hong, S.; Choi, S. Role of Computer-Aided Drug Design in Modern Drug Discovery. *Arch. Pharm. Res.* **2015**, 38, 1686-1701.
- (144) Song, C. M.; Lim, S. J.; Tong, J. C. Recent Advances in Computer-Aided Drug Design. *Brief. Bioinform.* **2009**, 10, 579-591.
- (145) Veselovsky, A. V.; Ivanov, A. S. Strategy of Computer-Aided Drug Design. *Curr. Drug Targets - Infect. Disord.* **2003**, 3, 33-40.
- (146) Yu, W.; Mackerell, A. D. Computer-Aided Drug Design Methods. *Methods Mol. Biol.*

- 2017**, *1520*, 85-106.
- (147) Andrews, L.; Ralston, S.; Blomme, E.; Barnhart, K. A Snapshot of Biologic Drug Development: Challenges and Opportunities. *Hum. Exp. Toxicol.* **2015**, *34*, 1279-1285.
- (148) Pushpakom, S.; Iorio, F.; Eyers, P. A.; Escott, K. J.; Hopper, S.; Wells, A.; Doig, A.; Williams, T.; Latimer, J.; McNamee, C.; Norris, A.; Sanseau, P.; Cavalla, D.; Pirmohamed, M. Drug Repurposing: Progress, Challenges and Recommendations. *Nature Reviews Drug Discovery* **2018**, *18*, 41-58.
- (149) Ko, Y. Computational Drug Repositioning: Current Progress and Challenges. *Applied Sciences* **2020**, *10*, 1-10.
- (150) Ashburn, T. T.; Thor, K. B. Drug Repositioning: Identifying and Developing New Uses for Existing Drugs. *Nat. Rev. Drug Discov.* **2004**, *3*, 673-683.
- (151) Breckenridge, A.; Jacob, R. Overcoming the Legal and Regulatory Barriers to Drug Repurposing. *Nat. Rev. Drug Discov.* **2018**, *18*, 1-2.

Isolation of Bioactives from Selected Medicinally Important Plants from *Zingiberaceae* Family and their Biological Evaluations

2.1. Abstract

The family *Zingiberaceae* provides a large repository of medicinal plants. In this chapter, we have selected three plants namely *Curcuma amada*, *Curcuma malabarica* and *Curcuma aromatica* from the *Zingiberaceae* family. Fifteen compounds were isolated and characterized from these plant species. Some of the phytochemicals are reported for the first time from these plants. Traditionally these plants are utilized in the treatment of skin diseases, inflammation, diabetes, obesity and other related metabolic disorders. Inhibition of pancreatic lipase activity is considered as an active therapy to control obesity. Thus, isolated compounds were evaluated for anti-obesity properties via inhibition of pancreatic lipase. From the pancreatic lipase inhibition studies, we found that coronarin D and zerumin A show better activity.

2.2. Introduction

Medicinal plants play a major role in traditional health care systems as well as in the pharmaceutical industry. Naturally occurring compounds have played a remarkable role in drug discovery for combating various human ailments.¹ The current knowledge of the usage of medicinal plants for various ailments is a result of years of struggle between man and illness, which led to the pursuit of drugs from different parts of plants. By experience, people have identified the therapeutic potency of medicinal plants for various illnesses and conveyed their knowledge to successive generations. The oldest written documents of medicinal plant usage in drug formulation have been found on approximately 5000 years old Sumerian clay slab from Nagpur. Indian holy books 'Vedas' mention the importance of plants for various treatments. Various indigenous systems such as Ayurveda, Siddha and Unani use many plant species to treat various illnesses. India is a large repository of medicinal plants. The therapeutic importance of plants lies in some phytoconstituents that produce a particular physiological action on the human body. The high cost and severe side effects associated

with many synthetic drugs also make the usage of natural products derived drugs interesting again.²⁻⁴

2.3. *Zingiberaceae* family

The family *Zingiberaceae* or the ginger family is a family of flowering plants and is well known for its medicinal and nutritional properties. It is widely distributed throughout the tropical and subtropical areas, particularly of Asia, Africa, America and in particular India and in Southeast Asia. It is one of the largest families of the plant kingdom. *Zingiberaceae* comprises 53 genera and more than 1600 species. India is one of the richest and diverse regions for *Zingiberaceae*, having 20 genera and around 200 species. The members belonging to *Zingiberaceae* are annual or perennial rhizomatous herbs.^{5,6} The systematic position of *Zingiberaceae* family is as follows

Kingdom	:	Plantae
Sub-kingdom	:	Phanerogamae
Division	:	Spermatophyta
Subdivision	:	Angiospermae
Class	:	Monocotyledonae
Series	:	Epigynae
Order	:	<i>Zingiberales</i>
Family	:	<i>Zingiberaceae</i>
Genus	:	<i>Curcuma</i>

The rhizomes of different species are variously coloured pale yellow, deep yellow, greenish blue, pink or a combination of these colours. Leaves are distichous and exhibit morphological differences in structure, size, shape, texture and venation.⁶ *Zingiberaceae* family is well known for its ethnomedicine value and it consists of large number of medicinal plants. It provides many useful products for food, spices, dyes, perfumes, cosmetics, medicine etc. and is a rich source of medicinal products. Medicinally important genera which belongs to *Zingiberaceae* are *Alpinia*, *Amomum*, *Curcuma*, *Elettaria*, *Hedychium*, *Kaempferia*, *Zingiber* and *Costus*. Some of the important genera with potential as medicinal and aromatic plants are listed below⁵ (**Table 2.1**).

Table 2.1. List of prominent genus in *Zingiberaceae* family with important medicinal plants

<i>Genus</i>	<i>Species</i>
<i>Curcuma</i>	: <i>C. amada, C. longa, C. zedoaria, C. aromatica</i>
<i>Kaempferia</i>	: <i>K. rotunda, K. galangal, K. pulchra</i>
<i>Hedychium</i>	: <i>H. spicatum, H. coronarium</i>
<i>Amomum</i>	: <i>A. subulatum</i>
<i>Zingiber</i>	: <i>Z. officinale, Z. zerumbet</i>
<i>Alpinia</i>	: <i>A. galanga, A. calcarata, A. allughas</i>
<i>Elettaria</i>	: <i>E. cardamomum</i>
<i>Costus</i>	: <i>C. speciosus</i>
<i>Gastrochilus</i>	: <i>G. pandurata</i>

There are several species from *Zingiberaceae* that have been reported to possess nutraceutical and medicinal activity. The plants belonging to this family are rich sources of volatile oils and oleoresins of export quality. The most important species are *Curcuma longa* and *Zingiber officinale*. *Curcuma longa* and *Zingiber officinale* has been used for many years as spices and in various traditional medicines.

C. longa rhizomes (turmeric) is an important constituent of curry powder and it gives colour and taste to food preparations. This spice has been used in Ayurveda and folk medicine for the treatment of various ailments as gynecological problems, gastric problems, infectious diseases, hepatic and blood disorders. Later modern science has scientifically validated the use of turmeric against such diseases. Curcumin is one of the active ingredients in turmeric. Curcumin is reported to have anti-inflammatory, anti-oxidant and anticancer potential. Many clinical studies have shown that turmeric exhibited potency against various human ailments including lupus nephritis, diabetes, irritable bowel syndrome, acne, cancer, fibrosis etc.⁷⁻⁹ The turmeric oil exhibits anti-bacterial and anti-fungal activity.^{10,11}

Ginger, the rhizomes of *Z. officinale* has a long history of its medicinal applications. Gingerol is the major constituents present in the essential oil and contributes the unique flavor and medicinal properties. Ginger is used as a carminative and digestive stimulant. It has a great demand in the kitchen, used as an ingredient in curries, cookies and pickles. Its preparations are used to alleviate cough and cold. Ginger is reported to possess anti-

inflammatory, anti-oxidant and anti-cancer potentials. It is also used in the treatment of stomach upset, diarrhoea and nausea.^{9,12,13}

In this regard our focus is on the phytochemical investigation and biological evaluations of plants from the genus *Curcuma*. A brief introduction about the genus *Curcuma* is given below.

2.4. The genus *Curcuma* L.

The genus curcuma belongs to the family *Zingiberaceae*. The genus consists of more than 120 species of perennial rhizomatous herbs native to tropical and sub-tropical regions in Asia, Australia and South America. It has been greatly valued for their immense therapeutic properties and also used as spices, perfumes, cosmetics, ornamental plants, flavoring and coloring agents. The genus was first identified by Carl Linnaeus in 1753. The word ‘curcuma’ is derived from the Arabic word “kurkum” which meant “saffron”, while now it is used for turmeric only. Many species from the genus curcuma are widely distributed in India, Pakistan, Indonesia, Malaysia, Bangladesh, Nepal and Thailand. Even though, more than 700 compounds have been isolated from this genus, only a few compounds are explored in detail. Curcumin is the most explored compound in this genus, which is mainly distributed in *C. longa*.¹⁴⁻¹⁶

It has been extensively used in traditional medicine for hundreds of years and it is reported to possess anti-inflammatory, anticancer, antiproliferative, gastrointestinal, hypoglycemic, anti-hyperlipidemic, neuroprotective, hepatoprotective, diuretic, carminative, hypotensive, antioxidant, insecticidal, antimicrobial, antiviral, anti-rheumatic and antivenomous properties. The biological potential of this genus is due to the presence of non-volatile curcuminoids and volatile terpenoids. Curcuma essential oils have exhibited a wide variety of pharmacological properties. *C. longa* is the most studied and medicinally relevant plant in the genus of curcuma. India is the world’s richest producer of commercially most important species. *C. longa*, *C. xanthorrhiza* and *C. zedoaria* are the most investigated species in this genus. Owing to this medicinal importance, the genus *curcuma* is a potential source for novel lead identification and drug discovery.^{15,17}

From the above discussion, it is clear that the genus *Curcuma* is an important genus in the *Zingiberaceae* family. Many plant species from the genus *Curcuma* are well known for

their nutraceutical and medicinal pertinence. Also from the literature, we found that the few species belonging to the *Curcuma* is not much explored for their pharmaceutical potential especially against metabolic disorders. Therefore, we have selected *Curcuma amada*, *Curcuma malabarica* and *Curcuma aromatica* from *Zingiberaceae*, which provide more scope to the isolation of bioactives and its biological studies.

2.5. A brief review on different plant species under present study

2.5.1. *Curcuma amada* Roxb.

Taxonomic position of the species *Curcuma amada* is as follows

Order	:	Zingiberales
Family	:	<i>Zingiberaceae</i>
Genus	:	<i>Curcuma</i>
Species	:	<i>C. amada</i> Roxb

Curcuma amada is a rhizomatous aromatic herb with a leafy tuft and 60-90 cm in height. The leaves are long and petiolate. Flowers are white or pale yellow in colour and arranged in spikes in the center of the tuft of the leaves and it is available from November to April. It has a morphological and phylogenic resemblance with ginger (*Zingiber officinale*) and commonly known as mango ginger because its rhizomes have characteristic aroma to raw mango (*Mangifera indica*). The presence of the volatile compounds, 3-carene, myrcene, β -ocimene and α -pinene are responsible for its characteristic aroma. Consequently, it has been used as a flavoring spice in dishes, candy, sauce, making pickles and salads.



Figure 2.1. *C. amada* plant and rhizomes

The rhizomes are rich in essential oil and more than 130 phytochemicals with diverse biological significance have been reported.¹⁸ It has a long history in folk medicine. In Ayurveda and Unani, it has been used as stomachic, appetizer, carminative, digestive, diuretic, in vitiated conditions of pitta, anorexia, dyspepsia, healing wounds, chronic ulcers, skin diseases, fever, constipation, cough, bronchitis, inflammation etc.¹⁵ Various solvent extracts and pure compounds from mango ginger provides antimicrobial, antifungal, hypotriglyceridemic, hypoglycemic, anthelmintic, antioxidant, anti-inflammatory, inhibition of platelet aggregation, cytotoxicity activities, CNS depressant and analgesic activities.¹⁹⁻²³ The compound zederone isolated from the methanol extract of *C. amada* is shown to exhibit excellent analgesic activity.²⁴ The important volatile constituents present in the essential oil of *C. amada* are given below (**Figure 2.2**).²⁵

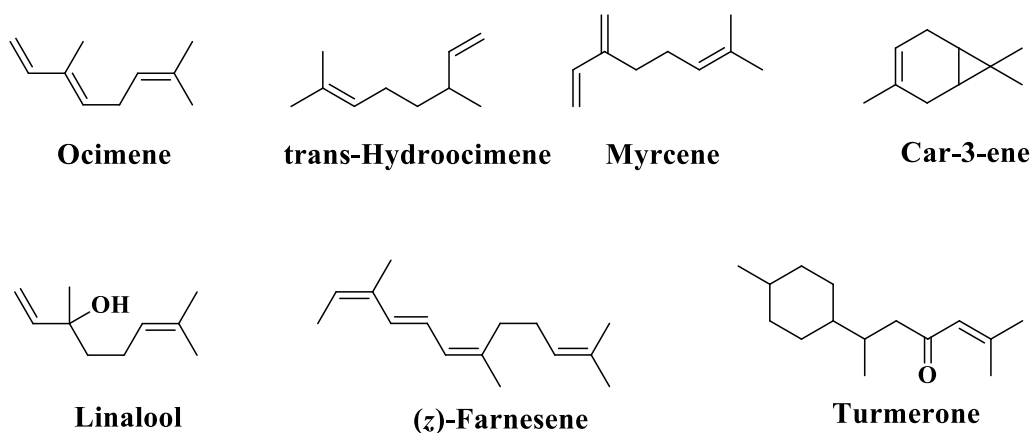


Figure 2.2. Volatile constituents from *C. amada*

Even though labdane diterpenes are the major bioactive constituents in the rhizomes, flavonoids, alkaloids and glycosides are also present. The labdane type diterpenes from *C. amada* rhizomes were first reported by Sheeja *et al.* in 2012 from chloroform extract except the compound (*E*)-labda-8(17),12-diene-15,16-dial, which was reported first time by Singh *et al.*²⁶ The six isolated labdane diterpenes are given below (**Figure 2.3**).²⁷

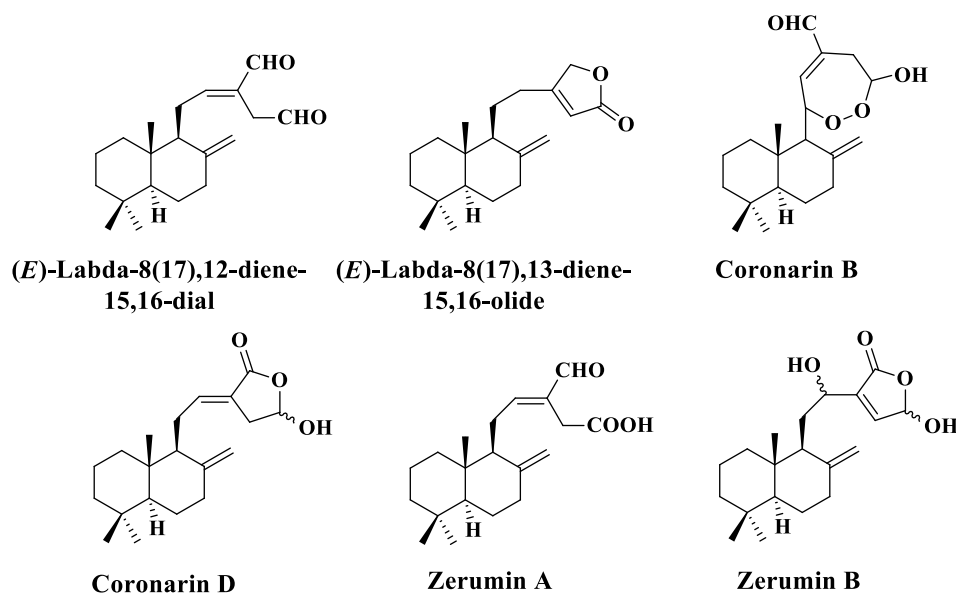


Figure 2.3. Labdane diterpenes isolated from *C. amada*

Policegoudra *et al.* in 2016 reported the novel compound difurocumenonol (**Figure 2.4**), a terpenoid from chloroform extract of mango ginger. It exhibited potent antibacterial activity against gram-negative and gram-positive bacteria.²⁸ In 2017 they have reported one novel terpenoid molecule, amadannulen (**Figure 2.4**) from chloroform extract, which shows anti-oxidant and anti-bacterial activity.²⁹ In 2010, Policegoudra *et al.* also reported another novel terpenoid, amadaldehyde (**Figure 2.4**) from chloroform extract, which is reported to possess antioxidant activity, cytotoxicity and platelet aggregation inhibitory activities.³⁰

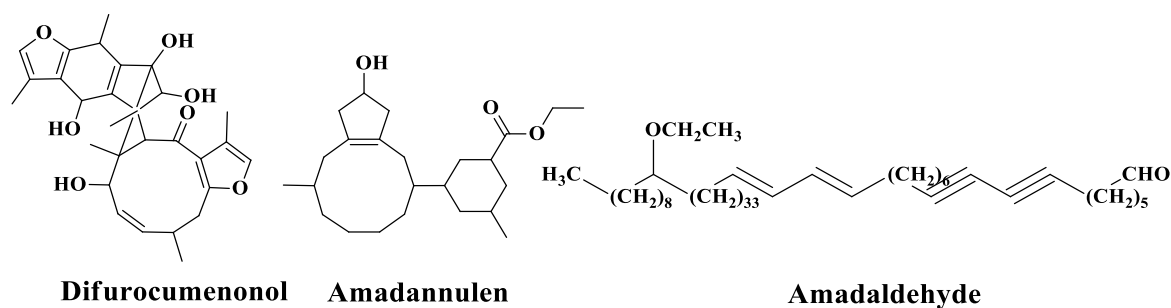


Figure 2.4. Terpenoids from *C. amada*

The important curcuminoids and phenolic acids present in the *C. amada* are given below (**Figure 2.5 & 2.6**).²⁵

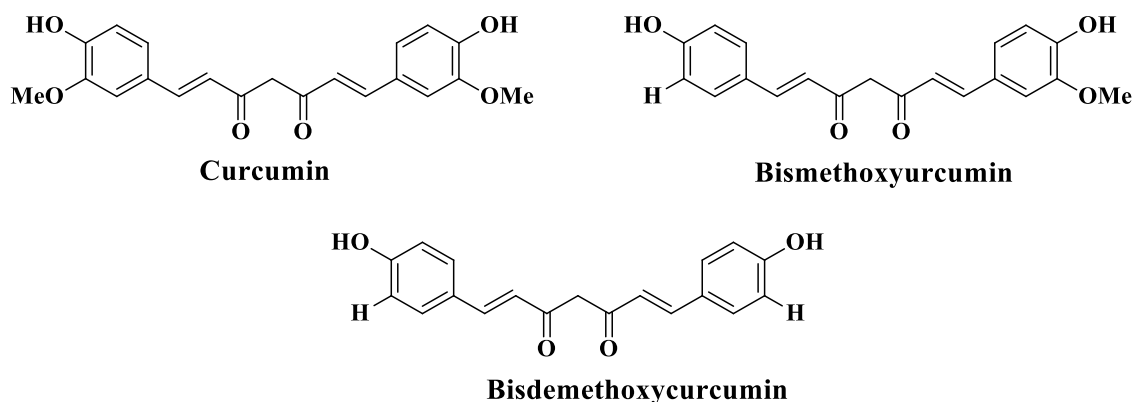


Figure 2.5. Curcuminoids from *C. amada*

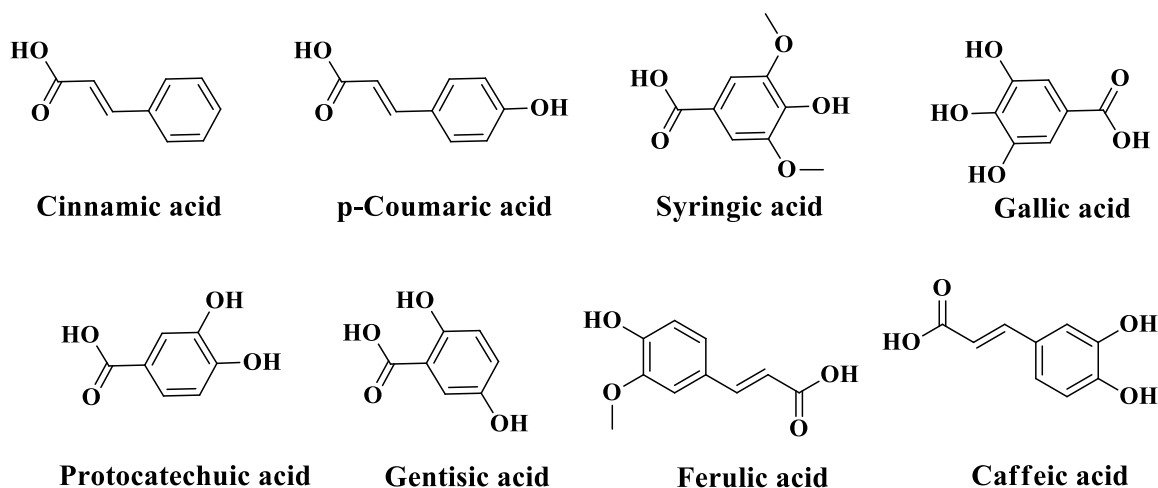


Figure 2.6. Phenolic acids from *C. amada*

The phenolic fractions of *C. amada* are reported to be a potent antiulcer agent viz., inhibiting proton potassium-ATPase activity and helicobacter pylori mediated ulcers. Gastric hyperacidity and ulcers are recurrent diseases of the gastrointestinal tract.³¹ Cholesterol lowering activity of mango ginger in induced hypercholesterolemic rats were studied by Srinivasan *et al.* in 2008 and shown to have beneficial anti-hypercholesterolemic activity.³²

Eventhough plant extracts and isolated compounds are shown to possess potent biological activities, the semi-synthetic transformation of isolated compounds also produces excellent therapeutic molecules. Modifications of isolated compounds may lead to the discovery of new leads. Singh *et al.* in 2010 isolated the compound labda-8(17),12-dien-15,16-dial first time from *C. amada*. Through semi-synthetic strategy, the molecule was

transformed it into three different analogues (**Figure 2.7**) and the products evaluated against mycobacterium tuberculosis. The studies found that one of the analogue (**2**) showed two fold increased activity over the isolated labda-8(17),12-dien-15,16-dial against tuberculosis.²⁶

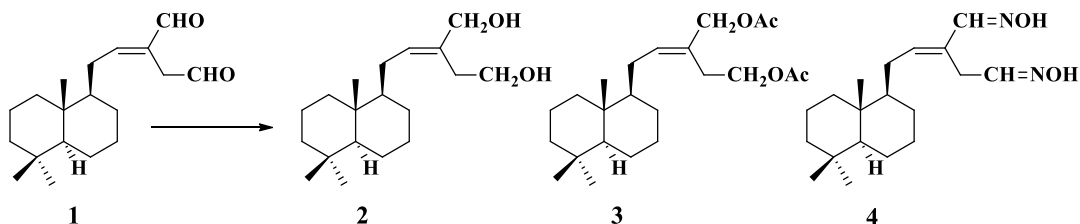


Figure 2.7. Modification of labda-8(17),12-dien-15,16-dial

From this literature survey, it became clear that constituents of *C. amada*, viz., (*E*)-labda-8(17),12-dien-15,16-dial had the potential for development to novel drug candidates.

2.5.2. *Curcuma malabarica*

Taxonomic position of the species *Curcuma malabarica* is as follows

Order	:	Zingiberales
Family	:	Zingiberaceae
Genus	:	<i>Curcuma</i>
Species	:	<i>C. malabarica</i>

Curcuma malabarica belongs to the family Zingiberaceae. It is a semi erect herb with green leaf sheath and light purple midrib. It possesses bluish white colour rhizomes with camphoraceous aroma. It is widely cultivated in South India. The rhizomes are used for the extraction of starch and the starch is used in diets for infants and convalescents since it possesses cooling and demulcent properties. This species has been reported for antimicrobial activity.^{33,34}



Figure 2.8. *C. malabarica* plant and rhizomes

The first phytochemical investigations of *C. malabarica* have been carried out by Sheeja *et al.* in 2009. They have isolated germacrane, guaiane, carabrane, diterpene types of sesquiterpene.³⁴ The reported compounds are given below (**Figure 2.9**).

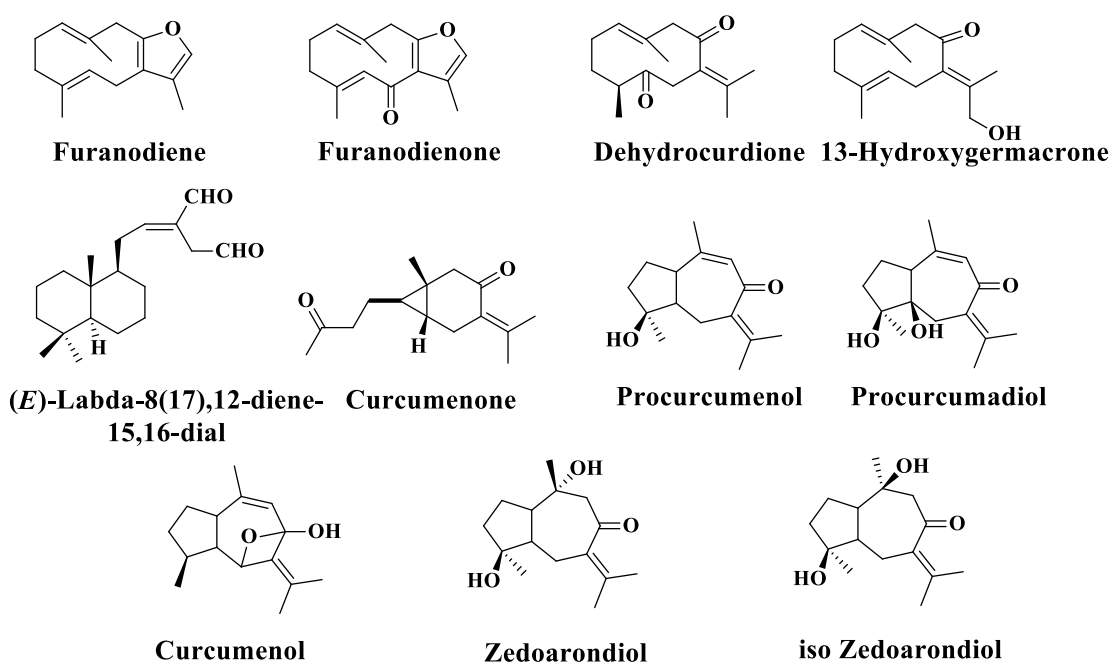


Figure 2.9. Chemical constituents of *C. malabarica*

A total of eleven compounds were reported from the essential oil of *C. malabarica* rhizomes, amongst which 1,8-cineole, curcumenone and camphor are the principal compounds.³⁵ Since the phytochemical investigation and biological evaluation of *C. malabarica* is not explored much, still there is much scope to explore the detailed phytopharmaceutical investigations on this species.

2.5.3. *Curcuma aromatica* Salisb.

The taxonomic position of *Curcuma aromatica* is given below.

Order	:	Zingiberales
Family	:	Zingiberaceae
Genus	:	<i>Curcuma</i>
Species	:	<i>C. aromatica</i> Salisb.

Curcuma aromatica, commonly known as wild turmeric or ‘vana haridra’, is a perennial aromatic herb with annulates. Inflorescence present in the base of rhizomes and leaves appears after the flowers. Rhizomes have an agreeable fragrant smell and having camphoraceous odour. It is commonly known as ‘kasturi manjal/arishne/pasuppu’ in South India. It grows in the tropical and subtropical regions and is widely distributed in India and particularly cultivated in Kerala and West Bengal. It has a long history in traditional medicine and is considered to be an effective remedy for various human ailments. In India, it has been extensively used as aromatic medicinal in cosmetics, for skin ailments and in vanishing creams. It has also been used as a base for making perfumes.^{36,37}



Figure 2.10. *C. aromatica* plant and rhizomes

C. aromatica is a rich reservoir for various phytochemicals and is known for its therapeutic effects. It is reported for its antimicrobial effects.³⁸ The essential oil of *C. aromatica* leaves and rhizomes consists of many compounds. The essential oil and various solvent extracts of leaves are reported to have anti-oxidant activities.^{38,39} Al-reza *et al.* in 2011 indicated the essential oil and various organic extracts from plant leaves exhibited remarkable antibacterial activity against different bacteria, and also these findings help food

industries to develop potent natural food preservatives.⁴⁰ Curdione isolated from the essential oil of *C. aromatica* alleviates pulmonary fibrosis, observed in the most common type of idiopathic interstitial pneumonia.⁴¹

Pintatum *et al.* reported the anti-inflammatory efficacy of crude extract of *C. aromatica* rhizomes and showed the highest inhibitory potential to NF- κ B activity.⁴² In 2016 Li *et al.* studied the cardioprotective effect of *C. aromatica* against acute myocardial ischemia (AMI) induced by isoproterenol (ISO) in rats. 70% hydroalcoholic extracts were shown to have the strongest cardioprotective effects amongst other concentrations.⁴³ The biogenic silver nanoparticles (AgNPs) synthesized by using the aqueous root extract of *C. aromatica* were shown to have potential anticancer activity against human cervical cancer cell lines (HeLa).⁴⁴ Dong *et al.* in 2018 reported four rare diarylheptanoids containing tetrahydropyran moieties and five known diarylheptanoids from the ethanol extract of *C. aromatica* root, along with a new phenol (**Figure 2.11**).⁴⁵

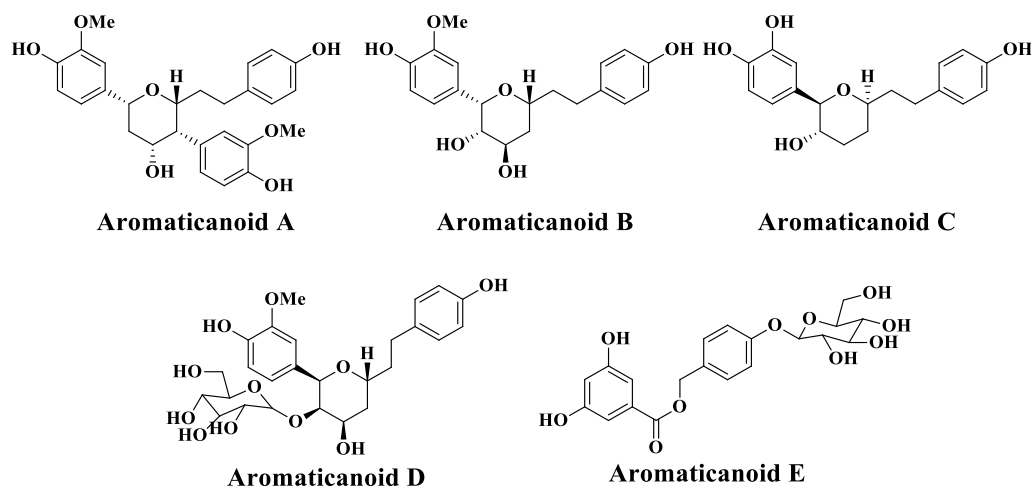


Figure 2.11. Structure of diarylheptanoids from *C. aromatica*

Recently in 2017, Dong *et al.* have isolated several novel sesqui and diterpenes from the radix of this plant and one of the novel compounds aromaticane I is the first atisane diterpenoid isolated from a curcuma species (**Figure 2.12**).⁴⁶ These studies all used *C. aromatica* from other countries. It was of interest to study *C. aromatica* grown in Kerala and therefore the investigation of *C. aromatica* was also included in the current study.

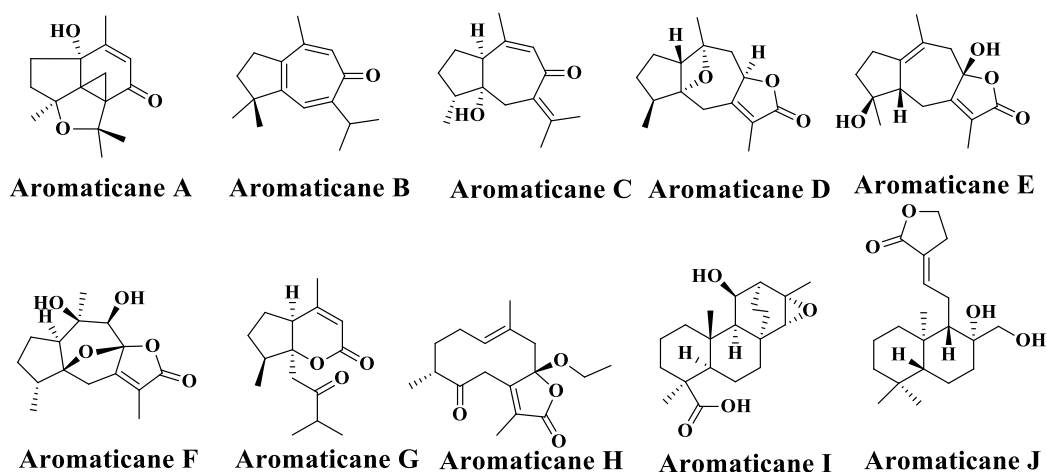


Figure 2.12. Sesqui and diterpenes from *C. aromatica*

2.6. Aim and scope of the present work

Since from ancient times, people always looked to nature for finding therapeutic agents for various diseases. Over the past twenty years, pharma companies have re-ignited their interest in natural product based drugs because of their potency and fewer adverse effects. As discussed in the introduction, *Zingiberaceae* is an important family in the plant kingdom and well known for its medicinal and nutritional properties in various traditional systems of medicine. *Curcuma* is an important genus in this family and a large number of bioactives have been isolated from this genus and most of the biological studies of these plants are carried out using various solvent extracts. However, there is relevance and scope for phytochemical investigation and evaluation of the biological efficacy of selected plants from the *Zingiberaceae* family. Therefore, as part of PhD program we selected *C. amada*, *C. malabarica* and *C. aromatica* for further investigations. We carried out a detailed Gas chromatography-mass spectrometry (GC-MS) analysis of essential oil of *C. amada* fresh rhizomes and the isolation of phytochemicals from *C. amada*, *C. malabarica* and *C. aromatica* from the *Zingiberaceae* family. After the isolation, inhibition of pancreatic lipase effect of bioactives was also carried out and the results are discussed in this chapter.

2.7. Gas Chromatography Mass Spectrometry (GC-MS) analysis of *C. amada*

GC-MS analysis of essential oils of *C. amada* cultivated in different geological regions have been studied and various volatile components are reported.^{15,47-49} Therefore to identify the

volatile organic compounds, here we have carried out the GC-MS profiling of essential oil of *C. amada* cultivated in Kerala.

2.7.1. Isolation of essential oil of *C. amada*

Clevenger apparatus was used for the extraction of essential oil. Around 250 g of freshly crushed rhizomes were subjected to steam distillation using 2.5 liters of distilled water for a period of 3 hrs. Around 0.1 ml of essential oil was obtained and subjected to GC-MS analysis.

2.7.2. GC-MS analysis of essential oil of *C. amada*

A total of 32 volatile organic compounds were identified from the essential oil of the *C. amada* rhizomes by GC-MS analysis with retention time in between 6.057-67.876 minutes. The major volatile phytoconstituents are represented in **Table 2.2**. The studies revealed that essential oil contains the following compounds present in highly abundant ratios viz., β -Pinene (25.90 %), β -Myrcene (21.73 %), trans- β -Ocimene (18.31 %), α -Pinene (4.97 %), α -Ocimene (1.69 %) and (-)-Limonene (1.71 %) representing 70.11% of total detected compounds and remaining compounds are present in minor amounts.

Table 2.2. GC MS profile of essential oil of *C. amada*

Peak	Ret. Time	Area	Area %	Height %	A/H	Name of compound
1	6.057	11026866	4.97	5.28	2.37	α -Pinene
2	6.552	3237282	1.46	1.51	2.44	Camphene
3	7.271	2273794	1.02	0.81	3.18	4(10)-Thujene
4	7.453	57559450	25.90	28.76	2.27	β -Pinene
5	7.814	48242695	22.50	30.33	1.80	β -Myrcene
7	9.272	3801114	1.71	1.37	3.15	(-)-Limonene
8	9.381	3607762	1.62	1.40	2.91	Eucalyptol (Cineole)
9	9.521	4157784	1.87	1.69	2.79	α -Ocimene
10	9.938	40652987	18.31	15.63	2.95	trans- β -Ocimene
11	10.116	1367904	0.62	0.45	3.42	3,5-Heptadien-2-one
12	11.722	3130120	1.41	0.86	4.13	2-Dodecanone
13	12.036	4380402	1.97	1.52	3.28	Perillene
14	12.149	1531971	0.69	0.41	4.21	Linalyl alcohol
15	12.246	2168416	0.98	0.51	4.83	2-Nonanol
16	15.231	723969	0.33	0.22	3.76	Borneol
17	15.612	836297	0.38	0.26	3.68	4-Terpineol
18	25.901	2935711	1.32	0.85	3.89	β -Caryophyllene
19	32.427	2530018	1.52	0.69	4.15	β -Caryophyllene epoxide
20	35.899	3777234	1.70	0.96	4.46	Longifolenaldehyde
21	40.395	4062041	1.83	1.02	4.51	1-[2-(2,2,6-trimethyl-bicyclo [4.1.0]hept-1-yl)-ethyl]-vinyl acetate
22	45.447	1240991	0.56	0.35	3.98	β -Springene
23	46.416	1801640	0.81	0.49	4.19	(+)- Saussurea lactone
24	57.383	3051264	1.37	0.73	4.73	Alloaromadendrene oxide
25	65.426	3166275	1.43	0.15	24.49	Campesterol
26	67.876	3410287	1.54	0.24	16.43	Stigmasterol
27	Other compounds		1.62			

2.8. Isolation and characterization of phytochemicals from *C. amada* rhizomes

2.8.1. Collection and extraction of *C. amada* rhizomes

The fresh rhizomes of *Curcuma amada* were collected from CTCRI, Thiruvananthapuram, Kerala, India. The voucher specimen was deposited in JNTBGRI, Palode, Thiruvananthapuram, Kerala (JNTBGRI 91073). The material was cleaned, washed, chopped and dried in a dehumidifying oven at 40 °C and then it was powdered. 1 kg of powdered rhizomes were subjected to extraction with chloroform (2Lx3) at room temperature, which yielded 70 g of crude extract. It was used for column chromatography.

2.8.2. Isolation and characterization of phytochemicals from chloroform extract

After studying the TLC profile of chloroform extract, 30 g of the extract was dissolved in a minimum quantity of hexane and loaded on the top of the column packed with silica gel (100-200 mesh) using hexane. Elution started with 100% hexane and the polarity of the solvent was increased gradually by adding ethyl acetate. A total of 300 fractions of approximately 100 ml each were collected. TLC of each fraction was studied and those fractions of which TLC profile were alike in UV were pooled together to get seven major fraction pools. Each of these pooled fractions were concentrated by removing the solvent under reduced pressure using Heidolph rotary evaporator and the above fractions on further purification led to the isolation of compounds 1-5.

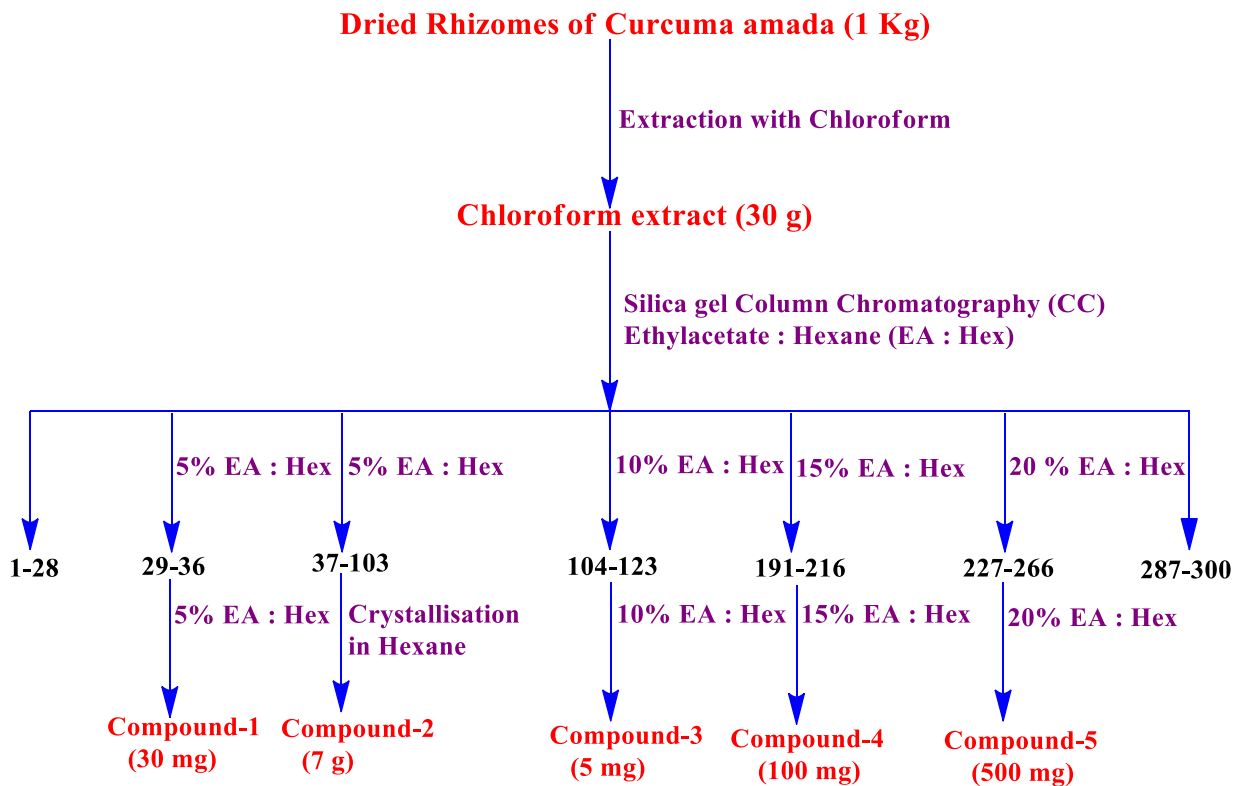
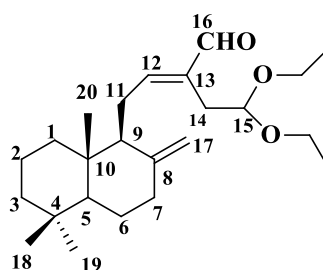


Figure 2.13. Pictorial representation for the isolation of phytochemicals from *C. amada* rhizomes

Fractions 29-36 obtained by eluting the column with 5% ethyl acetate-hexane showed a single UV active spot along with small upper impurities. After concentration, it was subjected to column chromatographic separation followed by preparative TLC which yielded a pure compound **1** (10 mg) as colourless oil. The IR spectrum of compound showed strong absorption at 1685 cm^{-1} confirms the presence of the carbonyl group. The bands at 2931 , 1641 and 890 cm^{-1} suggested the presence of an exo-cyclic double bond. Absorption at 1059 cm^{-1} indicated the compound have ether linkages. ^1H NMR spectrum (**Figure 2.14**) showed a singlet at δ 9.34 integrating for one proton, suggesting the presence of an aldehydic proton. A peak at δ 195.1 in the ^{13}C NMR spectrum (**Figure 2.15**) of the compound confirmed the presence of aldehyde group. From the signal at δ 6.55 integrating for one proton in the ^1H NMR spectrum and carbon signals at δ 160.1 and 138.4, could support that the aldehyde was an α , β -unsaturated system. The proton signals at δ 4.83 and δ 4.42, carbon signals at δ 148.3 and δ 108.0 were characteristic of an exo-methylene group. A triplet at δ 4.54 integrating for

one proton indicated the presence of methine proton attached to an electron withdrawing group. Multiplets at δ 3.67 and δ 3.48 could be attributed to the presence of deshielded protons. A doublet at δ 2.58 integrating for two protons suggests the presence of methylene protons. DEPT-135 confirms the presence of ten $-\text{CH}_2-$ groups. The three singlets at δ 0.89 (3H), 0.82 (3H) and 0.74 (3H) confirmed the presence of three quaternary methyl groups. The mass spectrum showed the molecular ion peak at m/z 399.2863, which is $(\text{M}+\text{Na})^+$ peak. Based on these spectral data and on comparison with the spectral data of compounds found in literature,⁵⁰ the structure of compound **1** was confirmed as a diterpene molecule, *(E)*-15,15-diethoxyabda-8 (17),12-diene-16-al. The structure of the compound is shown below.



Compound 1

15,15-Diethoxyabda-8 (17),12-diene-16-al

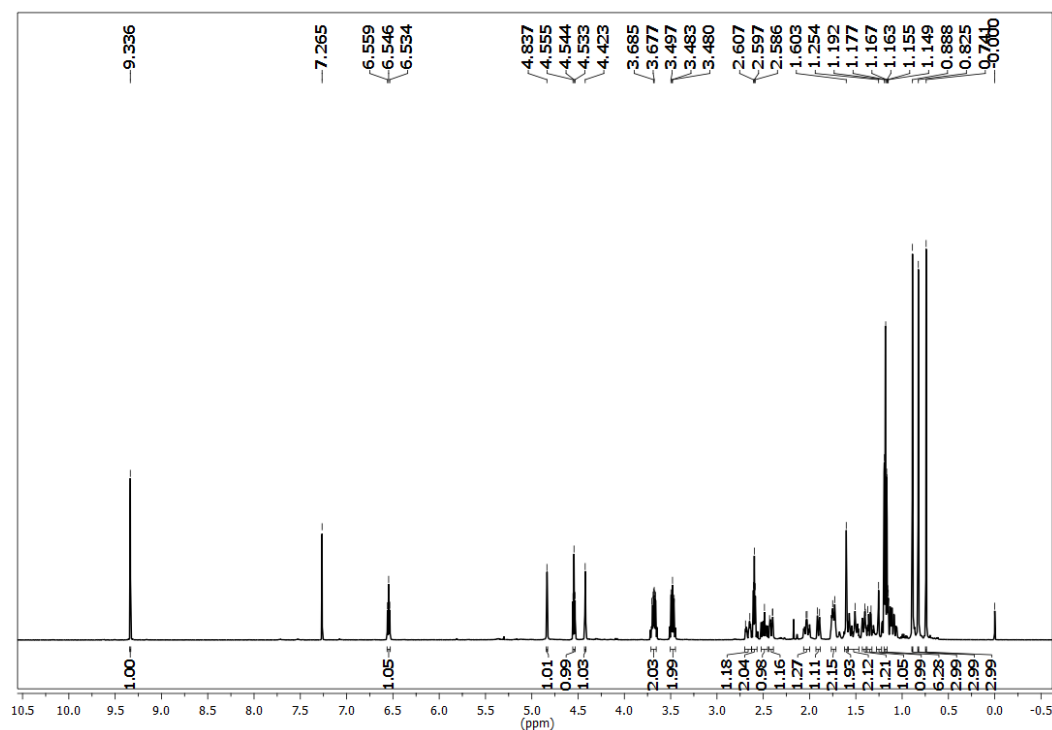


Figure 2.14. ^1H NMR spectrum of *(E)*-15,15-diethoxyabda-8 (17),12-diene-16-al in CDCl_3

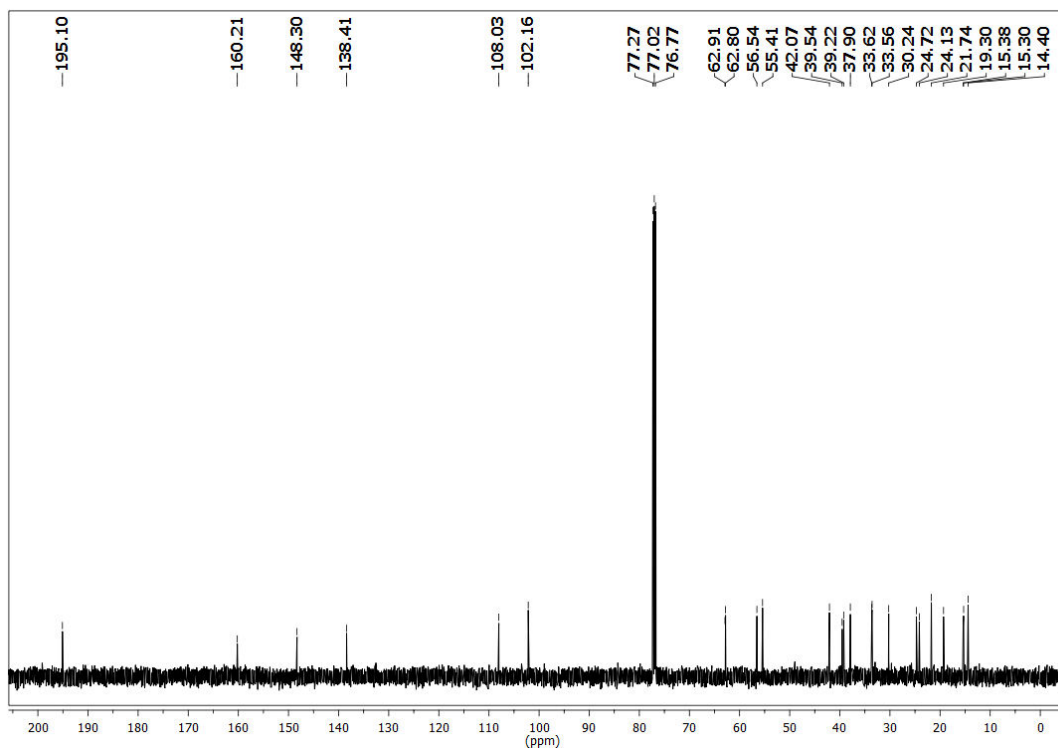
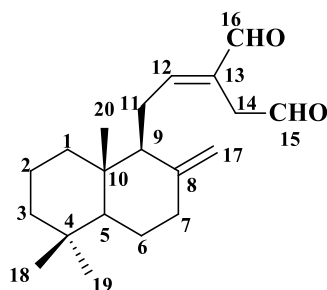


Figure 2.15. ^{13}C NMR spectrum of (*E*)-15,15-diethoxyabda-8 (17),12-diene-16-al in CDCl_3

Fractions 37-103 obtained on eluting the column with 5% ethyl acetate-hexane showed a UV active compound as the major constituent. After removing the solvent, it was subjected to crystallization in hexane which yielded 7g of pure compound **2** as a yellow solid that was separated from the mother liquor. The IR spectrum of compound showed strong absorptions at 1727 and 1684 cm^{-1} which suggest the presence of carbonyl and α , β -unsaturated carbonyl groups. Absorptions at 2931, 1642 and 890 cm^{-1} once again pointed to the presence of exo-cyclic double bond. ^1H NMR spectrum (**Figure 2.16**) of the compound showed the presence of one singlet and one triplet at δ 9.40 and 9.63 integrating for one proton each, suggesting the presence of two aldehydic groups. Two peaks at δ 193.5 and 197.3 in the ^{13}C NMR spectrum (**Figure 2.17**) confirmed the presence of two aldehyde groups. The proton signals at δ 4.86 and 4.37, carbon signals at δ 148.0 and 107.8 were characteristics of an exo-methylene group. The ^1H NMR spectrum clearly showed two deshielded protons appearing as a ABq at δ 3.42. That could be attributed to a methylene group (C-14) adjacent to an aldehyde. Three singlets at δ 0.89 (3H), 0.82 (3H) and 0.73 (3H) confirmed the presence of three quaternary methyl groups. The DEPT-135 spectrum

confirmed the presence of eight $-\text{CH}_2-$ groups as well as four quaternary carbons. The mass spectrum showed the molecular ion peak $(\text{M}+\text{Na})^+$ at 325.2132. From all these spectral data together and on comparing with the reported literature,²⁶ the structure of compound **2** could be identified as *(E)*-labda-8(17),12-diene-15,16-dial. The structure of the compound is shown below.



Compound 2
(E)-Labda-8(17),12-diene-1
 5,16-dial

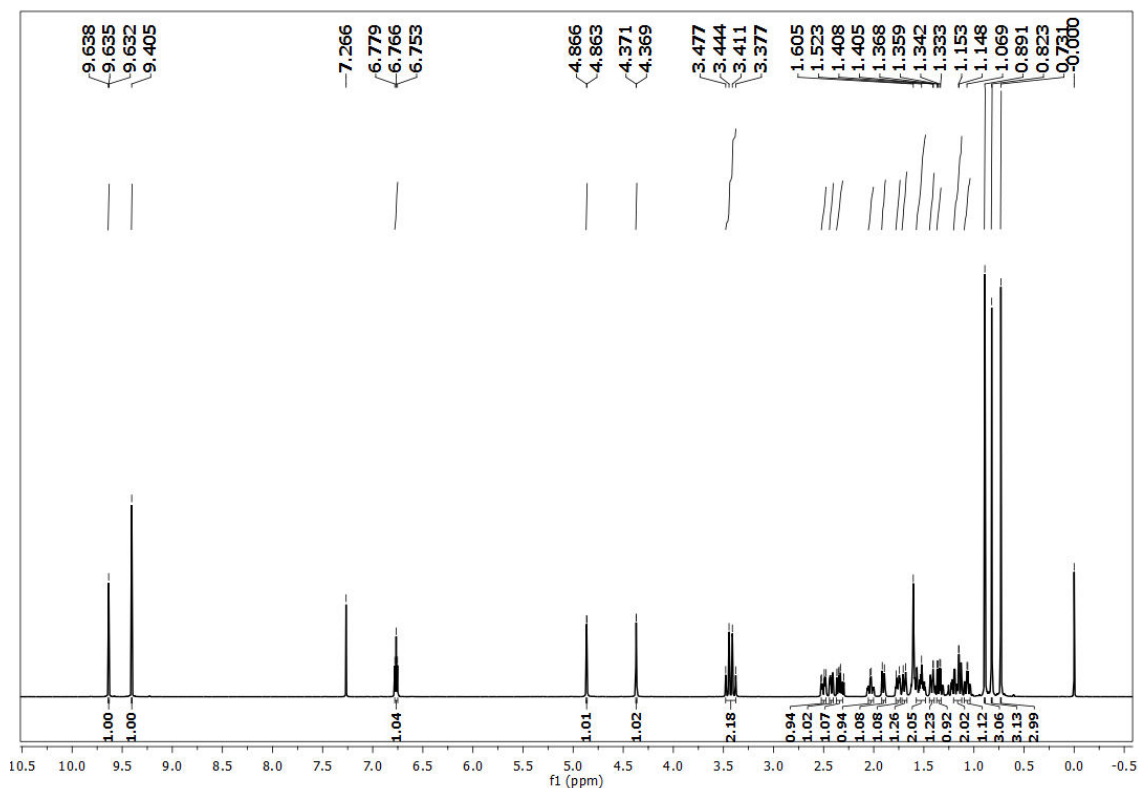


Figure 2.16. ^1H NMR spectrum of *(E)*-labda-8(17),12-diene-15,16-dial in CDCl_3

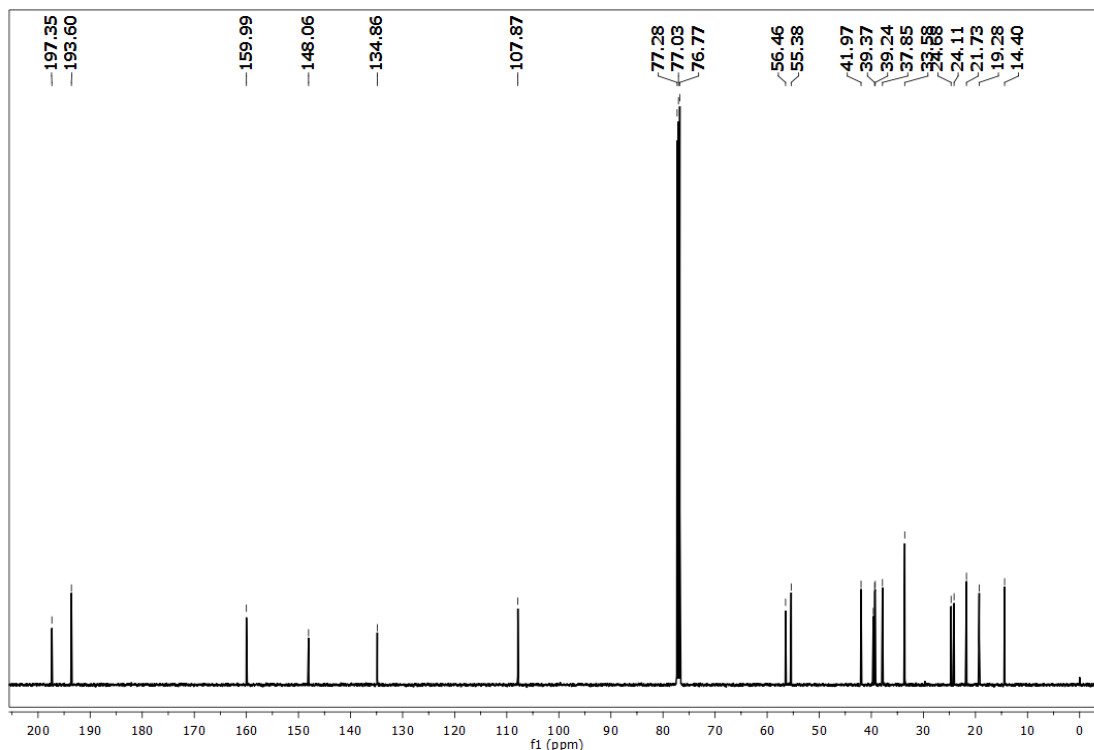
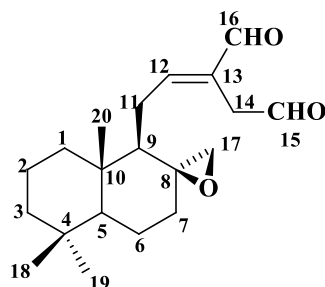


Figure 2.17. ^{13}C NMR spectrum of (*E*)-labda-8(17),12-diene-15,16-dial in CDCl_3

Fraction pool (104-123) obtained on eluting the column with 10% ethyl acetate-hexane showed a single UV active compound as the major constituent along with minor impurities. This fraction on further purification on silica gel column chromatography yielded 5 mg of compound **3** as a gummy solid. Two peaks at 1729 and 1684 cm^{-1} in the IR spectrum clearly indicated the presence of carbonyl groups in the molecule. In the ^1H NMR spectrum (**Figure 2.18**) one triplet and one singlet at δ 9.58 and 9.43 integrating for one proton each, suggests the presence of two aldehydic protons. Another triplet peak at δ 6.86 integrating for single proton could be ascribed to the presence of a proton attached to the double bond. The presence of two deshielded protons appearing as a singlet at δ 3.38, indicated the presence of a methylene group adjacent to an aldehyde. Three quarternary methyl groups are confirmed from the presence of three singlets at δ 0.91, 0.86 and 0.85, integrating for three protons each in the ^1H NMR. ^{13}C NMR spectrum (**Figure 2.19**) of the compound clearly showed the presence of twenty carbon atoms. The presence of two aldehyde groups is further confirmed by the presence of two peaks at δ 197.71 and 193.79 in the ^{13}C NMR spectrum. The peaks at δ 160.53 and 133.66 confirmed the presence of a double bond. ^{13}C NMR spectrum along

with DEPT-135 spectrum confirms the presence of three methyl, eight methylene, four methine and four quaternary carbons in the molecule. The mass spectrum of the compound showed the molecular ion peak at m/z 341.2089, which is $(M+Na)^+$ peak. From all these spectral data together and comparing with reported literature,^{51,52} compound **3** was found to be **afromodial** (*E*)-8 β ,(17)-epoxylabd-12-ene-15,16-dial. The structure of afromodial is shown below.



Compound 3
Afromodial

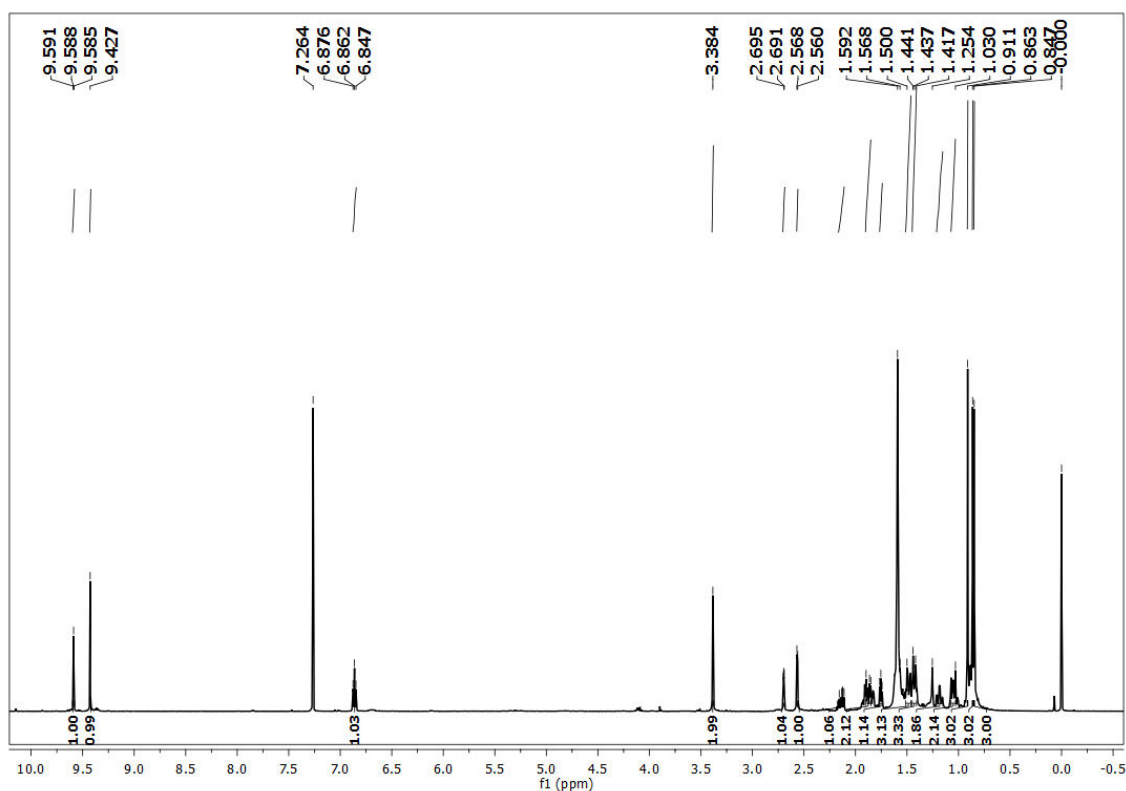


Figure 2.18. ^1H NMR spectrum of afromodial in CDCl_3

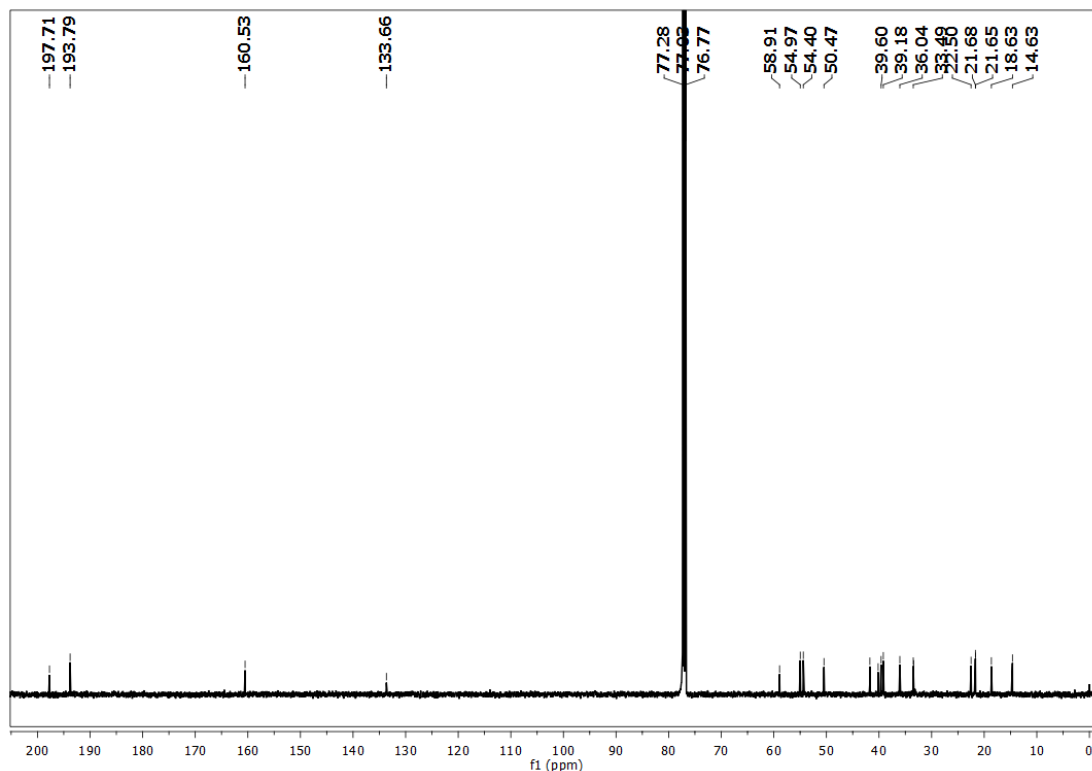


Figure 2.19. ^{13}C NMR spectrum of aframodial in CDCl_3

Fractions 191-216 obtained on eluting the column with 15% ethyl acetate-hexane showed a major UV active spot with some impurities. This was further purified by column chromatographic separation on silica gel using 15% ethyl acetate in hexane. This yielded 100 mg of compound **4** as colourless oil. The IR spectrum of compound showed absorption at 3363 cm^{-1} pointing the presence of a hydroxyl group. Absorption at 1737 and 1675 cm^{-1} suggested the presence of an α, β -unsaturated lactone carbonyl group. Two absorptions at 1644 and 888 cm^{-1} corresponds to the presence of an exo-cyclic double bond. ^1H NMR spectrum (**Figure 2.20**) showed the presence of three olefinic protons at δ 6.78, 4.84 and 4.36 of which, the first could be due to the β -proton in an α, β -unsaturated carbonyl system and the latter two could be attributed to exo-cyclic double bond. Peak at δ 5.93 supports the existence of the lactonic hemiacetal hydroxyl bearing methine proton. The three singlets observed at δ 0.89 (3H), 0.82 (3H) and 0.72 (3H) confirmed the presence of three quaternary methyl groups. ^{13}C NMR spectrum (**Figure 2.21**) showed twenty carbon signals which confirmed the structure as a labdane diterpenoid. The carbon signal appearing at δ 95.6 suggested a carbon atom connected by two oxygen functionalities (C-15). Peak at δ 169.6

was attributed to lactonic carbonyl carbon. Mass spectrum of the compound showed that molecular ion peak at m/z 341.2089, which is $(M+Na)^+$ peak. From all these spectral data along with DEPT-135 and on comparison with data of reported literature,⁵³ compound **4** was found to be **coronarin D**. The structure of coronarin D is shown below.

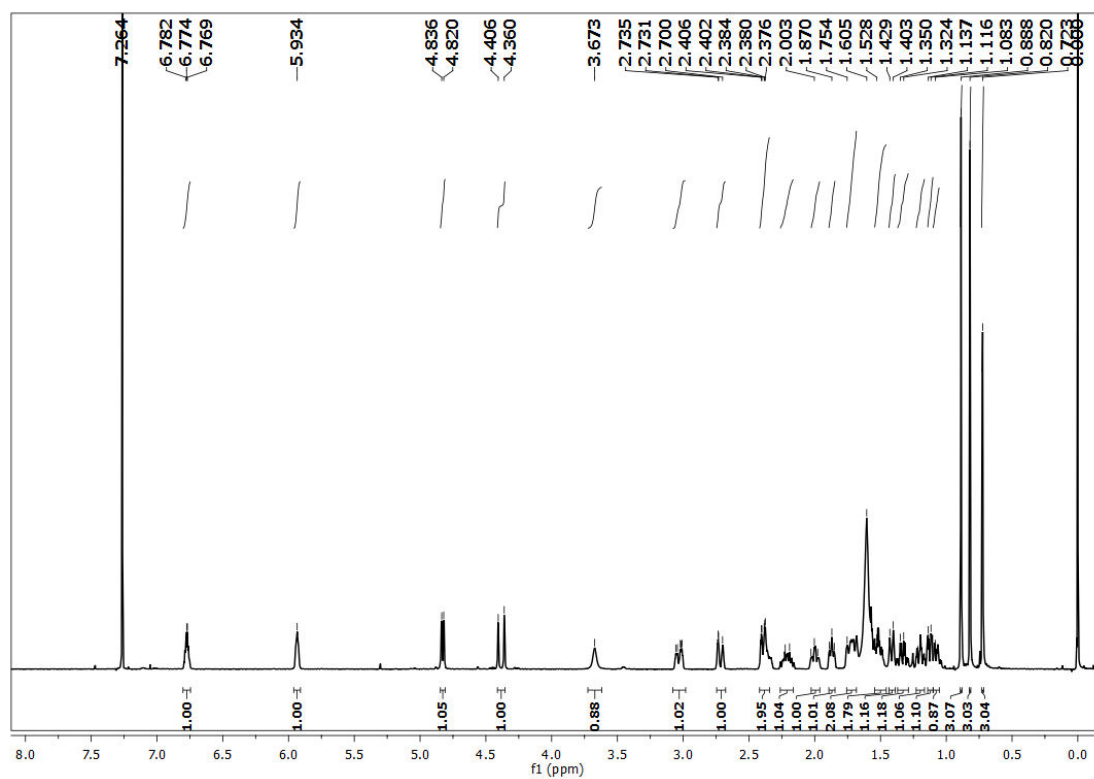
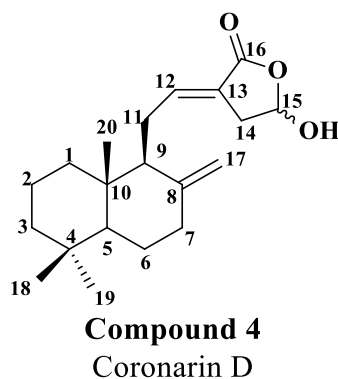


Figure 2.20. ¹H NMR spectrum of coronarin D in CDCl₃

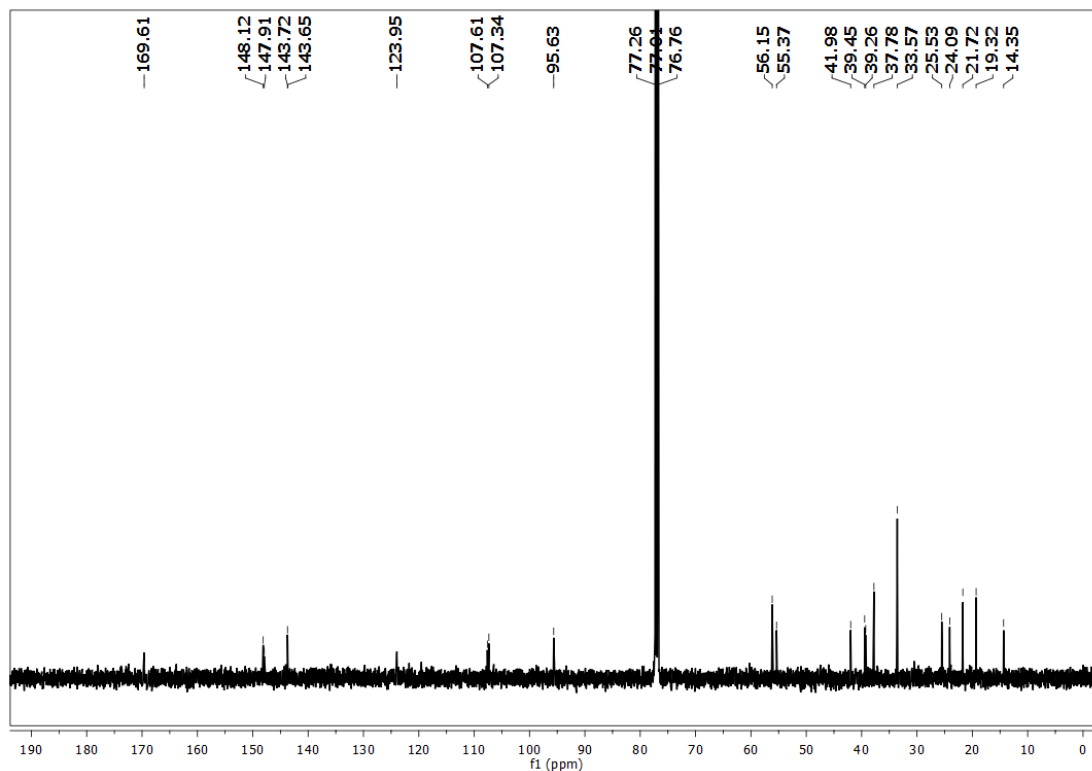


Figure 2.21. ^{13}C NMR spectrum of coronarin D in CDCl_3

Fractions 227-266 obtained on eluting the column with 20% ethyl acetate in hexane showed a single UV active spot along with some impurities. This fraction on further chromatographic purification using 20% ethyl acetate in hexane yielded 500 mg of viscous liquid, which was named as compound **5**. The IR spectrum of compound showed the presence of a carboxylic acid group through the broad absorption above 3000 cm^{-1} followed by the absorptions at 2847 cm^{-1} and 1713 cm^{-1} . Another strong absorption at 1689 cm^{-1} suggested the presence of an α, β -unsaturated aldehyde group. Absorptions at $2928, 1663$ and 890 cm^{-1} pointed to the presence of an exo-cyclic double bond. ^1H NMR spectrum (**Figure 2.22**) showed the presence of an aldehyde at $\delta 9.36$ integrating for one proton, which is confirmed by a peak at $\delta 193.6$ in the ^{13}C NMR spectrum (**Figure 2.23**). The signal at $\delta 6.69\text{ cm}^{-1}$ integrating for one proton in the ^1H NMR spectrum and carbon signals at $\delta 159.4$ and 135.7 , confirms that the aldehyde is an α, β -unsaturated aldehyde. The proton signals at $\delta 4.86$ and 4.40 , carbon signals at $\delta 148.0$ and 107.9 were characteristic of an exo-methylene group. The three singlets at $\delta 0.89$ (3H), 0.83 (3H) and 0.75 (3H) confirmed the presence of three quaternary methyl groups. Mass spectrum of the compound showed the molecular ion

peak at 341.2089, which is the mass of $(M+Na)^+$ peak. Thus the structure of compound **5** was confirmed on comparison with reported literature⁵⁴ as to be that of **zerumin A**. The structure of the compound is shown below.

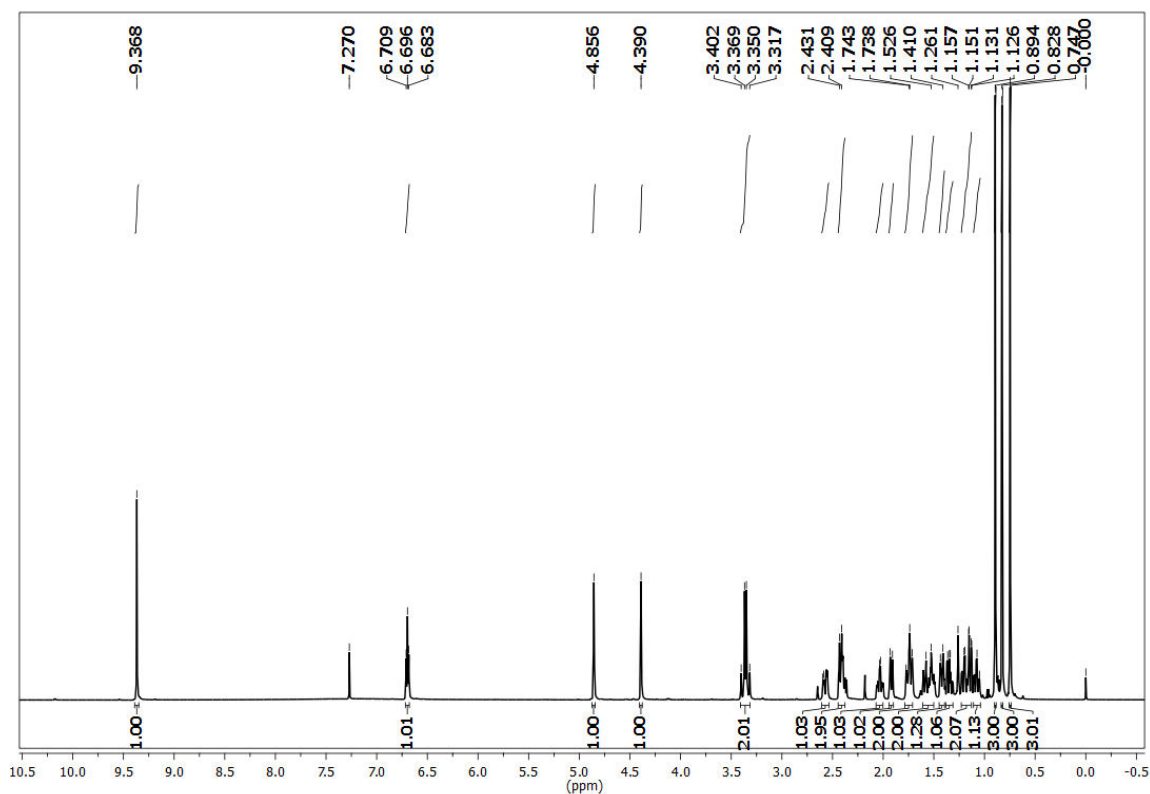
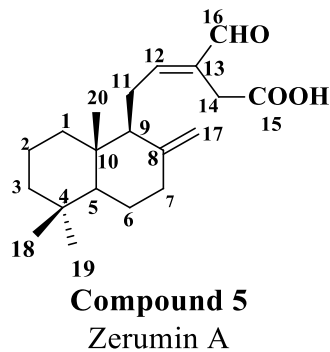


Figure 2.22. ¹H NMR spectrum of zerumin A in CDCl₃

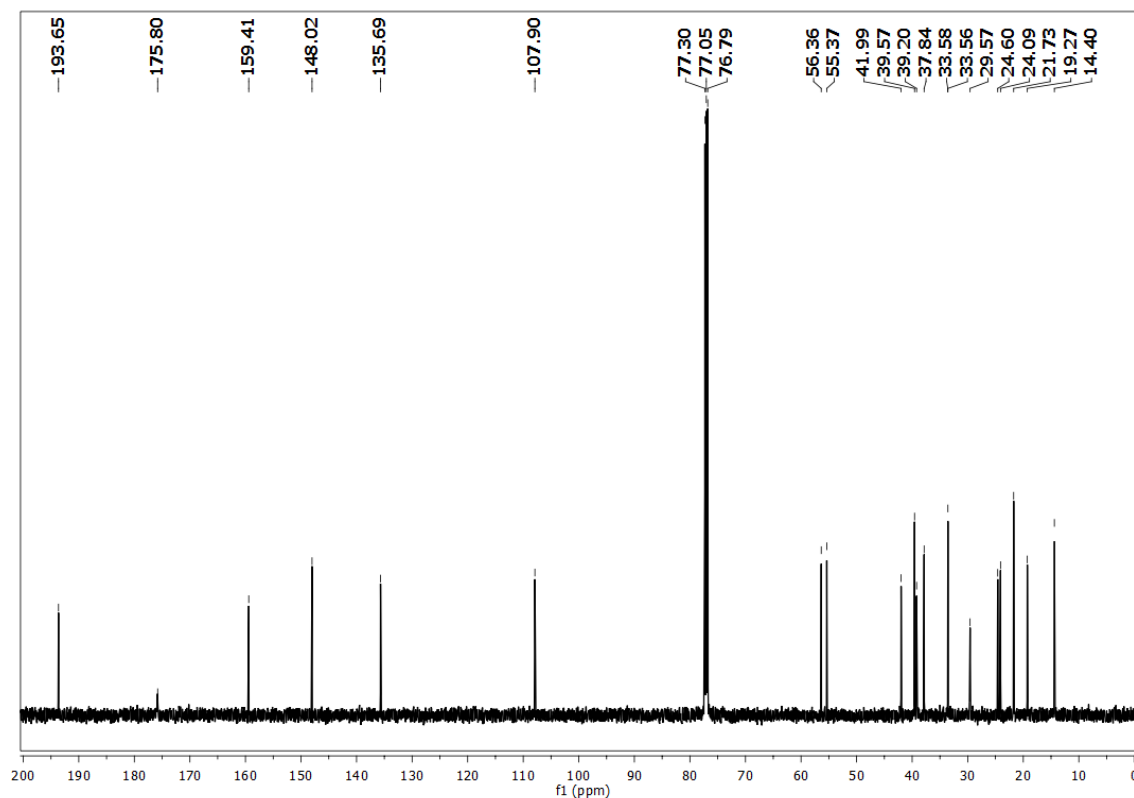


Figure 2.23. ^{13}C NMR spectrum of zerumin A in CDCl_3

2.9. Isolation and characterization of phytochemicals from *C. malabarica* rhizomes

2.9.1. Collection and extraction of *C. malabarica* rhizomes

15 kg of *Curcuma malabarica* rhizomes were collected from CTCRI, Thiruvananthapuram, Kerala, India and a voucher specimen was deposited in JNTBGRI, Palode, Thiruvananthapuram, Kerala (TBGT 54687). It was thoroughly washed, chopped, dried in a dehumidifying oven at 40 °C for two days and powdered mechanically. 1.6 kg of the powdered rhizomes were subjected to extraction with methanol (2Lx3) at room temperature, giving for each extraction 48 hrs at room temperature. The total extract was then concentrated under reduced pressure on Heidolph rotary evaporator, which yielded 90 g of methanol extract.

2.9.2. Isolation and characterization of phytochemicals from methanol extract

After studying the TLC profile of methanol extract, 33 g of the above extract was subjected for column chromatographic separation using chromatographic grade silica gel (100-200 mesh). Elution was started with 5% ethyl acetate in hexane and polarity was increased by adding ethyl acetate in hexane. The final elution was carried out with 5% methanol in hexane. A total of 395 fractions of approximately 100 ml each were collected. TLC of each fraction was checked and those fractions whose TLC profile was alike were pooled together to get seven major fraction pools. The pictorial representation of isolation of phytochemicals from *C. malabarica* is as shown below.

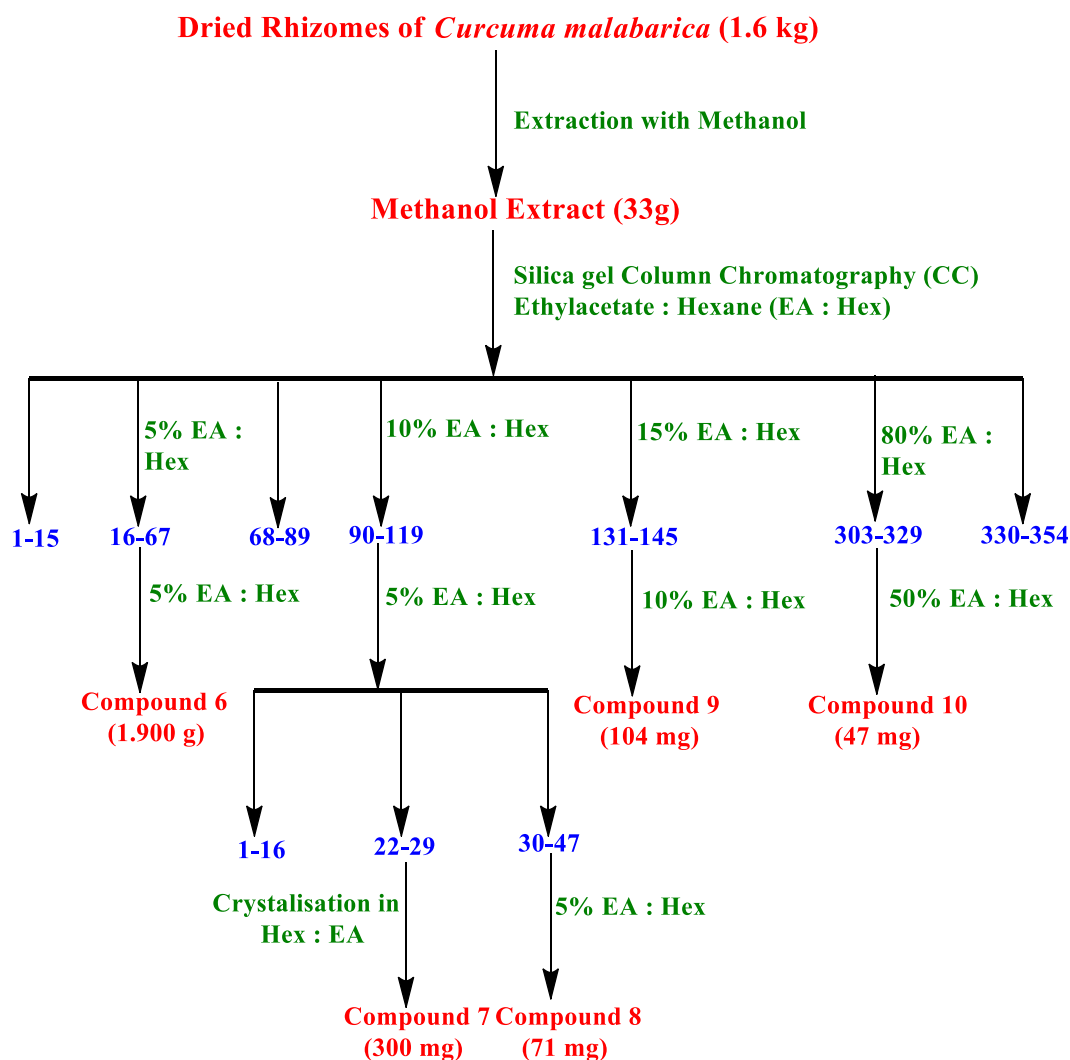
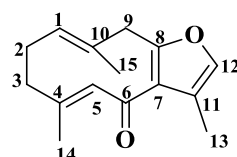
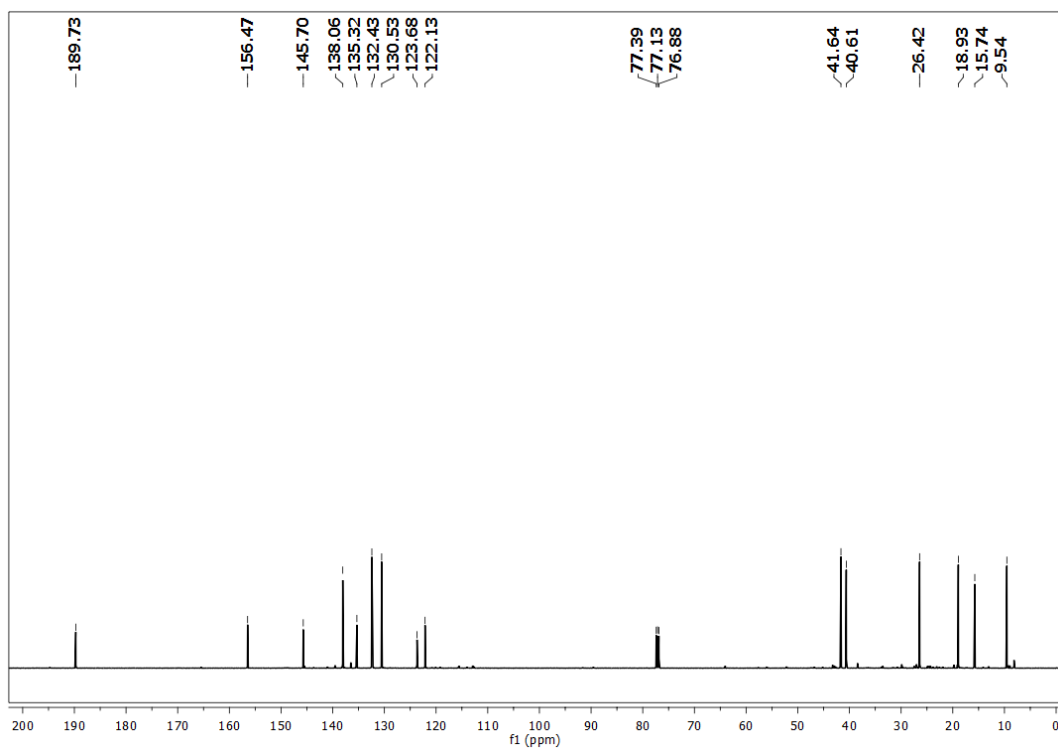
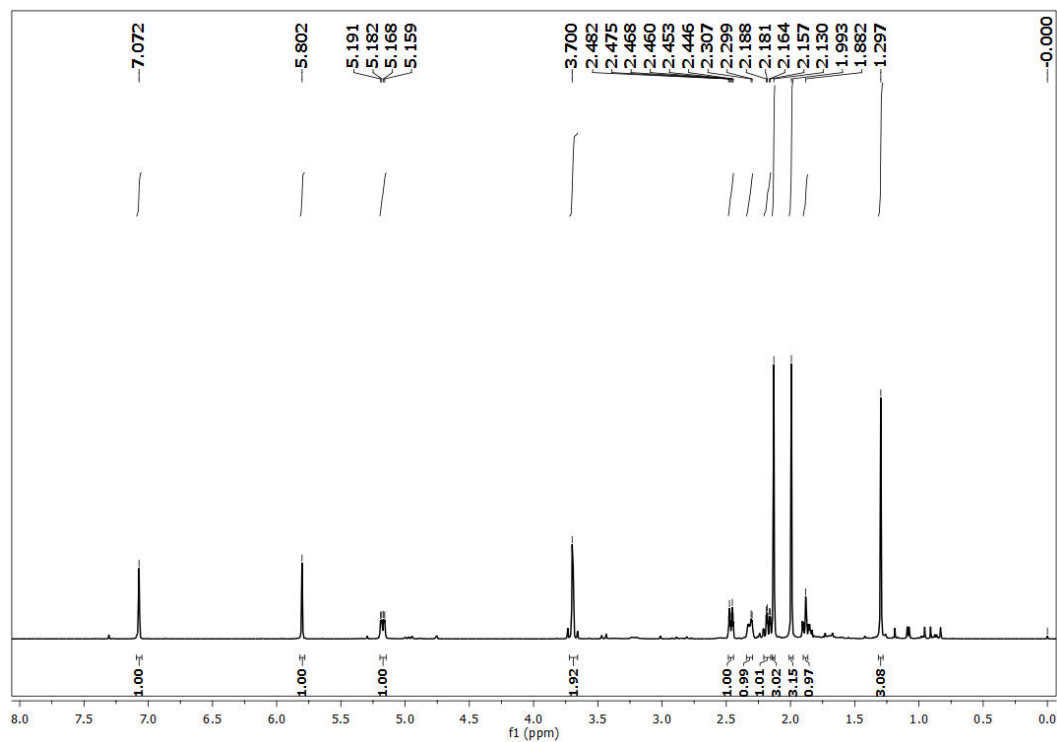


Figure 2.24. Pictorial representation for the isolation of phytochemicals from *C. malabarica* rhizomes

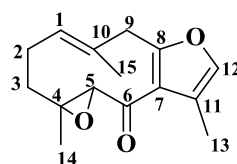
The pooled fraction 16-67 obtained by eluting the column with 5% ethyl acetate in hexane showed a single UV active spot along with small impurities, which on further column chromatography using 5% ethyl acetate in hexane furnished 1.900 g of pure compound **6** as a yellow solid. The IR spectrum showed a strong absorption at 1648 cm^{-1} , which suggested the presence of a highly conjugated carbonyl group. In the ^1H NMR spectrum (**Figure 2.25**) three singlets were observed at δ 2.13 (3H), 1.99 (3H) and 1.30 (3H), indicating the presence of 3 methyl groups attached to olefins. A singlet at δ 7.07 showed the presence of aromatic proton (H-12), whereas the signals at δ 5.17 and 5.80 ascribed the presence of two other olefinic protons centered at H-1 and H-5. ^{13}C NMR spectrum (**Figure 2.26**) of the compound showed the presence of 15 carbon atoms, of which the peak at δ 189.72 confirmed the presence of a carbonyl group. The presence of eight olefinic carbons was confirmed by the presence of 8 peaks in between δ 156.47-122.12 ppm. Further, mass spectrum of the compound showed the molecular ion peak at m/z 253.1508, which is $(\text{M}+\text{Na})^+$ peak. Based on these spectral data and on comparison with reported literature^{55,56} compound **6** was confirmed to be **furanodienone**. The structure of the compound is shown below.



Compound 6
Furanodienone



The pooled fraction 90-119 obtained on eluting the column with 10% ethyl acetate in hexane showed two strong UV active spots along with small impurities. This fraction on further column chromatography using 5% ethyl acetate in hexane led to three fraction pools. Subfraction (22-29) obtained by eluting the column with 5% ethyl acetate in hexane showed a single UV active spot with minor impurities, which on crystallization in ethyl acetate hexane mixture yield 300 mg of white needle shaped crystals, which was labeled as compound **7**. The IR spectrum of compound showed the peak at 1665 cm^{-1} due to an α, β -unsaturated ketone. Three singlets are seen at δ 1.35, 1.60, 2.12, each integrating for three protons in the ^1H NMR spectrum (**Figure 2.27**) assigned the presence of three quaternary methyl groups. Further, the spectrum also showed a characteristic aromatic peak at δ 7.09 due to methane proton for a trisubstituted furan ring (H-12). The peak at δ 5.49 (d, $J = 11.5$ Hz) suggested the presence of a vinylic proton (H-1). The ^{13}C NMR spectrum (**Figure 2.28**) showed the presence of fifteen carbon atoms in the compound. The peak at δ 192.2 confirmed the presence of a carbonyl group. Two oxygenated carbons showed the peaks at δ 64.0 and 66.5 respectively. The presence of three methyl groups was again confirmed by the presence of three peaks at δ 10.29, 15.15 and 15.74 in the ^{13}C NMR spectrum. The mass spectrum showed the molecular ion peak at m/z 269.1151, which is $(\text{M}+\text{Na})^+$ peak. From these data along with DEPT-135 and on comparison with literature^{57,58} compound **7** was confirmed to be **zederone**, which is being reported for the first time from this plant. The structure of the compound is shown below.



Compound 7
Zederone

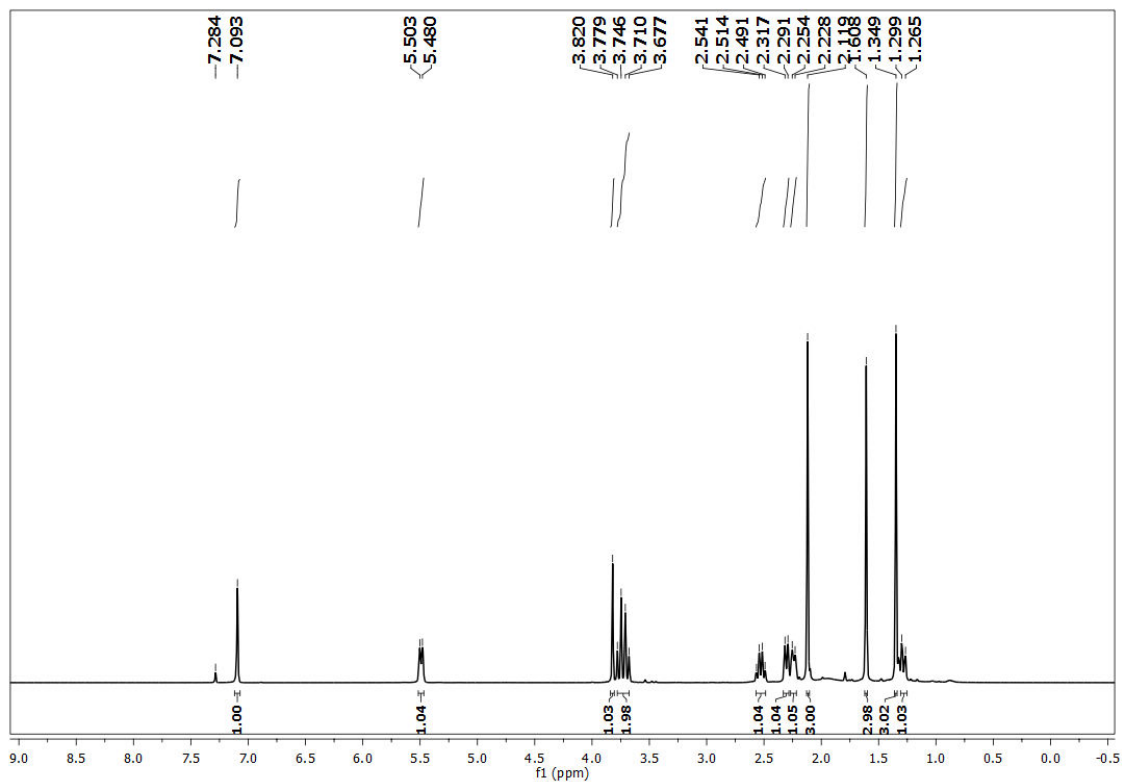


Figure 2.27. ^1H NMR spectrum of zederone in CDCl_3

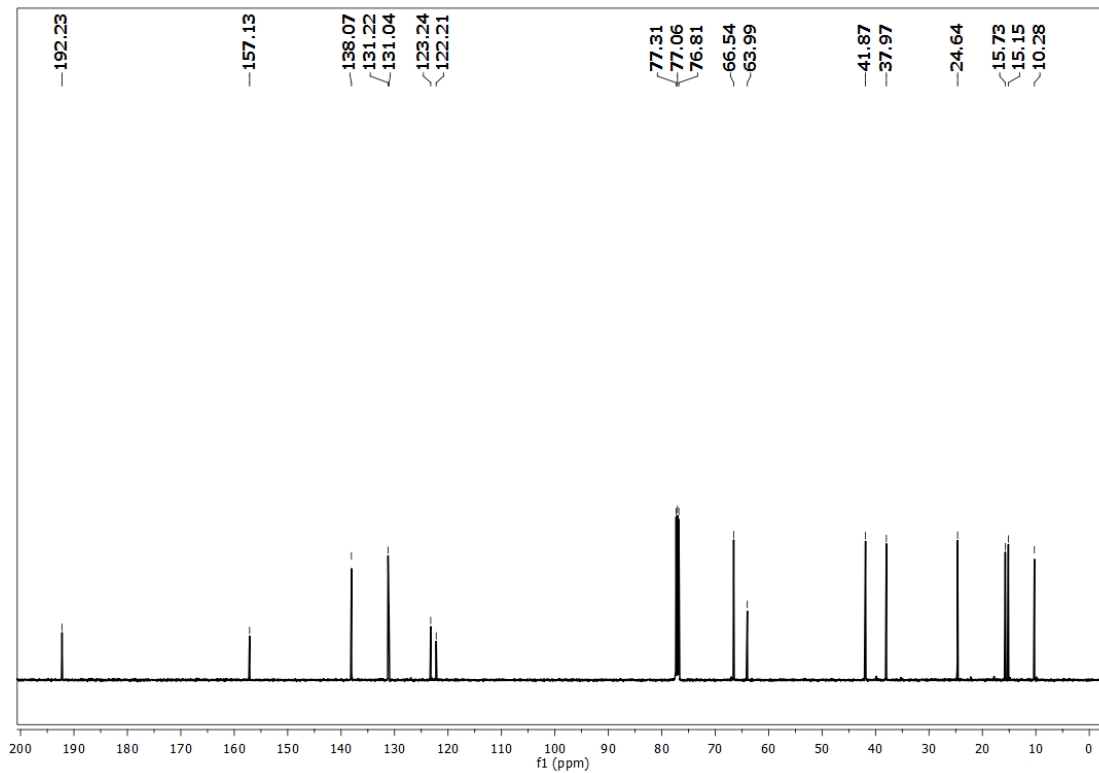
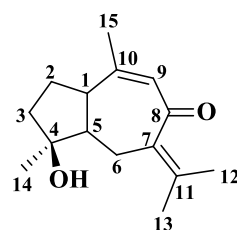


Figure 2.28. ^{13}C NMR spectrum of zederone in CDCl_3

The subfraction 30-47 obtained by eluting the column with 5% ethyl acetate in hexane was again subjected to column chromatographic purification by using 5% ethyl acetate in hexane, which yielded 71 mg of pure compound **8**. In the IR spectrum, the -OH group shows the absorption peak at 3427 cm^{-1} and 1645 cm^{-1} confirming the presence of a highly conjugated carbonyl group. In the ^1H NMR spectrum (**Figure 2.29**) a doublet centered at δ 5.81 indicated the presence of a deshielded olefinic proton. The appearance of four singlets at δ 1.81, 1.71, 1.68 and 1.54, integrating for three protons each attributed to the presence of four quaternary methyl groups in the compound. ^{13}C NMR spectrum (**Figure 2.30**) of the compound confirms the presence of 15 carbon atoms. The signal seen at 199.1 ppm confirmed the presence of a carbonyl group. The peaks in between δ 154.9-129.2 were confirming the presence of four olefinic carbons. The peak at δ 80.3 indicated the presence of oxygen attached carbon centered at the C-4 position. The mass spectra showed the molecular ion peak at m/z 257.1522, which is the $(\text{M}+\text{Na})^+$ peak. From these spectral data along with DEPT-135 and comparing with the data of compound found in literature reports,⁵⁹ the compound **8** was confirmed as **procurcumenol**. The structure of the compound is shown below.



Compound 8
Procurcumenol

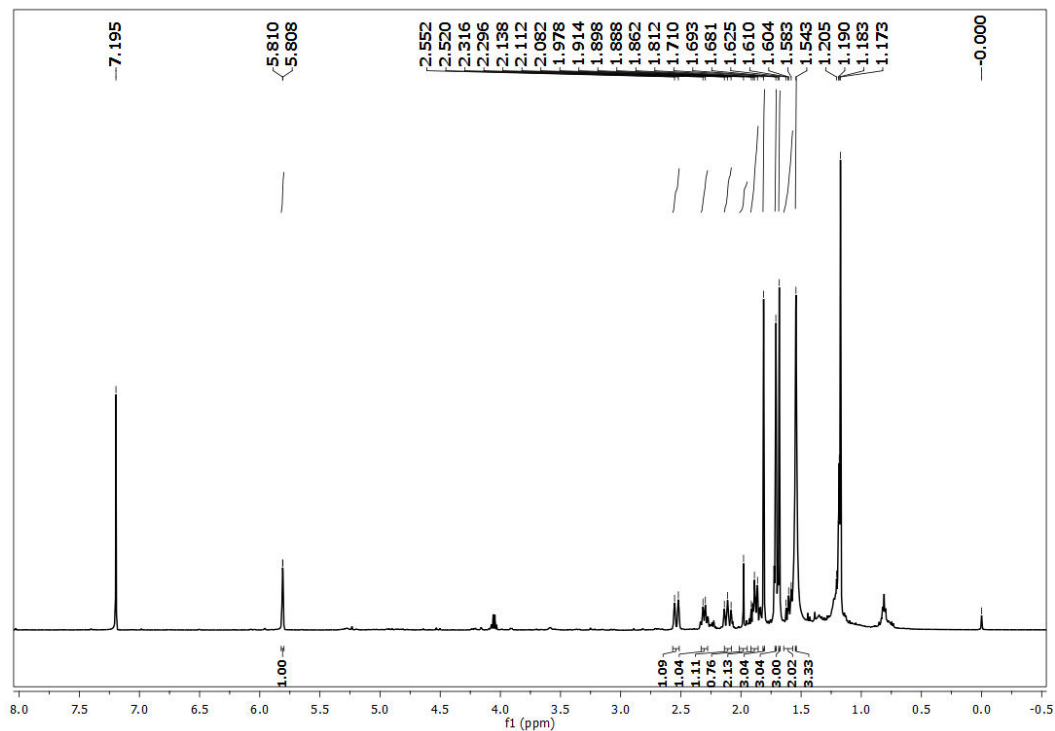


Figure 2.29. ^1H NMR spectrum of procurcumenol in CDCl_3

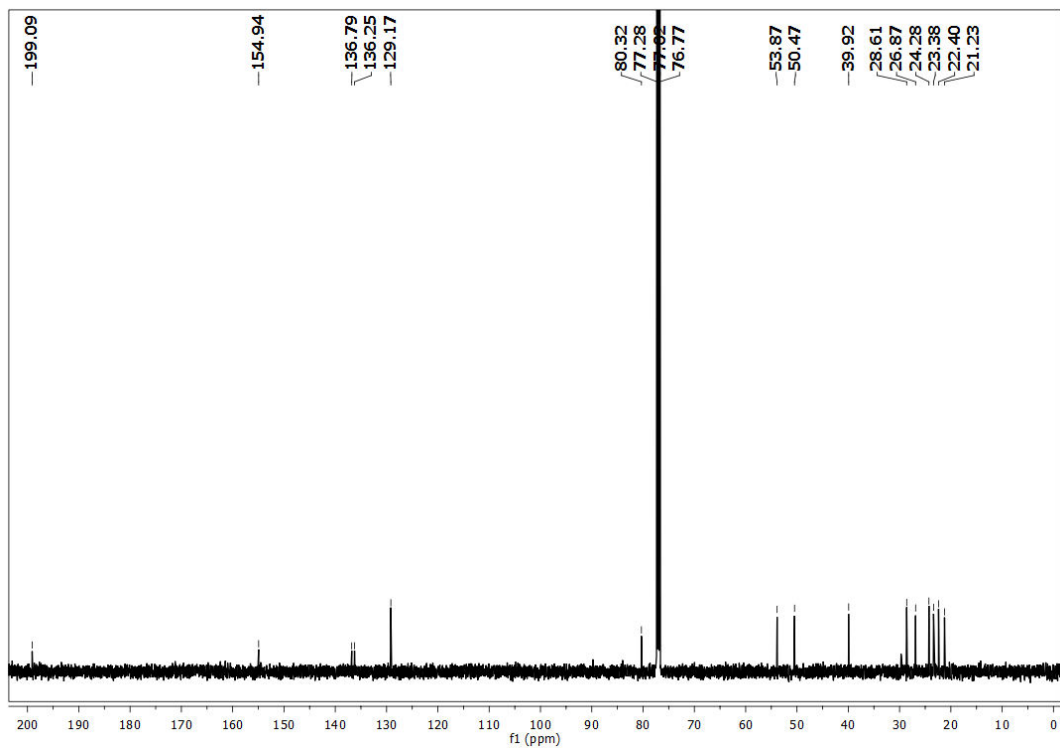
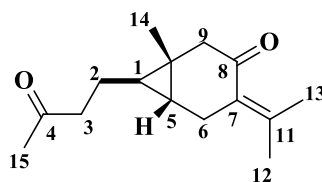


Figure 2.30. ^{13}C NMR spectrum of procurcumenol in CDCl_3

The pooled fraction 131-145 obtained on eluting the column with 10% ethyl acetate in hexane showed one strong UV active spot along with some other impurities. These fractions on further purification by column chromatography using 10% ethyl acetate in hexane, furnished 104 mg of pale yellow crystalline solid, which was named as compound **9**. IR spectrum of the compound showed sharp bands at 1766 cm^{-1} and 1701 cm^{-1} suggesting the presence of carbonyl and unsaturated carbonyl groups. ^1H NMR spectrum (**Figure 2.31**) of the compound showed four singlets observed at δ 2.13, 2.09, 1.80 and 1.12, integrating for 3 protons each, could be attributed to the presence of four quaternary methyl groups. The singlet at δ 0.67 and a multiplet at 0.45 indicated the presence of two methine protons. The ^{13}C NMR spectrum (**Figure 2.32**) of the compound showed the presence of fifteen carbon atoms. Further the two carbonyl groups are confirmed by the presence of peaks at δ 208.7 and 201.6. Mass spectra of the compound observed molecular ion peak m/z at 257.1517 for $(\text{M}+\text{Na})^+$ peak. Based on these spectral data along with DEPT-135 and on comparison with literature report⁶⁰ the compound **9** was confirmed to be **curcumenone**. The structure of the compound is as shown below.



Compound 9
Curcumenone

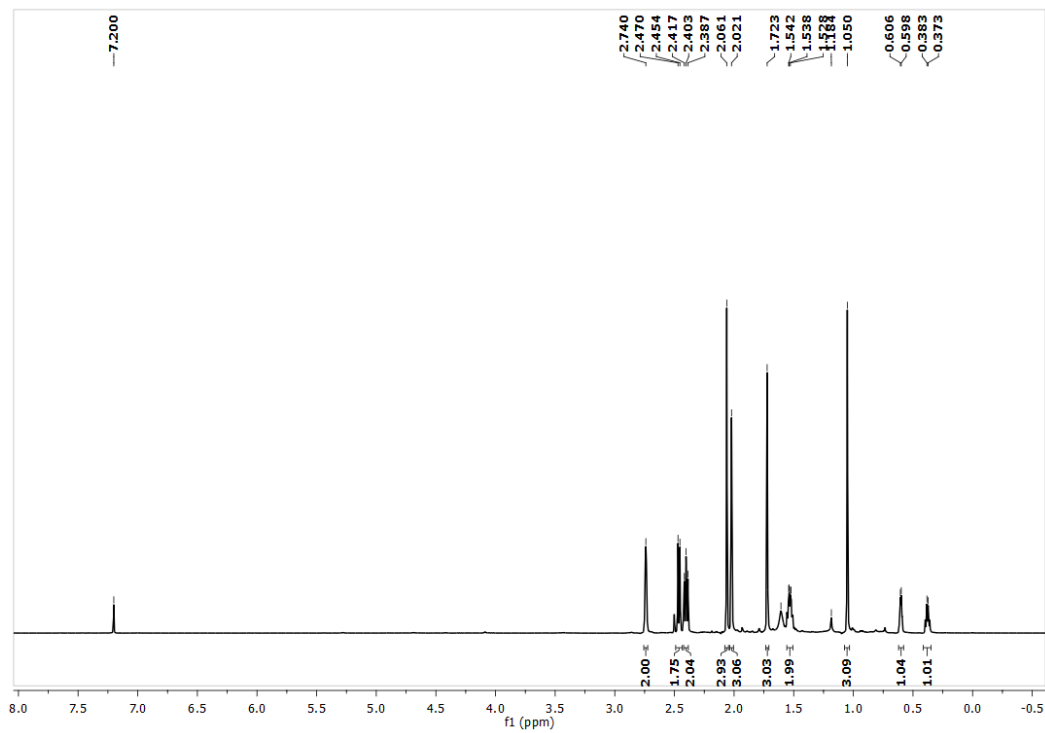


Figure 2.31. ^1H NMR spectrum of curcumenone in CDCl_3

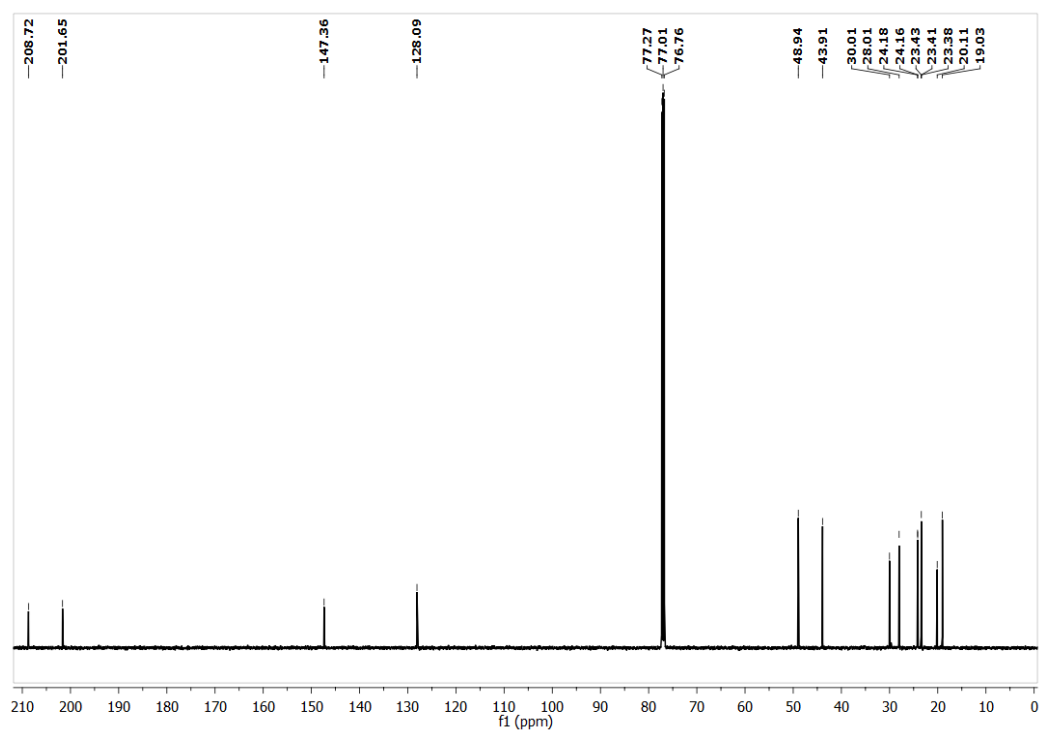
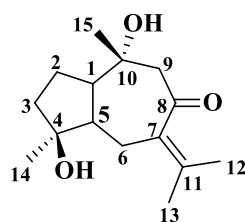


Figure 2.32. ^{13}C NMR spectrum of curcumenone in CDCl_3

Fraction 303-329 obtained by eluting the column with 80% ethyl acetate in hexane showed a strong UV active spot along with small impurities. It was again subjected to column chromatographic purification using 60% ethyl acetate in hexane to yield 47 mg of the pure compound as liquid, which was labeled as compound **10**. IR spectrum of the compound showed a band at 3405 cm^{-1} indicating the presence of hydroxyl group. The presence of an α , β -unsaturated carbonyl group was seen at 1660 cm^{-1} . The ^1H NMR spectrum (**Figure 2.33**) of the compound showed the presence of four quaternary methyl groups at δ 1.18, 1.20, 1.83 and 1.93 respectively. The doublets at δ 2.96 and 2.60 with J as 12.5 Hz and 13 Hz could be assigned to a methylene group adjacent to the carbonyl functionality. The ^{13}C NMR spectrum (**Figure 2.34**) of the compound clearly shows the presence of 15 carbon atoms. The peak at δ 202.9 confirms the presence of carbonyl group. The two peaks centered at δ 142.2 and 134.6 indicated the presence of olefinic carbons at positions C-11 and C-7. The two hydroxyl oxygen attached carbon show the peaks at δ 80.0 and 72.8. The molecular ion peak m/z was observed at 275.1627, which was $(\text{M}+\text{Na})^+$ peak. From these spectral data along with DEPT-135 and on comparison with literature report,⁶¹ compound **10** was confirmed to be **zedoarondiol**. The structure of the compound is shown below.



Compound 10
Zedoarondiol

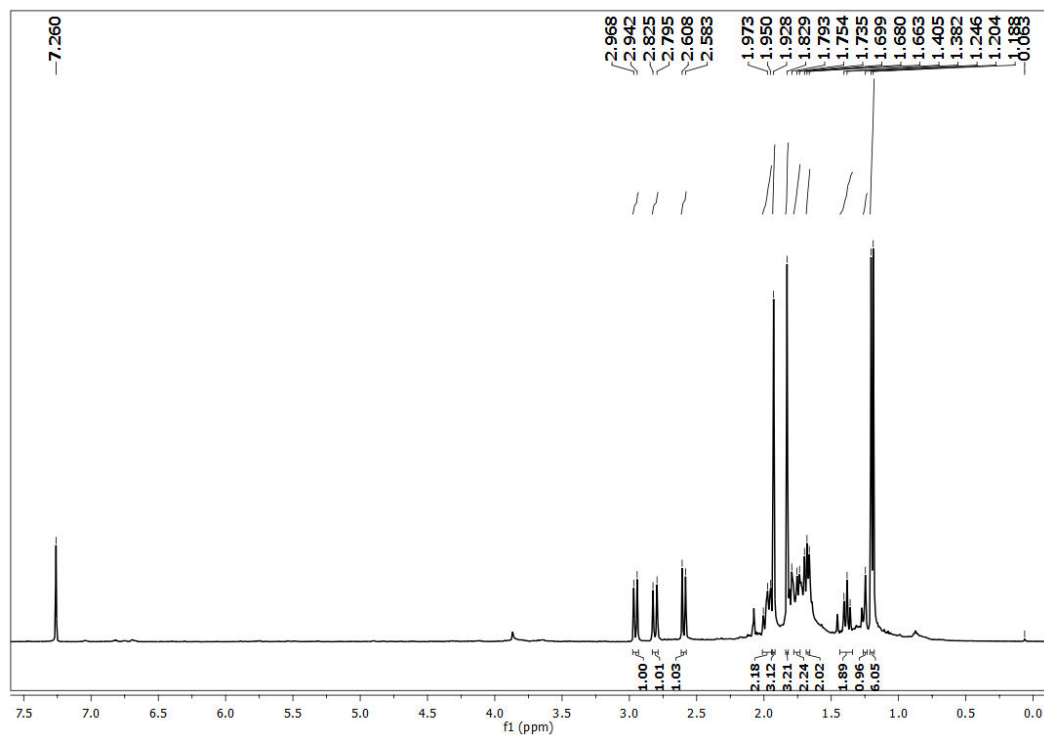


Figure 2.33. ^1H NMR spectrum of zedoarondiol in CDCl_3

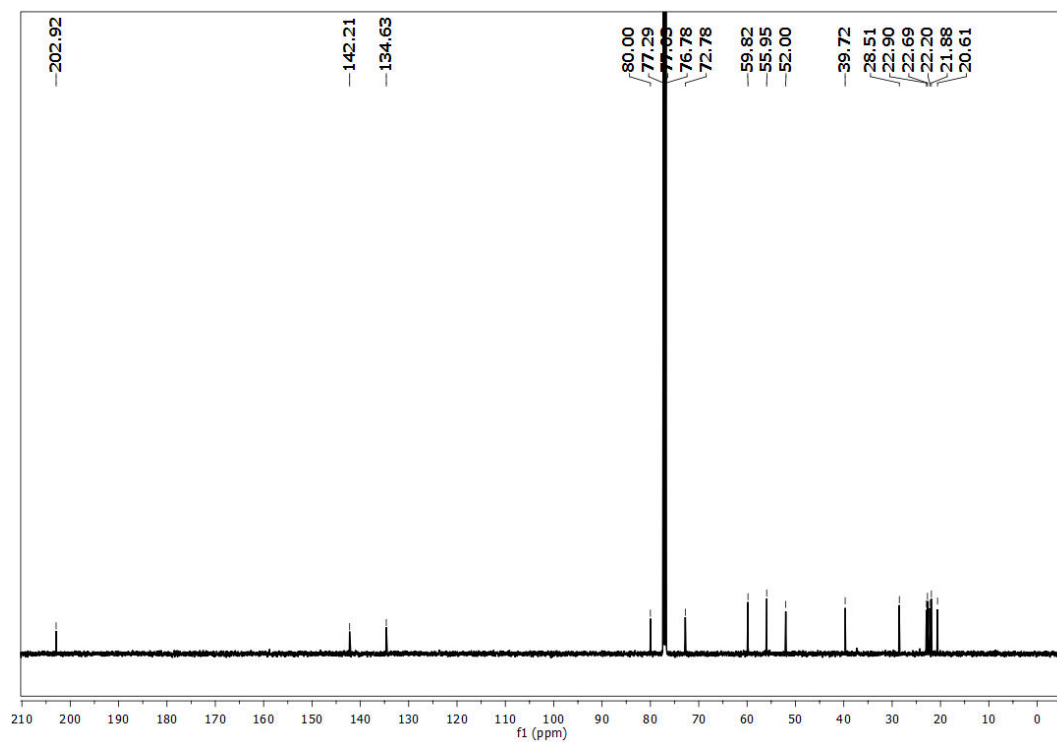


Figure 2.34. ^{13}C NMR spectrum of zedoarondiol in CDCl_3

2.10. Isolation and characterization of phytochemicals from *C. aromatica* rhizomes

2.10.1. Collection and extraction of *C. aromatica* rhizomes

C. aromatica rhizomes (6 kg) were collected from Indian Institute of Spices Research, Calicut, Kerala, India and a voucher specimen was deposited in JNTBGRI, Palode, Thiruvananthapuram (TBGT 91074). It was thoroughly washed, chopped, dried at room temperature and then dried in the dehumidifying oven at 40 °C for 2 days. The dried rhizomes were powdered mechanically. 800 g of the powdered material was subjected to extraction using hexane (2.5Lx3) at room temperature to yield 25 g of the crude hexane extract. The residue obtained after extraction using hexane was further subjected to extraction with chloroform (2.5Lx3), ethyl acetate (2.5Lx3), acetone (2.5Lx3) and methanol (2.5Lx3) as same as above, which yields 30 g, 10 g, 17 g and 24 g of the corresponding extracts. The pictorial representation of various solvent extractions is as shown below.

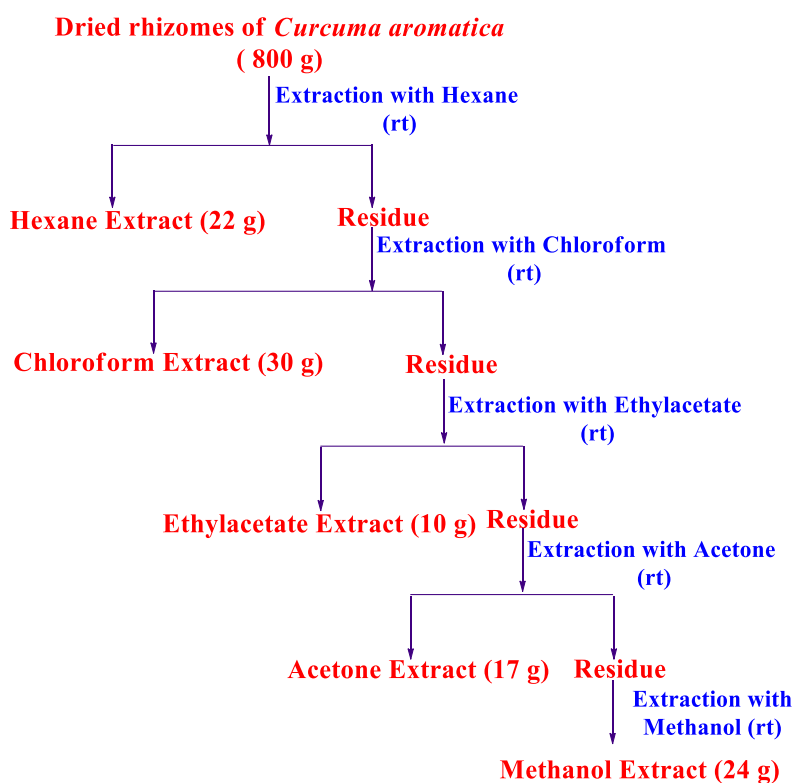


Figure 2.35. Pictorial representation for the extraction with various solvents of *C. aromatica* rhizomes

2.10.2. Isolation of compounds from hexane extract

After studying the TLC profile of extract at various polarities of ethyl acetate-hexane mixtures, 22 g of the hexane extract was subjected to column chromatographic separation using chromatographic grade silica gel. Elution was started with 100% hexane and increase in polarity was carried out by increasing the amount of ethyl acetate in hexane. Final elution was carried out with 100% ethyl acetate. A total of 243 fractions of approximately 150 ml volume each were collected. TLC of each fraction was checked and those fractions whose TLC profile was alike were pooled together to get 15 major fraction pools. The pictorial representation of isolation of phytochemicals from *C. aromatica* is as shown below.

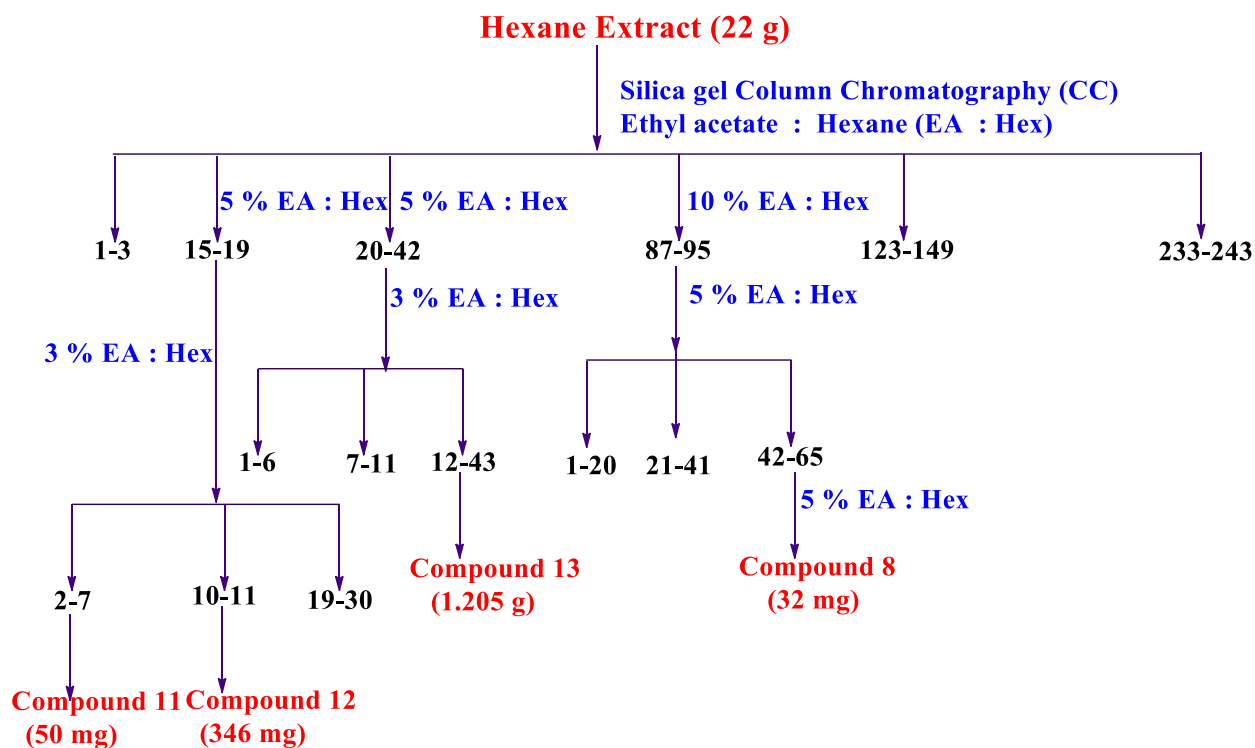
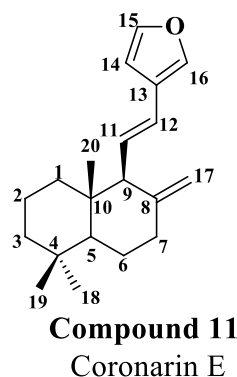


Figure 2.36. Pictorial representation for the isolation of phytochemicals from hexane extract of *C. aromatica* rhizomes

Fraction pool 15-19 obtained by eluting the column with 5% ethyl acetate in hexane showed four UV active spots along with impurities, which was further subjected to chromatographic separation using 3% ethyl acetate in hexane. The subfraction 2-7 obtained

by eluting the column with 3% ethyl acetate in hexane yielded 50 mg of the pure compound as pale yellow powder, which was labeled as compound **11**. IR spectrum of the compound showed peaks at 1160, 1070, 892, 776 cm^{-1} assigned the presence of a furan ring. The ^1H NMR spectrum (**Figure 2.37**) of the compound indicated the presence of 28 protons. A singlet at δ 7.36 integrating for two protons assigned the presence of two aromatic protons in the furan ring centered at H-15 and H-16. The third aromatic proton appeared as a singlet at δ 6.55. The presence of two olefinic protons corresponds to the presence of one doublet centered at δ 6.19 with $J = 15.5$ Hz and another doublet of doublet at δ 5.98 with $J = 16$ Hz and 10 Hz. The presence of exo-methylene protons is seen as two singlets at δ 4.76 and 4.53. The singlets at δ 0.89 (3H) and δ 0.85 (6H) suggested the compound has 3 methyl groups. ^{13}C NMR spectrum (**Figure 2.38**) confirms the presence of 20 carbon atoms in the compound. The chemical shifts at 150.3, 143.3, 139.6, 128.3, 124.5, 121.8, 107.9 and 107.7 ppm, which indicated the presence of eight carbon of the compound were located in a cyclic chain. ^{13}C NMR spectrum along with DEPT-135 spectrum confirmed the presence of exocyclic methylene group at δ 107.9. It also confirms the presence of 3 quaternary carbons at δ 150.3, 124.5 and 42.3. The mass spectrum showed the molecular ion peak at m/z 285.2225, which is $(\text{M}+\text{H})^+$ peak. Putting these spectral data together and on comparison with literature reports,^{62,63} compound **11** was confirmed to be **coronarin E**, a labdane type diterpene. To the best of our knowledge, this compound is being reported for the first time from this plant. The structure of the compound is shown below.



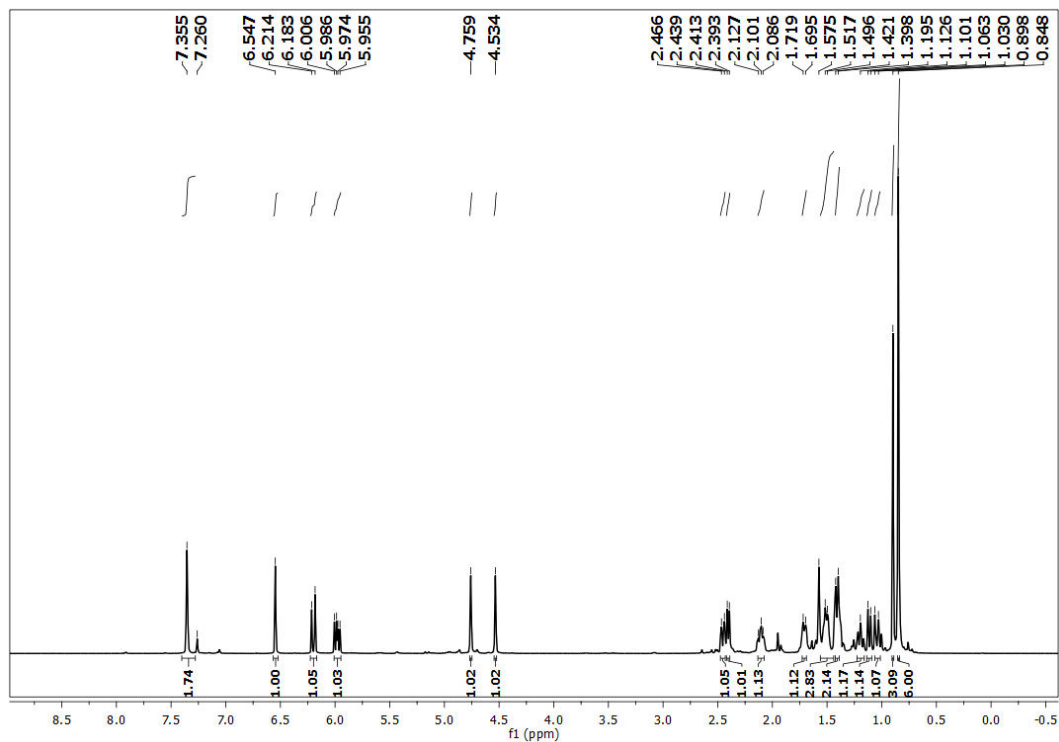


Figure 2.37. ^1H NMR spectrum of coronarin E in CDCl_3

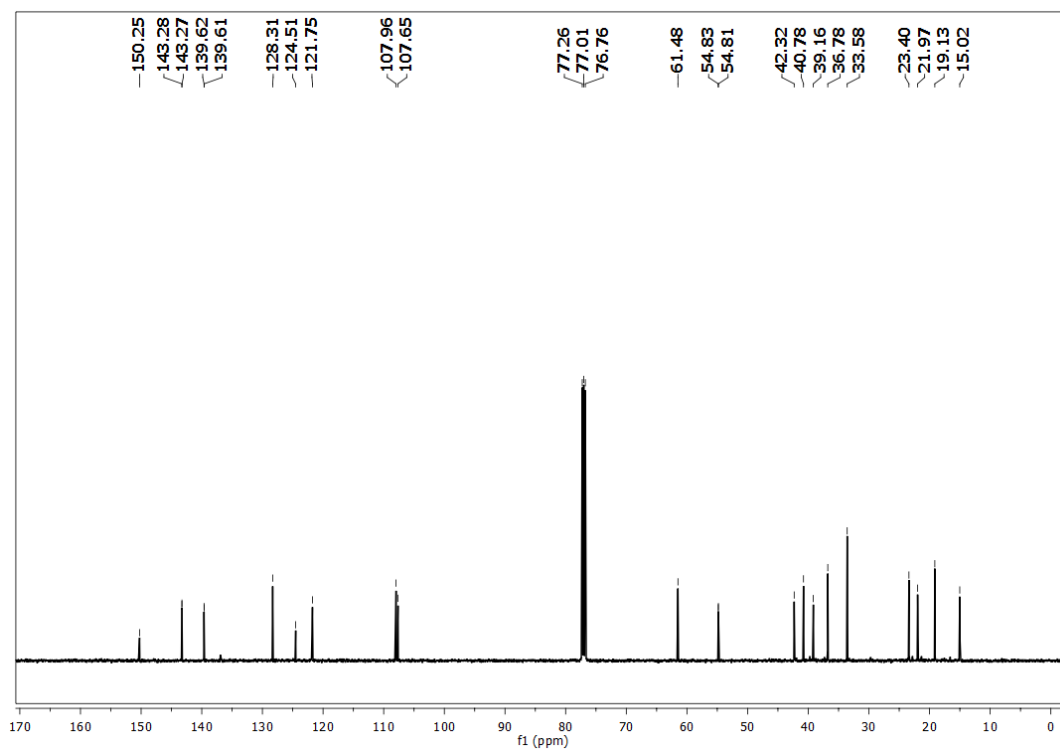
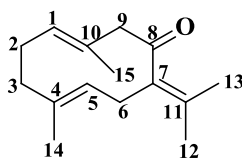


Figure 2.38. ^{13}C NMR spectrum of coronarin E in CDCl_3

The subfraction 10-11 obtained by eluting the column with 3% ethyl acetate in hexane furnished 346 mg of pure white solid, which was labeled as compound **12**. A sharp band at 1677 cm^{-1} in the IR spectrum confirms the presence of a carbonyl group. In the ^1H NMR spectrum (**Figure 2.39**) of compound **12**, the peaks at δ 1.44, 1.63, 1.73 and 1.78, each integrating for 3 protons showed the presence of four methyl groups, which was attached to three olefinic carbons. The doublets at δ 4.71 and 4.99 indicated the presence of two olefinic protons. ^{13}C NMR spectrum (**Figure 2.40**) of the compound assigned the signals for fifteen carbon atoms, which confirmed the structure as a sesquiterpenoid. The carbon signal appearing at δ 207.96 was confirming the presence of carbonyl group. Six peaks in between δ 137.26-125.40 ppm suggested the presence of six olefinic carbons in the molecule. The mass spectrum showed the molecular ion peak at m/z 241.1571, which is $(\text{M}+\text{Na})^+$ peak. Analysing all these spectral data and on comparison with literature report⁶⁴ compound **12** was confirmed to be **germacrone**. The structure of the compound is shown below.



Compound 12
Germacrone

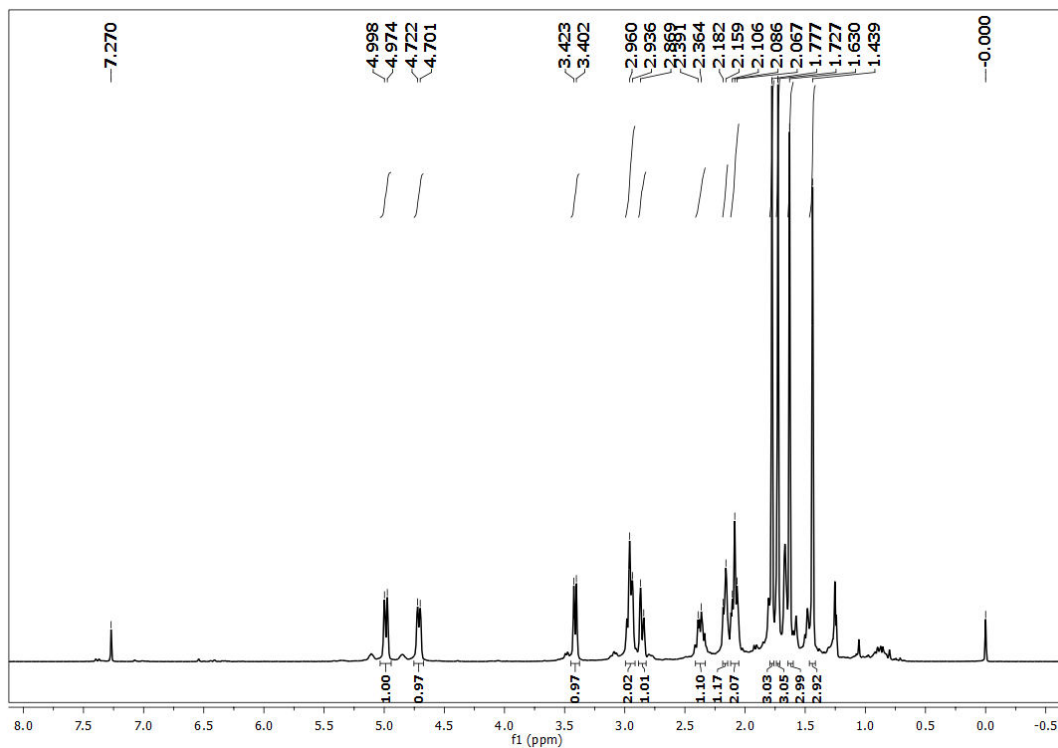


Figure 2.39. ^1H NMR spectrum of germacrone in CDCl_3

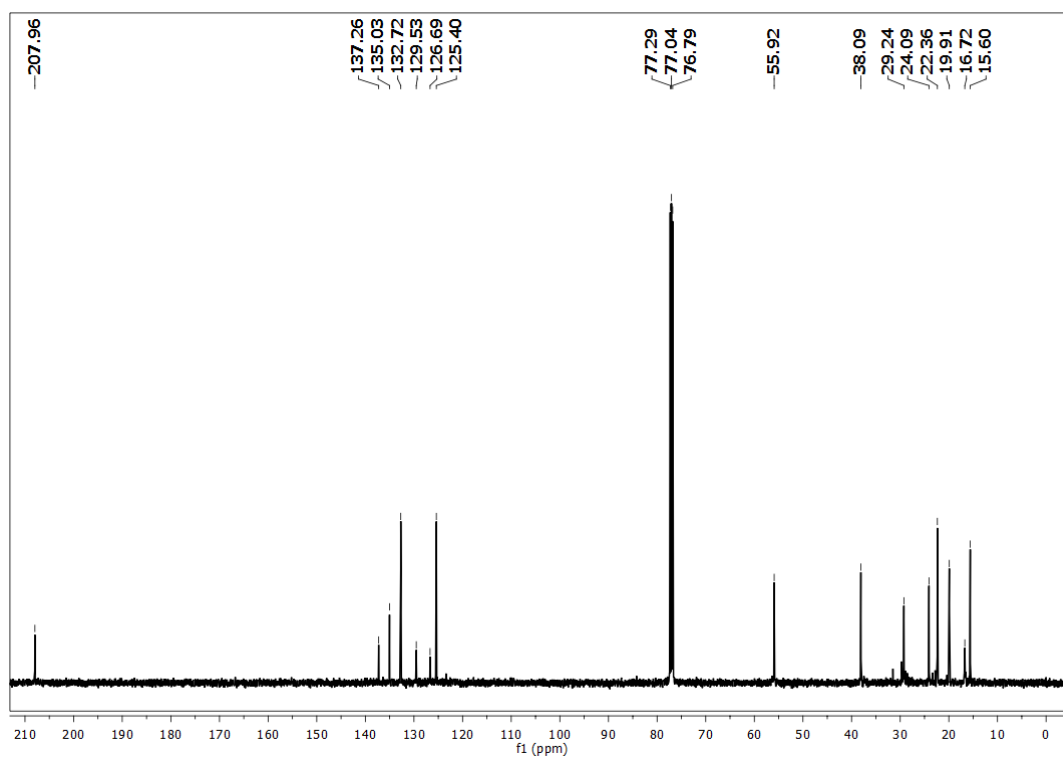
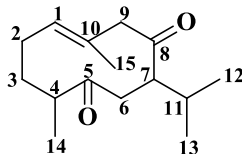


Figure 2.40. ^{13}C NMR spectrum of germacrone in CDCl_3

Fraction pool 20-42 obtained on eluting the column with 5% ethyl acetate in hexane showed a major UV active spot along with minor impurities, which on further purifications using 3% ethyl acetate in hexane furnished 1.205 g of pure compound **13** as a white solid. The IR spectrum showed a strong absorption at 1702 cm^{-1} pointed the presence of carbonyl group. ^1H NMR spectrum (**Figure 2.41**) of the compound showed a singlet resonating at δ 5.17 which is attributed the presence of olefinic proton (C-1). The four peaks at δ 0.88, 0.95, 0.98 and 1.66, integrating for 3 protons each indicated the presence of three tertiary and one quaternary methyl groups. The ^{13}C NMR spectrum (**Figure 2.42**) of the compound clearly confirms the presence of fifteen carbon atoms, which confirmed the structure as a sesquiterpenoid. The signal appearing at δ 214.3 and 211.0 confirmed the presence of two carbonyl groups. The peaks at δ 131.53 and 129.85 were attributed to the presence of two olefinic carbons. The mass spectrum showed the molecular ion peak m/z at 259.1675, which is $(\text{M}+\text{Na})^+$ peak. From all these spectral data together and comparing with literature reports,^{65,66} the compound **13** was confirmed to be **curdione**. The structure of the compound is as shown below.



Compound 13
Curdione

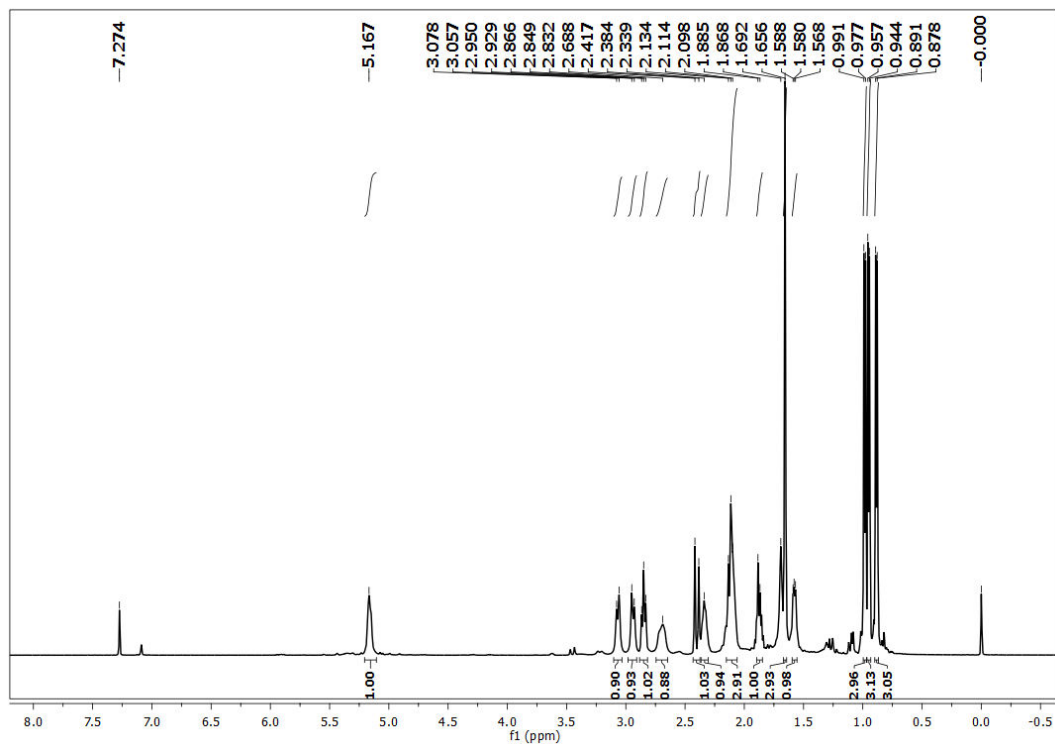


Figure 2.41. ^1H NMR spectrum of curdione in CDCl_3

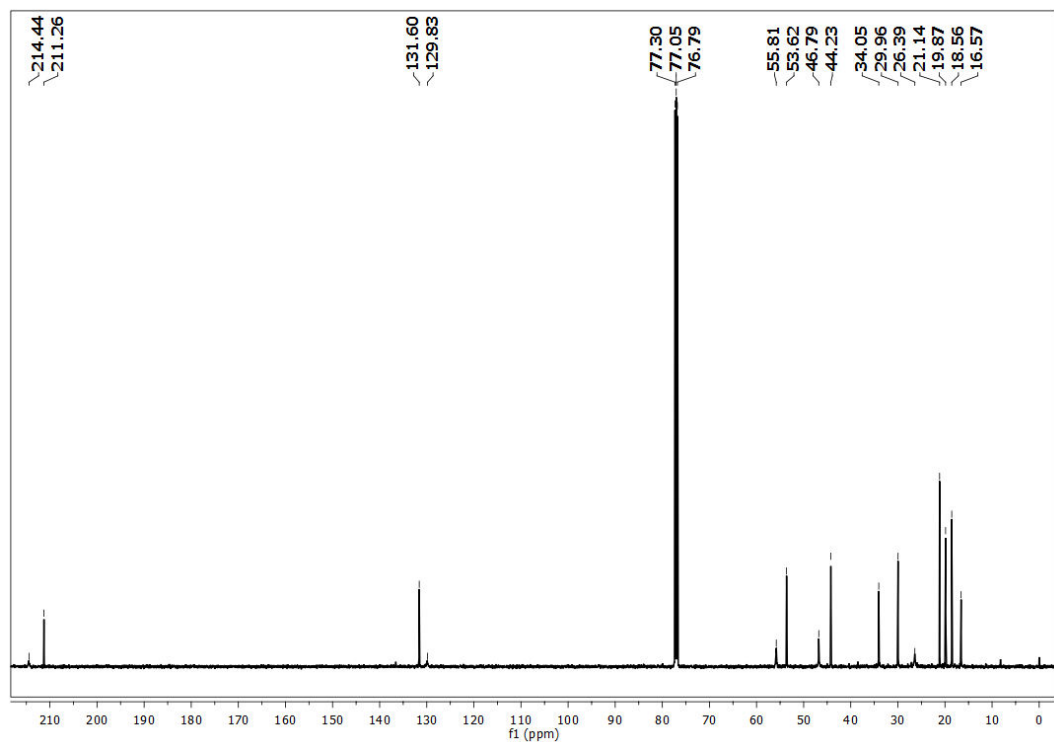


Figure 2.42. ^{13}C NMR spectrum of curdione in CDCl_3

The fourth compound isolated from the hexane extract of *C. aromatica* is **procurcumenol**, which was discussed in the section 2.7.2 (Compound 8)

2.10.3. Isolation of compounds from chloroform extract

After studying the TLC profile of chloroform extract, 25 g of the extract was subjected to column chromatographic separation. Elution was started with 100% hexane and increase in polarity was carried out by adding the amount of ethyl acetate in hexane. Final elution was carried out with 5% methanol in ethyl acetate. A total of 193 fractions of approximately 150 ml volume each were collected. TLC of each fraction was checked and those fractions whose TLC profile was alike were pooled together to get 16 major fraction pools. The pictorial representation of the isolation of phytochemicals from chloroform extract of *C. aromatica* is as shown below.

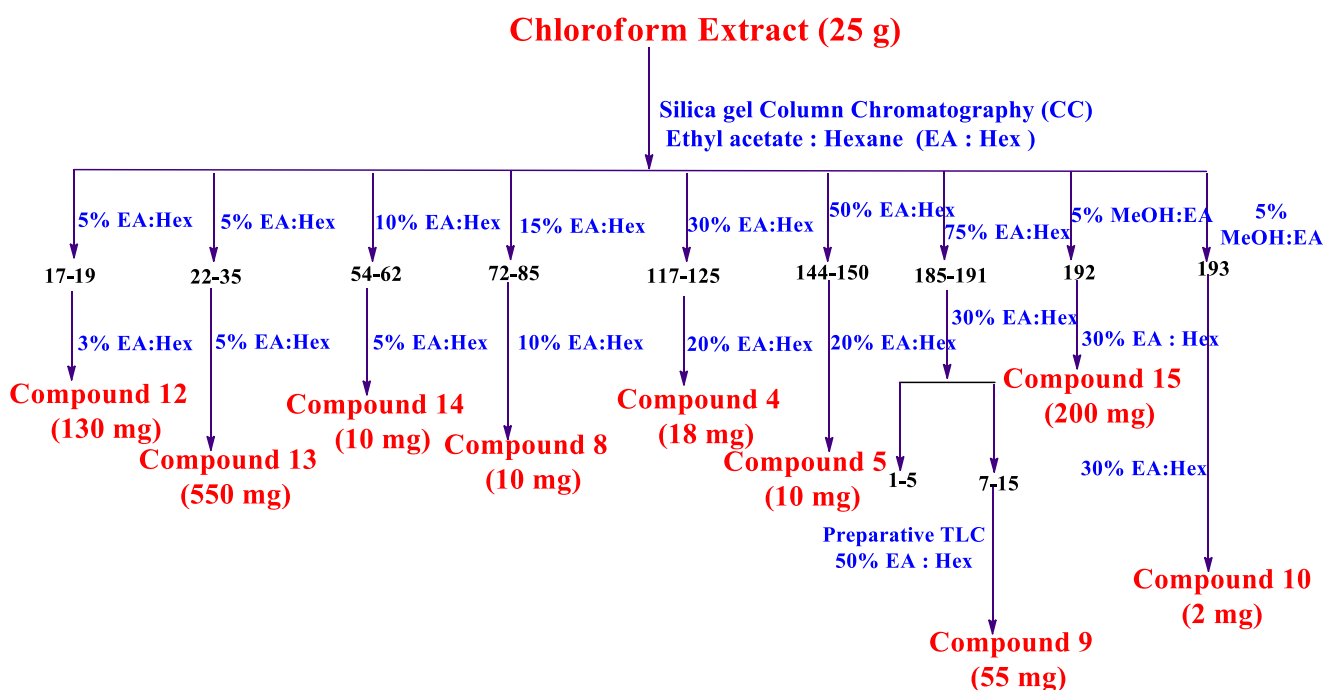
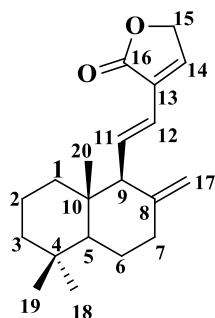


Figure 2.43. Pictorial representation for the isolation of phytochemicals from chloroform extract of *C. aromatica* rhizomes

Fraction pool 54-62 obtained by eluting the column with 10% ethyl acetate-hexane showed a single UV active spot along with minor impurities, which on further column chromatography using 5% ethyl acetate in hexane yielded 10 mg pure compound as a

colourless liquid, which was labeled as compound **14**. IR spectrum of the compound showed a sharp absorption band at 1755 cm^{-1} due to the presence of an α, β -unsaturated γ -lactone. An exo-cyclic double bond was identified by the presence of bands at $2924, 1644$ and 892 cm^{-1} . The ^1H NMR spectrum (**Figure 2.44**) of the compound showed the presence of two trans olefinic protons, which resonate at δ 6.83 and 6.04 with $J = 16\text{ Hz}$, the latter being shifted down field due to a conjugated carbonyl group. Another olefinic proton of the lactone ring appeared as a singlet at δ 7.08 (C-14). The peaks at δ 0.82 (3H), 0.80 (3H) and 0.77 (3H) attributed to the presence of three quaternary methyl groups. The ^{13}C NMR spectrum (**Figure 2.45**) of the compound confirmed the presence of 20 carbon atoms and a peak at δ 172.4, characteristics of the carbonyl group of the lactone ring. Six peaks in between δ 149.8-108.4 assigned the presence of six olefinic carbons. The mass spectrum showed the molecular ion peak m/z at 323.2001, which is $(\text{M}+\text{Na})^+$ peak. From all these spectral data along with DEPT-135 and on comparison with literature report⁶⁷ the compound **14** was confirmed to be **villosin**, which is a labdane diterpene. The structure of the compound is shown below.



Compound 14
Villosin

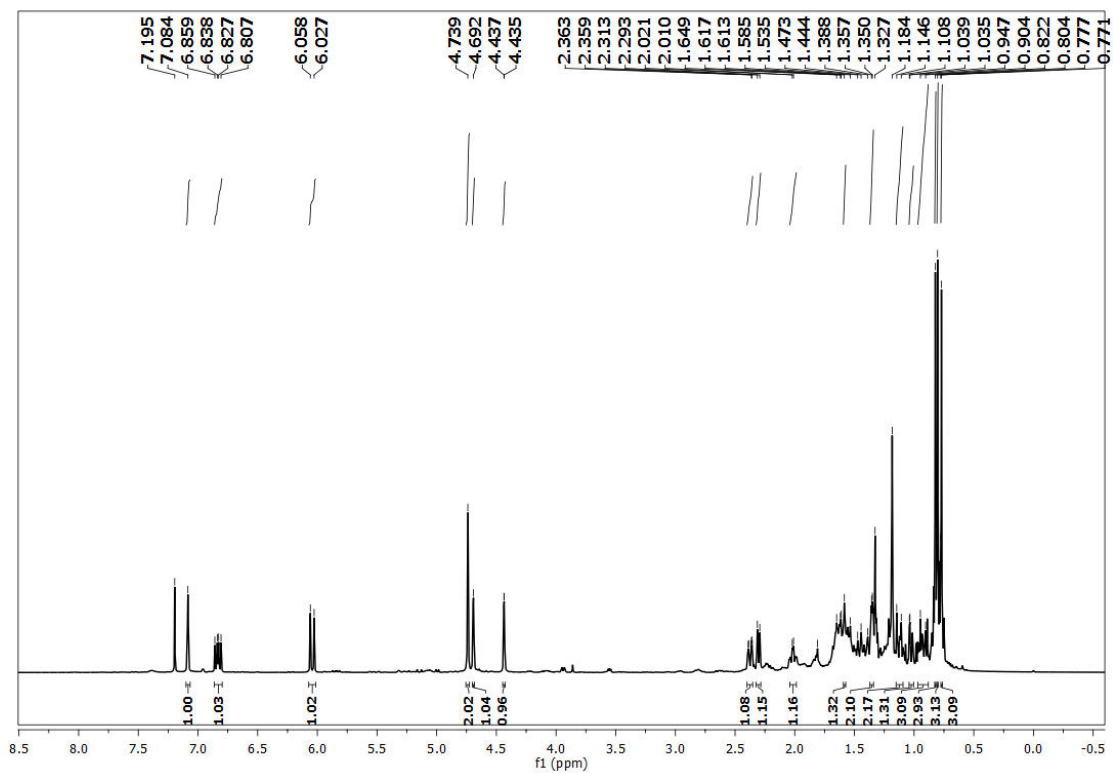


Figure 2.44. ^1H NMR spectrum of villosin in CDCl_3

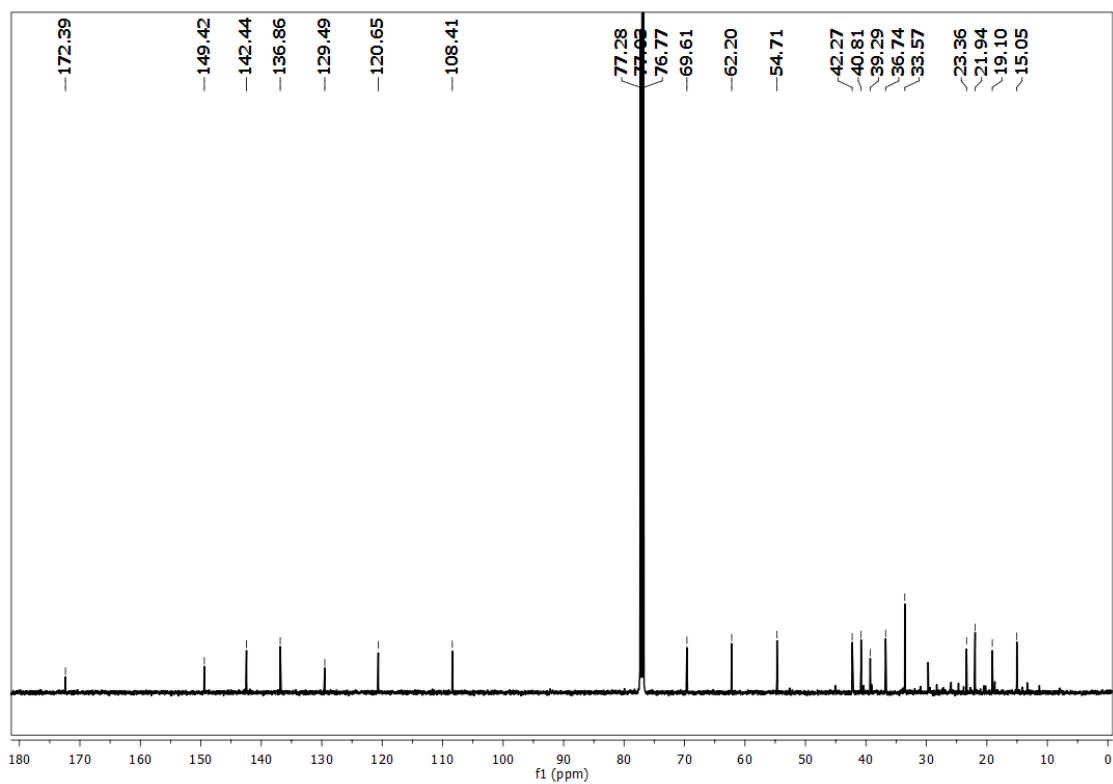
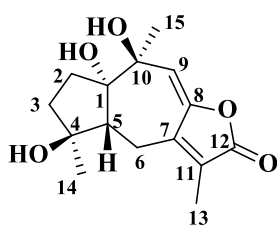


Figure 2.45. ^{13}C NMR spectrum of villosin in CDCl_3

Fraction 192 obtained by eluting the column with 50% methanol in ethyl acetate showed a single UV active spot along with minor impurities, which on further column chromatographic purification using 30% ethyl acetate in hexane yielded 200 mg of the pure compound as crystalline needles, which was labeled as compound **15**. The IR spectrum showed hydroxyl groups absorption band at 3452 cm^{-1} . The strong absorption band at 1743 cm^{-1} pointed to the presence of an α, β -unsaturated γ -lactone. The ^1H NMR spectrum (**Figure 2.47**) of the compound indicated the presence of three quaternary methyl groups at δ 1.84, 1.31 and 1.14 and a singlet seen at δ 5.48 attributed to the presence of olefinic proton centered at H-8. Three singlets at δ 5.14, 4.50 and 4.38 respectively confirmed the presence of three hydroxyl groups. The ^{13}C NMR spectrum (**Figure 2.48**) of the compound showed the presence of 15 carbon atoms, which is characteristic of a sesquiterpene. The ^{13}C NMR spectrum along with DEPT-135 confirming the presence of three quaternary methyl groups (δ 8.8, 23.4 and 25.6), three methylenes (δ 39.4, 34.5 and 21.2) and a methine group at δ 49.1 centered at C-5. The mass spectrum showed the molecular ion peak m/z at 303.1214, which is $(\text{M}+\text{Na})^+$ peak. From all these spectral data and on comparison with the literature report⁶⁸⁻⁷⁰ the compound **15** was confirmed to be **1-epihydroxy-zedoalactone D**, which is a gainane type sesquiterpene. In addition, structure was unambiguously confirmed by single crystal X-ray diffraction (**Figure 2.46**). The structure of the compound is shown below.



Compound 15
1-epihydroxy-Zedoalactone D

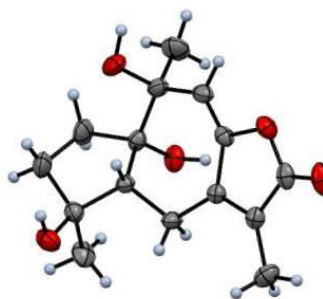


Figure 2.46. ORTEP diagram of 1-epihydroxy-zedoalactone D
CCDC Number: 2176358

This compound has been isolated first time from the plant *Curcuma wenyujin*, belonging to the *Zingiberaceae* family. To the best of our knowledge, this is the first report on the isolation of 1-epihydroxy-zedoalactone D from this plant.

In summary, a total of thirteen compounds were isolated, of which coronarin D, zerumin A, villosin and 1-epihydroxy-zedoalactone D are being reported for the first time from *C. aromatica* rhizomes.

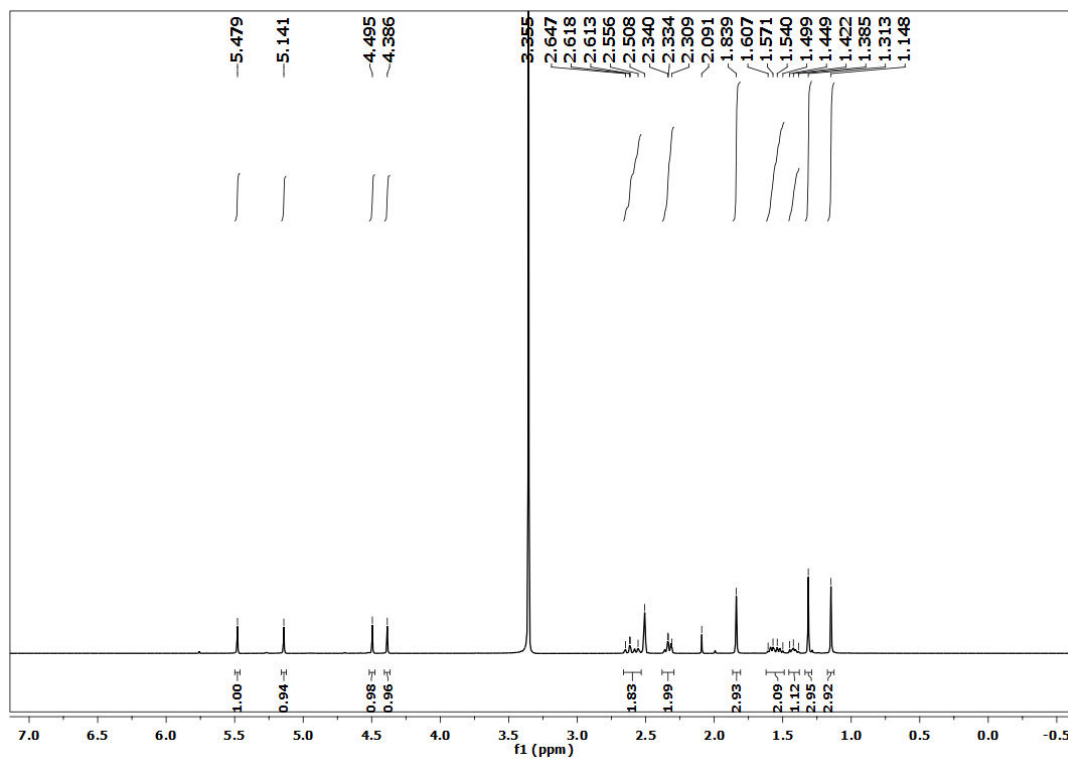


Figure 2.47. ^1H NMR spectrum of 1-epihydroxy-zedoalactone D in DMSO-d_6

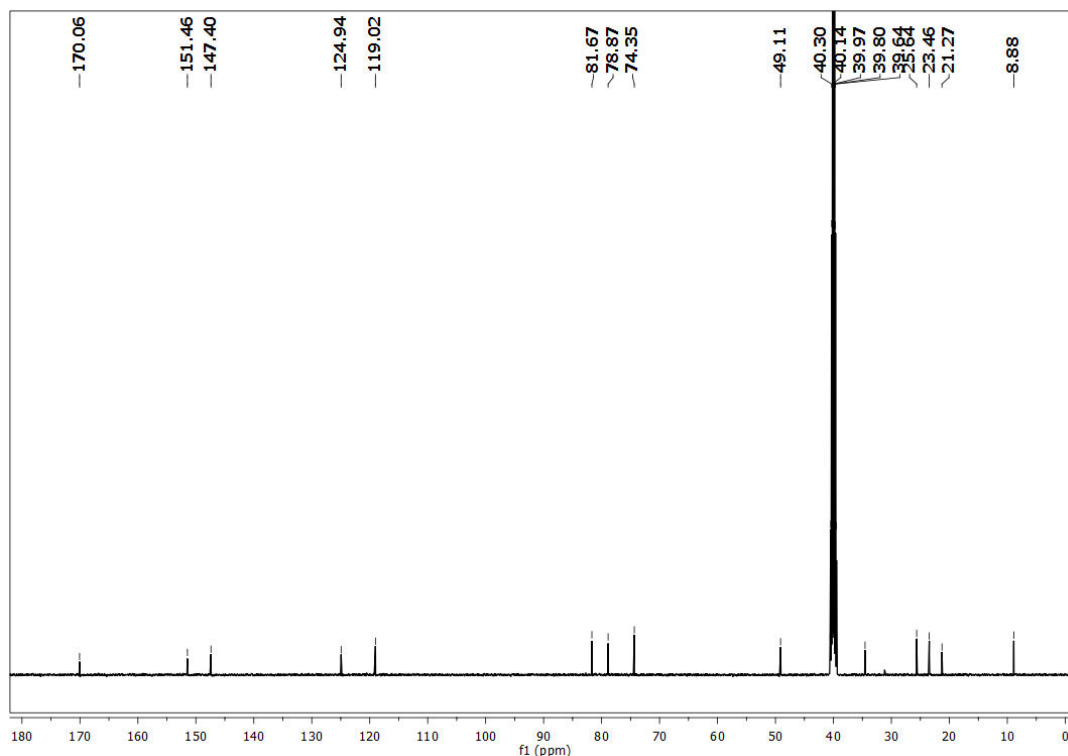


Figure 2.48. ^{13}C NMR spectrum of 1-epihydroxy-zedoalactone D in DMSO-d_6

2.11. Pancreatic lipase inhibition studies of isolated phytochemicals

The details regarding obesity and the importance of pancreatic lipase discussed in detail in chapter 1 and chapter 3. As discussed in chapter 1 and 3, obesity and pancreatic lipase are correlated. Inhibition of pancreatic lipase is the current method of choice for obesity. It was therefore of interest to study the effect of the isolated compounds on pancreatic lipase as well as to study whether they were non-toxic enough for use.

2.11.1. Cytotoxicity studies by MTT assay

In vitro toxicity of the compounds was tested by MTT assay to analyse the effect of compounds on Human liver cell lines (HepG2). The cytotoxic effect of each compound was estimated by calculating the percentage of cell viability in a dose-dependent manner ranging from 0.5-50 μM (**Figure 2.49**). The results showed that none of the tested compounds caused any sign of toxicity at all the tested concentrations.

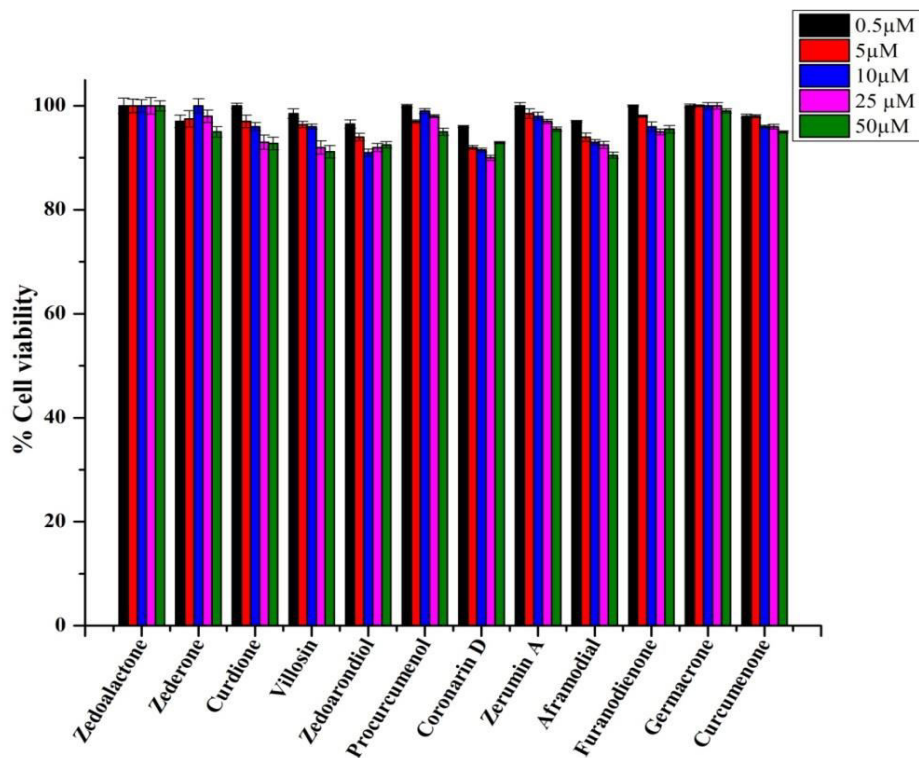


Figure 2.49. Cytotoxic study of phytochemicals by MTT assay (Cytotoxic effect of each compound is expressed as percentage of cell viability in dose dependent manner. Values are mean \pm SD of four independent experiments performed in duplicates)

2.11.2. Inhibition studies of bioactives against porcine pancreatic lipase

The isolated phytochemicals from three plants were investigated for the inhibitory activity against pancreatic lipase (PL, **Figure 2.50**). Among the tested compounds, coronarin D and zerumin A showed promising PL inhibitory activity. The compounds zederone, zedoarondiol and 1-epihydroxy-zedoalactone D also showed considerable activity to inhibit PL.

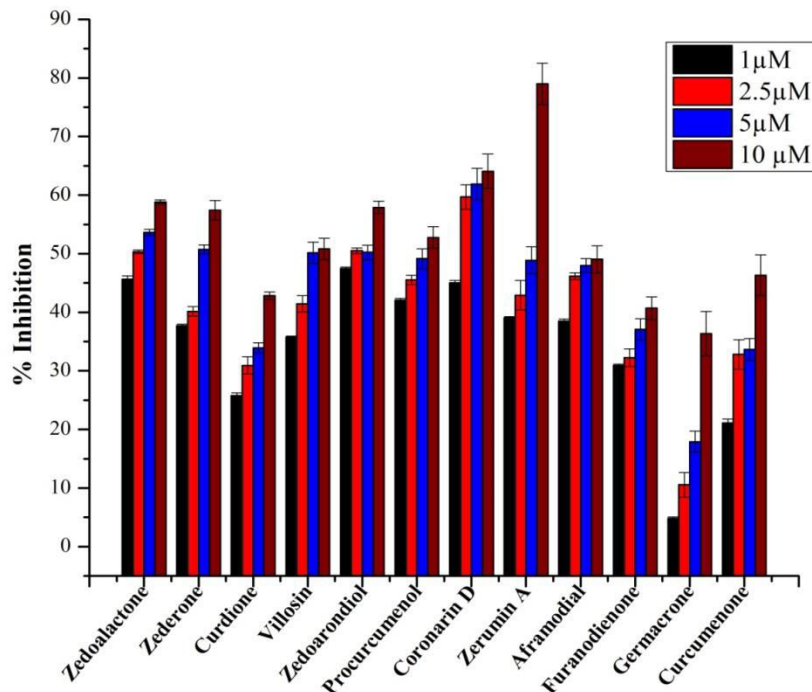


Figure 2.50. The percentage inhibition of phytochemicals against pancreatic lipase in various concentrations. (Phytochemicals are tested at concentrations 1-10 μM . Each experiment was independently performed four times in duplicates and expressed as mean \pm SD ($n = 4$))

2.12. Conclusion

Fifteen compounds were isolated from the dried rhizomes of *C. amada*, *C. malabarica* and *C. aromatica* respectively. Mainly diterpenes and sesquiterpenes are isolated and all the isolates were well characterized by using various spectroscopic techniques and on comparison with literature reports. The compound zederone was reported first time from the species *C. malabarica* and villosin, coronarin D, zerumin A, 1-epihydroxy-zedoalactone D was first time isolated from the species *C. aromatica*. The preliminary pancreatic lipase inhibition study demonstrated that the compounds coronarin D and zerumin A shows promising activity, which can be perceived further in determining the action of mechanism and identifying the potential semi-synthetic leads.

2.13. Experimental Section

2.13.1. General Experimental Details

The IR spectra were recorded on Bruker Alpha-T FT-IR spectrophotometer. The ^1H and ^{13}C NMR spectra were recorded at 500 MHz and 125 MHz respectively on Bruker AMX 500 MHz FT NMR and 125 MHz spectrometer, using deuterated chloroform (CDCl_3) or deuterated dimethylsulfoxide (DMSO-d_6) as the solvent. Tetramethylsilane (TMS) was used as internal standard, chemical shifts are expressed in δ scale in units of parts per million (ppm) downfield from tetramethylsilane (δ 0.0) and relative to the signal of solvent and coupling constants (J) in Hertz (Hz). In ^1H NMR the solvent (CDCl_3) peak appeared as a singlet at 7.26 ppm and the solvent (DMSO-d_6) peak appeared as a singlet at 2.50 ppm. In ^{13}C NMR the solvents CDCl_3 peak appeared as a triplet at 77.0 ppm and DMSO-d_6 appeared as a septet at 39.52 ppm. Abbreviations used in ^1H NMR are s-singlet, d-doublet, t- triplet, dd- doublet of doublet, brs-broad singlet and m-multiplet. Mass spectra were recorded under HRMS (ESI) at 60,000 resolutions using Thermo Scientific Exactive Orbitrap mass spectrometer. TLC was performed on Merck silica gel 60 F₂₅₄ aluminium sheets. The spots were first checked with UV light and second in the iodine chamber. Column chromatographic techniques were used for the isolation of natural compounds. All the solvents were commercial grade and were purified by distillation before use. Column chromatography was carried out using 100-200 mesh silica gel (Merck). Specific-rotation was recorded using Jasco P-2000 polarimeter. Melting points were determined on a Stuart SMP30 digital melting point apparatus and are uncorrected. Heidolph rotary evaporator was used for the removal of solvents. Hep G2 cell lines, Human liver carcinoma-derived cell lines were purchased from American Type Cell Culture (ATCC, Manassas, VA, USA), Pancreatic lipase, *p*-nitrophenyl butyrate, olive oil, taurochenodeoxycholate, taurocholate, cholesterol, L- α -phosphatidylcholine, calcium acetate, orlistat (Sigma Aldrich, USA) were used for biological study.

2.13.1.1. GC-MS profiling

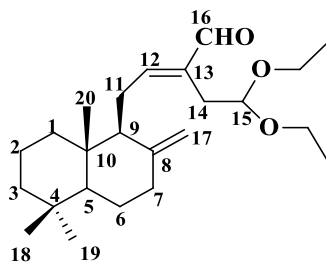
GC-MS analysis was performed on a GCMS-TQ8030 Shimadzu (Tokyo, Japan) instrument. The essential oil was dissolved in hexane solvent. Then, 1 μl of sample was injected to GC

with nonpolar Rxi 5Sil MS capillary column, full scan mode, injector mode-splitless, quadrapole mass selective detector (MSD), injection temperature 250 °C, GC-MS interface temperature 250 °C. Helium was employed as carrier gas, at a pressure of 57.5 KPa and flow rate was 1 ml/min. Mass spectra were detected at 70 eV. Temperature programming was set as follows: column temperature was started from 60 °C for 2 min and linearly increased by 5 °C/min to 200 °C for 2 min, after that it was increased by 3 °C/min to 220 °C for 1 min, further it was increased by 6 °C/min. to 250 °C for 7 min. The total instrument run time was 50 min. The mass m/z was scanned for a range of 100 - 1000. The chemical constituents were identified by matching their mass spectra and GC retention indices with spectra of reference compounds in NIST and WILEY mass spectral library. The relative amounts of individual components were expressed as percentage peak areas relative to total peak area.

2.13.2. Spectral data of the isolated compounds from *C. amada* rhizomes

2.13.2.1. Compound 1 ((*E*)-15,15-Diethoxyabda-8 (17),12-diene-16-al)

The compound 1 obtained from the fraction pool (29-36) of chloroform extract was confirmed to be (*E*)-15,15-Diethoxyabda-8 (17),12-diene-16-al based on the spectral data obtained along with HRMS and on comparison with literature reports. The obtained spectral data of the compound is as shown below.

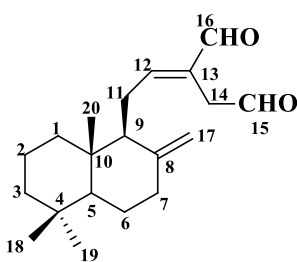


FT-IR (NaCl,	:	2931, 2844, 1685, 1642, 1560, 1459,
ν_{\max} , cm^{-1})		1367, 1164, 1059, 890.
^1H NMR (500	:	δ 9.34 (<i>s</i> , 1H, H-16), 6.56 (<i>t</i> , $J = 6.2$ Hz,
MHz, CDCl_3)		1H, H-12), 4.83 (<i>s</i> , 1H, H-17), 4.42 (<i>s</i> ,
		1H, H-17), 4.54 (<i>t</i> , $J = 5.5$ Hz, 1H, H-
		15), 3.70-3.66 (<i>m</i> , 2H, ethoxy- CH_2 -),
		3.49-3.46 (<i>m</i> , 2H, ethoxy- CH_2 -), 2.50
		and 2.63 (<i>m</i> , 2H, H-11), 2.58
		(<i>m</i> , 2H, H-14), 2.43-1.25 (<i>m</i> , 12H), 1.16
		(<i>dt</i> , 6H, ethoxy- CH_3), 0.89 (<i>s</i> , 3H, H-18),
		0.82 (<i>s</i> , 3H, H-19), 0.74 (<i>s</i> , 3H, H-20)
^{13}C NMR (125	:	δ 195.1 (C-16), 160.2 (C-12), 148.3 (C-

MHz, CDCl ₃)	8), 138.4 (C-13), 108.0 (C-17), 102.2 (C-15), 62.9 and 62.8 (ethoxy-CH ₂ -), 56.5 (C-9), 55.4 (C-5), 42.1 (C-3), 39.5 (C-10), 39.2 (C-1), 37.9 (C-7), 33.6 (C-4), 33.6 (C-18), 30.2 (C-14), 24.7 (C-11), 24.1 (C-6), 21.7 (C-19), 19.3 (C-2), 15.4 and 15.3 (ethoxy-CH ₃), 14.4 (C-20)
Mass (HRMS)	: 399.2863 (M+Na) ⁺ (calcd for C ₂₄ H ₄₀ O ₃ Na, 399.2875)

2.13.2.2. Compound 2 ((*E*)-Labda-8(17),12-diene-15,16-dial)

The compound 2 obtained from the fraction pool (37-103) of chloroform extract was confirmed to be (*E*)-labda-8(17),12-diene-15,16-dial based on the spectral data obtained along with HRMS and on comparison with literature reports. The obtained spectral data of the compound is as shown below.



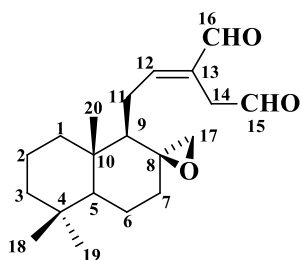
m.p. (°C)	: 54.5-55.5 °C
FT-IR (NaCl, v _{max} , cm ⁻¹)	: 2931, 2840, 1727, 1684, 1642, 1459, 1367, 890
¹ H NMR (500 MHz, CDCl ₃)	: δ 9.63 (<i>t</i> , <i>J</i> = 1.5 Hz, 1H, H-15), 9.41 (<i>s</i> , 1H, H-16), 6.76 (<i>t</i> , <i>J</i> = 6.5 Hz, 1H, H-12), 4.86 (<i>d</i> , <i>J</i> = 1.5 Hz, 1H, H-17), 4.37 (<i>d</i> , 1H, <i>J</i> = 1 Hz H-17), 3.42 (ABq, <i>J</i> = 16.5 Hz, 2H, H-14), 2.53-2.30 (<i>m</i> , 3H), 2.04-1.0 (<i>m</i> , 11H), 0.89 (<i>s</i> , 3H, H-18), 0.82 (<i>s</i> , 3H, H-19), 0.73 (<i>s</i> , 3H, H-20)
¹³ C NMR (500 MHz, CDCl ₃)	: δ 197.4 (C-15), 193.6 (C-16), 159.9 (C-12), 148.1 (C-8), 134.9 (C-13), 107.9 (C-17), 56.5 (C-9), 55.4 (C-5), 41.9 (C-3), 39.6 (C-10), 39.4 (C-14), 39.2 (C-1), 37.9 (C-7),

33.6 (C-4), 33.6 (C-18) 24.7 (C-11), 24.1 (C-6), 21.7 (C-19), 19.3 (C-2), 14.4(C-20)

Mass (HRMS) : 325.2132 (M+Na)⁺ (calcd for C₂₀H₃₀O₂Na, 325.2143)

2.13.2.3. Compound 3 (Aframodial)

The compound 3 obtained from the fraction pool (104-123) of chloroform extract was confirmed to be aframodial based on the spectral data obtained along with HRMS and on comparison with literature reports. The obtained spectral data of the compound is as shown below.



FT-IR (NaCl, : 2926, 2854, 1729, 1684, 1640, 1386, 1015
v_{max}, cm⁻¹)

¹H NMR (500 : δ 9.58 (*s*, 1H, H-15), 9.43 (*s*, 1H, H-16),
MHz, CDCl₃) 6.86 (*t*, *J* = 7.5 Hz, 1H, H-12), 3.38 (*s*, 2H,
H-14), 2.70-2.69 (*m*, 1H, H-17), 2.56 (*d*, *J*
= 4 Hz, 1H, H-17), 2.16-1.03 (*m*, 14H),
0.91 (*s*, 3H, H-20), 0.86 (*s*, 3H, H-18), 0.85
(*s*, 3H, H-19)

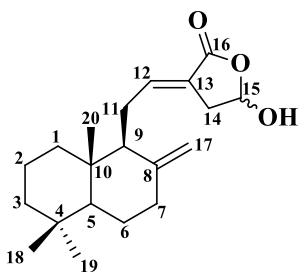
¹³C NMR (500 : 197.7 (C-15), 193.8 (C-16), 160.5 (C-12),
MHz, CDCl₃) 133.7 (C-13), 58.9 (C-8), 54.9 (C-9), 54.4
(C-5), 50.5 (C-17), 41.7 (C-3), 40.2 (C-10),
39.6 (C-7), 39.2 (C-1), 36.0 (C-14), 33.5
(C-4), 33.4 (C-18), 22.5 (C-11), 21.7 (C-
19), 21.6 (C-6), 18.6 (C-2), 14.3 (C-20)

Mass (HRMS) : 341.208 (M+Na)⁺ (calcd for C₂₀H₃₀O₃Na, 341.2093)

2.13.2.4. Compound 4 (Coronarín D)

The compound 4 obtained from the fraction pool (191-216) of chloroform extract was confirmed to be coronarín D based on the spectral data obtained along with HRMS and on

comparison with literature reports. The obtained spectral data of the compound is as shown below.

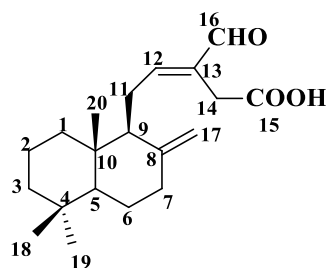


FT-IR (NaCl, ν_{\max} , cm^{-1})	: 3363, 3087, 2933, 2844, 1737, 1675, 1644, 1459, 1387
^1H NMR (500 MHz, CDCl_3)	: δ 6.77 (<i>t</i> , $J = 6.5$ Hz, 1H, H-12), 5.93 (<i>s</i> , 1H, H-15), 4.83 (<i>s</i> , 1H, H-17), 4.38 (<i>s</i> , 1H, H-17), 3.67 (<i>br s</i> , 1H, -OH attached to C-15), 3.03 (<i>m</i> , $J = 14$ Hz, 1H, H-14), 2.74 (<i>m</i> , 1H, H-14), 2.40-2.37 (<i>m</i> , 2H), 2.20 (<i>m</i> , 1H), 2.02- 1.08 (<i>m</i> , 12H), 0.88 (<i>s</i> , 3H, H-18), 0.82 (<i>s</i> , 3H, H-19), 0.72 (<i>s</i> , 3H, H-20)
^{13}C NMR (125 MHz, CDCl_3)	: δ 169.6 (C-16), 148.1 (C-8), 143.7 (C-12), 123.9 (C-13), 107.6 (C-17), 95.6 (C-15), 56.1 (C-9), 55.3 (C-5), 41.9 (C-3), 39.5 (C-10), 39.3 (C-14), 39.3 (C-1), 37.8 (C-7), 33.6 (C-18), 33.5 (C-4), 25.5 (C-11), 24.1 (C-6), 21.7 (C-19), 19.3 (C-2), 14.3 (C-20)
Mass (HRMS)	: 341.2089 ($\text{M}+\text{Na}$) ⁺ (calcd for $\text{C}_{20}\text{H}_{30}\text{O}_3\text{Na}$, 341.2093)

2.13.2.5. Compound 5 (Zerumin A)

The compound 5 obtained from the fraction pool (227-266) of chloroform extract was confirmed to be zerumin A based on the spectral data obtained along with HRMS and on comparison with literature reports. The obtained spectral data of the compound is as shown below.

FT-IR (NaCl, ν_{\max} , cm^{-1})	: 2928, 2828, 2867, 1713, 1689, 1643, 1389, 890
--	---



$^1\text{H NMR}$ (500 MHz, CDCl_3) : δ 9.37 (*s*, 1H, H-16), 6.71 (*t*, $J = 6.5$ Hz, 1H, H-12), 4.86 (*s*, 1H, H-17), 4.40 (*s*, 1H, H-17), 3.36 (*dd*, $J_1 = J_2 = 18$ Hz, 2H, H-14), 2.59-1.05 (*m*, H-14), 0.89 (*s*, 3H, H-18), 0.832 (*s*, 3H, H-19), 0.75 (*s*, 3H, H-20)

$^{13}\text{C NMR}$ (125 MHz, CDCl_3) : δ 193.6 (C-16), 175.8 (C-15), 159.4 (C-12), 148.0 (C-8), 135.6 (C-13), 107.9 (C-17), 56.4 (C-9), 55.4 (C-5), 41.9 (C-3), 39.6 (C-10), 39.2 (C-1), 37.8 (C-7), 33.6 (C-4), 33.6 (C-18), 29.6 (C-14), 24.6 (C-11), 24.1 (C-6), 21.7 (C-19), 19.3 (C-2), 14.4 (C-20)

Mass (HRMS) : 341.2089 ($\text{M}+\text{Na}^+$) (calcd for $\text{C}_{20}\text{H}_{30}\text{O}_3\text{Na}$, 341.2093)

2.13.3. Spectral data of the isolated compounds from *C. malabarica* rhizomes

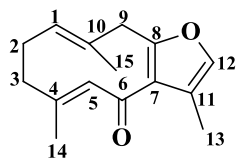
2.13.3.1. Compound 6 (Furanodienone)

The compound 6 obtained from the fraction pool (16-67) of methanol extract was confirmed to be furanodienone based on the spectral data obtained along with HRMS and on comparison with literature reports. The obtained spectral data of the compound is as shown below.

m.p. ($^{\circ}\text{C}$) : 61.5-63.5 $^{\circ}\text{C}$

FT-IR (NaCl) : 2932, 1648, 1612, 1527, 1237, 766

ν_{max} , cm^{-1})

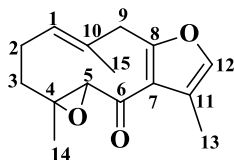


$^1\text{H NMR}$ (500 MHz, CDCl_3) : 7.07 (*s*, 1H, H-12), 5.80 (*s*, 1H, H-5), 5.18 (*br dd*, $J = 4.5$ Hz, 11.5 Hz, 1H, H-1), 3.70 (*br s*, 2H, H-9), 2.46 (*dt*, $J = 3.5$ Hz, 11 Hz, 1H, H-3), 2.30 (*m*, 1H, H-2), 2.17 (*dd*, $J = 3.5$ Hz, 12 Hz, 1H, H-2), 2.13 (*s*, 3H, H-13),

	1.99 (s, 3H, H-14), 1.30 (s, 3H, H-15), 1.88 (m, 1H, H-3)
^{13}C NMR (125 MHz, CDCl_3)	: 189.7 (C-6), 156.5 (C-8), 145.70 (C-4), 138.1 (C-12), 135.3 (C-10), 132.4 (C-5), 130.5 (C-1), 123.7 (C-11), 122.1 (C-7), 41.6 (C-3), 40.6 (C-9), 26.4 (C-2), 18.9 (C-14), 15.7 (C-15), 9.5 (C-13).
Mass (HRMS)	: 253.1202 ($\text{M}+\text{Na}^+$) (calcd for $\text{C}_{15}\text{H}_{18}\text{O}_2\text{Na}$, 253.1204)

2.13.3.2. Compound 7 (Zederone)

The compound 7 obtained from the fraction pool (90-119) of methanol extract was confirmed to be zederone based on the spectral data obtained along with HRMS and on comparison with literature reports. The obtained spectral data of the compound is as shown below.

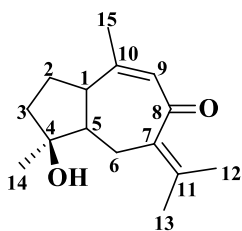


m.p. ($^{\circ}\text{C}$)	: 153.9-154.9 $^{\circ}\text{C}$
FT-IR (NaCl, ν_{max} , cm^{-1})	: 2930, 1665, 1530, 1404, 1237, 931
^1H NMR (500 MHz, CDCl_3)	: 7.09 (s, 1H, H-12), 5.49 (d, $J = 11.5$ Hz, 1H, H-1), 3.82 (s, 1H, H-5), 3.76 (d, $J = 16.5$ Hz, 1H, H-9), 3.69 (d, $J = 16.5$ Hz, 1H, H-9), 2.53 (m, 1H, H-2), 2.30 (brd, $J = 13$ Hz, 1H, H-3), 2.24 (brd, $J = 13$ Hz, 1H, H-2), 2.12 (s, 3H, H-15), 1.60 (s, 3H, H-13), 1.35 (s, 3H, H-14), 1.28 (m, 1H, H-3).
^{13}C NMR (125 MHz, CDCl_3)	: 192.2 (C-6), 157.1 (C-8), 138.1(C-12), 131.2 (C-1), 131.0 (C-10), 123.2 C-11), 122.2 (C-7), 65.5 (C-5), 63.9 (C-4), 41.9 (C-9), 37.9 (C-3), 24.6 (C-2), 15.7(C-13), 15.2 (C-15), 10.3 (C-14).
Mass (HRMS)	: 269.1152 ($\text{M}+\text{Na}^+$) (calcd for $\text{C}_{15}\text{H}_{18}\text{O}_3\text{Na}$

269.1154)

2.13.3.3. Compound 8 (Procurcumenol)

The compound 8 obtained from the fraction pool (90-119) of methanol extract was confirmed to be procurcumenol based on the spectral data obtained along with HRMS and on comparison with literature reports. The obtained spectral data of the compound is as shown below.

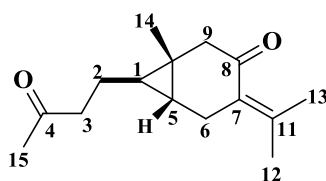


FT-IR (NaCl, ν_{\max} , cm^{-1})	: 3427, 2926, 1645, 1445, 1377
^1H NMR (500 MHz, CDCl_3)	: 5.81 (<i>d</i> , $J = 1$ Hz, 1H, H-9), 2.53 (<i>d</i> , $J = 15$ Hz, 1H, H-6), 2.31 (<i>d</i> , $J = 10$ Hz, 1H, H-1), 2.11 (<i>t</i> , $J = 15$ Hz, 1H, H-6), 1.98 (<i>s</i> , 1H, H-5), 1.91-1.86 (<i>m</i> , 2H, H-3), 1.62-1.58 (<i>m</i> , 2H, H-2), 1.81 (<i>s</i> , 3H, H-14), 1.71 (<i>s</i> , 3H, H-13), 1.68 (<i>s</i> , 3H, H-12), 1.54 (<i>s</i> , 3H, H-15)
^{13}C NMR (125 MHz, CDCl_3)	: 199.1 (C-8), 154.9 (C-10), 136.8 (C-7), 136.2 (C-11), 129.2 (C-9), 80.3 (C-4), 53.9 (C-5), 50.5 (C-1), 39.9 (C-3), 28.6 (C-6), 26.9 (C-2), 24.3 (C-15), 23.4 (C-14), 22.4 (C-13), 21.2 (C-12)
Mass (HRMS)	: 257.1522 ($\text{M}+\text{Na}$) ⁺ (calcd for $\text{C}_{15}\text{H}_{22}\text{O}_2\text{Na}$, 257.1517)

2.13.3.4. Compound 9 (Curcumenone)

The compound 9 obtained from the fraction pool (131-145) of methanol extract was confirmed to be curcumenone based on the spectral data obtained along with HRMS and on comparison with literature reports. The obtained spectral data of the compound is as shown below.

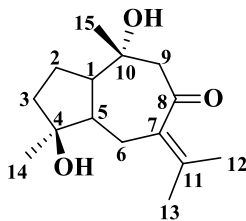
FT-IR (NaCl, ν_{\max} , cm^{-1}) : 2960, 1766, 1701, 1662, 1475, 1370, 1014



	$\nu_{\max}, \text{cm}^{-1}$	
$^1\text{H NMR}$ (500 MHz, CDCl_3)		: 0.38 (<i>q</i> , $J = 7$ Hz, 12 Hz, 1H, H-1), 0.60 (<i>q</i> , $J = 7$ Hz, 1H, H-5), 1.05 (<i>s</i> , 3H, H-15), 1.18 (<i>s</i> , 2H), 1.52-1.54 (<i>m</i> , 2H, H-2), 1.72 (<i>s</i> , 3H, H-13), 2.02 (<i>s</i> , 3H, H-12), 2.06 (<i>s</i> , 3H, H-14), 2.40 (<i>t</i> , $J = 7$ Hz, 15 Hz, 2H), 2.46 (<i>d</i> , $J = 8$ Hz, 2H, H-3), 2.74 (<i>br s</i> , 2H, H-6)
$^{13}\text{C NMR}$ (125 MHz, CDCl_3)		: 208.7 (C-4), 201.7 (C-8), 147.4 (C-11), 128.1 (C-7), 48.9 (C-9), 43.9 (C-3), 30.0 (C-14), 28.0 (C-6), 24.2 (C-1), 24.2 (C-5), 23.4 (C-12), 23.4 (C-13), 23.4 (C-2) 20.1 (C-10), 19.0 (C-15)
Mass (HRMS)		: 257.1523 ($\text{M}+\text{Na}^+$) (calcd for $\text{C}_{15}\text{H}_{24}\text{O}_2\text{Na}$, 257.1517)

2.13.3.5. Compound 10 (Zedoaronidiol)

The compound 10 obtained from the fraction pool (303-329) of methanol extract was confirmed to be curcumenone based on the spectral data obtained along with HRMS and on comparison with literature reports. The obtained spectral data of the compound is as shown below.



FT-IR (NaCl)		: 3405, 1660, 1442, 1345, 931
	$\nu_{\max}, \text{cm}^{-1}$	
$^1\text{H NMR}$ (500 MHz, CDCl_3)		: 2.96 (<i>d</i> , $J = 13$ Hz, 1H, H-9), 2.82 (<i>d</i> , $J = 15$ Hz, 1H, H-6), 2.59 (<i>d</i> , $J = 12.5$ Hz, 1H, H-9), 2.0-1.95 (<i>m</i> , 2H), 1.79-1.67 (<i>m</i> , 4H, H-2, H-3), 1.41-1.25 (<i>m</i> , 3H), 1.93 (<i>s</i> , 3H, H-12), 1.83 (<i>s</i> , 3H, H-13), 1.20 (<i>s</i> , 3H, H-14), 1.18 (<i>s</i> , 3H, H-15)
$^{13}\text{C NMR}$ (125 MHz, CDCl_3)		: 202.9 (C-8), 142.2 (C-11), 134.6 (C-7), 80.0 (C-4), 72.8 (C-10), 59.8 (C-9), 55.9 (C-1),

52.0 (C-5), 39.7 (C-6), 28.5 (C-3), 22.9 (C-2), 22.7 (C-14), 22.2 (C-13), 21.9 (C-12), 20.6 (C-15)

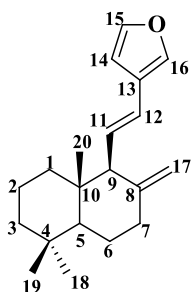
Mass (HRMS) : 275.1627 (M+Na)⁺ (calcd for C₁₅H₂₄O₃Na, 275.1623)

Optical activity : $[\alpha]_D^{25} = -32.8$ °C (c 0.5 MeOH)

2.13.4. Spectral data of the isolated compounds from hexane extract of *C. aromatica* rhizomes

2.13.4.1. Compound 11 (Coronarin E)

The compound 11 obtained from the fraction pool (15-19) of hexane extract was confirmed to be coronarin E based on the spectral data obtained along with HRMS and on comparison with literature reports. The obtained spectral data of the compound is as shown below.



FT-IR (NaCl, ν_{\max} , cm⁻¹) : 2928, 1766, 1643, 1160, 980, 892, 776, 732

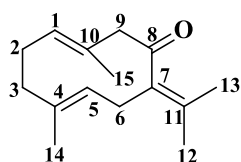
¹H NMR (500 MHz, CDCl₃) : 7.36 (s, 2H, H-15, H-16), 6.55 (s, 1H, H-14), 6.19 (d, *J* = 15.5 Hz, 1H, H-12), 5.98 (dd, *J* = 16 Hz, 10 Hz, 1H, H-11), 4.76 (s, 1H, H-17β), 4.53 (s, 1H, H-17α), 2.45 (d, *J* = 13.5 Hz, 1H, H-7β), 2.40 (d, *J* = 10 Hz, 1H, H-9), 2.10 (m, 1H, H-7α), 1.71 (m, 1H), 1.51 (m, 3H), 1.41 (m, 2H), 1.19 (m, 1H), 1.11 (d, *J* = 12.5 Hz, 1H, H-5), 1.05 (m, 1H), 0.89 (s, 3H, H-18), 0.85 (s, 2x3H, H-19, H-20)

¹³C NMR (125 MHz, CDCl₃) : 150.3 (C-8), 143.3 (C-15), 139.6 (C-16), 128.3 (C-11), 124.5 (C-13), 121.8 (C-12), 107.9 (C-17), 107.7 (C-14), 61.5 (C-9), 54.8 (C-5), 42.3 (C-3), 40.8 (C-1), 39.2 (C-10), 36.8 (C-7), 33.6 (C-4, C-18), 23.4 (C-6), 21.9 (C-19), 19.1 (C-2), 15.0 (C-20)

Mass (HRMS) : 285.2225 (M+H)⁺ (Calcd for C₂₀H₂₉O, 285.2218)

2.13.4.2. Compound 12 (Germacrone)

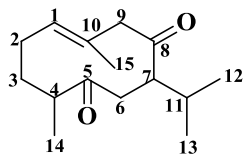
The compound 12 obtained from the fraction pool (15-19) of hexane extract was confirmed to be germacrone based on the spectral data obtained along with HRMS and on comparison with literature reports. The obtained spectral data of the compound is as shown below.



m.p. (°C) : 53.5-54.5 °C
 FT-IR (NaCl, ν_{\max} , cm⁻¹) : 2922, 1677, 1442, 1066, 750
¹H NMR (500 MHz, CDCl₃) : 1.44 (s, 3H, H-14), 1.63 (s, 3H, H-15), 1.73 (s, 3H, H-13), 1.78 (s, 3H, H-12), 2.06-2.39 (m, 4H, H-2, H-3), 2.86 (br d, *J* = 13.5 Hz, 1H, H-6β), 2.94-2.98 (m, 2H, H-6α, 9α), 3.41 (d, *J* = 10.5 Hz, 1H, H-9β), 4.71 (br d, *J* = 10.5 Hz, 1H, H-5), 4.99 (d, *J* = 12 Hz, 1H, H-1)
¹³C NMR (125 MHz, CDCl₃) : 207.9 (C-8), 137.3 (C-11), 135.0 (C-10), 132.7 (C-1), 129.5 (C-7), 126.7 (C-4), 125.4 (C-5), 55.9 (C-9), 38.0 (C-3), 29.2 (C-6), 24.1 (C-2), 22.4 (C-12), 19.9 (C-13), 16.7 (C-15), 15.6 (C-14)
 Mass (HRMS) : 241.1571 (M+Na)⁺ (calcd for C₁₅H₂₂ONa, 241.1568)

2.13.4.3. Compound 13 (Curdione)

The compound 13 obtained from the fraction pool (20-42) of hexane extract was confirmed to be curdione based on the spectral data obtained along with HRMS and on comparison with literature reports. The obtained spectral data of the compound is as shown below.



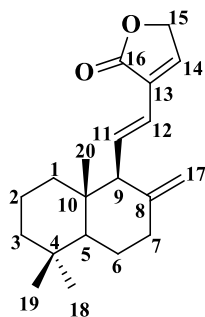
m.p. (°C)	: 58.1 °C
FT-IR (NaCl, ν_{\max} , cm^{-1})	: 2960, 1766, 1702, 1662, 1457, 1262, 1164, 1014, 768
^1H NMR (500 MHz, CDCl_3)	: 0.88 (<i>d</i> , $J = 6.5$ Hz, 3H), 0.95 (<i>d</i> , $J = 6.5$ Hz, 3H), 0.98 (<i>d</i> , $J = 7$ Hz, 3H), 1.66 (<i>d</i> , 3H), 1.88 (<i>m</i> , 1H), 2.09-2.15 (<i>m</i> , 3H, H-3 α , H-2 α , H-2 β), 2.33 (<i>m</i> , 1H, H-4 α), 2.40 (<i>d</i> , $J = 16.5$ Hz, 1H, H-6 β), 2.69 (<i>br s</i> , 1H, H-6 α), 2.85 (<i>t</i> , $J = 8.5$ Hz, 1H, 7 β -H), 2.94 (<i>d</i> , $J = 10.5$ Hz, 1H, H-9 α), 3.07 (<i>d</i> , $J = 10.5$ Hz, 1H, H-9 β), 5.17 (<i>s</i> , 1H, H-1)
^{13}C NMR (125 MHz, CDCl_3)	: 214.4 (C-8), 211.3 (C-5), 131.6 (C-1), 129.8 (C-10), 55.8 (C-9), 53.6 (C-7), 46.8 (C-4), 44.2 (C-6), 34.1 (C-3), 29.9 (C-11), 26.4 (C-2), 21.1 (C-12), 19.9 (C-13), 18.6 (C-14), 16.6 (C-15)
Mass (HRMS)	: 259.1675 (M+Na) $^+$ (calcd for $\text{C}_{15}\text{H}_{24}\text{O}_2\text{Na}$, 259.1674)

2.13.5. Spectral data of the isolated compounds from chloroform extract of *C. aromatica* rhizomes

2.13.5.1. Compound 14 (Villosin)

The compound 14 obtained from the fraction pool (54-62) of chloroform extract was confirmed to be villosin based on the spectral data obtained along with HRMS and on comparison with literature reports. The obtained spectral data of the compound is as shown below.

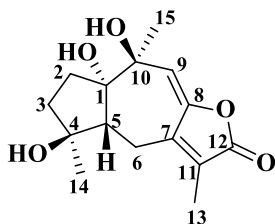
FT-IR (NaCl, ν_{\max} , cm^{-1})	: 2924, 1755, 1644, 1457, 1080, 892
--	-------------------------------------



- $^1\text{H NMR}$ (500 MHz, CDCl_3) : 7.08 (*s*, 1H, H-14), 6.83 (*dd*, $J = 16$ Hz, 10.5 Hz, 1H, H-11), 6.04 (*d*, $J = 15.5$ Hz, 1H, H-12), 4.74 (*br s*, 2H, H-15), 4.69 (*br s*, 1H, H-17 β), 4.44 (*d*, $J = 1$ Hz, 1H, H-17 α), 2.39-2.36 (*m*, 1H), 2.30 (*d*, $J = 10$ Hz, 1H), 2.02 (*m*, 1H), 1.65-1.54 (*m*, 1H), 1.37 (*m*, 2H), 1.15-1.11 (*m*, 2H), 1.04-1.01 (*m*, 1H), 0.98-0.89 (*m*, 3H), 0.82 (*s*, 3H, H-18), 0.80 (*s*, 3H, H-19), 0.77 (*s*, 3H, H-20)
- $^{13}\text{C NMR}$ (125 MHz, CDCl_3) : 172.4 (C-16), 149.4 (C-8), 142.4 (C-14), 136.9 (C-11), 129.5 (C-13), 120.7 (C-12), 108.4 (C-17), 69.6 (C-15), 62.2 (C-9), 54.7 (C-5), 42.3 (C-3), 40.8 (C-1), 39.3 (C-10), 36.7 (C-7), 33.6 (C-4, 18), 23.4 (C-6), 21.9 (C-19), 19.2 (C-2), 15.1 (C-20)
- Mass (HRMS) : 323.2001 ($\text{M}+\text{Na}$) $^+$ (calcd for $\text{C}_{20}\text{H}_{28}\text{O}_2\text{Na}$, 323.1987)

2.13.5.2. Compound 15 (1-epihydroxy-Zedoalactone D)

The compound 15 obtained from the fraction pool 192 of chloroform extract was confirmed to be 1-epihydroxy-zedoalactone D based on the spectral data obtained along with HRMS, single crystal X-ray structure and on comparison with literature reports. The obtained spectral data of the compound is as shown below.



- FT-IR (NaCl, $\nu_{\text{max,cm}^{-1}}$) : 3452, 2925, 1743, 1662, 1457, 1375, 1035, 736
- $^1\text{H NMR}$ (500 MHz, DMSO) : 5.48 (1H, *s*, H-9), 5.14 (1H, *s*), 4.50 (1H, *s*), 4.38 (1H, *s*), 2.64-2.61 (2H, *m*), 2.34-2.30 (2H, *m*), 1.60-1.50 (1H, *m*), 1.44-1.38 (1H, *m*), 1.84 (3H, *s*), 1.31 (3H, *s*), 1.14 (3H, *s*)

^{13}C NMR (125 MHz, DMSO) : 170.0 (C-12), 151.4 (C-7), 147.4 (C-8), 124.9 (C-11), 119.0 (C-9), 81.6 (C-10), 78.8 (C-4), 74.4 (C-1), 49.1 (C-5), 39.4 (C-3), 34.5 (C-2), 25.6 (C-15), 23.4 (C-14), 21.2 (C-6), 8.8 (C-13)

Mass (HRMS) : 303.1214 ($\text{M}+\text{Na}$)⁺ (calcd for $\text{C}_{15}\text{H}_{20}\text{O}_5\text{Na}$, 303.1208)

Optical activity : $[\alpha]_{\text{D}}^{25} = +124.3$ °C (c 0.15 MeOH)

2.14. References

- (1) Kumar, G.; Karthik, L.; Bhaskara Rao, K. V. A Review on Pharmacological and Phytochemical Properties of *Zingiber Officinale* Roscoe (*Zingiberaceae*). *J. Pharm. Res.* **2011**, *4*, 2963-2966.
- (2) Petrovska, B. B. Historical Review of Medicinal Plants' Usage. *Pharmacogn. Rev.* **2012**, *6*, 1-5.
- (3) Nair, R.; Shah, A.; Baluja, S.; Chanda, S. Comparison of Antibacterial Activities of Some Natural and Synthetic Compounds. *Asian J. Microbiol. Biotechnol. Environ. Sci.* **2006**, *8*, 503-508.
- (4) Verma, S.; Singh, S. P. Current and Future Status of Herbal Medicines. *Vet. World* **2008**, *1*, 347-350.
- (5) Tushar; Basak, S.; Sarma, G. C.; Rangan, L. Ethnomedical Uses of Zingiberaceous Plants of Northeast India. *J. Ethnopharmacol.* **2010**, *132*, 286-296.
- (6) Kumar, K. M.; Asish, G.; Sabu, M.; Balachandran, I. Significance of Gingers (*Zingiberaceae*) in Indian System of Medicine - Ayurveda: An Overview. *Anc. Sci. Life* **2013**, *32*, 253-261.
- (7) Gupta, S. C.; Sung, B.; Kim, J. H.; Prasad, S.; Li, S.; Aggarwal, B. B. Multitargeting by Turmeric, the Golden Spice: From Kitchen to Clinic. *Mol. Nutr. Food Res.* **2013**, *57*, 1510-1528.
- (8) Kocaadam, B.; Şanlıer, N. Curcumin, an Active Component of Turmeric (*Curcuma longa*), and Its Effects on Health. *Crit. Rev. Food Sci. Nutr.* **2017**, *57*, 2889-2895.
- (9) Ammon, H. P. T.; Wahl, M. A. Pharmacology of *Curcuma longa*. *Planta Med.* **1991**,

- 57, 1-7.
- (10) Negi, P. S.; Jayaprakasha, G. K.; Rao, L. J. M.; Sakariah, K. K. Antibacterial Activity of Turmeric Oil A Byproduct from Curcumin Manufacture. *J. Agric. Food Chem* **1999**, *47*, 4297-4300.
 - (11) Apisariyakul, A.; Vanittanakom, N.; Buddhasukh, D. Antifungal Activity of Turmeric Oil Extracted from *Curcuma longa* (Zingiberaceae). *J. Ethnopharmacol.* **1995**, *49*, 163-169.
 - (12) Shukla, Y.; Singh, M. Cancer Preventive Properties of Ginger: A Brief Review. *Food Chem. Toxicol.* **2007**, *45*, 683-690.
 - (13) Jiang, Y.; Huang, M.; Wisniewski, M.; Li, H.; Zhang, M.; Tao, X.; Liu, Y.; Zou, Y. Transcriptome Analysis Provides Insights into Gingerol Biosynthesis in Ginger (*Zingiber officinale*). *Plant Genome* **2018**, *11*, 1-11.
 - (14) Sun, W.; Wang, S.; Zhao, W.; Wu, C.; Guo, S.; Gao, H.; Tao, H.; Lu, J.; Wang, Y.; Chen, X. Chemical Constituents and Biological Research on Plants in the Genus *Curcuma*. *Crit. Rev. Food Sci. Nutr.* **2017**, *57*, 1451-1523.
 - (15) Dosoky, N. S.; Setzer, W. N. Chemical Composition and Biological Activities of Essential Oils of *Curcuma* Species. *Nutrients* **2018**, *10*, 10-17.
 - (16) Ravindran, P. N.; Nirmal Babu, K.; Sivaraman, K. Medicinal and Aromatic Plants- Industrial Profiles. **2020**, 1-506.
 - (17) Dosoky, N. S.; Satyal, P.; Setzer, W. N. Variations in the Volatile Compositions of *Curcuma* Species. *Foods* **2019**, *8*, 1-14.
 - (18) Jatoi, S. A.; Kikuchi, A.; Gilani, S. A.; Watanabe, K. N. Phytochemical, Pharmacological and Ethnobotanical Studies in Mango Ginger (*Curcuma amada* Roxb.; Zingiberaceae). *Phytother. Res.* **2007**, *21*, 507-516.
 - (19) Policegoudra, R. S.; Chandrashekhar, R. H.; Aradhya, S. M.; Singh, L. Cytotoxicity, Platelet Aggregation Inhibitory and Antioxidant Activity of *Curcuma amada* Roxb. Extracts. *Food Technol. Biotechnol.* **2011**, *49*, 162-168.
 - (20) Prema, D.; Kamaraj, M.; Achiraman, S.; Udayakumar, R. *In Vitro* Antioxidant and Cytotoxicity Studies of *Curcuma amada* Roxb . (Mango Ginger). *Int. J. Sci. Res. Publ.* **2014**, *4*, 1-6.
 - (21) Awin, T.; Mediani, A.; Maulidiani; Shaari, K.; Faudzi, S. M. M.; Sukari, M. A. H.;

- Lajis, N. H.; Abas, F. Phytochemical Profiles and Biological Activities of *Curcuma* Species Subjected to Different Drying Methods and Solvent Systems: NMR-Based Metabolomics Approach. *Ind. Crops Prod.* **2016**, *94*, 342-352.
- (22) Liu, Y.; Nair, M. G. Labdane Diterpenes in *Curcuma* Mangga Rhizomes Inhibit Lipid Peroxidation, Cyclooxygenase Enzymes and Human Tumour Cell Proliferation. *Food Chem.* **2011**, *124*, 527-532.
- (23) Samanth, L. R. *Curcuma amada* Roxb.: A Phytopharmacological Review. *J. Pharm. Res.* **2012**, *5*, 1992-1993.
- (24) Faiz Hossain, C.; Al-Amin, M.; Rahman, K. M. M.; Sarker, A.; Alam, M. M.; Chowdhury, M. H.; Khan, S. N.; Sultana, G. N. N. Analgesic Principle from *Curcuma amada*. *J. Ethnopharmacol.* **2015**, *163*, 273-277.
- (25) Policegoudra, R. S.; Aradhya, S. M.; Singh, L. Mango Ginger (*Curcuma amada* Roxb.) - A Promising Spice for Phytochemicals and Biological Activities. *J. Biosci.* **2011**, *36*, 739-748.
- (26) Singh, S.; Kumar, J. K.; Saikia, D.; Shanker, K.; Thakur, J. P.; Negi, A. S.; Banerjee, S. A Bioactive Labdane Diterpenoid from *Curcuma amada* and Its Semisynthetic Analogues as Antitubercular Agents. *Eur. J. Med. Chem.* **2010**, *45*, 4379-4382.
- (27) Alan Sheeja, D. B.; Nair, M. S. Phytochemical Constituents of *Curcuma amada*. *Biochem. Syst. Ecol.* **2012**, *44*, 264-266.
- (28) Policegoudra, R. S.; Divakar, S.; Aradhya, S. M. Identification of Difurocumenonol, a New Antimicrobial Compound from Mango Ginger (*Curcuma amada* Roxb.) Rhizome. *J. Appl. Microbiol.* **2007**, *102*, 1594-1602.
- (29) Policegoudra, R. S.; Abiraj, K.; Gowda, D. C.; Aradhya, S. M. Isolation and Characterization of Antioxidant and Antibacterial Compound from Mango Ginger (*Curcuma amada* Roxb.) Rhizome. *J. Chromatogr. B Anal. Technol. Biomed. Life Sci.* **2007**, *852*, 40-48.
- (30) Policegoudra, R. S.; Rehna, K.; Rao, L. J.; Aradhya, S. M. Antimicrobial, Antioxidant, Cytotoxicity and Platelet Aggregation Inhibitory Activity of a Novel Molecule Isolated and Characterized from Mango Ginger (*Curcuma amada* Roxb.) Rhizome. *J. Biosci.* **2010**, *35*, 231-240.
- (31) Siddaraju, M. N.; Dharmesh, S. M. Inhibition of Gastric H⁺,K⁺-ATPase and

- Helicobacter Pylori Growth by Phenolic Antioxidants of *Curcuma amada*. *J. Agric. Food Chem.* **2007**, *55*, 7377-7386.
- (32) Srinivasan, M. R.; Chandrasekhara, N.; Srinivasan, K. Cholesterol Lowering Activity of Mango Ginger (*Curcuma amada* Roxb.) in Induced Hypercholesterolemic Rats. *Eur. Food Res. Technol.* **2008**, *227*, 1159-1163.
- (33) Wilson, B.; Abraham, G.; Manju, V. S.; Mathew, M.; Vimala, B.; Sundaresan, S.; Nambisan, B. Antimicrobial Activity of *Curcuma zedoaria* and *Curcuma malabarica* Tubers. *J. Ethnopharmacol.* **2005**, *99*, 147-151.
- (34) Alan Sheeja, D. B.; Nair, M. S. Chemical Constituents of *Curcuma malabarica*. *Biochem. Syst. Ecol.* **2010**, *38*, 229-231.
- (35) Angel, G. R.; Menon, N.; Vimala, B.; Nambisan, B. Essential Oil Composition of Eight Starchy Curcuma Species. *Ind. Crops Prod.* **2014**, *60*, 233-238.
- (36) Pant, N.; Misra, H.; Jain, D. C. Phytochemical Investigation of Ethyl Acetate Extract from *Curcuma aromatica* Salisb. Rhizomes. *Arab. J. Chem.* **2013**, *6*, 279-283.
- (37) Sikha, A.; Harini, A.; Prakash, H. L. Pharmacological Activities of Wild Turmeric (*Curcuma aromatica* Salisb): A Review. *J. Pharmacogn. Phytochem.* **2015**, *3*, 1-4.
- (38) Al-Reza, S. M.; Rahman, A.; Sattar, M. A.; Rahman, M. O.; Fida, H. M. Essential Oil Composition and Antioxidant Activities of *Curcuma aromatica* Salisb. *Food Chem. Toxicol.* **2010**, *48*, 1757-1760.
- (39) Kojima, H.; Yanai, T.; Toyota, A. Essential Oil Constituents from Japanese and Indian *Curcuma aromatica* Rhizomes. *Planta Med.* **1998**, *64*, 380-381.
- (40) Al-Reza, S. M.; Rahman, A.; Parvin, T.; Rahman, M. M.; Rahman, M. S. Chemical Composition and Antibacterial Activities of Essential Oil and Organic Extracts of *Curcuma aromatica* Salisb. *J. Food Saf.* **2011**, *31*, 433-438.
- (41) Liu, P.; Miao, K.; Zhang, L.; Mou, Y.; Xu, Y.; Xiong, W.; Yu, J.; Wang, Y. Curdione Ameliorates Bleomycin-Induced Pulmonary Fibrosis by Repressing TGF- β -Induced Fibroblast to Myofibroblast Differentiation. *Respir. Res.* **2020**, *21*, 1-10.
- (42) Pintatum, A.; Maneerat, W.; Logie, E.; Tuenter, E.; Sakavitsi, M. E.; Pieters, L.; Berghe, W. V.; Sripisut, T.; Deachathai, S.; Laphookhieo, S. *In Vitro* Anti-inflammatory, Anti-oxidant and Cytotoxic Activities of Four *Curcuma* Species and the Isolation of Compounds from *Curcuma aromatica* Rhizome. *Biomolecules*

- 2020**, 10,1-14.
- (43) Li, Y.; Feng, J.; Mo, Y.; Liu, H.; Yang, B. Concordance between Cardio-Protective Effect on Isoproterenol-Induced Acute Myocardial Ischemia and Phenolic Content of Different Extracts of *Curcuma aromatica*. *Pharm. Biol.* **2016**, 54, 3226-3231.
- (44) Nadhe, S. B.; Tawre, M. S.; Agrawal, S.; Chopade, B. A.; Sarkar, D.; Pardesi, K. Anticancer Potential of AgNPs Synthesized Using *Acinetobacter* Sp. and *Curcuma aromatica* against HeLa Cell Lines: A Comparative Study. *J. Trace Elem. Med. Biol.* **2020**, 62, 1-8.
- (45) Dong, S.; Luo, X.; Liu, Y.; Zhang, M.; Li, B.; Dai, W. Diarylheptanoids from the Root of *Curcuma aromatica* and Their Antioxidative Effects. *Phytochem. Lett.* **2018**, 27, 148-153.
- (46) Dong, S.; Li, B.; Dai, W.; Wang, D.; Qin, Y.; Zhang, M. Sesqui- and Diterpenoids from the Radix of *Curcuma aromatica*. *J. Nat. Prod.* **2017**, 80, 3093-3102.
- (47) Mustafa, A.; Ali, M.; Khan, N. Z. Volatile Oil Constituents of the Fresh Rhizomes of *Curcuma amada* Roxb. *J. Essent. Oil Res.* **2005**, 17, 490-491.
- (48) Choudhury, S. N.; Rabha, L. C.; Kanjilal, P. B.; Ghosh, A. C.; Leclercq, P. A. Essential Oil of *Curcuma amada* Roxb. From Northeastern India. *J. Essent. Oil Res.* **1996**, 8, 79-80.
- (49) Padalia, R. C.; Verma, R. S.; Sundaresan, V.; Chauhan, A.; Chanotiya, C. S.; Yadav, A. Volatile Terpenoid Compositions of Leaf and Rhizome of *Curcuma amada* Roxb. from Northern India. *J. Essent. Oil Res.* **2013**, 25, 17-22.
- (50) Duker-Eshun, G.; Jaroszewski, J. W.; Asomaning, W. A.; Oppong-Boachie, F.; Olsen, C. E.; Christensen, S. B. Antiplasmodial Activity of Labdanes from *Aframomum latifolium* and *Aframomum sceptrum*. *Planta Med.* **2002**, 68, 642-644.
- (51) Ayafor, J. F.; Tchuendem, M. H. K.; Nyasse, B.; Tillequin, F.; Anke, H. Aframodial and Other Bioactive Diterpenoids from *Aframomum* Species. *Pure Appl. Chem.* **1994**, 66, 2327-2330.
- (52) Morita, H.; Itokawa, H. Cytotoxic and Antifungal Diterpenes from the Seeds of *Alpinia galanga*. *Planta Med.* **1988**, 54, 117-120.
- (53) Itokawa, H.; Morita, H.; Katou, I.; Takeya, K.; Cavalheiro, A. J.; De Oliveira, R. C. B.; Ishige, M.; Motidome, M. Cytotoxic Diterpenes from the Rhizomes of *Hedychium*

- coronarium. Planta Med.* **1988**, *54*, 311-315.
- (54) Xu, H. X.; Dong, H.; Sim, K. Y. Labdane Diterpenes from *Alpinia zerumbet*. *Phytochemistry* **1996**, *42*, 149-151.
- (55) Dekebo, A.; Dagne, E.; Hansen, L. K.; Gautun, O. R.; Aasen, A. J. Crystal Structures of Two Furanosesquiterpenes from *Commiphora Sphaerocarpa*. *Tetrahedron Lett.* **2000**, *41*, 9875-9878.
- (56) Makabe, H.; Maru, N.; Kuwabara, A.; Kamo, T.; Hirota, M. Anti-inflammatory Sesquiterpenes from *Curcuma zedoaria*. *Nat. Prod. Res.* **2006**, *20*, 680-685.
- (57) Pant, N.; Jain, D. C.; Bhakuni, R. S.; Prajapati, V.; Tripathi, A. K.; Kumar, S. Zederone: A Sesquiterpenic Keto-Dioxide from *Curcuma aromatica*. *Indian J. Chem. - Sect. B Org. Med. Chem.* **2001**, *40*, 87-88.
- (58) Asem, S. D.; Laitonjam, W. S. Investigation of the Structure-Nonlinearity Relationship of Zederone from the Rhizomes of *Curcuma caesia* Roxb. *Indian J. Chem. - Sect. B Org. Med. Chem.* **2012**, *51*, 1738-1742.
- (59) Hamdi, O. A. A.; Ye, L. J.; Kamarudin, M. N. A.; Hazni, H.; Paydar, M.; Looi, C. Y.; Shilpi, J. A.; Kadir, H. A.; Awang, K. Neuroprotective and Antioxidant Constituents from *Curcuma zedoaria* Rhizomes. *Rec. Nat. Prod.* **2015**, *9*, 349-355.
- (60) Shiobara, Y.; Asakawa, Y.; Kodama, M.; Yasuda, K.; Takemoto, T. Curcumenone, Curcumanolide A and Curcumanolide B, Three Sesquiterpenoids from *Curcuma zedoaria*. *Phytochemistry* **1985**, *24*, 2629-2633.
- (61) Win Tun, K. N.; Aminah, N. S.; Kristanti, A. N.; Ramadhan, R.; Takaya, Y.; Aung, H. T. Isolation of Cytotoxic Sesquiterpenes from *Curcuma comosa* and Characterization of Their Structures. *J. Indian Chem. Soc.* **2019**, *96*, 1513-1517.
- (62) Jang, M. H.; Piao, X. L.; Kim, J. M.; Kwon, S. W.; Park, J. H. Inhibition of Cholinesterase and Amyloid- β Aggregation by Resveratrol Oligomers from *Vitis Amurensis*. *Phyther. Res.* **2008**, *22*, 544-549.
- (63) Hartati, R.; Suganda, A. G.; Fidrianny, I. Chemical Composition and Antimicrobial Activity of Diterpene and Essential Oils of *Hedychium roxburghii* Blume Rhizome. *Asian J. Pharm. Clin. Res.* **2015**, *8*, 221-226.
- (64) Firman, K.; Kinoshita, T.; Itai, A.; Sankawa, U. Terpenoids from *Curcuma heyneana*. *Phytochemistry* **1988**, *27*, 3887-3891.

-
- (65) Xia, Q.; Wang, X.; Xu, D. J.; Chen, X. H.; Chen, F. H. Inhibition of Platelet Aggregation by Curdione from *Curcuma wenyujin* Essential Oil. *Thromb. Res.* **2012**, *130*, 409-414.
- (66) Yang, F. Q.; Li, S. P.; Chen, Y.; Lao, S. C.; Wang, Y. T.; Dong, T. T. X.; Tsim, K. W. K. Identification and Quantitation of Eleven Sesquiterpenes in Three Species of *Curcuma* Rhizomes by Pressurized Liquid Extraction and Gas Chromatography-Mass Spectrometry. *J. Pharm. Biomed. Anal.* **2005**, *39*, 552-558.
- (67) Nakatani, N.; Kikuzaki, H.; Yamaji, H.; Yoshio, K.; Kitora, C.; Okada, K.; G. Padolina, W. Labdane Diterpenes from Rhizomes of *Hedychium Coronarium*. *Phytochemistry* **1994**, *37*, 1383-1388.
- (68) Takano, I.; Yasuda, I.; Takeya, K.; Itokawa, H. Guaiane Sesquiterpene Lactones from *Curcuma aeruginosa*. *Phytochemistry* **1995**, *40*, 1197-1200.
- (69) Loua, Y.; Zhaob, F.; Hea, H.; Penga, K.; Zhoua, X.; Chena, L.; Qiua, F. Guaiane-type Sesquiterpenes from *Curcuma wenyujin* and Their Inhibitory Effects on Nitric oxide Production. *J. Asian Nat. Prod. Res.* **2009**, *11*, 737-747.
- (70) Li, Y.; Wu, Y.; Li, Y.; Guo, F. Review of the Traditional Uses, Phytochemistry, and Pharmacology of *Curcuma wenyujin* Y. H. Chen et C. Ling. *J. Ethnopharmacol.* **2021**, *269*, 1-65.

Design and Synthesis of Labdane Appended Triazoles as Potent Pancreatic Lipase Inhibitors

3.1. Abstract

Obesity contributes to the genesis of many metabolic disorders including dyslipidemia, coronary heart disease (CHD), non-alcoholic fatty liver, type 2 diabetes, etc. Pancreatic lipase (PL) plays a vital role in the digestion and absorption of fat. Therefore to control obesity, inhibition of pancreatic lipase is the active therapy. Thus, in this chapter, novel natural product derived labdane appended triazoles with pancreatic lipase inhibition potential was designed and synthesized. Among these hybrids, **6b** and **6f** exhibited excellent inhibitory activity (IC_{50} $0.75 \pm 0.02 \mu\text{M}$ and $0.77 \pm 0.01 \mu\text{M}$), higher than that of the positive control Orlistat (IC_{50} $0.8 \pm 0.03 \mu\text{M}$). Compounds **6c**, **6e** and **6g-i** inhibited the PL comparable to that of the positive control. Interestingly, none of the compounds showed cytotoxicity (H9c2) in the concentration ranging from $1 \mu\text{M}$ - $100 \mu\text{M}$. Overall results reveal the potential of labdane appended triazoles as anti-obesity agents.

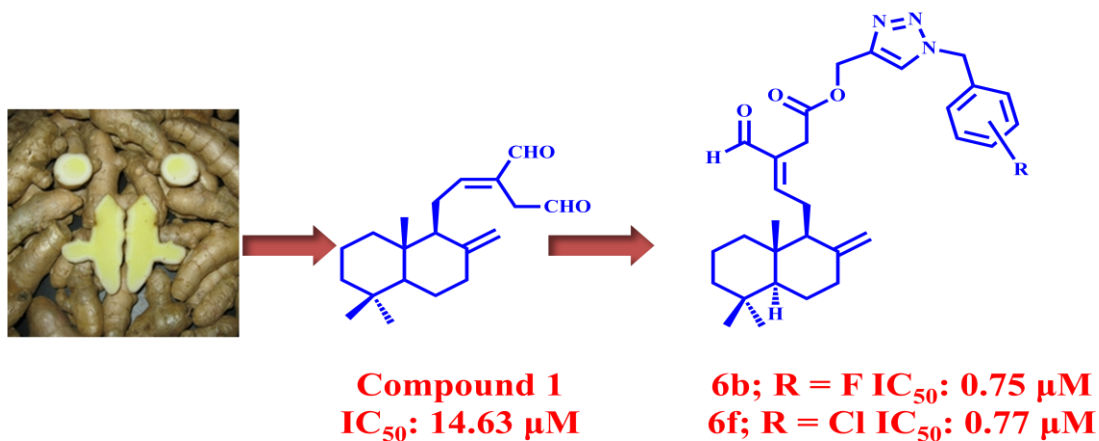


Figure 3.1. Pancreatic lipase inhibitory activity

3.2. Introduction

Obesity is a medical condition with excess body fat accumulation to the extent which leads to serious health consequences. Obesity contributes to the genesis of many metabolic disorders including dyslipidemia,¹ coronary heart disease (CHD),² non-alcoholic fatty liver,³ type 2 diabetes⁴ etc. Obesity affects metabolic health and leads to morbidity and premature mortality globally. In 2018 WHO reported that global obesity has almost tripled since 1975.⁵ As per literature, more than 340 million children and adolescents between 5 and 19 aged are overweight or obese.⁵ As a result, physicians are prompted to take aggressive treatments in lifestyle changes, pharmacological interventions and surgical therapies before severe consequences become clinically apparent. Among these various treatments, pharmacotherapy is the most commonly used one.⁶⁻⁷ Pancreatic lipase is an enzyme secreted from the pancreas and it plays a vital role in the digestion and absorption of fat.⁸ Therefore to control obesity, inhibition of pancreatic lipase is the active therapy. Among the existing medicines, orlistat is one such precise drug used for the inhibition of pancreatic lipase.

In recent times, natural/herbal products also been considered as an alternative medicine for the treatment of obesity and related disorders.⁹⁻¹⁰ Many plant-based extracts are reported for the treatment of obesity and associated diseases. For instance, ethanolic extracts of *Terminalia paniculata* showed very good anti-lipase and anti-obesity activities.¹¹ Likewise, some terpenoid saponins from the leaves of *Acanthopanax senticosus*,¹² the phenolic acids from fermented oats,¹³ apple polyphenols,¹⁴ and flavan-3-ol digalate esters of oolong tea are found to have substantial pancreatic lipase inhibitory property.¹⁵ In light of these observations we selected the plant species *Curcuma amada* from the Zingiberaceae family. The anti-obesity properties of *C. amada* and important heterocyclic core triazoles are discussed below in review of literature.

3.3. Review of literature

3.3.1. Anti-obesity properties of *Curcuma amada*

In 2019, Nissankara Rao *et al.* evaluated the anti-obesity effects of acetone extract of *Curcuma amada* (mango ginger) on high-fat high-sugar (HFHS) diet-induced rat. HFHS diet leads to increased body weight, increased lipid parameters such as total cholesterol, low

density lipoprotein (LDL), very low density lipoprotein (VLDL) and triglycerides (TGs). There is no increase in the level high density lipoprotein (HDL). The HFHS diet also induces the cognitive deficit and there is a relationship between obesity and Alzheimer's disease. The treatment of 300 mg/kg acetone extract of *C. amada* in HFHS diet induced rats showed a dose dependent activity and was effective against lipid parameters related to obesity and memory loss.¹⁶

Yoshioka *et al.* in 2019 reported diterpenes isolated from *C. amada* was effective for inhibiting α -glucosidase and pancreatic lipase. One of the abundant diterpenes (*E*)-labda-8(17),12-diene-15,16-dial isolated from mango ginger was the most prominent compound and showed remarkable α -glucosidase inhibitory activities. Its enzymatic action is slightly less than that of the antidiabetic drug acarbose.¹⁷ These literatures showed that *C. amada* may be effective for the treatment of obesity and being overweight. Additionally, it is an edible ginger, exploring its potential as an anti-obesity agent of future as food supplement/nutraceutical looks promising and was taken up as part of this study.

3.3.2. Anti-obesity properties of triazole

Triazole and its derivatives are well known for their extended pharmacological applications. Triazole nucleus is present as a core structural component in many drugs belonging to antimicrobial, anti-inflammatory, analgesic, antiepileptic, antiviral, antineoplastic, antihypertensive, antimalarial, antianxiety, antidepressant, antihistaminic, antioxidant, antitubercular, anti-Parkinson's, antidiabetic, local anaesthetic as well as immunomodulatory agents.¹⁸ It also serves as an important scaffold for many anti-obesity drugs and drug candidates. 3-Amino-1,2,4-triazole (ATZ) is shown to reduce both fat deposition and body weight in high fat diet (HFD) induced obese rat via improved lipid and glucose metabolism.¹⁹ In 2014, Holubova *et al.*, reported the growth hormone secretagogue receptor 1a (GHS-R1a) antagonists such as JMV4208 (**Figure 3.2**) and JMV3002 (**Figure 3.2**), trisubstituted 1,2,4-triazole derivatives are effective for the treatment of obesity. The mechanism of GHS-R1a is via decreased food intake and body weight, and it is also effective for other conditions associated with hyperphagia.²⁰

LH-21(5-(4-chlorophenyl)-1-(2,4-dichlorophenyl)-3-hexyl-1H-1,2,4-triazole) (**Figure 3.2**) is another important anti-obesity agent and it is a cannabinoid CB1 receptor antagonist. This may effectively promote weight loss via modulation of visceral adipose tissue. CB1 receptors have been pursued as a highly promising, safe and effective therapeutic strategy against obesity.²¹⁻²² Synthetic semicarbazone-triazole hybrids (**Figure 3.2**) exhibited excellent anti-obesity benefits.²³

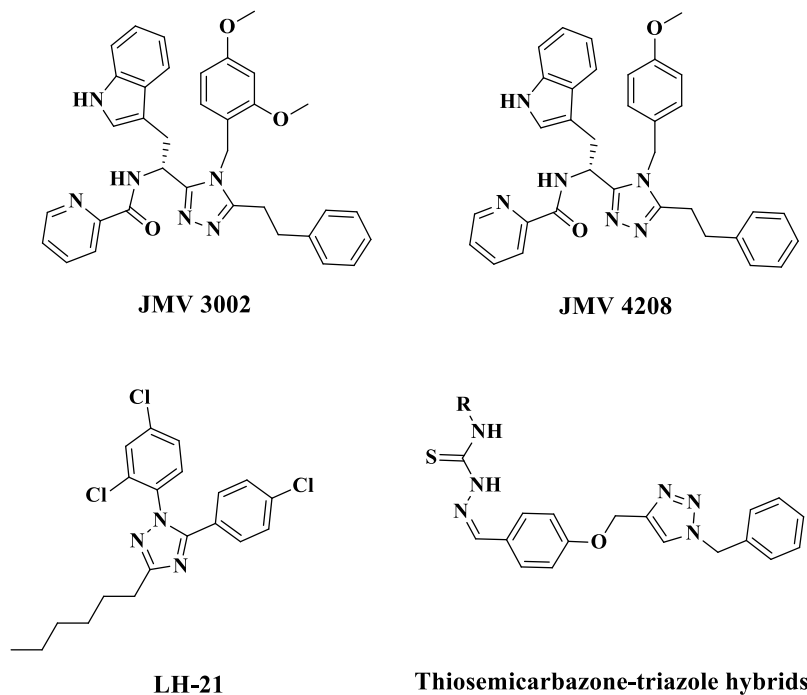


Figure 3.2. Triazoles having anti-obesity properties

3.4. Aim and scope of the present study

As discussed in the introduction (section 3.2), inhibition of pancreatic lipase is an effective way to reduce obesity. Many reports are available on the potency of plants on the inhibition of lipase. Based on the traditional applications and its large medicinal properties in a long history of Ayurvedic medicine, we have selected *Curcuma amada Roxb.* to explore its inhibition properties against the pancreatic lipase. Therefore, in continuation of our focused ongoing research interest on natural products and natural product based lead molecule²⁴⁻²⁶ identification for therapeutic applications, as part of Ph.D. programme, we have isolated the

major compound (*E*)-labda-8(17),12-diene-15,16-dial from *C. amada* (Chapter 2, section 2.6). This was synthetically transformed to rationally designed triazole appended analogues and evaluated for their pancreatic lipase inhibitory potential is discussed in this chapter.

3.5. Design strategy for the synthesis of labdane appended triazoles

Based on the traditional applications and its large medicinal properties in a long history of Ayurvedic medicine, we have selected *C. amada* for the exploration of its inhibition properties against the pancreatic lipase. *C. amada*, an edible ginger is one of the rhizomatous species in the *Zingiberaceae* family. The rhizomes of *C. amada* are a rich source of essential oils, and more than 130 phytochemicals are isolated,²⁷ which possesses various biological properties viz. antimicrobial, antioxidant, anti-inflammatory, anticancer, cardiovascular and gastrointestinal disorders etc.²⁷⁻³⁰ The phytochemical, (*E*)-labda-8(17),12-diene-15,16-dial was the marker compound and we have isolated in large quantity.

From the literature background, we have found that molecules having labdane functionality and triazoles are exhibiting promising anti-obesity potential. Therefore we have designed novel labdane appended triazoles by incorporating triazole pharmacophore into labdane core, in order to enhance the biological potential. The rationale for the targeted synthesis of triazole appended analogues is based upon its broad spectrum of biological properties.³¹⁻³² Triazole and pyrazole based synthetic drugs are also well-known for the treatment of obesity and related disorders (**Figure 3.3**).^{23, 33-34}

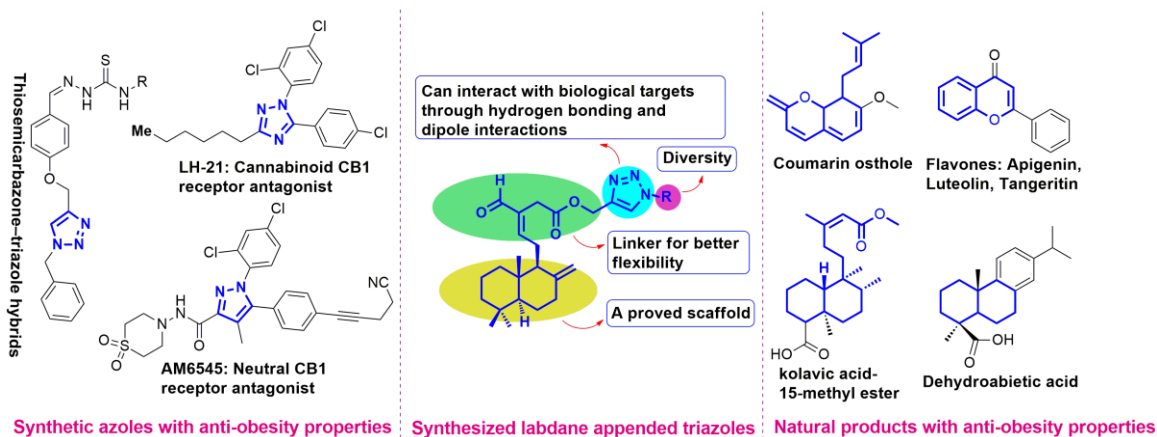
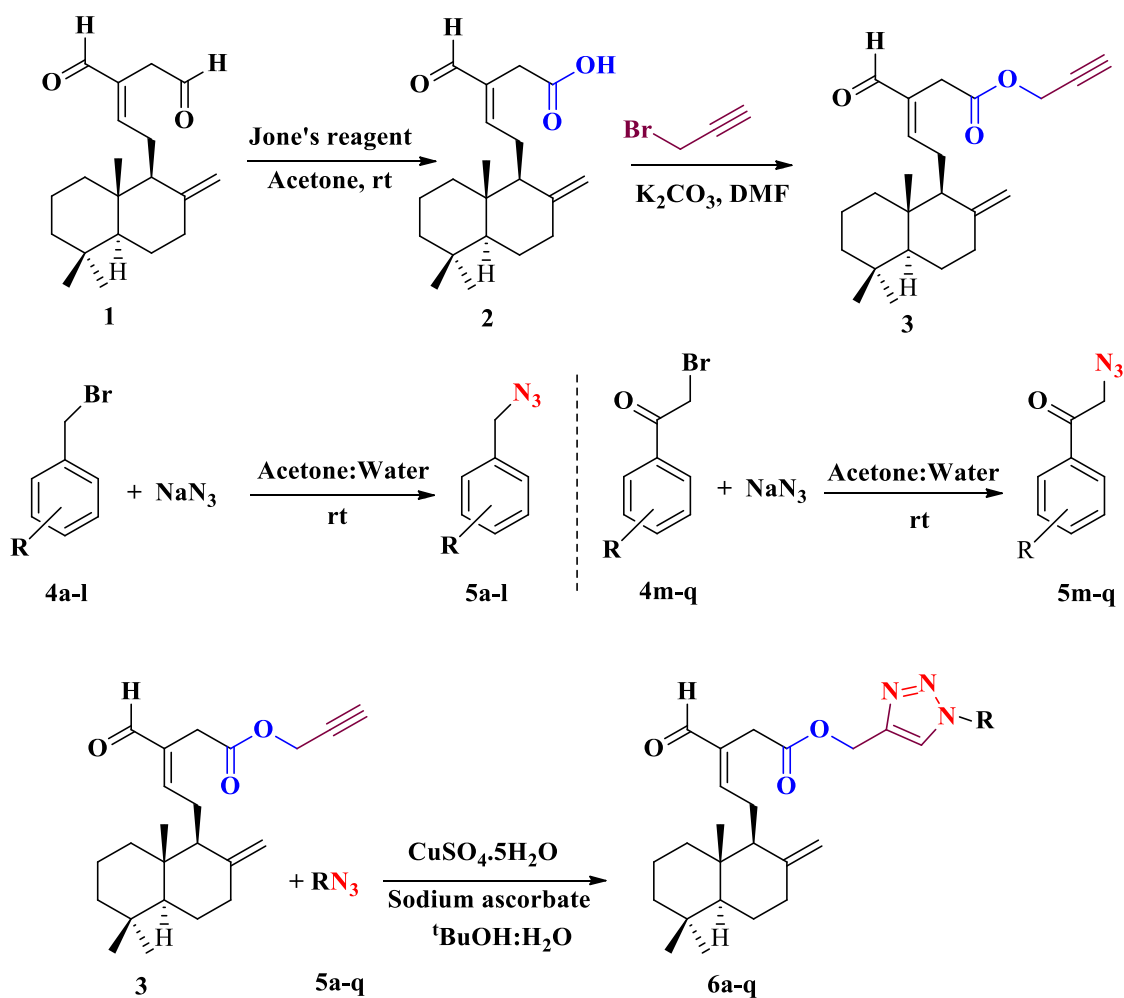


Figure 3.3. Rationale for the synthesis of labdane appended triazoles

After designing labdane appended triazole molecules, we have performed molecular docking studies by using Auto-dock 3.0 version to determine whether/how our designed molecules are docking Human pancreatic lipase. From the docking studies we found that all our molecules can dock the target site and then synthesize all the designed molecules.

3.6. Results and discussion

(*E*)-Labda-8(17),12-diene-15,16-dial (Compound **1**) was isolated from the chloroform extract of *C. amada* as a colorless solid and the structure was confirmed using various spectroscopic data such as IR, ¹H NMR, ¹³C NMR, HRMS, etc.³⁵ A series of variously substituted triazole appended labdane derivatives were prepared by a three-step protocol starting from compound **1**. Compound **1**, when subjected to Jones's oxidation, one of the aldehydes of compound **1** is selectively oxidized into acid derivative leading to zerumin A (**2**). The alkyne intermediate (**3**) of zerumin A could be prepared in excellent yields by treating compound **2** with propargyl bromide (**Scheme 3.1**). The propargylated labdane undergoes the click reaction with various substituted benzyl and phenacyl azides (**5**) at room temperature to provide 1,2,3-triazole appended labdane derivatives (**6a-q**) in good to excellent yields (**Scheme 3.1**). All the synthesized derivatives are fully characterized by IR, NMR and HRMS spectral data.



Scheme 3.1. Synthesis of propargylated labdane (**3**), substituted benzyl and phenacyl azides (**5a-q**) and labdane appended triazoles (**6a-q**)

Spectral data leading to the structural characterization is exemplified using compound **6j** (Figure 3.4). The IR spectrum of the compound **6j** showed two strong absorption bands at 1739 and 1682 cm^{-1} which indicated the presence of two different carbonyl groups. The absorption peak seen at 2115 cm^{-1} attributed to the presence of azide functionality. The absorption bands at 2933, 1643 and 891 cm^{-1} suggested the presence of an exo-cyclic double bond. The 1H NMR spectrum (Figure 3.5) of the compound showed the aldehydic proton at δ 9.33 and two singlets at δ 4.82 and 4.34 attributed to the presence of exo-methylene group. Two doublets observed at δ 7.23 and 6.89 integrating two protons each, with $J = 8.5$ Hz indicated the presence of *p*-substituted aromatic protons. The aromatic proton present in the triazole ring resonated at δ 7.50. Two singlets observed at δ 5.44 and 5.19, both integrating

for two protons each could be attributed to the presence of methylene groups attached to oxygen and nitrogen atoms respectively. A singlet integrating for two protons at δ 3.32 showed the presence of allylic methylene group near carbonyl group. A singlet at δ 3.81 integrating for three protons indicated the presence of methoxy protons. Presence of aldehyde and ester carbonyl groups confirmed by the presence of peaks at δ 193.5 and 170.0 in the ^{13}C NMR spectrum (**Figure 3.6**). The eight peaks between δ 159.9-107.9 confirmed the presence of aromatic and aliphatic double bonds. The mass spectrum of the compound showed the molecular ion peak at m/z 542.3003, which is $(\text{M}+\text{Na})^+$ peak. From these data, along with DEPT-135 and 2D spectra, the structure of the compound **6j** (is confirmed as shown below.

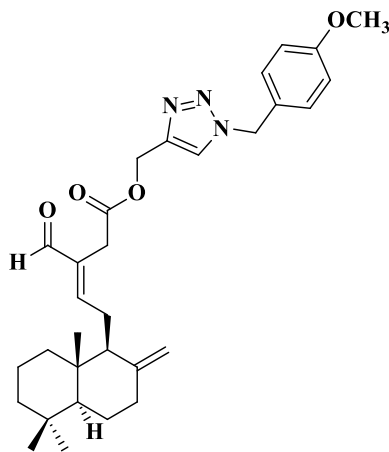


Figure 3.4. Compound 6j

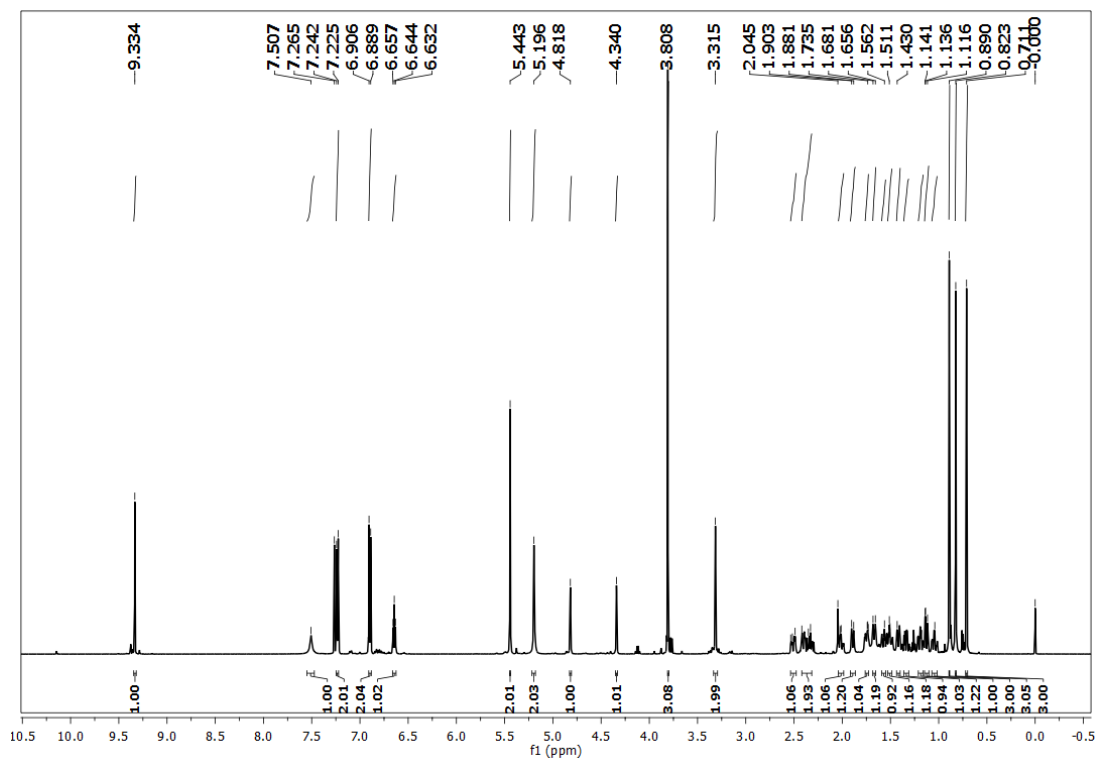


Figure 3.5. ^1H NMR spectrum of compound 6j in CDCl_3

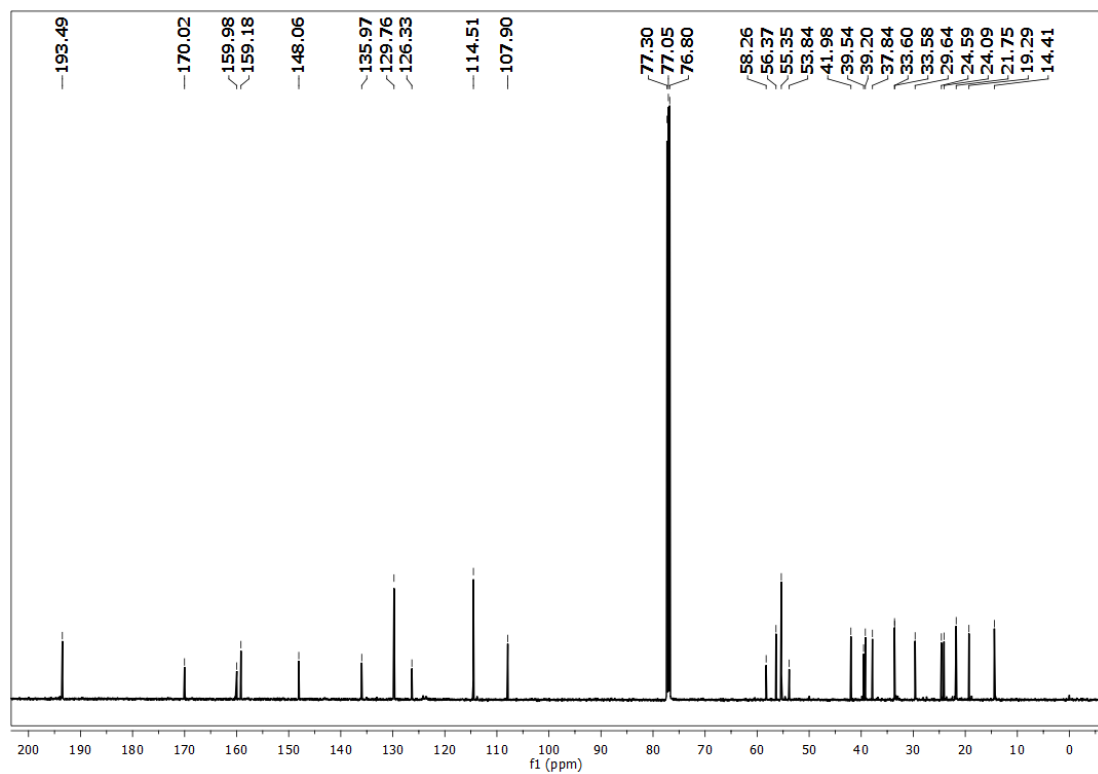


Figure 3.6. ^{13}C NMR spectrum of compound 6j in CDCl_3

3.6.1. Diversity of triazole appended labdane molecules

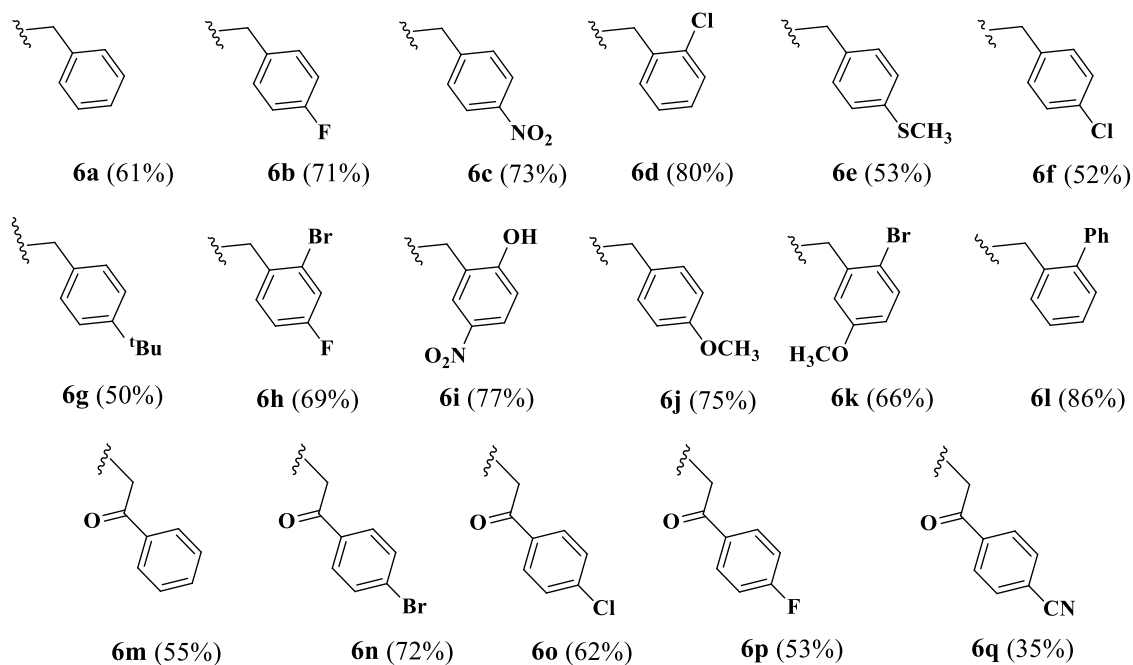


Figure 3.7. Diversity of the reaction

3.6.2. Cytotoxicity studies by MTT assay

Further, *in vitro* toxicity of isolated and semi-synthetic derivatives was carried out to analyze the effect of compounds on Human liver cell lines. This method is primarily used to identify potentially hazardous compounds and their toxic effect in the early stage of development of therapeutic drugs. The cytotoxicity of compounds on Hep G2 Human liver carcinoma-derived cell lines was measured by MTT assay.³⁶ The cytotoxic effect of each compound was estimated by calculating the percentage of cell viability in a dose-dependent manner ranging from 0.5 μM to 100 μM (**Figure 3.8**). Based on the percentage of cell viability, compounds **6a**, **6c**, **6f**, **6g**, **6h**, **6j**, **6k** and **6q** were found to be the least toxic on Hep G2 Human liver cell lines, and none of the compounds showed any signs of toxicity at all the tested concentrations.

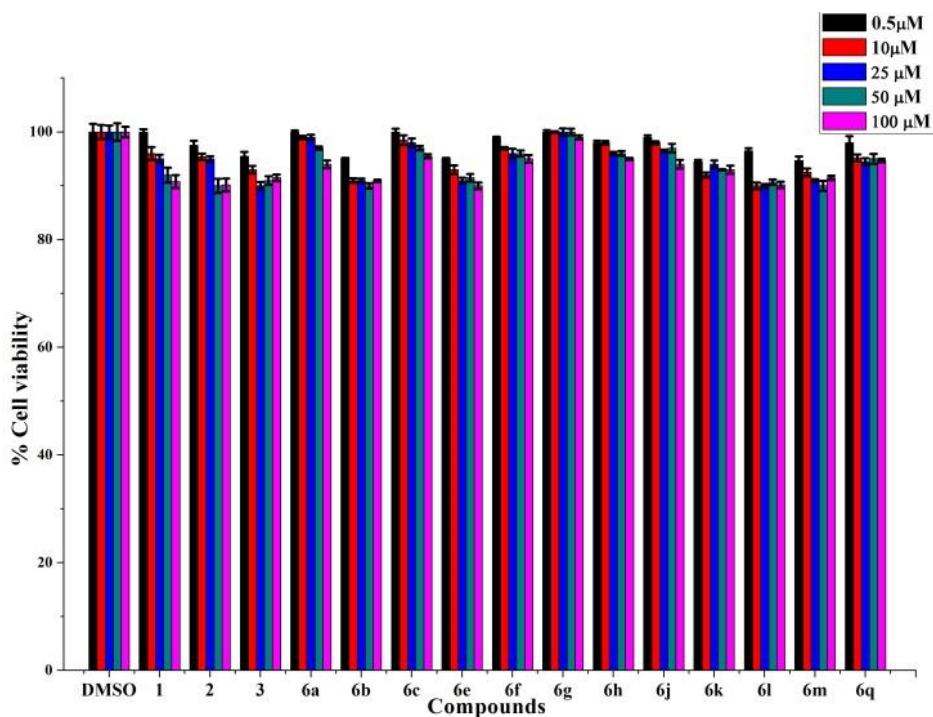


Figure 3.8. Cytotoxic study of isolates and selected semi-synthetic derivatives by MTT assay (Cytotoxic effect of each compound is expressed as percentage of cell viability in dose dependent manner. Values are mean \pm SD of four independent experiments performed in duplicates)

3.6.3. Inhibition studies of compounds against porcine pancreatic lipase (Method A)

The isolated (*E*)-labda-8(17),12-diene-15,16-dial (**1**), semi-synthetic intermediates and targeted triazole appendages were evaluated for the inhibitory activity against pancreatic lipase (PL) (**Method A**).³⁷ The parent molecule labdane dial exhibited moderate activity. Among the tested, majority of the triazole hybrids showed strong PL inhibitory activity in the concentration ranging from 0.75-14.63 μ M. Initially, the percentage of enzyme inhibition of compounds at various concentrations (1, 5, 10 and 20 μ M) was performed. At lower concentration of 1 μ M, compounds **6b** and **6f** showed inhibition of 75 to 80 %. At 20 μ M concentration the derivatives **6b**, **6c**, **6e**, **6f**, **6g**, **6h** and **6j** exhibited maximum inhibition percentage of 80 to 85 (**Figure 3.9**). The other compounds (**6a**, **6k**, **6l**, **6m** and **6q**) also showed better tendency to inhibit the PL. In contrast, few derivatives (**6d**, **6i**, **6n**, **6o** and **6p**)

failed to show any significant effect on pancreatic lipase. Overall, the labdane-triazole hybrids inhibited the PL through a concentration dependent manner.

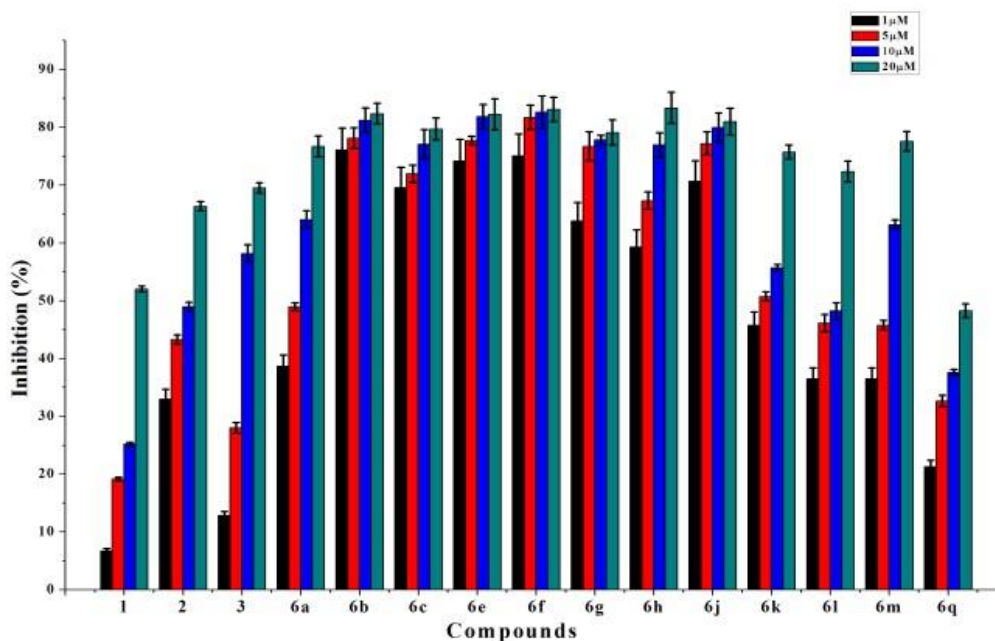


Figure 3.9. The percentage inhibition of isolates and synthetic derivatives against pancreatic lipase in various concentrations. (Isolates and synthetic derivatives are tested at concentrations 1-20 μM . Each experiment was independently performed four times in duplicates and expressed as mean \pm SD (n=4))

3.6.4. Inhibition studies of compounds against Human pancreatic lipase (Method B)

In an attempt to validate the potential of the compounds, the PL inhibitory activity was repeated using Human Pancreatic lipase (**Method B**).³⁸ As expected, the compounds followed the similar trend in exhibiting the inhibitory potential with IC_{50} values in the range of 1.10 - 14.48 μM concentration. The derivatives **6b**, **6c**, **6g** and **6h** presented maximum PL inhibition percentage of 80 to 85 at 15 μM concentration (**Figure 3.10**). Similarly, triazole analogues **6d**, **6i**, **6n**, **6o** and **6p** have failed to inhibit the Human pancreatic lipase. The IC_{50} values of active compounds with maximum inhibitory potential are calculated and summarized in **Table 3.1**.

The IC_{50} results revealed (**Method A**) that the labdane triazole appendages **6b** and **6f** exhibited an excellent inhibitory activity with $0.75 \pm 0.02 \mu\text{M}$ and $0.77 \pm 0.01 \mu\text{M}$ respectively, which is slightly better than that of the positive control orlistat ($\text{IC}_{50} 0.8 \pm 0.03$

μM). Compounds **6c**, **6e** and **6g-j** inhibited the pancreatic lipase comparable to that of positive control in the range IC_{50} 0.8 to 0.9 μM . Whereas, the parent molecule **1**, semi-synthetic intermediates **2** and **3**, and labdane triazole derivatives **6a**, **6k**, **6l** and **6m** showed moderate potency in the range of IC_{50} 5.35 - 14.63 μM . However, against the Human pancreatic lipase (**Method B**), labdane triazole appendages **6b** and **6f** being the more potent analogues exhibited the inhibitory activities with IC_{50} values $1.1 \pm 0.53 \mu\text{M}$ and $1.25 \pm 0.78 \mu\text{M}$ respectively. Compounds **6c**, **6e** and **6g-j** also showed promising ability in inhibiting the PL with IC_{50} values in the range of 1.65 to 2.31 μM . The parent molecule and other derivatives showed moderate activity. The preliminary studies also revealed that the compounds are bound to the active site of PL and probably exhibited a covalent interaction with PL. Nevertheless, extended kinetics and crystallographic studies are to be conducted for further authentication of a mode of interaction. We believe this is the first report on the pancreatic lipase inhibitory activity of labdane dial and its semi-synthetic triazole appendages.

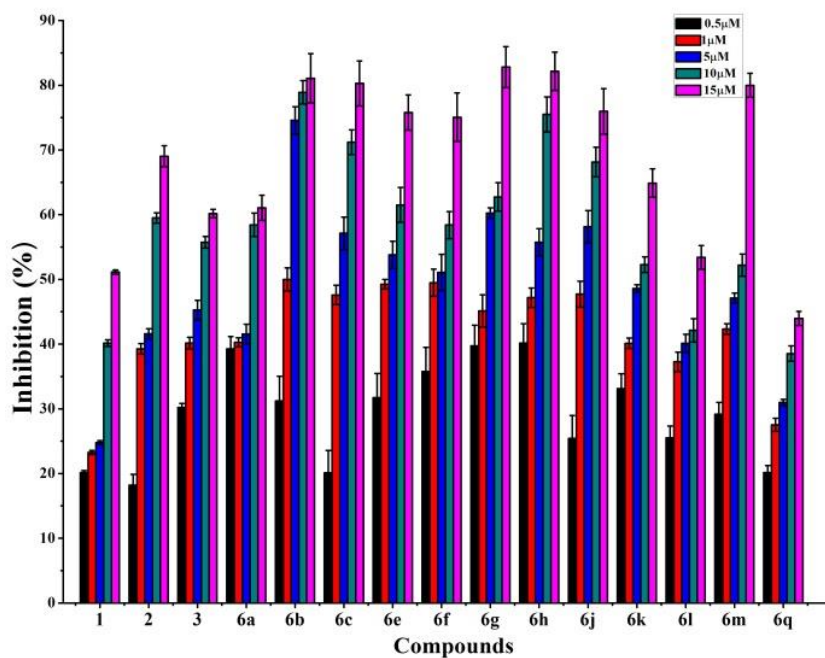


Figure 3.10. The percentage of isolates and synthetic derivatives against Human pancreatic lipase in various concentrations (Isolates and synthetic derivatives are tested at concentrations 0.5-15 μM . Each experiment was independently performed four times in duplicates and expressed as means \pm SD (n=4))

Table 3.1. 50% inhibitory concentration (IC₅₀) evaluation of labdane appended Triazoles

Compound	IC ₅₀ (μM) ^a	
	Method A	Method B
1	14.63 ± 0.11	14.48 ± 0.51
2	10.30 ± 2.71	11.75 ± 0.64
3	8.64 ± 3.13	7.38 ± 0.77
6a	5.35 ± 1.20	9.15 ± 0.27
6b	0.75 ± 0.02	1.1 ± 0.53
6c	0.85 ± 0.03	2.01 ± 0.73
6e	0.80 ± 0.05	1.65 ± 0.93
6f	0.77 ± 0.01	1.25 ± 0.78
6g	0.91 ± 0.02	2.28 ± 0.88
6h	0.95 ± 0.02	2.31 ± 0.62
6j	0.84 ± 0.07	1.87 ± 0.14
6k	4.43 ± 1.02	6.90 ± 0.73
6l	10.36 ± 2.20	13.48 ± 0.53
6m	6.22 ± 2.04	7.82 ± 0.48
Orlistat	0.80 ± 0.03	0.19 ± 0.62

^aThe IC₅₀ values of PL inhibitory activity for selected compounds and the positive control Orlistat. Values are mean ± SD of four independent experiments performed in duplicates.

3.6.5. Structure-activity relationships (SAR) studies

In a structure-activity relationship point of view, we observed that the labdane-triazole hybrids incorporating benzyl azides (6a-l) were more active than the phenacyl azides (6m-q). Most of the analogues synthesized from benzyl azides exhibited excellent inhibition property slightly better than or equal to that of orlistat. In contrast, the triazole analogues synthesized from phenacyl azides (6m-q) did not show any significant inhibition potential except for the compound 6m. In precise, among the triazoles incorporated from the variously substituted benzyl azides, all the para-substituted analogues showed the lowest IC₅₀. However, the unsubstituted (6a), ortho- and meta- substituted benzyl azide incorporated triazole

appendages showed moderate activity. Interestingly, there was no clear trend followed by the nature of the para- substitution, *i.e.*, among the halogen, electron donating and electron withdrawing groups. Overall, among the various substituted hybrids, **6b** and **6f** with *p*-F and *p*-Cl substituted benzyl azide incorporated triazole appendages were found to be the most potent candidates of the series.

3.6.6. Molecular docking studies

The molecular docking studies have also been performed³⁹ in the present study to understand the basic knowledge on how these compounds have blocked Human pancreatic lipase activity. There were twenty compounds docked on Human pancreatic lipase to understand their possible binding site with respect to the binding energies of structure conformations of compounds (**Figure 3.11**). The top ranked stable structure conformations on protein have shown least Gibb's free binding energies. The docking results have shown that all the triazole derivatives can interact with lipase at possible predicted site with different binding energies (**Table 3.2**). However, further experimental studies (*i.e.*, site directed mutagenesis) are much needed to understand the precise mechanism of action of these compounds. This data provided us a vital clue about the interaction sites, which helps in our future in-depth studies towards lipase inhibition.

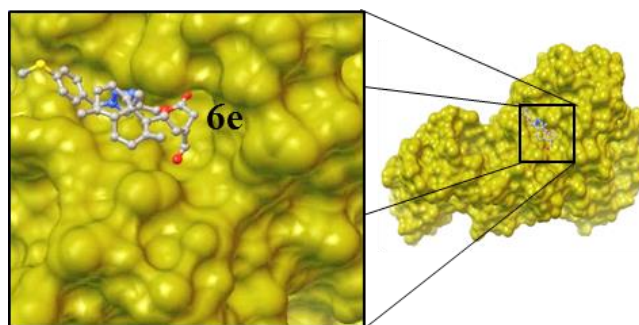


Figure 3.11. The representative molecular docking studies of compound **6e**

3.7. Conclusion

In conclusion, a new series of natural product derived labdane-triazole hybrids were designed, synthesized and evaluated for pancreatic lipase inhibitory potential. Among the semi-synthetic derivatives, **6b** and **6f** are the most active candidates of the series with

excellent PL inhibitory activity, which is interestingly slightly better than that of the positive control orlistat. Hybrids **6c**, **6e** and **6g-i** inhibited the PL comparable to that of positive control. The structure-activity relationship studies suggested that the *p*-substitution on benzyl azides seems to be vital for improved PL inhibition. Cytotoxicity of the compounds on Hep G2 Human liver carcinoma-derived cell line was measured by MTT assay. Based on the percentage of cell viability, none of the compounds showed any signs of toxicity at all the tested concentrations. This is the first report on the PL inhibitory activity of labdane dial and its semi-synthetic triazole appendages. Our findings will provide useful insights for the design and synthesis of novel PL inhibitors. Presently, a detailed study to elucidate the molecular mechanistic action of an anti-obesity effect of the compounds **6b** and **6f** using *in vitro* and *in vivo* experimental models and structural optimization are in progress in our laboratory.

3.8. Experimental section

3.8.1. Chemistry

All reagents used for the isolation and triazole preparation were purchased from Sigma-Aldrich and Spectrochem. Hep G2 cell lines, Human liver carcinoma-derived cell lines were purchased from American Type Cell Culture (ATCC, Manassas, VA, USA), Pancreatic lipase, *p*-nitrophenyl butyrate, Human Pancreatic lipase (EC 3.1.13), olive oil, taurochenodeoxycholate, taurocholate, cholesterol, L- α -phosphatidylcholine, calcium acetate, Orlistat (Sigma Aldrich, USA) were used for biological study. Solvents were purchased from Merck and were distilled before use. TLC plates (silica gel 60 F₂₅₄) were used for monitoring the purity of the isolated compounds and the reaction progress. Column chromatographic techniques were used for the isolation of natural compounds and its analogues. Heidolph rotary evaporator was used for the removal of solvents. The absorbance was recorded at 540 nm by the Elisa reader. The IR spectra were recorded on Bruker Alpha-T FT-IR spectrophotometer. The ¹H and ¹³C NMR spectra were recorded at 500 MHz and 125 MHz respectively, on Bruker AMX 500 MHz FT NMR spectrometer. Tetramethylsilane (TMS) was used as an internal standard, chemical shifts are expressed in δ scale and coupling constants in Hertz (Hz). In ¹H NMR spectra the solvent (CDCl₃) peak appeared as a singlet at

7.26 ppm and in ^{13}C NMR spectra the peak appeared as a triplet at 77.0 ppm. Mass spectra were recorded under HRMS (ESI) using Thermo Scientific Exactive Orbitrap mass spectrometer.

3.8.1.1. Isolation of (*E*)-labda-8(17),12-diene-15,16-dial (1)

The isolation protocol is discussed in chapter 2 (section 2.8)

3.8.1.2. Procedure for the synthesis of zerumin A (2)

To a stirred solution of the compound (*E*)-labda-8(17),12-diene-15,16-dial (**1**) (1 g) in acetone, Jones's reagent (CrO_3 and H_2SO_4) was added drop wise until the reddish colour persisted. After the completion of the reaction, as indicated by TLC, excess reagent was quenched by the addition of isopropanol. The reaction mixture was then filtered through celite, concentrated, further extracted with diethyl ether, washed with distilled water and dried with anhydrous Na_2SO_4 . Solvent was removed and the residue was subjected to column chromatography on silica gel which afforded the compound zerumin A (**2**) (1.5 g, 71% yield). The structure of the compound was confirmed by various spectroscopic data and by comparison with the reported literature.³⁵

3.8.1.3. Procedure for the synthesis of (*E*)-prop-2-yn-1-yl 3-formyl-5-(5,5,8a-trimethyl-2-methylenedecahydronaphthalen-1-yl)pent-3-enoate (3)

The propargyl bromide (0.3736 g, 1 equiv.) was added drop wise to a solution of zerumin A (1g, 1 equiv.) in DMF at 0 °C. K_2CO_3 (0.6510 g, 1.5 equiv.) was added and allowed to stir continuously at room temperature until the completion of the reaction as indicated by TLC. The compound was extracted with ethyl acetate, dried over anhydrous Na_2SO_4 and the solvent was removed under reduced pressure which afforded the compound **3**.

3.8.1.4. General procedure for the synthesis of azides (5a-5q)

Benzyl/Phenacyl bromide (1 equiv.) was added drop wise to a stirred solution of NaN_3 (2 equiv.) in 3:1 mixture of acetone and water, and the resulting mixture was stirred at room temperature for 1 hr. The reaction was diluted with water and extracted with ethyl acetate.

The combined layer was washed with brine, dried over anhydrous Na₂SO₄ and the solvent was removed under reduced pressure.

3.8.1.5. General procedure for the synthesis of triazole analogues (6a-6q)

To a solution of azide (1 equiv.) and compound **3** (1 equiv.) in ^tBuOH-water (1:2) mixture, CuSO₄·5H₂O (0.1 equiv.) and sodium ascorbate (0.25 equiv.) were added and the reaction mixture was allowed to stir at room temperature. Progress of the reaction was monitored by TLC. After completion of the reaction, the content was extracted with ethyl acetate, washed with brine and the compound was dried over anhydrous Na₂SO₄ and the solvent was removed under reduced pressure. The product was purified by column chromatography using ethyl acetate and hexane as solvents.

3.8.2. Spectral data

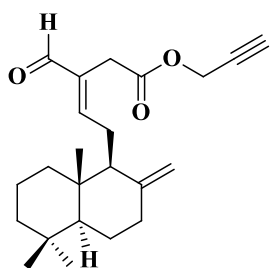
3.8.2.1. (*E*)-Labda-8(17),12-diene-15,16-dial (**1**)

The spectral details of (*E*)-labda-8(17),12-diene-15,16-dial has been discussed in section 2.11.2.2 (Chapter 2)

3.8.2.2. Zerumin A (**2**)

The spectral details of zerumin A has been discussed in section 2.11.2.5 (Chapter 2)

3.8.2.3. (*E*)-prop-2-yn-1-yl-3-formyl-5-(5,5,8a-trimethyl-2-methylenedecahydronaphthalen-1-yl) pent-3-enoate (**3**)



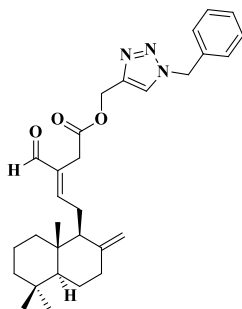
FT-IR (NaCl, ν _{max} , cm ⁻¹)	:	3279, 3080, 2933, 2845, 2719, 2130, 1747, 1686, 1644, 891
¹ H NMR (500 MHz, CDCl ₃)	:	9.37 (s, 1H), 6.69 (t, <i>J</i> = 6.5 Hz, 1H), 4.86 (s, 1H), 4.69 (d, <i>J</i> = 2.5 Hz, 2H), 4.40 (s, 1H), 3.37 (d, <i>J</i> = 8.5 Hz, 2H), 2.55-1.13 (m, 15H), 0.89 (s, 3H), 0.82 (s, 3H), 0.74 (s, 3H)
¹³ C NMR (125 MHz, CDCl ₃)	:	193.2, 169.3, 159.2, 148.0, 135.8, 107.9, 77.4, 75.0, 56.4, 55.3, 52.4, 41.9, 39.6, 39.2,

37.8, 33.6, 29.4, 24.6, 24.0, 21.7, 19.2, 14.4

HRMS (ESI) : m/z: 379.2235 [M+Na]⁺ (calcd for C₂₃H₃₂O₃Na is 379.2249)

3.8.2.4. Synthesis of (*E*)-(1-benzyl-1*H*-1,2,3-triazol-4-yl)methyl 3-formyl-5-(5,5,8a-trimethyl-2-methylenedecahydronaphthalen-1-yl) pent-3-enoate (**6a**)

The compound **6a** was prepared by the reaction of benzyl azide (11.20 mg, 1 equiv.) and compound **3** (30 mg, 1 equiv.) in ^tBuOH-water (1:2) mixture (3 ml) as per the method described in the section 3.8.1.5. Yield: 61% (25 mg).



FT-IR (NaCl, : 3082, 2930, 2846, 2719, 2122, 1739, 1683, v_{max}, cm⁻¹) 1644, 891

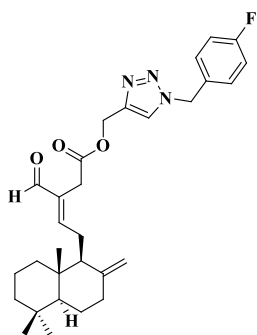
¹H NMR (500 : 9.33 (s, 1H), 7.52 (s, 1H), 7.38-7.27 (m, 5H), 6.64 (t, *J* = 6.5Hz, 1H), 5.51 (s, 2H), 5.21(s, 2H), 4.82 (s, 1H), 4.34 (s, 1H), 3.31 (s, 2H), 2.53-1.04 (m, 14H), 0.89 (s, 3H), 0.82 (s, 3H), 0.71 (s, 3H)

¹³C NMR (125 : 193.4, 169.9, 159.0, 148.0, 143.1, 135.9, MHz, CDCl₃) 134.4, 129.2, 128.8, 128.1, 123.6, 107.8, 58.2, 56.4, 55.4, 54.2, 41.9, 39.6, 39.2, 37.8, 33.6, 29.6, 24.6, 24.0, 21.7, 19.3, 14.4

HRMS (ESI) : m/z: 512.2885 [M+Na]⁺ (calcd for C₃₀H₃₉N₃O₃Na is 512.2889)

3.8.2.5. Synthesis of (*E*)-(1-(4-fluorobenzyl)-1*H*-1,2,3-triazol-4-yl)methyl 3-formyl-5-(5,5,8a-trimethyl-2-methylenedecahydronaphthalen-1-yl)pent-3-enoate (**6b**)

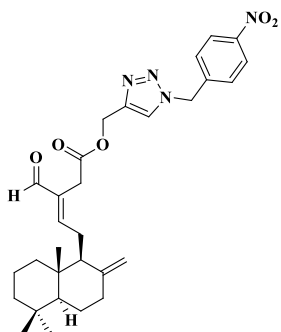
The compound **6b** was prepared by the reaction of 4-fluorobenzyl azide (12.71 mg, 1 equiv.) and compound **3** (30 mg, 1 equiv.) in ^tBuOH-water (1:2) mixture (3 ml) as per the method described in the section 3.8.1.5. Yield: 71% (32 mg).



FT-IR (NaCl, ν_{\max} , cm^{-1})	: 3080, 2932, 2845, 2720, 2102, 1739, 1682, 1643, 892
^1H NMR (500 MHz, CDCl_3)	: 9.33 (s, 1H), 7.54 (s, 1H), 7.29-7.27 (m, 2H), 7.08-7.05 (m, 2H), 6.65 (t, $J = 6.5\text{Hz}$, 1H), 5.48 (s, 2H), 5.22 (s, 2H), 4.82 (s, 1H), 4.34 (s, 1H), 3.32 (s, 2H), 2.54-1.04 (m, 14H), 0.89 (s, 3H), 0.82 (s, 3H), 0.71 (s, 3H)
^{13}C NMR (500 MHz, CDCl_3)	: 193.4, 170.0, 159.2, 148.0, 143.2, 135.9, 130.0, 130.0, 123.6, 116.2, 116.0, 107.8, 58.2, 56.4, 55.3, 53.4, 41.9, 39.5, 39.2, 37.8, 33.6, 33.6, 29.6, 24.6, 24.0, 21.7, 19.2, 14.4
HRMS (ESI)	: m/z : 530.2775 $[\text{M}+\text{Na}]^+$ (calcd for $\text{C}_{30}\text{H}_{38}\text{FN}_3\text{O}_3\text{Na}$ is 530.2795)

3.8.2.6. Synthesis of (*E*)-1-(4-nitrobenzyl)-1*H*-1,2,3-triazol-4-ylmethyl 3-formyl-5-(5,5,8*a*-trimethyl-2-methylenedecahydronaphthalen-1-yl)pent-3-enoate (**6c**)

The compound **6c** was prepared by the reaction of 4-nitrobenzyl azide (14.99 mg, 1 equiv.) and compound **3** (30 mg, 1 equiv.) in $t\text{BuOH}$ -water (1:2) mixture (3 ml) as per the method described in the section 3.8.1.5. Yield: 73% (32 mg).

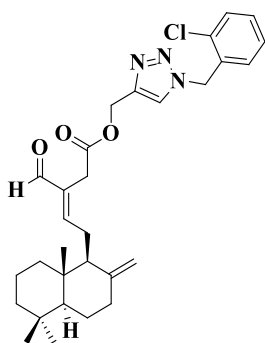


FT-IR (NaCl, ν_{\max} , cm^{-1})	: 3081, 2931, 2846, 2720, 2253, 1739, 1682, 1643, 893
^1H NMR (500 MHz, CDCl_3)	: 9.32 (s, 1H), 8.24 (d, $J = 8.5\text{ Hz}$, 2H), 7.64 (s, 1H), 7.42 (d, $J = 9\text{ Hz}$, 2H), 6.66 (t, $J = 6.5\text{ Hz}$, 1H), 5.64 (s, 2H), 5.25 (s, 2H), 4.82 (s, 1H), 4.34 (s, 1H), 3.32 (s, 2H), 2.55-1.05 (m, 14H), 0.89 (s, 3H), 0.82 (s, 3H), 0.72 (s, 3H)
^{13}C NMR (125 MHz, CDCl_3)	: 193.6, 170.0, 159.2, 148.1, 143.7, 141.4, 135.9, 128.6, 124.3, 124.0, 107.8, 58.2, 56.4, 55.3, 53.1, 41.9, 39.6, 39.2, 37.8, 33.6, 29.8, 24.6, 24.0, 21.7, 19.2, 14.4

HRMS (ESI) : m/z : 557.2760 $[M+Na]^+$ (calcd for $C_{30}H_{38}N_4O_5Na$ is 557.2740)

3.8.2.7. Synthesis of (*E*)-(1-(2-chlorobenzyl)-1*H*-1,2,3-triazol-4-yl)methyl 3-formyl-5-(5,5,8a-trimethyl-2-methylenedecahydronaphthalen-1-yl)pent-3-enoate (**6d**)

Compound **6d** was prepared by the reaction of 2-chlorobenzyl azide (14.10 mg, 1 equiv.) and compound **3** (30 mg, 1 equiv.) in ^tBuOH-water (1:2) mixture (3 ml) as per the method described in the section 3.8.1.5. Yield: 80% (35 mg).



FT-IR (NaCl) : 3078, 2929, 2845, 2718, 2359, 2120, 1739, ν_{max} , cm^{-1} 1683, 1643, 891

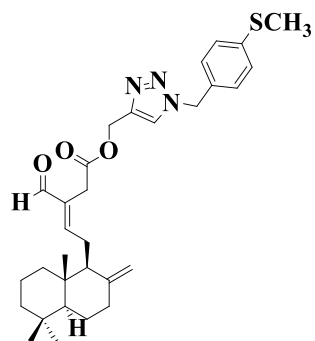
¹H NMR (500 MHz, $CDCl_3$) : 9.34 (s, 1H), 7.62 (s, 1H), 7.44-7.18 (m, 4H), 6.65 (t, $J = 6.5$ Hz, 1H), 5.66 (s, 2H), 5.22 (s, 2H), 4.82 (s, 1H), 4.34 (s, 1H), 3.32 (d, $J = 1.5$ Hz, 2H), 2.54-1.02 (m, 14H), 0.89 (s, 3H), 0.82 (s, 3H), 0.71 (s, 3H)

¹³C NMR (125 MHz, $CDCl_3$) : 193.4, 169.9, 159.0, 148.0, 142.9, 135.9, 133.5, 132.2, 130.4, 130.3, 129.9, 127.6, 124.0, 107.9, 58.2, 56.4, 55.4, 51.4, 41.9, 39.5, 39.2, 37.8, 33.6, 33.6, 29.6, 24.6, 24.0, 21.7, 19.2, 14.4

HRMS (ESI) : m/z : 546.2509 $[M+Na]^+$ (calcd for $C_{30}H_{38}ClN_3O_3Na$ is 546.2499)

3.8.2.8. Synthesis of (*E*)-(1-(4-(methylthio)benzyl)-1*H*-1,2,3-triazol-4-yl)methyl 3-formyl-5-(5,5,8a-trimethyl-2-methylenedecahydronaphthalen-1-yl)pent-3-enoate (**6e**)

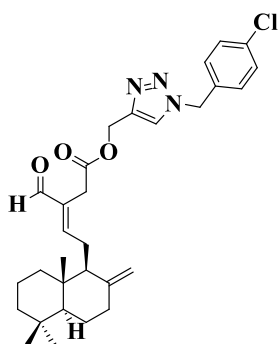
The compound **6e** was prepared by the reaction of 4-thiomethylbenzyl azide (15.08 mg, 1 equiv.) and compound **3** (30 mg, 1 equiv.) in ^tBuOH-water (1:2) mixture (3 ml) as per the method described in the section 3.8.1.5. Yield: 53% (24 mg).



FT-IR (NaCl, ν_{\max} , cm^{-1})	: 3082, 2930, 2846, 2720, 2100, 1739, 1682, 1643, 892
^1H NMR (500 MHz, CDCl_3)	: 9.33 (s, 1H), 7.52 (s, 1H), 7.23 (s, 2H), 7.21 (s, 2H), 6.64 (t, $J = 6.5$ Hz, 1H), 5.46 (s, 2H), 5.20 (s, 2H), 4.82 (s, 1H), 4.34 (s, 1H), 3.32 (s, 2H), 2.48 (s, 3H), 2.04-1.04 (m, 14H), 0.89 (s, 3H), 0.82 (s, 3H), 0.71 (s, 3H)
^{13}C NMR (125 MHz, CDCl_3)	: 193.4, 170.0, 159.1, 148.0, 143.1, 139.8, 135.9, 130.8, 128.6, 126.8, 123.5, 107.8, 58.2, 56.4, 55.4, 53.8, 41.9, 39.5, 39.2, 37.8, 33.6, 33.6, 29.6, 24.6, 24.0, 21.7, 19.3, 15.5, 14.4
HRMS (ESI)	: m/z : 558.2769 $[\text{M}+\text{Na}]^+$ (calcd for $\text{C}_{31}\text{H}_{41}\text{N}_3\text{O}_3\text{S}$ is 558.2766)

3.8.2.9. Synthesis of (*E*)-(1-(4-chlorobenzyl)-1*H*-1,2,3-triazol-4-yl)methyl 3-formyl-5-(5,5,8*a*-trimethyl-2-methylenedecahydronaphthalen-1-yl)pent-3-enoate (**6f**)

The compound **6f** was prepared by the reaction of 4-chlorobenzyl azide (14.10 mg, 1 equiv.) and compound **3** (30 mg, 1 equiv.) in t BuOH-water (1:2) mixture (3 ml) as per the method described in the section 3.8.1.5. Yield: 52% (23 mg).



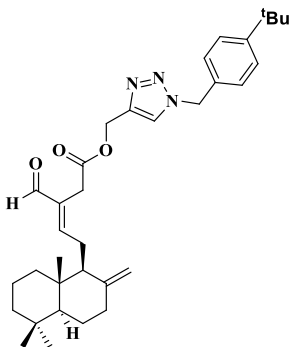
FT-IR (NaCl, ν_{\max} , cm^{-1})	: 3083, 2931, 2845, 2720, 2118, 1739, 1682, 1643, 891
^1H NMR (500 MHz, CDCl_3)	: 9.33 (s, 1H), 7.54 (s, 1H), 7.35 (d, $J = 8.5$ Hz, 2H), 7.22 (d, $J = 8.5$ Hz, 2H), 6.65 (t, $J = 6.5$ Hz, 1H), 5.48 (s, 2H), 5.22 (s, 2H), 4.82 (s, 1H), 4.34 (s, 1H), 3.32 (s, 2H), 2.54-1.04 (m, 14H), 0.89 (s, 3H), 0.82 (s, 3H), 0.71 (s, 3H)
^{13}C NMR (125 MHz, CDCl_3)	: 193.4, 170.0, 159.1, 148.0, 143.3, 135.9

134.9, 132.9, 129.4, 129.4, 123.6, 107.8,
58.2, 56.4, 55.4, 53.4, 41.9, 39.6, 39.2, 37.8,
33.6, 29.6, 24.6, 24.0, 21.7, 19.3, 14.4

HRMS (ESI) : m/z: 546.2512 [M+Na]⁺ (calcd for
C₃₀H₃₈ClN₃O₃Na is 546.2499)

3.8.2.10. Synthesis of (*E*)-(1-(4-(tert-butyl)benzyl)-1*H*-1,2,3-triazol-4-yl)methyl 3-formyl-5-(5,5,8a-trimethyl-2-methylenedecahydronaphthalen-1-yl)pent-3-enoate (**6g**)

The compound **6g** was prepared by the reaction of 4-^tbutylbenzyl azide (10.65 mg, 1 equiv.) and compound **3** (20 mg, 1 equiv.) in ^tBuOH-water (1:2) mixture (3 ml) as per the method described in the section 3.8.1.5. Yield: 50% (15 mg).



FT-IR (NaCl, : 3081, 2957, 2867, 2718, 2132, 1739, 1684,
v_{max}, cm⁻¹) 1643, 891

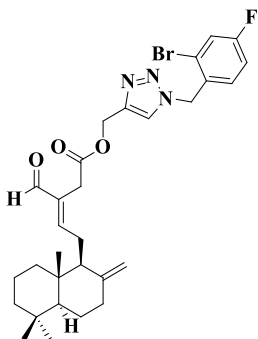
¹H NMR (500 : 9.33 (s, 1H), 7.52 (s, 1H), 7.40 (d, *J* = 8 Hz,
MHz, CDCl₃) 2H), 7.22 (d, *J* = 8.5 Hz, 2H), 6.64 (t, *J* =
6.5 Hz, 1H), 5.48 (s, 2H), 5.20 (s, 2H), 4.82
(s, 1H), 4.34 (s, 1H), 3.32 (s, 2H), 2.54-1.05
(m, 14H), 1.31 (s, 9H), 0.89 (s, 3H), 0.82 (s,
3H), 0.72 (s, 3H)

¹³C NMR (125 : 193.4, 170.0, 159.1, 151.9, 148.0, 135.9,
MHz, CDCl₃) 131.3, 127.8, 126.0, 107.9, 58.2, 56.4, 55.4,
53.9, 41.9, 39.6, 39.2, 37.8, 34.6, 33.6, 33.6,
31.2, 29.6, 24.6, 24.0, 21.7, 19.3, 14.4

HRMS (ESI) : m/z: 544.3560 [M-H]⁺ (calcd for
C₃₄H₄₆N₃O₃ is 544.3534)

3.8.2.11. (*E*)-(1-(2-bromo-5-fluorobenzyl)-1*H*-1,2,3-triazol-4-yl) methyl 3-formyl-5-((1*S*, 4*aS*, 8*aS*)-5, 5, 8*a*- trimethyl-2-methylenedecahydronaphthalen-1-yl)pent-3-enoate (6h**)**

The compound **6h** was prepared by the reaction of 2-bromo-5-fluorobenzyl azide (14.77 mg, 1 equiv.) and compound **3** (23 mg, 1 equiv.) in ^tBuOH-water (1:2) mixture (3 ml) as per the method described in the section 3.8.1.5. Yield: 69% (25 mg).

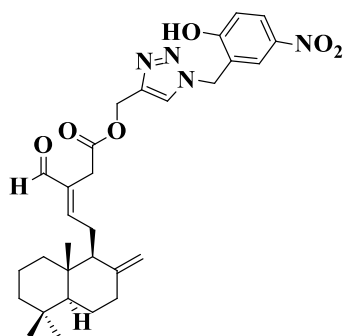


FT-IR (NaCl, ν_{\max} , cm^{-1})	: 3079, 2928, 2848, 2719, 2121, 1739, 1683, 1643, 891
¹ H NMR (500 MHz, CDCl ₃)	: 9.34 (s, 1H), 7.63-7.16 (m, 4H), 6.65 (t, <i>J</i> = 6.5 Hz, 1H), 5.65 (s, 2H), 5.22 (s, 2H), 4.82 (s, 1H), 4.34 (s, 1H), 3.32 (s, 2H), 2.54-1.04 (m, 14H), 0.89 (s, 3H), 0.82 (s, 3H), 0.71 (s, 3H)
¹³ C NMR (125 MHz, CDCl ₃)	: 193.4, 170.0, 159.1, 148.0, 142.9, 135.9, 133.9, 133.2, 130.4, 130.4, 128.2, 124.0, 123.5, 107.9, 58.2, 56.4, 55.4, 53.8, 41.9, 39.6, 39.2, 37.8, 33.6, 33.6, 29.6, 24.6, 24.0, 21.8, 19.3, 14.4
HRMS (ESI)	: <i>m/z</i> : 608.1921 [M+Na] ⁺ (calcd for C ₃₀ H ₃₇ BrFN ₃ O ₃ Na is 608.1900)

3.8.2.12. Synthesis of (*E*)-(1-(2-hydroxy-5-nitrobenzyl)-1*H*-1,2,3-triazol-4-yl)methyl 3-formyl-5-((5,5,8*a*-trimethyl-2-methylenedecahydronaphthalen-1-yl)pent-3-enoate (6i**)**

The compound **6i** was prepared by the reaction of 2-hydroxy-5-nitrobenzyl azide (10.88 mg, 1 equiv.) and compound **3** (20 mg, 1 equiv.) in ^tBuOH-water (1:2) mixture (3 ml) as per the method described in the section 3.8.1.5. Yield: 77% (23 mg).

FT-IR (NaCl, ν_{\max} , cm^{-1})	: 3081, 2928, 2847, 2118, 1740, 1681, 1644, 893
--	---



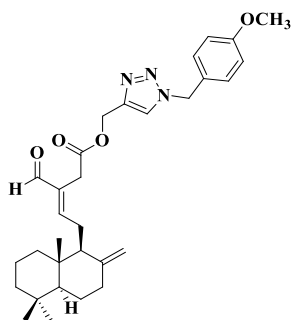
$^1\text{H NMR}$ (500 MHz, CDCl_3) : 9.94 (bs, 1H), 9.30 (s, 1H), 8.20 (d, $J = 2.5$ Hz 1H), 8.12 (dd, $J = 9$ Hz, 3Hz, 1H), 7.82 (s, 1H), 7.04 (d, $J = 9$ Hz, 1H), 6.70 (t, $J = 6.5$ Hz, 1H), 5.58 (s, 2H), 5.23 (s, 2H), 4.81 (s, 1H), 4.32 (s, 1H), 3.30 (s, 2H), 2.56-1.02 (m, 14H), 0.88 (s, 3H), 0.82 (s, 3H), 0.70 (s, 3H)

$^{13}\text{C NMR}$ (125 MHz, CDCl_3) : 194.3, 170.0, 161.2, 160.5, 148.1, 142.8, 140.8, 135.8, 126.8, 126.8, 124.9, 121.8, 116.8, 107.8, 57.9, 56.4, 55.4, 49.5, 41.9, 39.6, 39.2, 37.8, 33.6, 29.8, 24.7, 24.0, 21.7, 19.2, 14.4

HRMS (ESI) : m/z: 573.2689 $[\text{M}+\text{Na}]^+$ (calcd for $\text{C}_{30}\text{H}_{38}\text{N}_4\text{O}_6\text{Na}$ is 573.2689)

3.8.2.13. Synthesis of (*E*)-(1-(4-methoxybenzyl)-1*H*-1,2,3-triazol-4-yl)methyl 3-formyl-5-(5,5,8*a*-trimethyl-2-methylenedecahydronaphthalen-1-yl)pent-3-enoate (**6j**)

The compound **6j** was prepared by the reaction of 4-methoxybenzyl azide (10.06 mg, 1 equiv.) and compound **3** (22 mg, 1 equiv.) in $t\text{BuOH}$ -water (1:2) mixture (3 ml) as per the method described in the section 3.8.1.5. Yield: 75% (24 mg).



FT-IR (NaCl, ν_{max} , cm^{-1}) : 3081, 2933, 2843, 2115, 1739, 1682, 1643, 891

$^1\text{H NMR}$ (500 MHz, CDCl_3) : 9.33 (s, 1H), 7.50 (bs, 1H), 7.23 (d, $J = 8.5$ Hz, 2H), 6.90 (d, $J = 8.5$ Hz, 2H), 6.64 (t, $J = 6.5$ Hz, 1H), 5.44 (s, 2H), 5.20 (s, 2H), 4.82 (s, 1H), 4.34 (s, 1H), 3.80 (s, 3H), 3.32 (s, 2H), 2.52-1.04 (m, 14H), 0.89 (s, 3H), 0.82 (s, 3H), 0.71 (s, 3H)

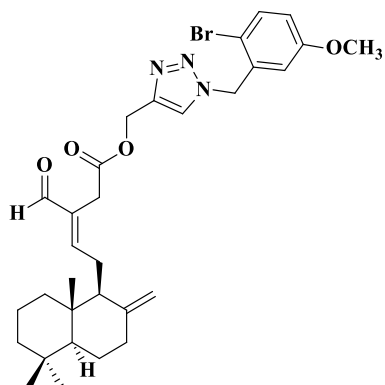
$^{13}\text{C NMR}$: 193.4, 170.0, 159.9, 159.2, 148.0, 135.9,

(125 MHz, CDCl_3) 129.8, 126.3, 114.5, 107.9, 58.2, 56.4, 55.3, 53.8, 41.9, 39.5, 39.2, 37.8, 33.6, 33.6, 29.6, 24.6, 24.0, 21.7, 19.2, 14.4

HRMS (ESI) : m/z: 542.3003 $[\text{M}+\text{Na}]^+$ (calcd for $\text{C}_{31}\text{H}_{41}\text{N}_3\text{O}_4\text{Na}$ is 542.2995)

3.8.2.14. Synthesis of (*E*)-(1-(2-bromo-5-methoxybenzyl)-1*H*-1,2,3-triazol-4-yl)methyl 3-formyl-5-(5,5,8a-trimethyl-2-methylenedecahydronaphthalen-1-yl)pent-3-enoate (**6k**)

The compound **6k** was prepared by the reaction of 2-bromo-5-methoxybenzyl azide (16.89 mg, 1 equiv.) and compound **3** (25 mg, 1 equiv.) in $^t\text{BuOH}$ -water (1:2) mixture (3 ml) as per the method described in the section 3.8.1.5. Yield: 66% (27 mg).



FT-IR (NaCl, ν_{max} , cm^{-1}) : 3080, 2932, 2844, 2115, 1739, 1682, 1643, 890

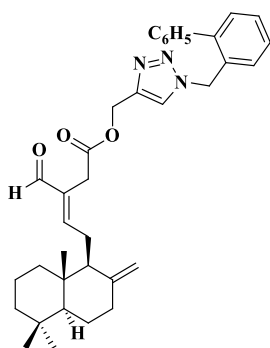
^1H NMR (500 MHz, CDCl_3) : 9.34 (s, 1H), 7.65 (s, 1H), 7.49 (d, $J = 9$ Hz, 1H), 6.79 (dd, $J_1 = 9$ Hz, 3 Hz, 1H), 6.72 (d, $J = 3$ Hz, 1H), 6.65 (t, $J = 6.5$ Hz, 1H), 5.60 (s, 2H), 5.22 (s, 2H), 4.82 (s, 1H), 4.35 (s, 1H), 3.75 (s, 3H), 3.33 (s, 2H), 2.54-1.04 (m, 14H), 0.90 (s, 3H), 0.82 (s, 3H), 0.71 (s, 3H)

^{13}C NMR (125 MHz, CDCl_3) : 193.4, 169.9, 159.4, 159.2, 148.0, 142.9, 135.9, 134.7, 133.8, 124.0, 116.3, 115.9, 113.6, 107.9, 58.2, 56.4, 55.6, 55.3, 53.9, 41.9, 39.5, 39.2, 37.8, 33.6, 33.6, 29.6, 24.6, 24.0, 21.8, 19.3, 14.4

HRMS (ESI) : m/z: 598.2278 $[\text{M}+\text{H}]^+$ (calcd for $\text{C}_{31}\text{H}_{40}\text{BrN}_3\text{O}_4$ is 598.2280)

3.8.2.15. Synthesis of (*E*)-(1-([1,1'-biphenyl]-2-ylmethyl)-1*H*-1,2,3-triazol-4-yl)methyl 3-formyl 5-(5,5,8a-trimethyl-2-methylenedecahydronaphthalen-1-yl)pent-3-enoate (**6l**)

The compound **6l** was prepared by the reaction of 1,1'-biphenyl azide (15.82 mg, 1 equiv.) and compound **3** (27 mg, 1 equiv.) in ^tBuOH-water (1:2) mixture (3 ml) as per the method described in the section 3.8.1.5. Yield: 86% (36 mg).



FT-IR (NaCl, ν_{\max} , cm^{-1}) : 3060, 2932, 2844, 2719, 2095, 1740, 1684, 1643, 891

¹H NMR (500 MHz, CDCl_3) : 9.33 (s, 1H), 7.44-7.24 (m, 10H), 6.64 (t, $J = 6.5$ Hz, 1H), 5.48 (s, 2H), 5.16 (s, 2H), 4.80 (s, 1H), 4.33 (s, 1H), 3.30 (s, 2H), 2.52-1.01 (m, 14H), 0.88 (s, 3H), 0.82 (s, 3H), 0.70 (s, 3H)

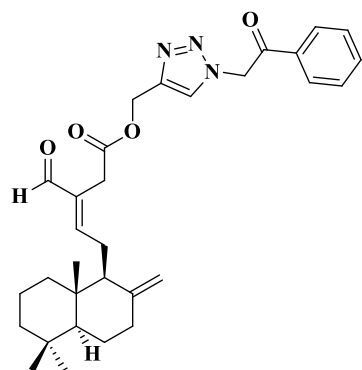
¹³C NMR (125 MHz, CDCl_3) : 193.4, 169.9, 159.0, 148.0, 142.6, 141.9, 139.8, 135.9, 131.8, 130.5, 129.0, 129.0, 128.7, 128.6, 128.2, 127.8, 123.8, 107.9, 58.2, 56.4, 55.3, 51.8, 41.9, 39.5, 39.2, 37.8, 33.6, 33.6, 29.6, 24.6, 24.0, 21.7, 19.2, 14.4

HRMS (ESI) : m/z : 588.3181 [$\text{M}+\text{Na}$]⁺ (calcd for $\text{C}_{36}\text{H}_{43}\text{N}_3\text{O}_3\text{Na}$ is 588.3202)

3.8.2.16. Synthesis of (*E*)-(1-(2-oxo-2-phenylethyl)-1*H*-1,2,3-triazol-4-yl)methyl 3-formyl-5-(5,5,8a-trimethyl-2-methylenedecahydronaphthalen-1-yl)pent-3-enoate (**6m**)

The compound **6m** was prepared by the reaction of phenacyl azide (10.39 mg, 1 equiv.) and compound **3** (23 mg, 1 equiv.) in ^tBuOH-water (1:2) mixture (3 ml) as per the method described in the section 3.8.1.5. Yield: 55% (18 mg).

FT-IR (NaCl, ν_{\max} , cm^{-1}) : 3082, 2929, 2848, 2121, 1738, 1682, 1643, 892



$^1\text{H NMR}$ (500 : 9.36 (s, 1H), 8.00 (d, $J = 7$ Hz, 2H), 7.78
 MHz, CDCl_3) (s, 1H), 7.68 (t, $J = 7.5$ Hz, 1H), 7.56 (t, J
 = 8 Hz, 2H), 6.67 (t, $J = 6.5$ Hz, 1H),
 5.86 (s, 2H), 5.30 (s, 2H), 4.84 (s, 1H),
 4.38 (s, 1H), 3.36 (d, $J = 4$ Hz, 2H), 2.56-
 1.06 (m, 14H), 0.88 (s, 3H), 0.82 (s, 3H),
 0.72 (s, 3H)

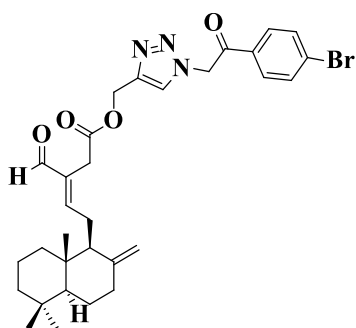
$^{13}\text{C NMR}$ (125 : 193.5, 189.9, 169.9, 159.2, 148.0, 135.9,
 MHz, CDCl_3) 134.6, 133.9, 129.2, 128.1, 125.6, 107.9,
 58.2, 56.4, 55.4, 55.4, 41.9, 39.6, 39.2,
 37.8, 33.6, 29.6, 24.6, 24.0, 21.7, 19.2,
 14.4

HRMS (ESI) : m/z : 540.2828 $[\text{M}+\text{Na}]^+$ (calcd for
 $\text{C}_{31}\text{H}_{39}\text{N}_3\text{O}_4\text{Na}$ is 540.2838)

3.8.2.17. Synthesis of (*E*)-1-(2-(4-bromophenyl)-2-oxoethyl)-1*H*-1,2,3-triazol-4-ylmethyl 3-formyl-5-(5,5,8a-trimethyl-2-methylenedecahydronaphthalen-1-yl) pent-3-enoate (**6n**)

The compound **6n** was prepared by the reaction of 4-bromo phenacyl azide (17.43 mg, 1 equiv.) and compound **3** (26 mg, 1 equiv.) in $^t\text{BuOH}$ -water (1:2) mixture (3 ml) as per the method described in the section 3.8.1.5. Yield: 72% (31 mg).

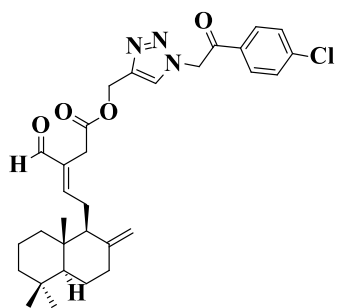
FT-IR (NaCl, : 3086, 2929, 2848, 2170, 1738, 1683,
 ν_{max} , cm^{-1}) 1644, 911



$^1\text{H NMR}$ (500 MHz, CDCl_3)	: 9.35 (s, 1H), 7.86 (d, $J = 8.5$ Hz, 2H), 7.76 (s, 1H), 7.70 (d, $J = 8.5$ Hz, 2H), 6.67 (t, $J = 6.5$ Hz, 1H), 5.81 (s, 2H), 5.29 (s, 2H), 4.84 (s, 1H), 4.37 (s, 1H), 3.34 (d, $J = 3.5$ Hz, 2H), 2.57-1.06 (m, 14H), 0.88 (s, 3H), 0.82 (s, 3H), 0.72 (s, 3H)
$^{13}\text{C NMR}$ (125 MHz, CDCl_3)	: 193.5, 189.2, 169.9, 159.2, 148.0, 135.9, 132.6, 130.1, 129.6, 125.6, 107.8, 58.2, 56.4, 55.4, 55.2, 41.9, 39.6, 39.2, 37.8, 33.6, 29.7, 24.6, 24.0, 21.7, 19.2, 14.4
HRMS (ESI)	: m/z : 618.1917 $[\text{M}+\text{Na}]^+$ (calcd for $\text{C}_{31}\text{H}_{38}\text{BrN}_3\text{O}_4\text{Na}$ is 618.1943)

3.8.2.18. Synthesis of (*E*)-1-(2-(4-chlorophenyl)-2-oxoethyl)-1*H*-1,2,3-triazol-4-ylmethyl 3-formyl 1-5-(5,5,8a-trimethyl-2-methylene decahydronaphthalen-1-yl) pent-3-enoate (**60**)

The compound **60** was prepared by the reaction of 4-chlorophenacyl azide (7.65 mg, 1 equiv.) and compound **3** (14 mg, 1 equiv.) in $t\text{BuOH}$ -water (1:2) mixture (3 ml) as per the method described in the section 3.8.1.5. Yield: 62% (13 mg).



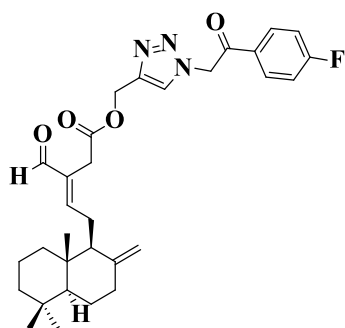
FT-IR (NaCl, ν_{max} , cm^{-1})	: 3085, 2930, 2847, 2130, 1739, 1705, 1683, 1643, 891
$^1\text{H NMR}$ (500 MHz, CDCl_3)	: 9.35 (s, 1H), 7.94 (d, $J = 9$ Hz, 2H), 7.77 (s, 1H), 7.53 (d, $J = 8.5$ Hz, 2H), 6.67 (t, $J = 6.5$ Hz, 1H), 5.82 (s, 2H), 5.29 (s, 2H), 4.84 (s, 1H), 4.38 (s, 1H), 3.35 (d, $J = 3.5$ Hz, 2H), 2.57-1.06 (m, 14H), 0.88 (s, 3H), 0.82 (s, 3H), 0.72 (s, 3H)
$^{13}\text{C NMR}$ (125 MHz, CDCl_3)	: 193.5, 188.9, 169.9, 159.1, 148.06, 141.3, 135.9, 132.2, 129.6, 129.5, 125.6, 107.8,

99.9, 58.2, 56.4, 55.4, 55.2, 41.9, 39.6,
39.2, 37.8, 33.6, 29.7, 24.6, 24.0, 21.7,
19.2, 14.4

HRMS (ESI) : m/z: 574.2438 [M+Na]⁺ (calcd for
C₃₁H₃₈ClN₃O₄Na is 574.2438)

3.8.2.19. Synthesis of (*E*)-(1-(2-(4-fluorophenyl)-2-oxoethyl)-1*H*-1,2,3-triazol-4-yl)methyl 3-formyl-5-(5,5,8a-trimethyl-2-methylenedecahydronaphthalen-1-yl)pent-3-enoate (**6p**)

The compound **6p** was prepared by the reaction of 4-fluorophenacyl azide (6.53 mg, 1 equiv.) and compound **3** (13 mg, 1 equiv.) in ^tBuOH-water (1:2) mixture (3 ml) as per the method described in the section 3.8.1.5. Yield: 53% (10 mg).



FT-IR (NaCl, : 3079, 2927, 2850, 2115, 1739, 1683, 1644,
v_{max}, cm⁻¹) 891

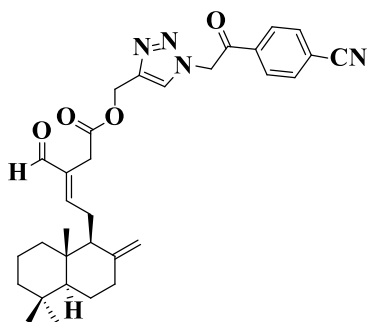
¹H NMR (500 : 9.36 (s, 1H), 8.06-8.03 (m, 2H), 7.77 (s,
MHz, CDCl₃) 1H), 7.23 (t, *J* = 8.5 Hz, 2H), 6.67 (t, *J* =
6.5 Hz, 1H), 5.82 (s, 2H), 5.30 (s, 2H),
4.84 (s, 1H), 4.38 (s, 1H), 3.35 (d, *J* = 4
Hz, 2H), 2.56-1.06 (m, 14H), 0.88 (s, 3H),
0.82 (s, 3H), 0.72 (s, 3H)

¹³C NMR : 193.5, 188.4, 169.9, 159.1, 152.06, 148.0,
(125 MHz, 144.8, 135.9, 130.9, 116.6, 116.4, 107.9,
CDCl₃) 58.2, 56.4, 55.4, 55.2, 41.9, 39.8, 39.2,
37.8, 33.6, 29.6, 24.6, 24.0, 21.7, 19.2,
14.4

HRMS (ESI) : m/z: 558.2737 [M+Na]⁺ (calcd for
C₃₁H₃₈FN₃O₄Na is 558.2744)

3.6.2.20. Synthesis of (*E*)-(1-(2-(4-cyanophenyl)-2-oxoethyl)-1*H*-1,2,3-triazol-4-yl)methyl 3-formyl-5-(5,5,8a-trimethyl-2-methylenedecahydronaphthalen-1-yl)pent-3-enoate (**6q**)

The compound **6q** was prepared by the reaction of 4-cyano phenacyl azide (17.74 mg, 1 equiv.) and compound **3** (34 mg, 1 equiv.) in ^tBuOH-water (1:2) mixture (3 ml) as per the method described in the section 3.8.1.5. Yield: 35 % (18 mg).



FT-IR (NaCl, : 3095, 2928, 2848, 2232, 1738, 1683,
 v_{\max} , cm^{-1}) 1643, 892

¹H NMR (500 : 9.34 (s, 1H), 8.10 (d, J = 8.5 Hz, 2H),
 MHz, CDCl₃) 7.86 (d, J = 8.5 Hz, 2H), 7.78 (s, 1H),
 6.68 (t, J = 6.5 Hz, 1H), 5.86 (s, 2H),
 5.30 (s, 2H), 4.84 (s, 1H), 4.38 (s, 1H),
 3.34 (d, J = 2.5 Hz, 2H), 2.57-1.04 (m,
 14H), 0.89 (s, 3H), 0.82 (s, 3H), 0.73 (s,
 3H)

¹³C NMR (125 : 193.6, 189.1, 170.0, 159.2, 148.0, 136.74,
 MHz, CDCl₃) 135.9, 133.0, 128.6, 125.6, 117.9, 117.4,
 107.9, 58.2, 56.4, 55.5, 55.4, 41.9, 39.58,
 39.2, 37.8, 33.6, 29.7, 24.6, 24.09, 21.7,
 19.3, 14.4

HRMS (ESI) : m/z : 541.2828 [M-H]⁺ (calcd for
 C₃₂H₃₈N₄O₄Na is 541.2809)

3.8.3. Biology

3.8.3.1. *In vitro* cytotoxic evaluation of compounds by MTT assay

In vitro toxicity of the synthesized compounds was assessed by standard MTT bioassay³⁸ in HepG2 cell line (American Type Cell Culture, ATCC, Manassas, VA, USA) at 24 hr of drug administration. In brief, the cells were seeded in 96-well plates (10⁴ cells/well in 200 μ L of medium) and incubated for 24 hr for attachment. Test compounds were prepared prior to the experiment by dissolving in 0.1% DMSO and diluted with the medium. The cells were then

exposed to different concentrations of the compounds (0.5-100 μM) in the volume of 200 μL /well. Cells in the control wells received the same volume of medium containing 0.1% DMSO. After 24 hr, the medium was removed, and cell cultures were incubated with 100 μL MTT reagent (5 mg/mL) for 4 hr at 37 $^{\circ}\text{C}$. The formazan crystals formed by the viable cells was solubilized by addition of 200 μL DMSO. The suspension was placed on the shaker for 5 min, and absorbance was recorded at 540 nm by the plate reader (Biotek, USA). The experiment was performed in triplicate. The percentage of cytotoxicity and percentage cell viability was calculated using the following formula.

$$\text{Cell viability (\%)} = [\text{Abs sample} / \text{Abs control}] \times 100$$

Where Abs (absorbance) is calculated as, $\text{Abs}_{\text{sample}} = \text{OD of sample-blank}$, $\text{Abs}_{\text{control}} = \text{OD of control-blank}$.

3.8.3.2. Pancreatic lipase inhibitory activity assay

3.8.3.2.1. Method A

The pancreatic lipase assay was performed as described by Bustanji *et al.* with some modifications.³⁶ Briefly, a volume of 50 μL porcine pancreatic lipase (Sigma, St. Louis, MO) (1 mg/mL in 2.5 mM tris-hydrochloride buffer pH 7.4 with 0.125 mM sodium chloride) was pre-mixed with 100 μL of different concentration of compounds (Stock solutions of the isolates, synthetic derivatives and orlistat were prepared in DMSO with concentrations ranging from 0.25 μM -20 μM and 0.2 μM -1.4 μM , respectively) and incubated at 37 $^{\circ}\text{C}$ for 15 min. Following pre-incubation, 100 μL *p*-nitrophenyl butyrate (PNPB) (25 mM) was added to the enzyme-sample mixture, and the volume was made up to 300 μL using tris hydrochloride buffer. The amount of DMSO in the final concentration did not exceed 1%. The reaction mixture was incubated at 37 $^{\circ}\text{C}$ for 60 min, and the amount of *p*-nitrophenol produced was measured at 405 nm using a plate reader (Biotek, USA). The percentage inhibition of pancreatic lipase was calculated as follows.

$$\% \text{ inhibition} = \frac{\text{Abs}_{\text{control}} - \text{Abs}_{\text{sample}}}{\text{OD}_{\text{control}}} \times 100$$

Absorbance (Abs) of control (DMSO) or sample was calculated by subtracting ODs for each sample from their corresponding blank. A bar diagram was plotted with % inhibition against test compounds (concentrations 1, 5, 10, 20 μM) where $n = 4$.

The IC_{50} , the concentration of the compounds /positive control that causes 50% inhibition of the enzyme were calculated from the results of isolated and synthetic derivatives of concentrations (0.25 μM -20 μM) for both methods A and B from the dose-response curves using a logistic model in Origin software (Origin Lab Corp.).

3.8.3.2.2. Method B

The pancreatic lipase activity was assayed as narrated by Kido *et al.* (2003) with slight modifications.³⁷ The activity was measured based on the amount of free fatty acids released from the emulsified olive oil substrate. Emulsion mixture consisting of bile salts, cholesterol and phospholipid were taken to imitate *in vivo* conditions. The bile salts concentration was adjusted to approximate that of duodenal aspirates.⁴⁰ The substrate emulsion (0.6 mL) was formulated by ultrasonification of olive oil (48 g/L) in a solution containing 1 mmol/L taurochenodeoxycholate, 9 mmol/L taurocholate, 0.1 mmol/L cholesterol, 0.8 g/L L- α -phosphatidylcholine, 1 mmol/L calcium acetate and 100 mmol/L Tris-HCl (pH 8.0). After addition of the test compounds in 75 μL of 100 mmol/L Tris- HCl (pH 8.0), or vehicle alone, the assay mixture was pre-incubated for 5 min at 37 $^{\circ}\text{C}$. The reaction was initiated by the addition of 75 μL lipase solution containing 0.1 g/L of 100 mmol/L Tris-HCl (pH 8.0). After incubation for 30 min at 37 $^{\circ}\text{C}$, free fatty acids concentration in the reaction was calculated as described by Duncombe (1963).⁴¹ Human pancreatic lipase was used in all experiments. The inhibitory activity of test materials was calculated from the relative fatty acid concentration liberated compared with the control value. The concentration ranges of isolates and synthetic derivatives tested in the method B were in the range 0.25-20 μM . A bar diagram was plotted with % inhibition against test compound (concentrations 0.5, 1, 5, 10, 15 μM) since the results of method A showed IC_{50} values starting from 0.77 μM concentration.

The IC_{50} values were calculated from the dose-response curves (Test compounds concentration ranging from 0.25 μM to 20 μM using a logistic model in Origin software (Origin Lab Corp.).

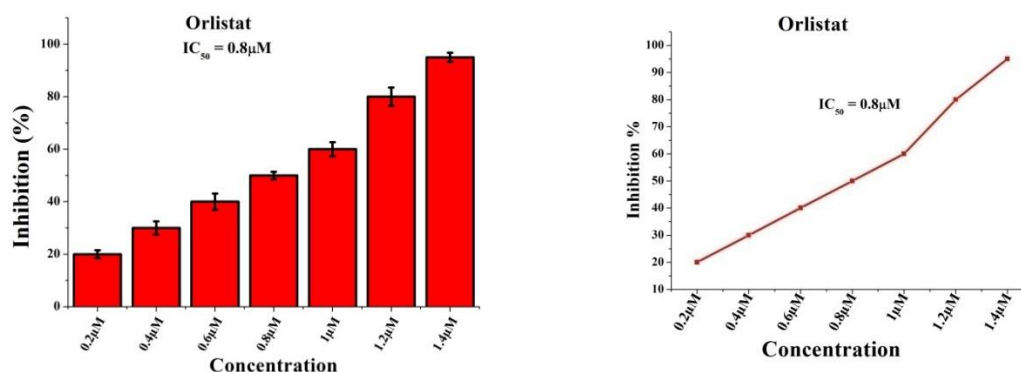


Figure 3.12 (Method A). The percentage inhibition of orlistat against porcine pancreatic lipase in various concentrations

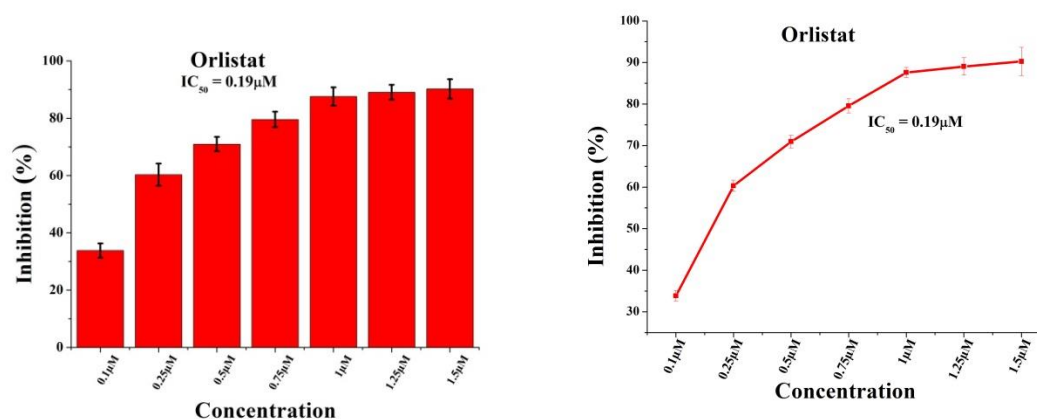
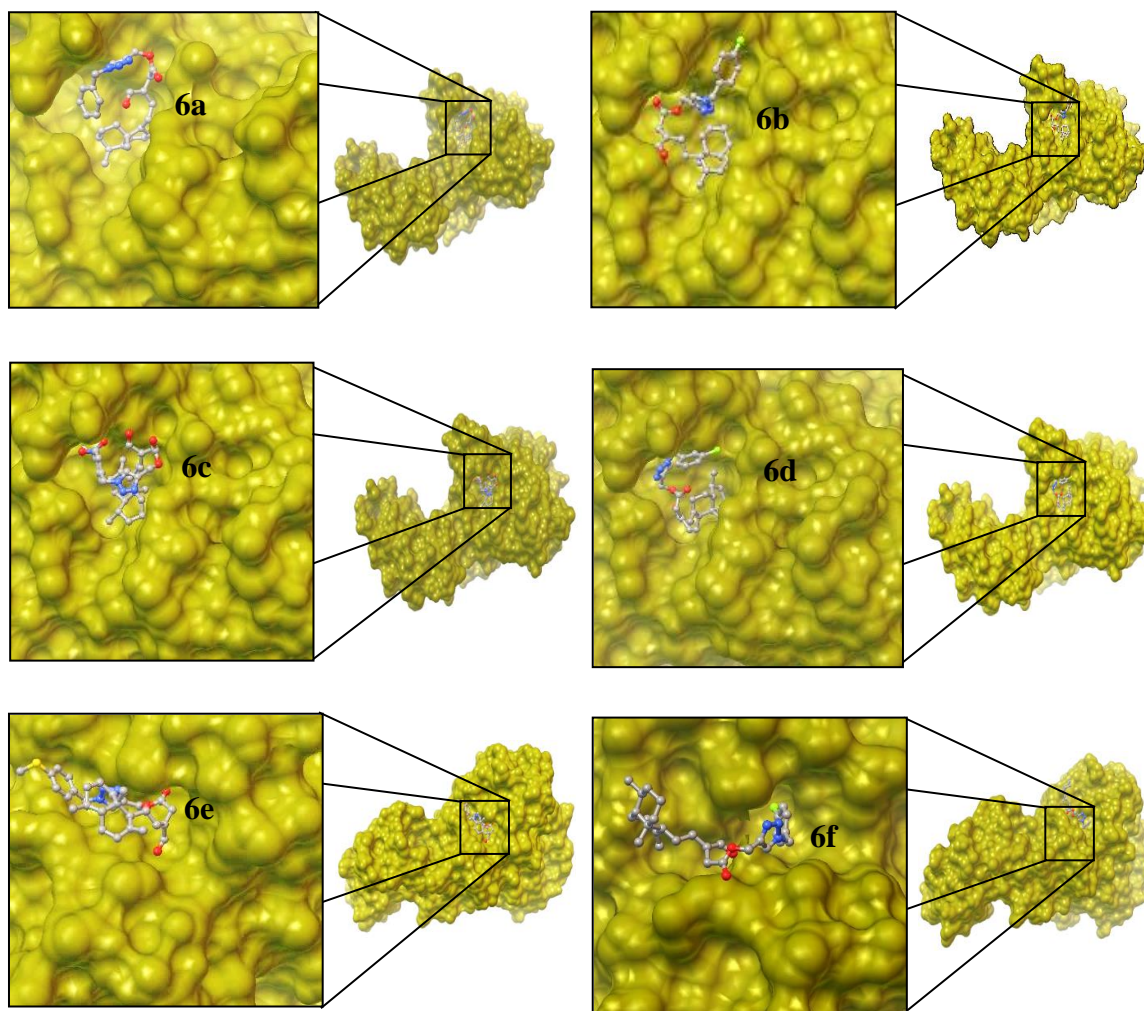


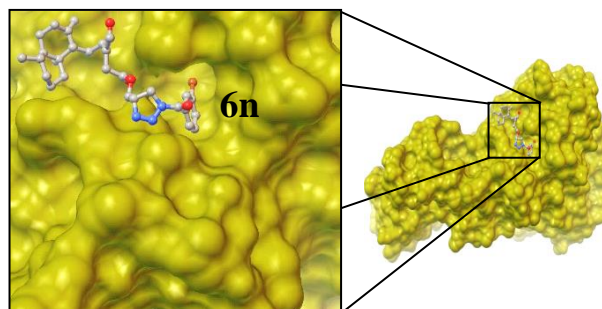
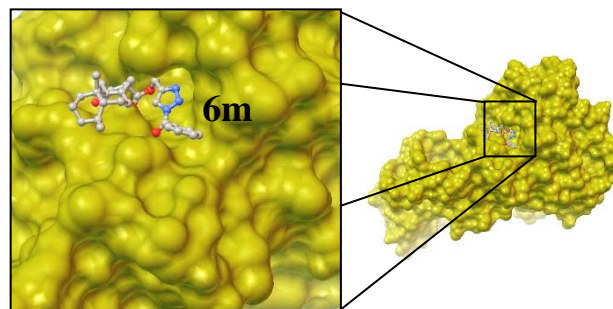
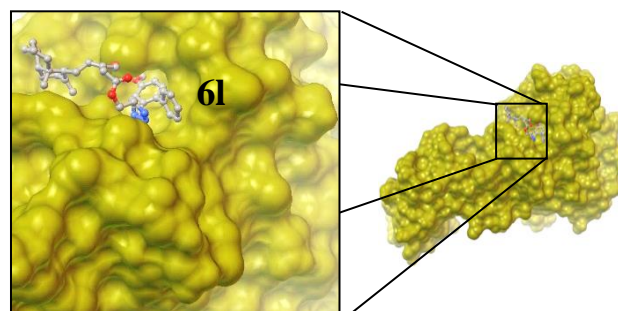
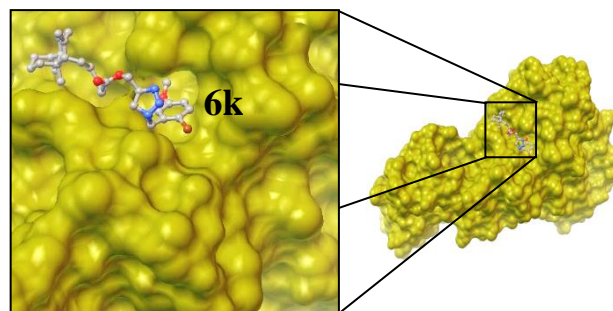
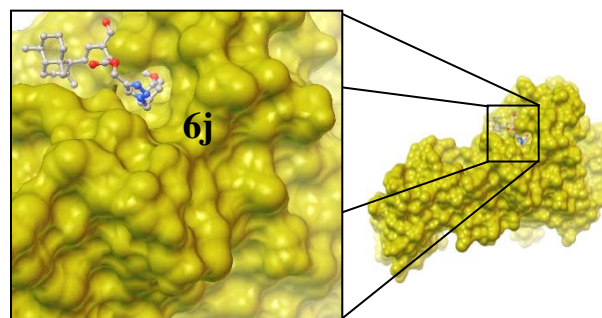
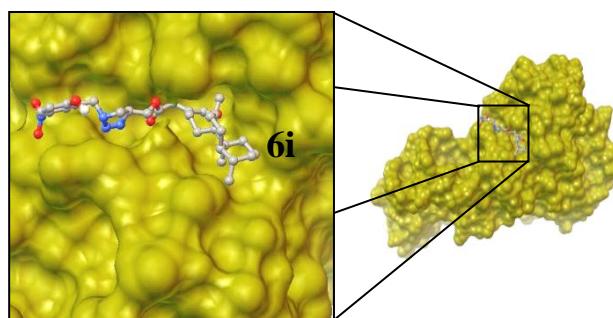
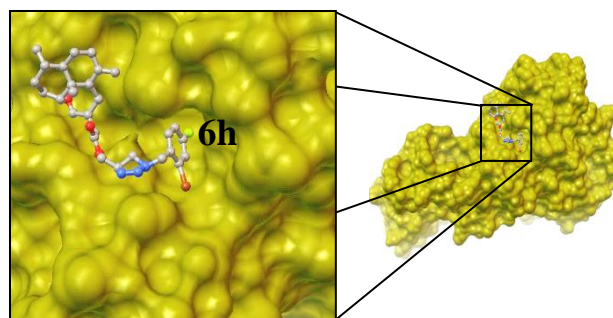
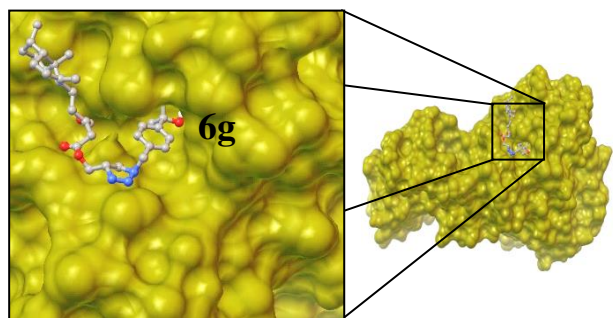
Figure 3.13 (Method B). The percentage inhibition of orlistat against Human pancreatic lipase in various concentrations

3.8.4. Molecular docking studies of various triazole derivatives and intermediates

The molecular docking studies of various triazole derivatives were carried out using the Autodock 3.0 version (Morris *et al.*, 1998).³⁹ In brief, the X-ray Human pancreatic lipase structure coordinates were obtained from protein data bank (PDB ID: 1LPA-B; Van Tilburgh *et al.*, 1993),⁴² and the 2D structures of compounds were created using JME editor (Bienfait and Ertl, 2013).⁴³ The protonation state and energy minimizations of these compounds were done with PRODRG tool (Schuttelkopf and Alten., 2004).⁴⁴ The predefined grid space on lipase structure was created using the autogrid program. The docking was

carried out using the Lamarkian genetic algorithm. A total 50 GA runs were performed, and Gibb's free energy of binding was evaluated best ranked conformation of compound/s. The possible binding site of compound/s was visualized using MGL software (Michel, 1999).





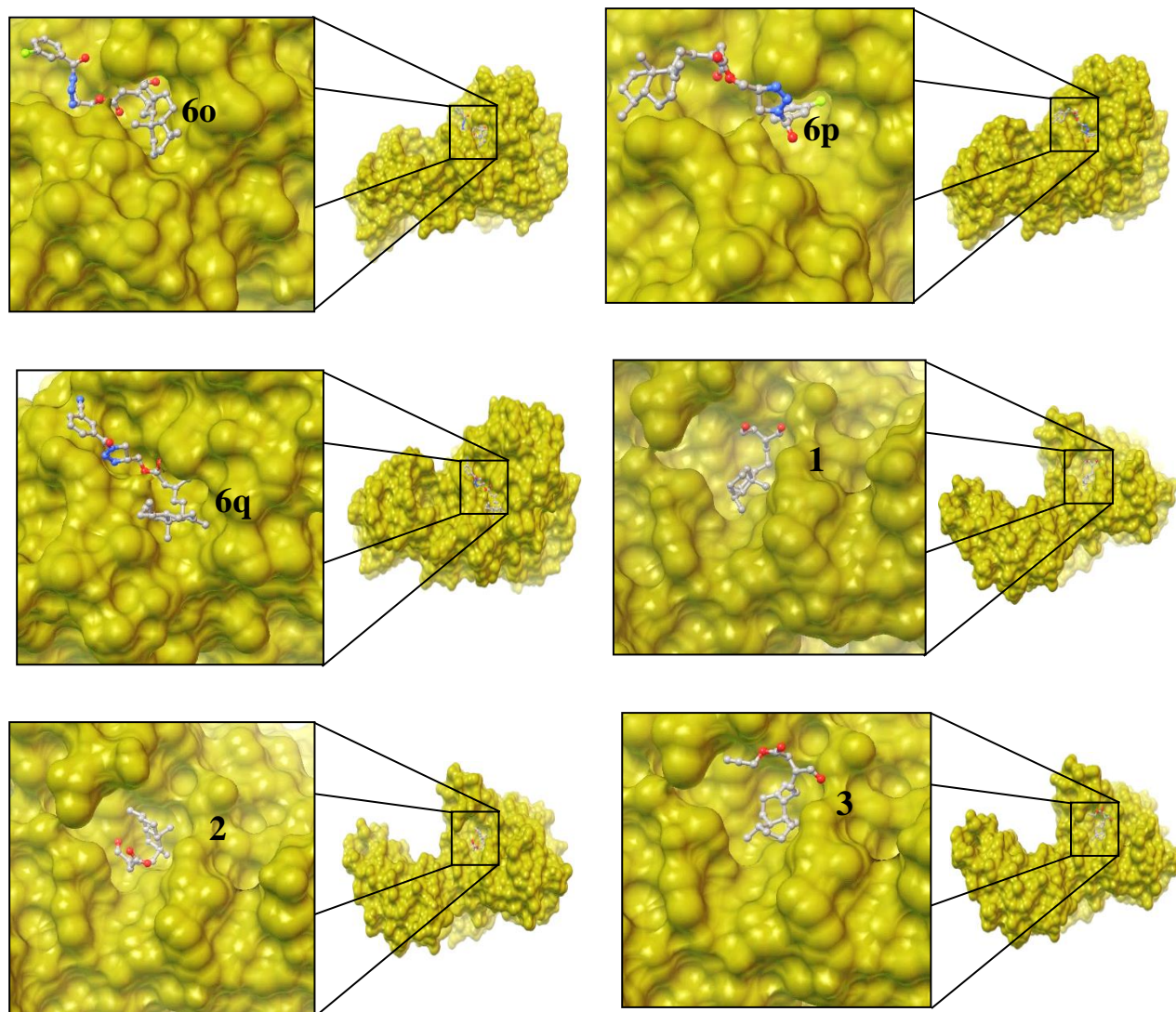


Figure 3.14. The representative molecular docking studies of isolates and semi-synthetic derivatives

Table 3.2. List of compounds used in docking study and the estimated free energy of binding

Compound code	Predicted free energy of binding (kcal/mol)
6a	-8.24
6b	-8.50
6c	-6.08
6d	-6.80
6e	-7.00
6f	-4.90
6g	-5.43
6h	-4.90
6i	-6.16
6j	-8.09
6k	-3.75
6l	-2.17
6m	-3.77
6n	-3.29
6o	-5.04
6p	-7.25
6q	-6.14
1	-4.13
2	-1.19
3	-7.07

3.9. References

- (1) Barnes, A. Overweight versus Obese: Different Risk and Different Management. *Tex Heart Inst. J.* **2015**, *42*, 237-238.
- (2) Donahue, R. P.; Abbott, R. D.; Bloom, E.; Reed, D. M.; Yano, K. Central Obesity and Coronary Heart Disease in Men. *The Lancet* **1987**, *11*, 821-824.

- (3) Fabbrini, E.; Sullivan, S.; Klein, S. Obesity and Nonalcoholic Fatty Liver Disease: Biochemical, Metabolic, and Clinical Implications. *Hepatology* **2010**, *51*, 679-89.
- (4) Golay, A.; Ybarra, J. Link between obesity and type 2 diabetes. *Best Pract. Res. Clin. Endocrinol. Metab.* **2005**, *19*, 649-63.
- (5) Obesity facts from: <http://www.who.int/mediacentre/factsheets/fs311/en/index.html>.
- (6) Fu, C.; Jiang, Y.; Guo, J.; Su, Z. Natural Products with Anti-obesity Effects and Different Mechanisms of Action. *J. Agric. Food Chem.* **2016**, *64*, 9571-9585.
- (7) Cosentino, G.; Conrad, A. O.; Uwaifo, G. I. Phentermine and Topiramate for the Management of Obesity: A Review. *Drug Des. Devel. Ther.* **2013**, *7*, 267-278.
- (8) Wang, T. Y.; Liu, M.; Portincasa, P.; Wang, D. Q. New Insights into the Molecular Mechanism of Intestinal Fatty Acid Absorption. *Eur. J. Clin. Invest.* **2013**, *43*, 1203-23.
- (9) Sun, N. N.; Wu, T. Y.; Chau, C. F. Natural Dietary and Herbal Products in Anti-obesity Treatment. *Molecules* **2016**, *21*, 1351.
- (10) Fu, C.; Jiang, Y.; Guo, J.; Su, Z. Natural Products with Anti-obesity Effects and Different Mechanisms of Action. *J. Agric. Food Chem.* **2016**, *64*, 9571-9585.
- (11) Mopuri, R.; Meriga, B. Anti-lipase and Anti-obesity Activities of *Terminalia paniculata* Bark in High Calorie Diet-Induced Obese Rats. *Global J. Pharmacol.* **2014**, *8*, 114-119.
- (12) Jiang, W.; Li, W.; Han, L.; Liu, L.; Zhang, Q.; Zhang, S.; Nikaido, T.; Koike, K. Biologically Active Triterpenoid Saponins from *Acanthopanax senticosus*. *J. Nat. Prod.* **2006**, *69*, 1577-1581.
- (13) Cai, S.; Wang, O.; Wang, M.; He, J.; Wang, Y.; Zhang, D.; Zhou, F.; Ji, B. *In vitro* Inhibitory Effect on Pancreatic Lipase Activity of Subfractions from Ethanol Extracts of Fermented Oats (*Avena sativa* L.) and Synergistic Effect of Three Phenolic Acids. *J. Agric. Food Chem.* **2012**, *60*, 7245-7251.
- (14) Sugiyama, H.; Akazome, Y.; Shoji, T.; Yamaguchi, A.; Yause, M.; Kanda, T.; Ohtake, Y. Oligomeric Procyanidins in Apple Polyphenol are Main Active Components for Inhibition of Pancreatic Lipase and Triglyceride Absorption. *J. Agric. Food Chem.* **2007**, *55*, 4604-4609.

- (15) Nakai, M.; Fukui, Y.; Asami, S.; Toyoda-Ono, Y.; Iwashita, T.; Shibata H.; Mitsunaga, T.; Hashimoto, F.; Kiso, Y. Inhibitory Effects of Oolong Tea Polyphenols on Pancreatic Lipase *In vitro*. *J. Agric. Food Chem.* **2005**, *53*, 4593-4598.
- (16) Nissankara Rao, L. S.; Kilari, E. K.; Kola, P. K. Protective Effect of *Curcuma amada* Acetone Extract Against High-Fat and High-Sugar Diet-Induced Obesity and Memory Impairment. *Nutr. Neurosci.* **2019**, 1-15.
- (17) Yoshioka, Y.; Yoshimura, N.; Matsumura, S.; Wada, H.; Hoshino, M.; Makino, S.; Morimoto, M. α -Glucosidase and Pancreatic Lipase Inhibitory Activities of Diterpenes from Indian Mango Ginger (*Curcuma amada* Roxb.) and its Derivatives. *Molecules* **2019**, *24*, 1-12.
- (18) Kharb, R.; Sharma, P. C.; Yar, M. S. Pharmacological Significance of Triazole Scaffold. *J. Enzyme Inhib. Med. Chem.* **2011**, *26*, 1–21.
- (19) Nunes-Souza, V.; Dias-Júnior, N. M.; Eleutério-Silva, M. A.; Ferreira-Neves, V. P.; Moura, F. A.; Alenina, N.; Bader, M.; Rabelo, L. A. 3-Amino-1,2,4-Triazole Induces Quick and Strong Fat loss in Mice with High Fat-Induced Metabolic Syndrome. *Oxid. Med. Cell. Longev.* **2020**, 1-14.
- (20) Holubova, M.; Nagelova, V.; Lacinova, Z.; Haluzik, M.; Sykora, D.; Moulin, A.; Blayo, A.L.; Fehrentz, J.A.; Martinez, J.; Stofkova, A.; Jurcovicova, J.; Zelezna, B.; Maletinska, L. Triazole GHS-R1a Antagonists JMV4208 and JMV3002 Attenuate Food Intake, Body Weight, and Adipose Tissue Mass in Mice. *Mol. Cell. Endocrinol.* **2014**, 1-8.
- (21) Alonso, M.; Serrano, A.; Vida, M.; Crespillo, A.; Hernandez-Folgado, L.; Jagerovic, N.; Goya, P.; Reyes-Cabello, C.; Perez-Valero, V.; Decara, J.; Macias-Gonzalez, M.; Bermúdez-Silva, F. J.; Suarez, J.; Fonseca, F. R.; Pavon, F. J. Antiobesity Efficacy of LH-21, A Cannabinoid CB1 Receptor Antagonist with Poor Brain Penetration, in Diet-Induced Obese Rats, *Br. J. Pharmacol.* **2012**, *165*, 2274-2291.
- (22) Pavon, F. J.; Bilbao, A.; Hernandez-Folgado, L.; Cippitelli, A.; Jagerovic, N.; Abellan, G.; Rodriguez-Franco, M. I.; Serrano, A.; Macias, M.; Gomez, R.; Navarro, M.; Goya, P.; Fonseca, F. R. Antiobesity Effects of the Novel *In vivo*

- Neutral Cannabinoid Receptor Antagonist 5-(4-chlorophenyl)-1-(2,4-dichlorophenyl)-3-hexyl-1H-1,2,4-triazole LH 21. *Neuropharmacology* **2006**, *51*, 358-366.
- (23) Kinfé, H. H.; Belay, Y. H.; Joseph, J. S.; Mukwevho, E. Evaluation of the Influence of Thiosemicarbazone-Triazole Hybrids on Genes Implicated in Lipid Oxidation and Accumulation as Potential Antiobesity Agents. *Bioorg. Med. Chem. Lett.* **2013**, *23*, 5275-5278.
- (24) Shilpa, G.; Renjitha, J.; Saranga, R.; Sajin, K. F.; Nair, M. S.; Joy, B.; Sasidhar, B. S.; Priya, S. Epoxyazadiradione Purified from the *Azadirachta indica* Seed Induced Mitochondrial Apoptosis and Inhibition of NF κ B Nuclear Translocation in Human Cervical Cancer Cells. *Phytother. Res.* **2017**, *31*, 1892-1902.
- (25) Kumar, V. P.; Renjitha, J.; Salfeena, C. T. F.; Ashitha, K. T.; Keri, R. S.; Varughese, S.; Sasidhar, B.S. Antibacterial and Antitubercular Evaluation of Dihydronaphthalenone-indole Hybrid Analogs. *Chem. Biol. Drug Des.* **2017**, *90*, 703-708.
- (26) Ashitha, K. T.; Kumar, V. P.; Salfeena, C. T. F.; Sasidhar, B. S. BF₃-OEt₂-Mediated Tandem Annulation: A Strategy To Construct Functionalized Chromeno- and Pyrano-Fused Pyridines. *J. Org. Chem.* **2018**, *83*, 113-124.
- (27) Jatoi, S. A.; Kikuchi, A.; Gilani, S. A.; Watanabe, K. N. Phytochemical, Pharmacological and Ethnobotanical Studies in Mango Ginger. *Phytother. Res.* **2007**, *21*, 507-516.
- (28) Behera, K. K. Ethnomedicinal Plants used by the Tribals of Similipal Bioserve, Orissa, India: A Pilot Study. *Ethnobot. Leaflet.* **2006**, *10*, 149-173.
- (29) Ramachandran, C.; Quirin, K. W.; Escalon, E. A.; Lollett, I. V.; Melnick, S. J. Therapeutic Effect of Supercritical CO₂ Extracts of Curcuma Species with Cancer Drugs in Rhabdomyosarcoma Cell Lines. *Phytother. Res.* **2015**, *29*, 1152-1160.
- (30) Singh, S.; Kumar, J. K.; Saikia, D.; Shanker, K.; Thakur, J. P.; Negi, A. S.; Banerjee, S. A bioactive Labdane diterpenoid from *Curcuma amada* and its semi-synthetic analogues as antitubercular agents. *Eur. J. Med. Chem.* **2010**, *45*, 4379-4382.

- (31) Narasimha, S.; Battula, K. S.; Nukala, S. K.; Gondru, R.; Reddy, Y. N.; Nagavelli, V. R. One-pot Synthesis of Fused Benzoxazino[1,2,3]triazolyl [4,5-c]quinolinone Derivatives and their Anticancer Activity. *RSC Adv.* **2016**, *6*, 74332.
- (32) Tantray, M. A.; Khan, I.; Hamid, H.; Alam, M. S.; Umar, S.; Ali, Y.; Sharma, K.; Hussain, F. Synthesis of Novel Oxazolo[4,5-b]pyridine-2-one Based 1,2,3-Triazoles as Glycogen Synthase Kinase-3b Inhibitors with Anti-inflammatory Potential. *Chem. Biol. Drug. Des.* **2016**, *87*, 918-926.
- (33) Kharb, R.; Sharma, P. C.; Yar, M. S. Pharmacological Significance of Triazole Scaffold. *J. Enzyme Inhib. Med. Chem.* **2011**, *26*, 1-21.
- (34) Sharma, M. K.; Machhi, J.; Murumkar, P.; Yadav, M. R. New Role of Phenothiazine Derivatives as Peripherally Acting CB1 Receptor Antagonizing Anti-obesity agents. *Sci. Rep.* **2018**, *8*, 1650.
- (35) Sheeja, A. D. B.; Nair, M. S. Facile Isolation of *E*-labda 8(17),12-diene-15,16-dial from *Curcuma amada* and Its Conversion to Other Biologically Active Compounds. *Indian. J. Chem. Sect. B.* **2014**, *53*, 319-324
- (36) Wilson, A. P. Cytotoxicity and Viability Assay, in *Animal Cell Culture: A Practical Approach*, 2nd edition, Masters JRW, Oxford University Press, Oxford, **2000**, 175-219.
- (37) Bustanji, Y.; Issa, A.; Mohammad, M.; Hudaib, M.; Tawah, K. Inhibition of Hormone Sensitive Lipase and Pancreatic Lipase by *Rosmarinus officinalis* Extract and Selected Phenolic Constituents. *J. Med. Plants Res.* **2010**, *4*, 2235-2242.
- (38) Kido, Y.; Hiramoto, S; Murao, M.; Horio, Y; Miyazaki, T; Kodama, T.; Nakabou, Y. Epsilon-polylysine Inhibits Pancreatic Lipase Activity and Suppresses Postprandial Hypertriacylglyceridemia in Rats. *J. Nutr.* **2003**, *133*, 1887-91.
- (39) Morris, G. M.; Goodsell, D. S.; Halliday, R.S.; Huey, R.; Hart, W. E.; Belew, R. K.; Olson, A. J. Automated Docking Using a Lamarckian Genetic Algorithm and Empirical Binding Free Energy Function. *J. Comput. Chem.* **1998**, *19*, 1639-1662.
- (40) Mansbach, C.; Cohen, R.; Leff, P. Isolation and Properties of the Mixed Lipid Micelles Present in Intestinal Content During Fat Digestion in Man. *J. Clin. Investig.* **1975**, *56*, 781-791.

- (41) Duncombe, W. G. The Colorimetric Micro-determination of Long-chain Fatty Salts. *Biochem. J.* **1963**, 88, 7-10.
- (42) VanTilbeurgh, H.; Egloff, M. P.; Martinez, C.; Rugani, N.; Verger, R.; Cambillau, C. Interfacial Activation of the Lipase-procolipase Complex by Mixed Micelles Revealed by X-ray Crystallography. *Nature* **1993**, 362, 814-820.
- (43) Bienfait, B.; Ertl, P. JSME: A Free Molecule Editor in Java Script. *J. Cheminformatics.* **2013**, 5, 1-6.
- (44) Schüttelkopf, A. W.; Van Aalten, D. M. F. PRODRG - A Tool for High-throughput Crystallography of Protein-ligand Complexes. *Acta Crystallogr.* **2004**, 60, 1355-1363.

Anti-hyperlipidemic Potential of Labdane-Pyrroles via Inhibition of Cholesterol and Triglycerides Synthesis

4.1. Abstract

Hyperlipidemia is the clinical condition where blood has an increased level of lipids, such as cholesterol and triglycerides. Therefore controlling hyperlipidemia is considered to be a protective strategy to treat many associated diseases. Thus, novel natural product derived pyrrole and pyrazole-(*E*)-labda-8(17),12-diene-15,16-dial conjugates with cholesterol and triglycerides synthesis inhibition potential were designed through scaffold hopping approach and synthesized via one-pot selective cycloaddition. Amongst the tested hybrids, **3i** exhibited excellent activity against triglyceride and cholesterol synthesis with percentage inhibition of 71.73 ± 0.78 and 68.61 ± 1.19 , which was comparable to the positive controls Fenofibrate and Atorvastatin respectively. Compounds **3j** and **3k** also exhibited considerable potential as promising leads. The HMG CoA reductase inhibitory activity of the compounds was consistent with that of inhibitory activity of cholesterol synthesis. Compound **3i** showed the highest inhibitory potential (78.61 ± 2.80), which was comparable to that of the positive control Pravastatin (78.05 ± 5.4). Favourably, none of the compounds showed cytotoxicity (HepG2) in the concentration ranging from 0.5-100 μ M.

4.2. Introduction

Hyperlipidemia is a metabolic disorder characterized by higher levels of total cholesterol (TC), triglycerides (TGs), or both in plasma,¹ and it is a major known risk factor for atherosclerosis, coronary heart diseases (CHD), myocardial infarction, ischemic stroke, pancreatitis, etc.² The lipids consist of cholesterol, lipoproteins such as very low density lipoprotein (VLDL), low density lipoprotein (LDL), high density lipoprotein (HDL) and TG. The elevated level of LDL cholesterol, known as bad cholesterol in the blood is a major risk for CHD. Hyperlipidemia is of two types, primary hyperlipidemia and secondary hyperlipidemia. Primary hyperlipidemia, which is a genetic disorder, is inherited through

birth and secondary hyperlipidemia is acquired by a patient through an unhealthy diet, sedentary lifestyle, etc. The World Health Organization (WHO) has reported that elevated levels of plasma cholesterol concentrations affect approximately 40% of the global population's health.³ Therefore, to control hyperlipidemia is one of the major challenges worldwide. Hyperlipidemia is closely associated with CHD, since it leads to the accumulation or build-up of plaques (cholesterol-containing deposits) in the artery walls. CHD is a leading cause of death and people having hyperlipidemia are at twice the risk of developing cardiovascular diseases. It is well reported that a 10 % drop in serum cholesterol level will reduce the risk of CHD by 30 %.⁴⁻⁵ Hyperlipidemia is most commonly associated with high-fat diets, a sedentary lifestyle, obesity and diabetes. The pathophysiology of obesity is closely allied with dyslipidemia, in particular the formation of excessive lipid deposits in non-adipose tissue, such as the liver.⁶⁻⁸ Thus, controlling hyperlipidemia is considered to be a protective strategy to treat obesity.⁹⁻¹⁰

As we know, the synthesis of TG and cholesterol is essential for the normal physiological function of the body. Cholesterol, a type of lipid is very essential for the functioning of all human organs and to synthesize hormones, vitamin D, etc. But if the integration exceeds its breakdown, that will deposit on adipose tissue as well as non-adipose tissue which leads to hyperlipidemia and related consequences. It has been reported that the inhibitions of lipid accumulation, inhibition of TG and cholesterol synthesis are effective strategies to control hyperlipidemia and related complications. Statins are the most widely used mainstay therapeutic agents to reduce hyperlipidemia by inhibiting the 3-hydroxy-3-methylglutaryl-coenzyme (HMG CoA) reductase, a natural enzyme responsible for cholesterol synthesis. Many synthetic and natural products derived statins are available to treat hyperlipidemia¹¹⁻¹⁴ (Chapter 1 Section 1.7.3). Atorvastatin, a synthetic statin, which is a blockbuster drug is currently used for the treatment of cholesterol. However, several unwarranted side effects are reported for the existing statins.¹⁵ In light of these reports, medicinal chemists are actively engaged in the development of new and safer therapeutic agents from natural product based approaches. Natural products from plants are rich source of therapeutic agents for various diseases since ancient times. The families such as, *Amaranthus*, *Apiaceae*, *Asteraceae*, *Fabaceae*, *Lamiaceae*, *Malvaceae*, *Myrtaceae* and *Zingiberaceae* contribute a large number of lipid-lowering agents. The active

phytoconstituents such as flavonoids, polyphenols, terpenoids, alkaloids, saponins, etc., are responsible for the therapeutic potential of this plant species.²⁹

4.3. Review of Literature

4.3.1. Anti-hyperlipidemic properties of *Curcuma amada*

Nature is the reservoir of medicine for various diseases. Because of the high cost and lack of safety associated with many of the synthetic anti-hyperlipidemic drugs, natural products are the safe and effective alternatives to develop anti-hyperlipidemic drugs. Even though many plant species are reported for their anti-hyperlipidemic potential, only a few reports are available on the anti-hyperlipidemic efficacy of *C. amada*.

Srinivasan and Chandrasekhara studied the effects of *C. amada* for hyperlipidemia. In 1992, they have disclosed the effects of mango ginger (*C. amada*) on serum total lipids and triglycerides in normal and hypertriglyceridemic rats. 10 % dry mango ginger was administered for finding the efficacy of mango ginger and results have shown that it was effective in reducing total lipids and TGs.¹⁶ In 1993 they have also studied the effect of mango ginger against lipid level and found that 10 % dry curcumin-free mango ginger was effective in lowering lipids in a high-sucrose diet rat model.¹⁷ In 2008, the anti-hypercholesterolemic effect of mango ginger was investigated in experimental rats and they have revealed that the curcumin containing 10 % mango ginger powder fed along with 1 % cholesterol supplemented diets in Wistar rats was effectively decreasing liver and serum total cholesterol, LDL+VLDL associated cholesterol and increased the HDL associated cholesterol, but it did not affect the cholesterol levels in normal diet-induced animals.¹⁸ These literature highlighted the importance of *C. amada* in the daily diet for preventing hyperlipidemia and related consequences.

4.3.2. Anti-hyperlipidemic properties of pyrrole and pyrazole

Pyrrole and pyrazole constitute an important class of heterocycles by virtue of their pharmaceutical properties. Pyrrole scaffolds possess a wide spectrum of biological activity whether they have been isolated from natural sources or synthetic. The most important pyrrole-containing natural compounds are heme derivatives and chlorophyll. Pyrrole-

containing compounds are common in natural products of marine origin too. Lamellarin isolated from the marine invertebrates exhibits antitumor and anti-HIV activity.¹⁹ One of the top selling drugs Atorvastatin (**Figure 4.1**), is a pyrrole-containing drug and is the most widely used cholesterol-lowering agent acting via inhibition of HMG CoA reductase.

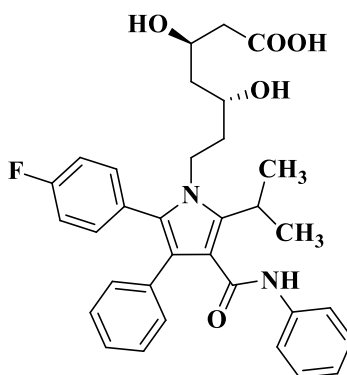


Figure 4.1. Atorvastatin

Pyrazole possesses extensive therapeutic activities such as anti-inflammatory, antipsychotic, anti-obesity, antidepressant, analgesic, etc.²⁰ AM6545 (**Figure 4.2**) is an important anti-obesity agent and is a neutral cannabinoid CB1 receptor antagonist. It reduces caloric intake of high fat and carbohydrate diets. Rimonabant hydrochloride (**Figure 4.2**) belonging to the diaryl pyrazole family, is the first therapeutically most efficient CB1 receptor antagonist and it is considered as an anti-obesity drug.²¹ Rimonabant (**Figure 4.2**) was another important anti-obesity drug containing pyrazole scaffold, which is a synthetic drug and considered the most potent weight-lowering agent. It was the first commercial CB1 receptors antagonist. Since it possesses serious psychiatric side effects, it was withdrawn from the market in 2008. 3,4-diaryl dihydro pyrazole is also a potent CB1 antagonist. 8-Chloro-1-(2,4-dichlorophenyl)-N-piperidin-1-yl-1,4,5,6-tetrahydrobenzo-[6,7]-cyclohepta-[1,2-c]-pyrazole-3-carboxamide 5 (**Figure 4.2**), is a very potent CB1 antagonist in cell-based *in vitro* assays and *ex vivo* screens and is considered as an efficient anti-obesity agent.^{19, 22-23}

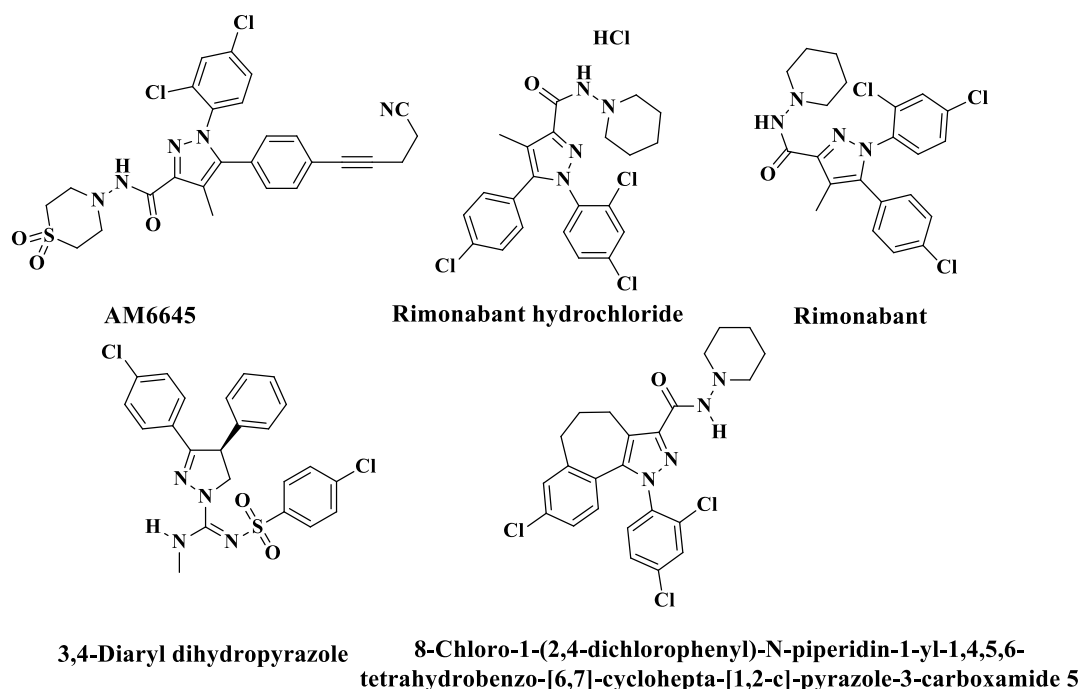


Figure 4.2. Anti-obesity agents having pyrazole core

4.4. Aim and scope of the present study

In literature, a few plant species are well documented for their anti-hyperlipidemic potential. This includes plant extracts, phytochemicals and semi-synthetic derivatives of phytochemicals.²⁴⁻²⁸ A few reports reveal the anti-hyperlipidemic efficacy of *C. amada*, which belongs to the *Zingiberaceae* family.¹⁶⁻¹⁸ In the third chapter, we have identified promising anti-obesity leads of triazole appended-labdanes via pancreatic lipase inhibition studies.³⁰ In continuation of our discovery programme on natural products and bioactive heterocycles,³¹⁻³⁶ our aim was to further explore the anti-hyperlipidemic potential of the abundant bioactive molecule (*E*)-labda-8(17),12-diene-15,16-dial isolated from *C. amada* (Chapter 2, section 2.8) and its semi-synthetic derivatives (*E*)-labda-8(17),12-diene-15,16-dial-pyrrole and (*E*)-labda-8(17),12-diene-15,16-dial-pyrazoles. As part of the research program, we have isolated (*E*)-labda-8(17),12-diene-15,16-dial and synthetically modified it to the corresponding pyrroles and pyrazoles. The efficacy of these compounds on the inhibition of lipid droplet formation, inhibition of TG and cholesterol synthesis in the culture medium of Human liver carcinoma cell lines, viz., HepG2 cells has been successfully evaluated in this chapter.

4.5. Design strategy for the synthesis of labdane appended pyrroles and pyrazoles

The rationale for the designed hybrids is schematically represented by the ligand- based molecular hybridization approach (**Figure 4.3**). As depicted in Figure 4.3, labdane terpenes, pyrroles, and pyrazoles constitute a crucial central core in many of the FDA approved statin drugs.¹²⁻¹⁴ Moreover, pyrrole and pyrazole represent a vital scaffold in medicinal chemistry with their diverse pharmacological properties.³⁷⁻⁴⁰ Therefore, we emphasize that the molecular hybridization of these pharmacophores in a single entity will enrich the pharmacological properties in finding the potent “leads” as anti-hyperlipidemic agents.

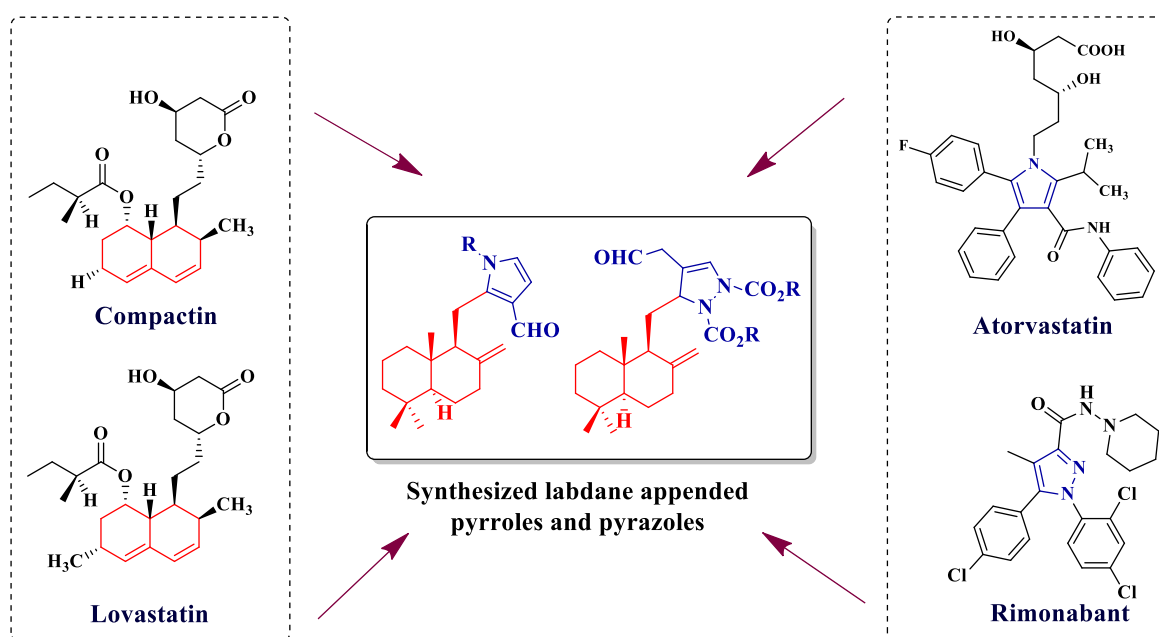


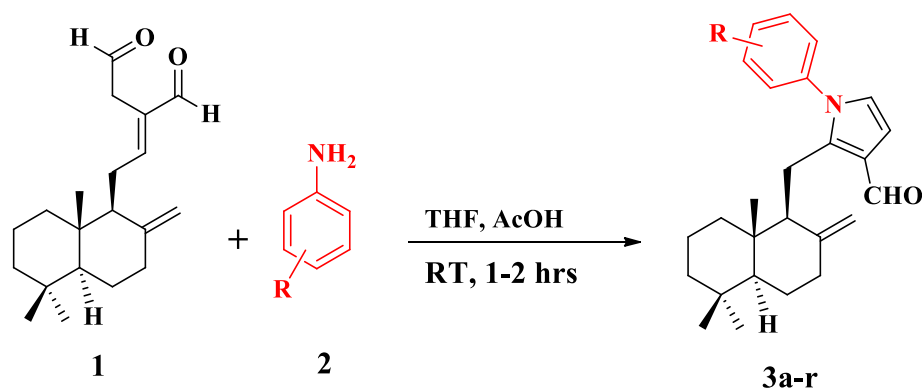
Figure 4.3. Molecular hybridization approach led to the discovery of novel (*E*)-labda-8(17),12-diene-15,16-dial hybrids

4.6. Results and discussion

Many researchers have already demonstrated that natural compounds from medicinal plants are capable of controlling hyperlipidemia. To develop alternative, safe and more effective therapeutic entities from natural products, we have isolated the compound (*E*)-labda-8(17),12-diene-15,16-dial from *C. amada*³⁰ and synthesized a series of (*E*)-labda-8(17),12-diene-15,16-dial appended pyrrole and pyrazole targets. Further, we examined the efficacy of these compounds on the inhibition of lipid droplet formation, inhibition of TG and

cholesterol synthesis in the culture medium of Human liver carcinoma cell lines, viz., HepG2 cells. The HMG CoA reductase inhibitory activity of the compounds further confirms the inhibitory potential of cholesterol synthesis.

From (*E*)-labda-8(17),12-diene-15,16-dial (**1**), a library of (*E*)-labda-8(17),12-diene-15,16-dial appended pyrroles (**Scheme 4.1**) and pyrazoles (**Scheme 4.2**) were synthesized via one-pot cascade protocol. (*E*)-labda-8(17),12-diene-15,16-dial (**1**) undergoes metal-free, acid catalysed cyclo-condensation with various substituted anilines (**2**) in THF at room temperature to produce (*E*)-labda-8(17),12-diene-15,16-dial appended-1H-pyrrole-3-carbaldehydes (**3**) (**Scheme 4.1**). Similarly, a [3+2] cycloaddition of **1** and dialkyl azodicarboxylate (**4**) in DCM at room temperature has led to the formation of 1H-pyrazole-1,2(3H)-dicarboxylate (*E*)-labda-8(17),12-diene-15,16-dial appendages (**5**) (**Scheme 4.2**). All the semi-synthetic derivatives are well characterized by using IR, ¹H, ¹³C NMR and HRMS analysis.



Scheme 4.1. One-pot synthetic strategy for the (*E*)-labda-8(17),12-diene-15,16-dial appended pyrroles^a. ^aReagents and conditions: THF, AcOH, RT (1-2 hrs).

Spectral data leading to the structural elucidation is exemplified using compound 3k. IR spectrum of the compound **3k** showed the absorption band at 1736 cm⁻¹ due to the presence of carbonyl group of the aldehyde. The peak at δ 9.98 in the ¹H NMR spectrum (**Figure 4.5**) indicated the presence of aldehyde proton. The peaks between δ 7.25-6.60 integrating for 5 protons suggested the presence of two aromatic rings. Two singlets at δ 4.61 and 4.36 could be attributed to the presence of the exo-methylene group. ¹³C NMR spectrum (**Figure 4.6**) of the compound confirmed the aldehydic carbonyl group at δ 186.1. The peaks

between 147.9-107.3 suggested the presence of both aromatic ring carbons and exo-methylene carbon. The mass spectrum of the compound showed the molecular ion peak at m/z 426.2783, which is $(M+Na)^+$ peak. From these data along with DEPT-135 and 2D spectra, the structure of the compound **3k** was confirmed as shown below (**Figure 4.4**).

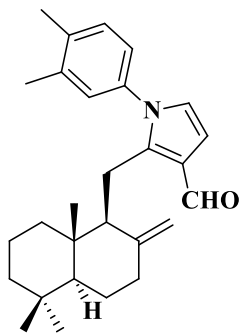


Figure 4.4. Compound **3k**

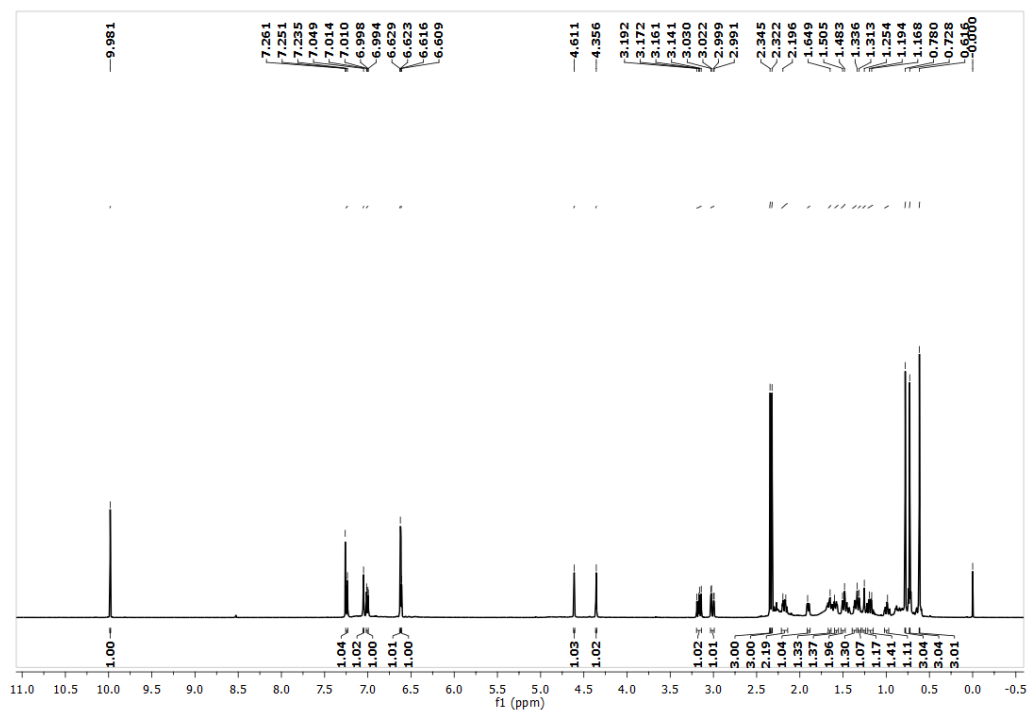


Figure 4.5. ^1H NMR spectrum of compound **3k** in CDCl_3

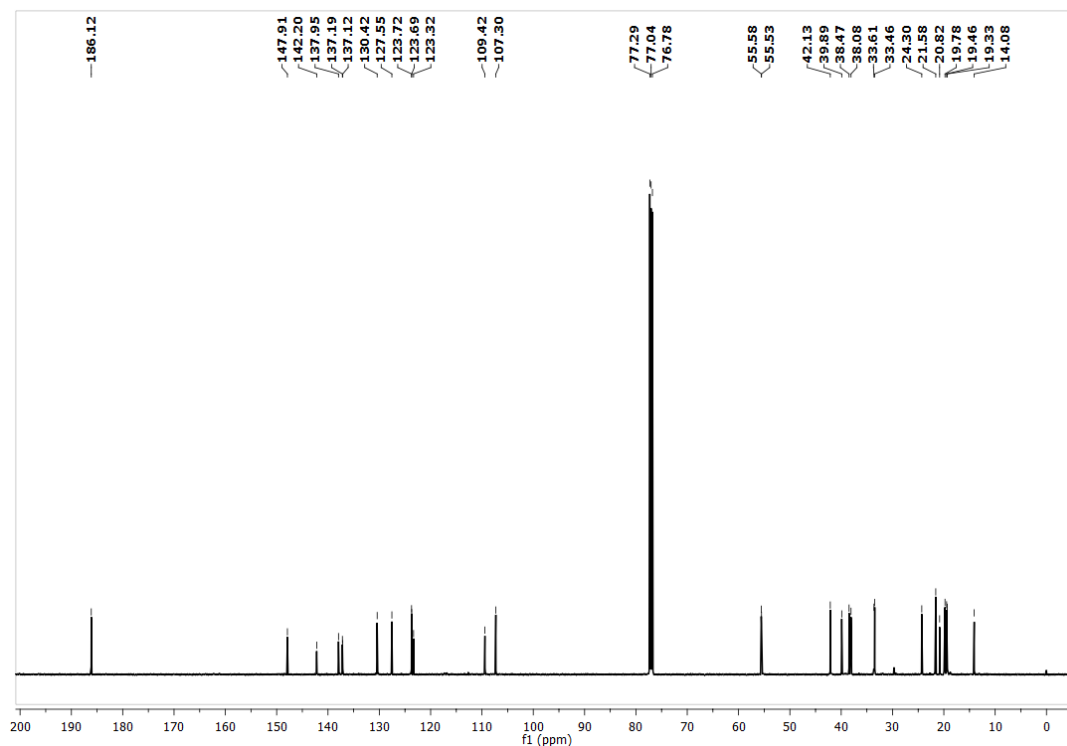


Figure 4.6. ^{13}C NMR spectrum of compound 3k in CDCl_3

4.6.1. Optimization of the reaction

To optimize the reaction, we have tried different solvents and catalysts at 0 °C to 50 °C. The reaction was monitored by checking the TLC at various time intervals. From the optimization **Table 4.1.**, it was found that the best reaction condition was the use of 1 equiv. of reactant 1a and 1.5 equiv. of reactant 2a, THF as the solvent, 6 equiv. of AcOH as a catalyst and stirring at RT for 1-2 hours. The maximum optimized yield obtained was 45%.

Table 4.1. Optimization of the reaction^a

Sl. No.	Solvent	Catalyst	Temperature (°C)	Yield (%)
1	CH ₂ Cl ₂	pTSA	0	-
2	CH ₂ Cl ₂	pTSA	RT	-
3	CH ₂ Cl ₂	AcOH	0	10
4	CH ₂ Cl ₂	AcOH	RT	15
5	CH ₂ Cl ₂	NaBH ₄	RT	-
6	EtOH	AcOH	RT	-
7	EtOAc	AcOH	RT	20
8	EtOAc	BF ₃ OEt ₂	RT	-
9	Toluene	AcOH	RT	-
10	Acetonitrile	AcOH	RT	-
11	THF	AcOH	0	15
12	THF	AcOH	RT	45
13	THF	AcOH	50	-
14	THF	pTSA	RT	-
15	THF	pTSA	50	-
16	DMF	AcOH	RT	25
17	DMF	TFA	RT	-

^aReaction conditions: 1a (1 equiv.), 2a (1.5 equiv.) in 3 ml of solvent without inert atmosphere. Reaction time: 1-2 hrs.

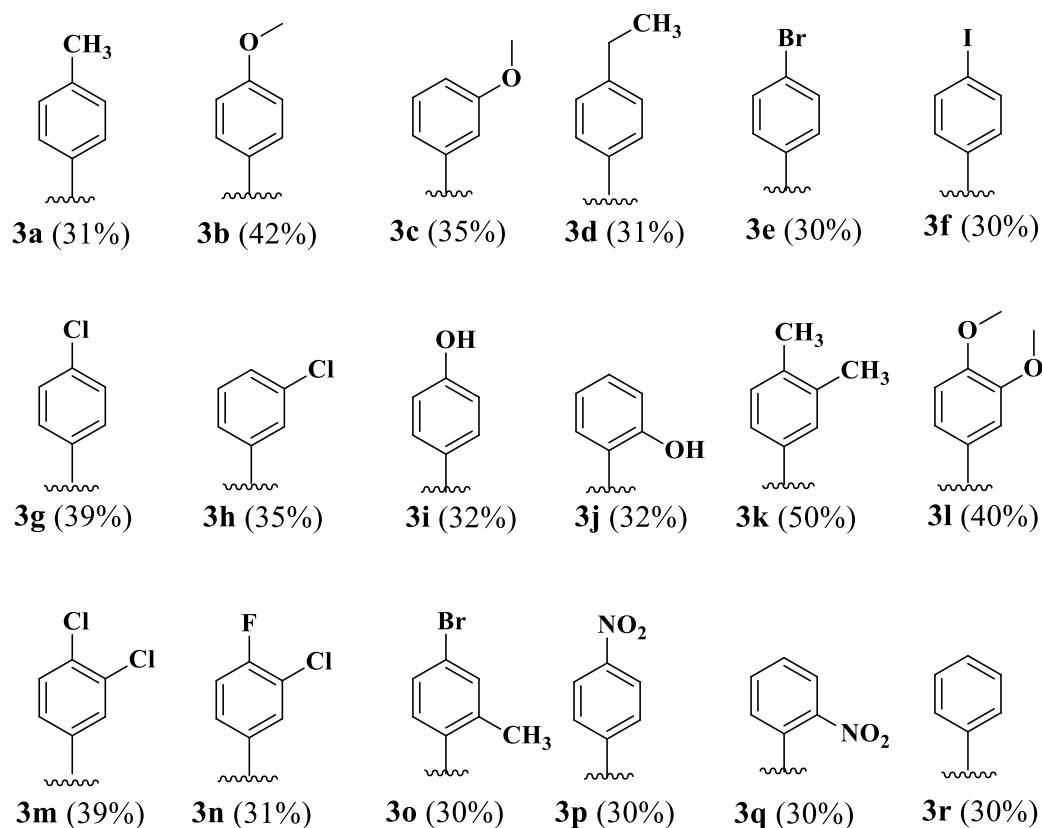
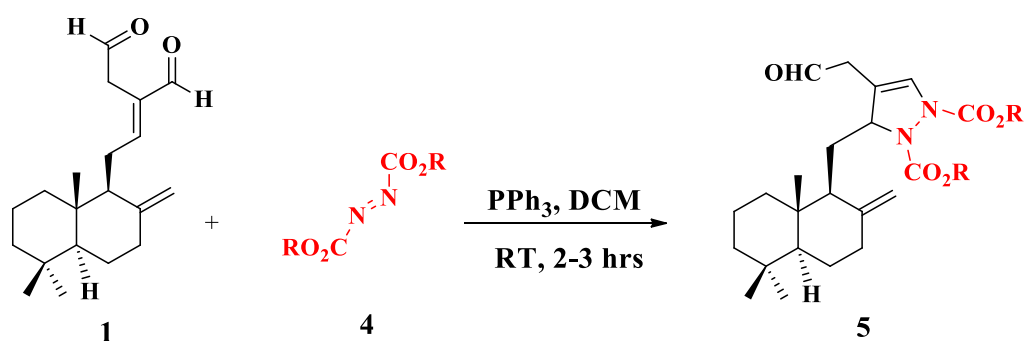


Figure 4.7. Scope of the reaction



Scheme 4.2. One-pot access for the (*E*)-labda-8(17),12-diene-15,16-dial appended pyrazoles^a. ^aReagents and conditions: DCM, PPh₃, RT (2-3 hrs).

The salient features of the spectral data of this group of compounds is exemplified using that of compound 5c. The IR spectrum of the compound 5d showed carbonyl absorption at 1723 cm⁻¹. In the ¹H NMR spectrum (Figure 4.9), a singlet seen at δ 9.29 suggested the presence of an aldehydic proton. The peak at δ 8.04 was assigned to the proton

in the pyrazole ring. In the ^{13}C NMR spectrum (**Figure 4.10.**), aldehyde carbon is confirmed by the presence of a peak observed at δ 194.4. The mass spectrum of the compound showed the molecular ion peak at m/z 539.3480, which is $(\text{M}+\text{Na})^+$ peak. From these data along with DEPT-135 and 2D spectra, the compound structure was confirmed as shown below (**Figure 4.8.**).

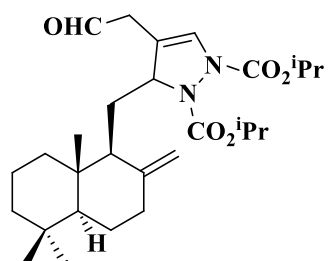


Figure 4.8. Compound 5c

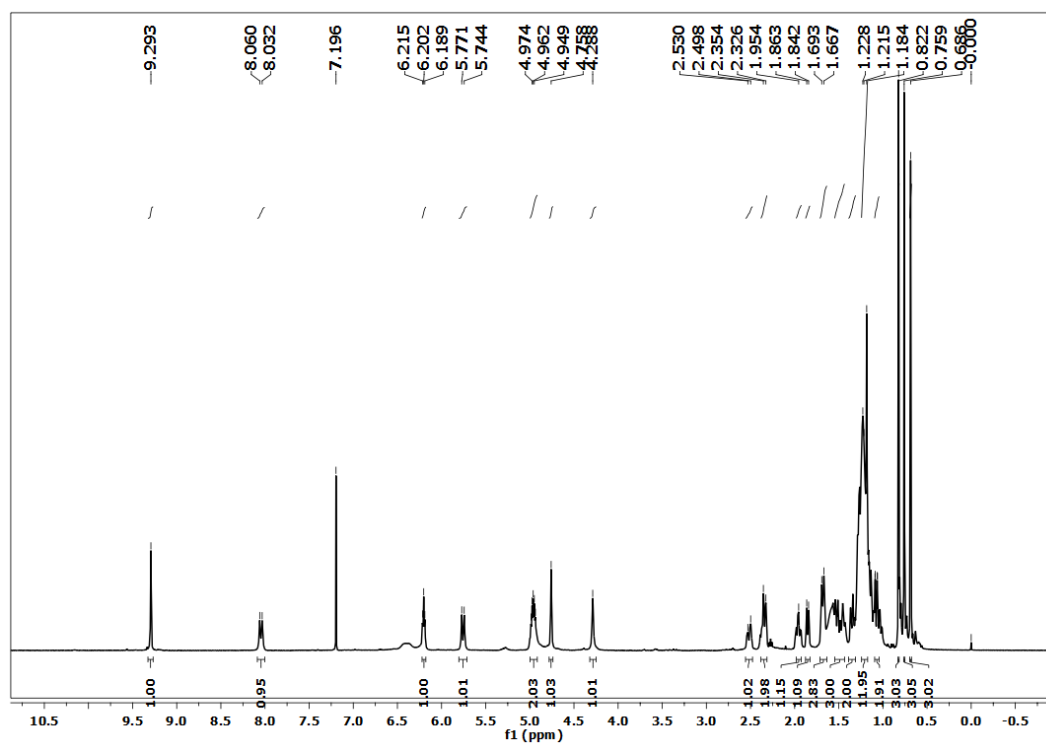


Figure 4.9. ^1H NMR spectrum of compound 5c in CDCl_3

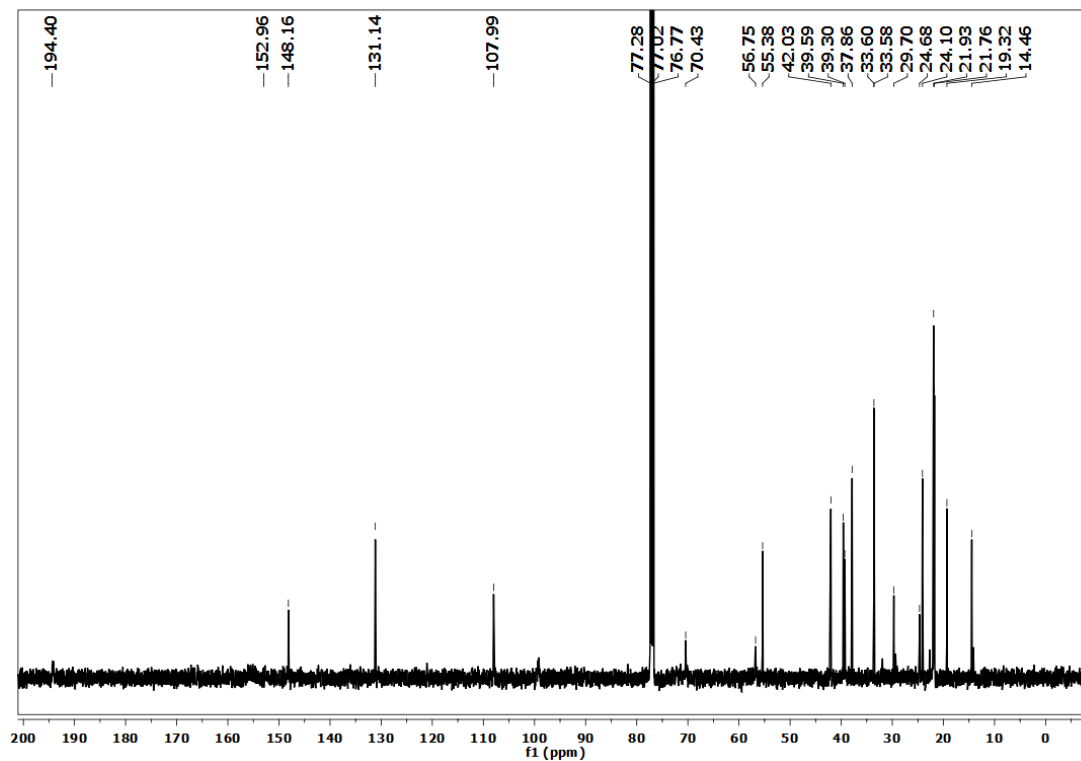


Figure 4.10. ^{13}C NMR spectrum of compound 5c in CDCl_3

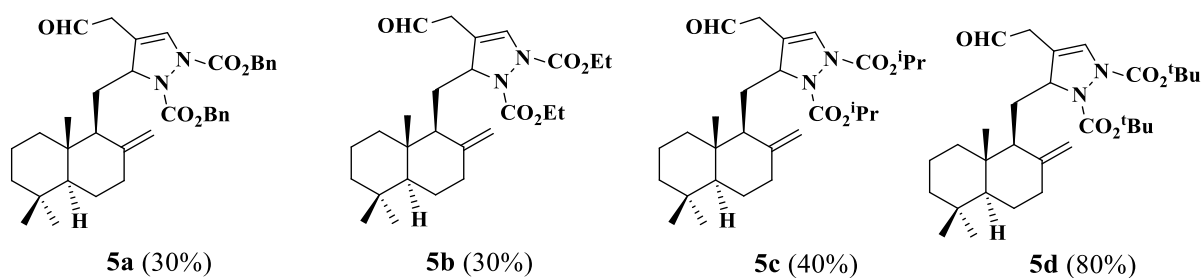


Figure 4.11. Scope of the reaction

4.6.2. MTT assay

To begin with, the toxicity of the compounds was tested in HepG2 cell lines by MTT assay (Figure 4.12).⁴¹⁻⁴² Cytotoxic effect of each compound was expressed as a percentage of cell viability in a dose-dependent manner. Values are mean \pm SD of four independent experiments performed in duplicates. The results of the study displayed that none of the compounds

caused any toxicity at all the tested concentrations. More than 91 percent of cell viability was observed when cells were pretreated with 100 μM levels of test compounds for 48 hrs.

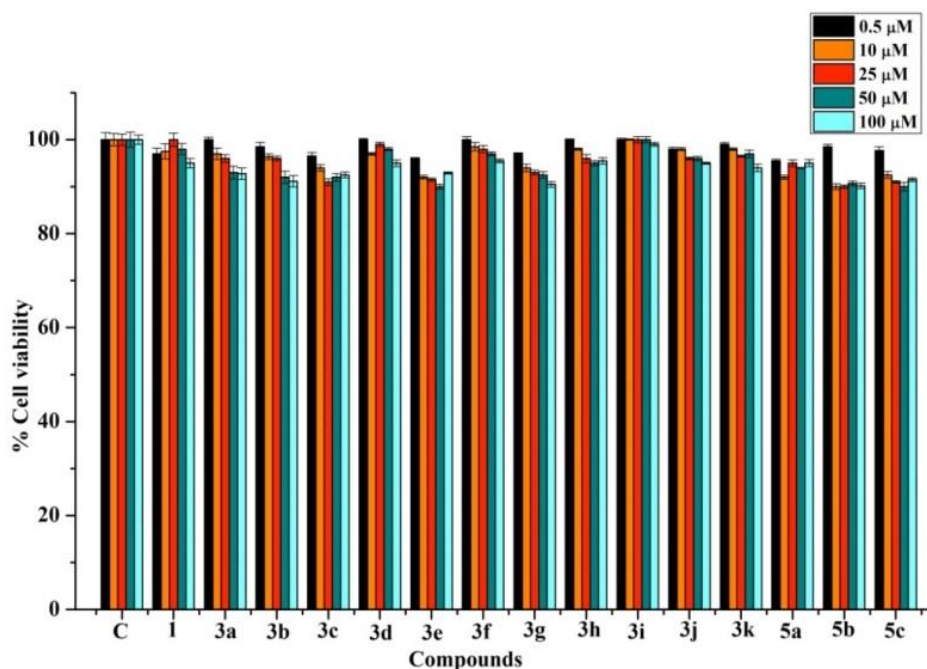


Figure 4.12. Cytotoxic study of isolates and selected semi-synthetic derivatives by MTT assay

4.6.3. Effect of compounds on lipid droplet accumulation in HFA treated HepG2 cells

Next, to see the effect of compounds on lipid droplet accumulation in high fatty acid rich (HFA) medium treated HepG2 cells, oil red O staining assay was performed (**Figure 4.13 & 4.14**).⁴¹⁻⁴² Initially, we have conducted a preliminary screening of the compounds with concentration ranging from 0.5 μM to 100 μM on HFA medium treated HepG2 cells to identify the most potent concentration with a maximum inhibition of lipid accumulation. It was observed that most of the compounds showed maximum efficacy at 10 μM concentration. Hence, all the comparative studies were performed at 10 μM concentration. The relative intensity of lipid accumulation was also analyzed (**Figure 4.14**). The results showed that the number of lipid droplets formation in HepG2 cells treated with the compounds were less than the control groups. As depicted in **Figure 4.14**, compound **3i** showed the highest lipid accumulation inhibitory activity, which was comparable to that of

the positive control Fenofibrate (FF). Compounds **3j** and **3k** also showed significant activity when compared to other derivatives. The labdane appended pyrazole molecules **5a**, **5b** and **5c** exhibited the lowest activity. However, compounds **3l-3r** and **5d** failed to show any effect on lipid accumulation.

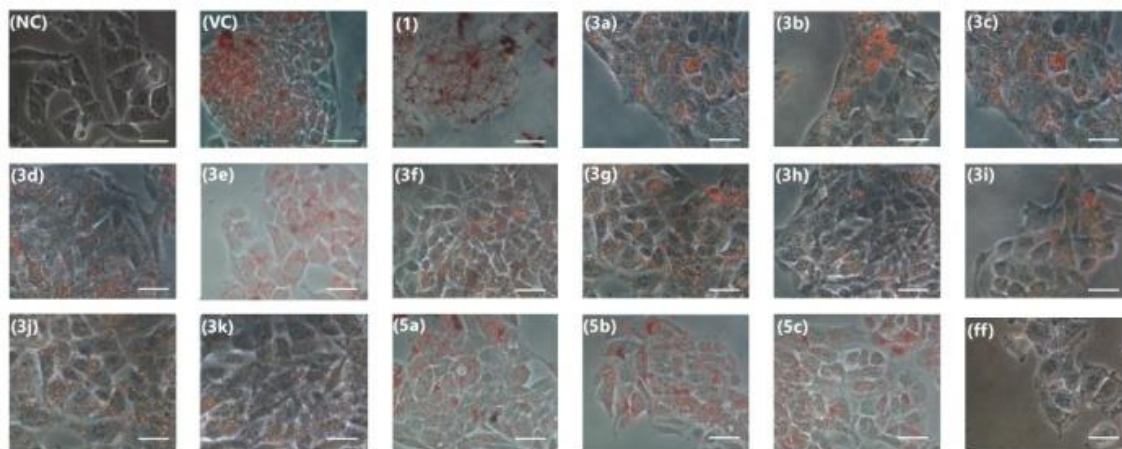


Figure 4.13. The effect of compounds and standard drug FF (Fenofibrate) on lipid droplet accumulation in HepG2 cells by oil red O staining: Representative microscopic images of oil red O stained HepG2 cells treated with compounds or FF (10 μ M). NC (normal control), without any treatment; VC (vehicle control) -0.1% DMSO treated cells cultured in high fatty acid rich medium.

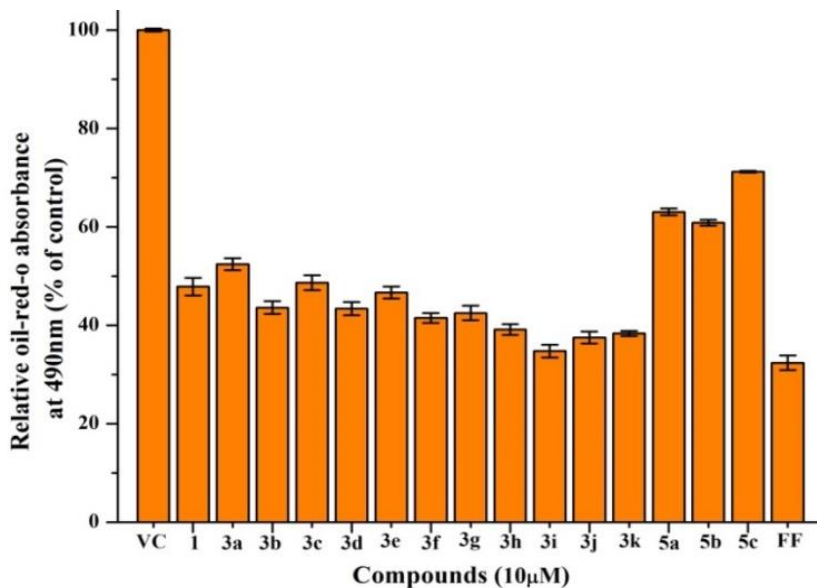


Figure 4.14. The effect of compounds and standard drug FF (Fenofibrate) on lipid droplet accumulation in HepG2 cells by oil red O staining: Absorbance measured at 490 nm after oil-red-O staining and data is presented as % of control. Results are mean \pm SD, (n = 4).]. VC (vehicle control) -0.1% DMSO treated cells cultured in high fatty acid rich medium.

4.6.4. Effect of compounds on the inhibition of triglyceride synthesis in HepG2 cells

Subsequently, we investigated whether the synthesized derivatives could inhibit triglyceride (TG) accumulation in HepG2 cells.⁴¹⁻⁴² The TG levels were analyzed in HepG2 cells in HFA induced medium and test compounds for 24 hrs (**Table 4.1**) at two different concentrations viz., 5 and 10 μ M. The findings reveal that the synthesis of TG has significantly decreased in a dose-dependent manner in compound treated HepG2 cells. The percentage inhibition of TG synthesis at 10 μ M varies from 71.73 ± 0.78 to 37.25 ± 1.13 (**Table 4.2**). All the compounds except 3a, 3c, 5a, 5b and 5c showed significant efficacy than the parent molecule 1. One of the derivative **3i** exhibited the highest percentage of the inhibitory potential of TG synthesis with 71.73 ± 0.78 , which is comparable to that of the positive control **FF** (74.01 ± 0.33). Also, the compounds **3j**, **3k**, **3f** and **3g** showed a considerable TG synthesis inhibitory potential of 64.22 ± 0.61 , 62.30 ± 0.38 , 53.94 ± 1.32 and 51.51 ± 1.21 percent respectively. Surprisingly, pyrazole derivatives **5a**, **5b** and **5c** exhibited weak inhibition of TG synthesis.

Table 4.2. The effect of compounds on percentage inhibition of TG synthesis in high fatty acid treated HepG2 cells.^a

Compounds	TG level (mg/dl) 5 μ M	TG level (mg/dl) 10 μ M	% Inhibition (10 μ M)
NC	15.00 \pm 0.15		
VC	90.50 \pm 0.49		
1	55.00 \pm 1.41	49.50 \pm 0.70	45.51 \pm 0.71
3a	66.00 \pm 1.21	54.05 \pm 0.91	40.51 \pm 1.02
3b	50.00 \pm 0.70	49.50 \pm 1.41	45.51 \pm 0.68
3c	64.60 \pm 1.06	51.65 \pm 2.33	43.15 \pm 1.17
3d	50.00 \pm 1.41	46.75 \pm 2.19	48.54 \pm 0.85
3e	50.10 \pm 1.97	46.00 \pm 0.42	49.37 \pm 0.46
3f	45.00 \pm 1.41	41.85 \pm 1.41	53.94 \pm 1.32
3g	49.30 \pm 1.83	44.05 \pm 3.11	51.51 \pm 1.21
3h	42.00 \pm 2.82	38.70 \pm 1.90	46.96 \pm 0.24
3i	39.00 \pm 2.12	27.50 \pm 0.70	71.73 \pm 0.78
3j	42.50 \pm 1.76	32.50 \pm 0.60	64.22 \pm 0.61
3k	45.00 \pm 0.70	34.25 \pm 2.12	62.30 \pm 0.38
5a	64.00 \pm 2.12	55.85 \pm 1.41	38.52 \pm 0.23
5b	60.00 \pm 2.12	55.00 \pm 1.41	39.46 \pm 0.52
5c	68.00 \pm 0.70	57.00 \pm 1.41	37.25 \pm 1.13
FF(10 μM)	-----	23.00 \pm 2.12	74.01 \pm 0.33

^aData is presented as mean \pm SD of five different experiments at $P \leq 0.05$. % inhibition of TG synthesis in HepG2 cells were calculated at 10 μ M concentration. FF (Fenofibrate) at 10 μ M concentration is used as positive control. NC (normal control), without any treatment, VC (vehicle control)-0.1% DMSO treated cells cultured in high fatty acid rich medium.

4.6.5. Evaluation of effect of compounds on the inhibition of cholesterol synthesis in HepG2 cells

We further examined the effect of test compounds on the inhibition of cholesterol synthesis in HFA rich medium treated HepG2 cells (**Table 4.3**).⁴¹⁻⁴² The results revealed that the inhibition of cholesterol synthesis showed a concentration-dependent effect. The percentage inhibition of cholesterol synthesis at 10 μ M varies from 68.61 \pm 1.19 to 46.32 \pm 1.34. All the compounds except 3a, 5a, 5b and 5c showed a marked increase in the inhibition of

cholesterol synthesis. As anticipated, compound **3i** showed a consistent activity in the inhibition of cholesterol synthesis with the highest (**68.61 ± 1.19**) percentage of suppression, which was comparable to that of the positive control Atorvastatin (AS) (**70.19 ± 0.64**). Compounds **3j**, **3k**, **3h**, **3f** and **3g** also showed a substantial percentage of inhibition with **65.81 ± 0.85**, **63.51 ± 0.04**, **62.07 ± 1.65**, **60.48 ± 1.09** and **57.65 ± 1.92** respectively at 10 μ M concentration. In line with other assays, here also the pyrazole derivatives showed the lowest efficiency among the tested compounds.

Table 4.3. The effect of compounds on inhibition of cholesterol synthesis in high fatty acid treated HepG2 cells.^a

Compounds	Total cholesterol (mg/dl) 5 μ M	Total cholesterol (mg/dl)10 μ M	% Inhibition (10 μ M)
NC	26.58 ± 1.73		
VC	71.36 ± 0.08		
1	41.01 ± 0.68	33.56 ± 1.07	52.98 ± 1.57
3a	43.74 ± 0.71	35.32 ± 0.98	50.51 ± 1.45
3b	40.82 ± 0.98	32.66 ± 0.64	54.23 ± 0.83
3c	48.14 ± 0.30	33.69 ± 1.32	52.79 ± 1.78
3d	37.98 ± 0.79	31.50 ± 1.24	55.86 ± 1.80
3e	40.00 ± 0.21	33.13 ± 0.96	53.57 ± 1.41
3f	40.03 ± 0.14	28.19 ± 0.82	60.48 ± 1.09
3g	35.71 ± 1.01	30.22 ± 1.32	57.65 ± 1.92
3h	37.32 ± 0.76	27.07 ± 1.21	62.07 ± 1.65
3i	29.75 ± 1.06	22.40 ± 0.82	68.61 ± 1.19
3j	32.43 ± 1.31	24.39 ± 0.64	65.81 ± 0.85
3k	32.27 ± 1.37	26.04 ± 0.07	63.51 ± 0.04
5a	45.68 ± 0.64	36.95 ± 1.16	48.22 ± 1.71
5b	43.23 ± 0.12	36.03 ± 0.70	49.50 ± 1.05
5c	46.71 ± 1.05	38.31 ± 0.90	46.32 ± 1.34
AS (10 μM)	-----	21.27 ± 0.48	70.19 ± 0.64

^aData is presented as mean ± SD at P ≤ 0.05 of five different experiments. % inhibition of cholesterol synthesis in HepG2 cells were calculated at 10 μ M concentration. AS (Atorvastatin) at 10 μ M concentration is used as positive control. NC (normal control), without any treatment, VC (vehicle control) -0.1% DMSO treated cells cultured in high fatty acid rich medium.

4.6.6. Evaluation of effect of compounds on the inhibition of HMG CoA reductase enzyme

We further examined the effect of test compounds on the inhibition of HMG CoA reductase enzyme, a rate limiting enzyme in the cholesterol synthesis pathway (**Figure 4.15**). We used an *in vitro* HMG CoA reductase detection assay kit, which is designed to screen for different inhibitors/activators of the purified catalytic subunit of the enzyme. Since most of the compounds showed maximum efficacy at 10 μ M concentration, we evaluated the % of HMG CoA reductase enzyme inhibition at 10 μ M concentration and presented below is the data for the same. The percentage inhibition of cholesterol synthesis at 10 μ M varies from 78.51 ± 2.80 to 45.87 ± 2.50 . The HMG CoA reductase inhibitory activity of the compounds was consistent with that of the inhibitory activity of cholesterol synthesis. All the compounds except 3a, 5a, 5b and 5c exhibited significant inhibition of HMG CoA reductase. Consistent with the results of cholesterol synthesis, compound **3i** showed the highest percentage of inhibitory potential (78.61 ± 2.80), which was comparable to that of the positive control Pravastatin (PS) (78.05 ± 5.4). Compounds **3j**, **3k**, **3h**, **3f** and **3g** also showed a considerable percentage of inhibition with 77.59 ± 6.9 , 74.94 ± 8.27 , 71.81 ± 1.84 , 68.47 ± 9.42 and 65.47 ± 6.03 respectively at 10 μ M concentration. Similar to cholesterol synthesis, the pyrazole derivatives (5a-c) displayed the lowest activity among the tested compounds.

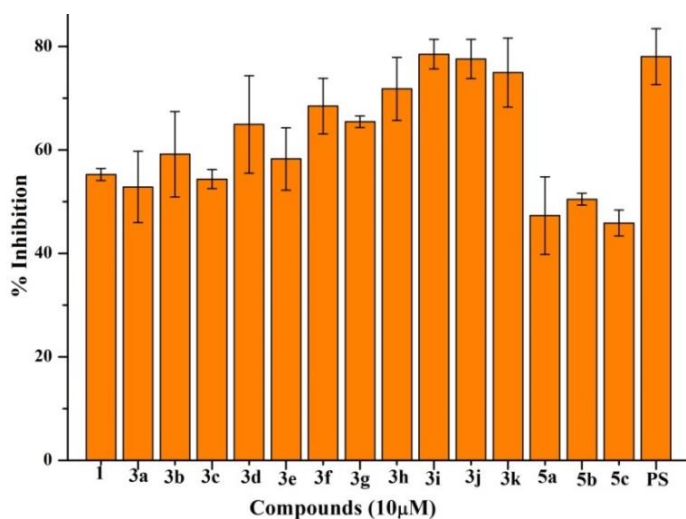


Figure 4.15. The effect of compounds on the inhibition of HMG CoA reductase enzyme. PS (Pravastatin, positive control)

4.6.7. Structure activity relationship (SAR) studies

From the structure-activity relationship (SAR) studies, amongst the novel pyrrole and pyrazole conjugated (*E*)-labda-8(17),12-diene-15,16-dial, the pyrroles (3a-k) are more potent than pyrazole derivatives (5a-c). In pyrrole series, 1-(4-hydroxyphenyl)-2-((5,5,8a-trimethyl-2-methylenede-cahydronaphthalen-1-yl)methyl)-1H-pyrrole-3-carbaldehyde (**3i**) exhibited highest efficacy, which is more potent than the parent molecule (*E*)-labda-8(17), 12-diene-15, 16-dial (1) and comparable to that of positive controls. Analogues 3j and 3k with *m*-OH and *m*, *p*-disubstituted-CH₃ functionality respectively, also exhibited excellent efficacy. However, the analogues 3l-r did not show any significant inhibition potential. The potency of these molecules may be attributed to the synergistic interaction of the (*E*)-labda-8(17),12-diene-15,16-dial core, pyrrole ring and aromatic ring linked to the nitrogen atom on the pyrrole ring. Even though, all the molecules possess these scaffolds, precisely the improved activity of some molecules amongst others may be due to the electronic properties of an aromatic ring which comes from various substitutions. In molecule 3i, there is an electron-donating -OH group present in the para position of the aromatic ring. Here the *p*-OH group may play an important role in the inhibition of TG and cholesterol synthesis through hydrogen bonding interactions. The molecules 3j and 3k with *m*-OH and *m*, *p*-disubstituted-CH₃ functionality also showed better activity. Compound 3a with electron-donating *p*-CH₃ substitution on the aromatic ring possesses the least activity among the other tested derivatives of pyrroles. However, there is no significant trend in the activity of the molecules followed by the nature of electron-donating and electron-withdrawing groups on the aromatic ring. Overall, among the variously substituted pyrrole conjugated (*E*)-labda-8(17),12-diene-15,16-dial, 3i with *p*-OH substituted aromatic ring was found to be the most potent molecule. These findings established that the synthesized hybrids could be utilized as effective lead candidates in the treatment of hyperlipidemia and related complications. However, further detailed molecular biology studies are required to confirm its mechanism of action and other pharmacological properties to be promoted as a safe clinical candidate.

4.7. Conclusion

In conclusion, the design of tailor-made analogues conceived from the structural features of known ligands has paved the way for the discovery of promising pyrrole appended (*E*)-labda-

8(17),12-diene-15,16-dial synthesized via semi-synthetic strategy. The study reveals (*E*)-labda-8(17),12-diene-15,16-dial derived pyrroles play a significant role in controlling hyperlipidemia by inhibiting TG and cholesterol synthesis in HepG2 cells. The HMG CoA reductase inhibitory activity of the compounds was consistent with that of inhibitory activity of cholesterol synthesis. Amongst synthesized pyrrole derivatives, **3i** possess the highest efficacy, which is comparable to the positive control Fenofibrate, Atorvastatin and Pravastatin. To the best of our knowledge this is the first report on the natural product derived (*E*)-labda-8(17),12-diene-15,16-dial appended pyrrole and pyrazole analogues as anti-hyperlipidemic agents. Nonetheless, further detailed investigations are in progress to explore the lead analogue **3i** as a potent and safe therapeutic clinical candidate.

4.8. Experimental section

All the reagents used for the isolation, pyrrole and pyrazole synthesis were purchased from Sigma-Aldrich and Spectrochem. Dulbecco's Modified Eagle's Medium (DMEM-high glucose), trypsin-EDTA and 100 U/Lml penicillin-streptomycin (100 µg/ml) mix were purchased from Himedia Pvt Ltd (Mumbai, India). Fetal bovine serum (FBS) was from Gibco (Grand Island, NY). 3-[4,5-dimethylthiazol-2-yl]-2,5-diphenyl tetrazolium bromide (MTT), linoleic acid, palmitic acid, BSA, paraformaldehyde, oil red O, Fenofibrate, Atorvastatin and Pravastatin were purchased from Sigma-Aldrich (U.S.A). Total cholesterol assay kit was purchased from Cell Biolabs, Inc (CA, U.S.A) and triglyceride quantification colorimetric assay kit was purchased from Biovision (CA, U.S. A). Human hepatoma cells were obtained from the NCBS (National Centre for Biological Sciences, Pune). HMG CoA reductase activity was assessed based on the oxidation of NADPH by using a screening assay kit (Sigma Aldrich, USA) as per the manufacturer's instructions. Solvents were purchased from Merck and were distilled before use. TLC plates (silica gel 60 F₂₅₄) were used for monitoring the purity of the isolated compounds and the reaction progress. Column chromatographic techniques were used for the isolation of natural compounds and their analogues. Heidolph-rotary evaporator was used for the removal of solvents. The absorbance was recorded at 540 nm by the Elisa reader. The IR spectra were recorded on Bruker Alpha-T FT-IR spectrophotometer. The ¹H and ¹³C NMR spectra were recorded at 500 MHz and 125 MHz respectively on the Bruker AMX 500 MHz FT NMR spectrometer.

Tetramethylsilane (TMS) was used as an internal standard. Chemical shifts are expressed in δ scale and coupling constants in Hertz (Hz). Mass spectra were recorded under HRMS (ESI) using Thermo Scientific Exactive Orbitrap mass spectrometer.

4.8.1. Isolation of (*E*)-labda-8(17),12-diene-15,16-dial (1)

The isolation protocol of (*E*)-labda-8(17),12-diene-15,16-dial was discussed in section 2.8 (Chapter 2)

4.8.2. General procedure for the synthesis of (*E*)-labda-8(17),12-diene-15,16-dial-pyrrole analogues (3a-3r)

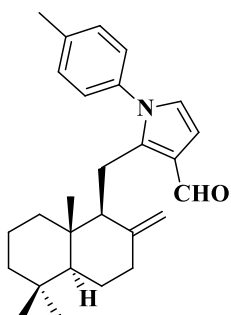
To a solution of (*E*)-labda-8(17),12-diene-15,16-dial (1equiv.) and various substituted aniline (1.5 equiv.) in THF solvent, acetic acid (6 equiv.) was added dropwise. The resulting mixture was stirred at room temperature for 1-2 hours and the progress of the reaction was monitored by TLC. After completion of the reaction, the content was extracted with ethyl acetate, washed with brine, the compound was dried over anhydrous Na₂SO₄ and the solvent was removed under reduced pressure. The product was purified by column chromatography using hexane and ethyl acetate as solvents.⁴³

4.8.3. Spectral Details

4.8.3.1. Synthesis of 1-(*p*-tolyl)-2-((5,5,8a-trimethyl-2-methylenedecahydronaphthalen-1-yl) methyl)-1H-pyrrole-3-carbaldehyde (3a)

The compound **3a** was prepared by the reaction of (*E*)-labda-8(17),12-diene-15,16-dial (30 mg, 1equiv.) and 4-methylaniline (15.96 mg, 1.5 equiv.) in THF (3 ml) as per the method described in section 4.8.2. Yield: 31% (12 mg).

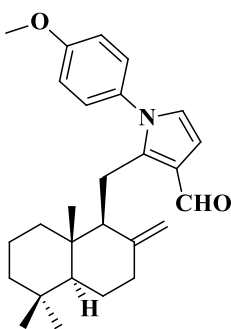
FT-IR (NaCl, : 3308, 2960, 2848, 1944, 1732, 1666, 1530,
v_{max}, cm⁻¹) 1495



$^1\text{H NMR}$ (500 MHz, CDCl_3)	: 9.98 (s, 1H), 7.30 (d, $J = 8$ Hz, 2H), 7.16 (d, $J = 8.5$ Hz, 2H), 6.64 (d, $J = 3$ Hz, 1H), 6.62 (d, $J = 3$ Hz, 1H), 4.60 (s, 1H), 4.32 (s, 1H), 3.07 (m, 2H), 2.44 (s, 3H), 2.20-1.01 (m, 12H), 0.78 (s, 3H), 0.73 (s, 3H), 0.61 (s, 3H)
$^{13}\text{C NMR}$ (125 MHz, CDCl_3)	: 186.0, 147.9, 142.2, 138.5, 136.9, 129.9, 126.2, 123.6, 123.4, 109.5, 107.3, 55.6, 55.5, 42.0, 39.9, 38.5, 38.0, 33.6, 33.4, 24.3, 21.6, 21.1, 20.9, 19.2, 14.0
HRMS (ESI)	: m/z: $[\text{M}+\text{H}]^+$ calcd for $\text{C}_{27}\text{H}_{36}\text{NO}$ is 390.2797, found 390.2809

4.8.3.2. Synthesis of 1-(4-methoxyphenyl)-2-((5,5,8a-trimethyl-2-methylenedecahydro-naphthalen-1-yl)methyl)-1H-pyrrole-3-carbaldehyde (3b)

The compound 3b was prepared by the reaction of (*E*)-labda-8(17),12-diene-15,16-dial (30 mg, 1equiv.) and 4-methoxyaniline (18.34 mg, 1.5 equiv.) in THF (3 ml) as per the method described in section 4.8.2. Yield: 42% (18 mg).

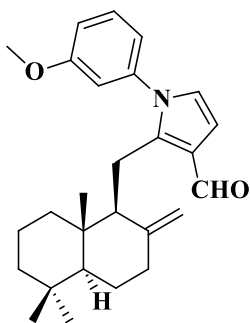


FT-IR (NaCl, ν_{max} , cm^{-1})	: 3642, 3273, 2924, 2851, 1870, 1896, 1737, 1718, 1701, 1652, 1591, 1543, 1513, 1460
$^1\text{H NMR}$ (500 MHz, CDCl_3)	: 9.98 (s, 1H), 7.20 (d, $J = 9$ Hz, 2H), 7.00 (d, $J = 9$ Hz, 2H), 6.63 (d, $J = 3.5$ Hz, 1H), 6.60 (d, $J = 3$ Hz, 1H), 4.62 (s, 1H), 4.33 (s, 1H), 3.88 (s, 3H), 3.16-2.98 (m, 2H), 2.21-0.84 (m, 12H), 0.79 (s, 3H), 0.74 (s, 3H), 0.62(s, 3H)
$^{13}\text{C NMR}$ (125 MHz, CDCl_3)	: 186.0, 159.6, 147.9, 147.6, 142.2, 132.4, 127.6, 123.8, 123.3, 114.6, 109.5, 107.4, 55.7, 55.6, 42.0, 39.9, 38.6, 38.1, 33.6, 33.4, 24.3, 21.6, 20.9, 19.2, 14.0
HRMS (ESI)	: m/z: $[\text{M}+\text{Na}]^+$ calcd for $\text{C}_{27}\text{H}_{35}\text{NO}_2\text{Na}$ is

428.2565, found 428.2571

4.8.3.3. Synthesis of 1-(3-methoxyphenyl)-2-((5,5,8a-trimethyl-2-methylenedecahydro-naphthalene-1-yl)methyl)-1H-pyrrole-3-carbaldehyde (3c)

The compound 3c was prepared by the reaction of (*E*)-labda-8(17),12-diene-15,16-dial (30 mg, 1 equiv.) and 3-methoxyaniline (18.34 mg, 1.5 equiv.) in THF (3 ml) as per the method described in section 4.8.2. Yield: 35% (15 mg).



FT-IR (NaCl, ν_{\max} , cm^{-1}) : 3428, 2934, 2841, 2101, 1663, 1607, 1533, 1495, 1459, 1438

^1H NMR (500 MHz, CDCl_3) : 9.99 (s, 1H), 7.40 (t, $J = 8$ Hz, 1H), 7.00 (dd, $J_1 = 2$ Hz, $J_2 = 8$ Hz, 1H), 6.88 (d, $J = 7.5$ Hz, 1H), 6.81 (t, $J = 2$ Hz, 1H), 6.64 (s, 2H), 4.62 (s, 1H), 4.36 (s, 1H), 3.84 (s, 3H), 3.22-3.04 (m, 2H), 2.20-0.88 (m, 12H), 0.78 (s, 3H), 0.73 (s, 3H), 0.64 (s, 3H)

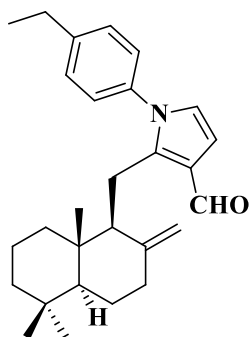
^{13}C NMR (125 MHz, CDCl_3) : 186.1, 160.4, 147.9, 141.9, 140.6, 130.2, 123.6, 118.6, 114.2, 112.2, 109.7, 107.3, 55.6, 55.4, 42.0, 39.9, 38.6, 38.1, 33.6, 33.4, 24.3, 21.6, 20.9, 19.3, 14.0

HRMS (ESI) : m/z : $[\text{M}+\text{Na}]^+$ calcd for $\text{C}_{27}\text{H}_{35}\text{NO}_2\text{Na}$ is 428.2565, found 428.2565

4.8.3.4. Synthesis of 1-(4-ethylphenyl)-2-((5,5,8a-trimethyl-2-methylenedecahydro-naphthalene-1-yl)methyl)-1H-pyrrole-3-carbaldehyde (3d)

The compound 3d was prepared by the reaction of (*E*)-labda-8(17),12-diene-15,16-dial (30 mg, 1 equiv.) and 4-ethylaniline (18.04 mg, 1.5 equiv.) in THF (3 ml) as per the method described in section 4.8.2. Yield: 31% (13 mg).

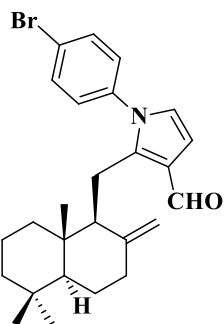
FT-IR (NaCl, ν_{\max} , cm^{-1}) : 3283, 2934, 2852, 1737, 1665, 1538, 1439



ν_{\max} , cm^{-1}	
$^1\text{H NMR}$ (500 MHz, CDCl_3)	: 9.98 (s, 1H), 7.32 (d, $J = 7.5\text{Hz}$, 2H), 7.20 (d, $J = 8\text{ Hz}$, 2H), 6.62 (s, 2H), 4.62 (s, 1H), 4.38 (s, 1H), 3.21 (dd, $J = 10.5\text{ Hz}$, 1H), 2.99 (dd, $J = 3.5\text{ Hz}$, 1H), 2.74 (q, $J_1 = 7.5\text{ Hz}$, $J_2 = 15\text{ Hz}$, 2H), 2.17 (br d, $J = 12.5\text{ Hz}$, 1H), 1.82 (br d, $J = 9\text{ Hz}$, 1H), 1.66-0.87 (m, 10H), 1.30 (d, 7.5 Hz, 3H), 0.76 (s, 3H), 0.72 (s, 3H), 0.62 (s, 3H)
$^{13}\text{C NMR}$ (125 MHz, CDCl_3)	: 186.1, 147.8, 145.0, 142.0, 137.2, 128.8, 126.4, 123.7, 123.4, 109.6, 107.4, 55.6, 55.2, 42.0, 39.8, 38.4, 38.0, 33.5, 33.4, 28.6, 24.3, 21.58, 20.8, 19.2, 15.9, 14.0
HRMS (ESI)	: m/z : $[\text{M}+\text{Na}]^+$ calcd for $\text{C}_{28}\text{H}_{37}\text{NONa}$ is 426.2773, found 426.2775

4.8.3.5. Synthesis of 1-(4-bromophenyl)-2-((5,5,8a-trimethyl-2-methylenedecahydronaphthalen-1-yl)methyl)-1H-pyrrole-3-carbaldehyde (3e)

The compound 3e was prepared by the reaction of (*E*)-labda-8(17),12-diene-15,16-dial (30 mg, 1equiv.) and 4-bromoaniline (25.62 mg, 1.5 equiv.) in THF (3 ml) as per the method described in section 4.8.2. Yield: 29% (13.5 mg).



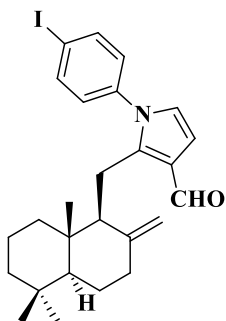
FT-IR (NaCl, ν_{\max} , cm^{-1})	: 3339, 2942, 2848, 1666, 1593, 1533, 1496, 1460, 1439
$^1\text{H NMR}$ (500 MHz, CDCl_3)	: 9.99 (s, 1H), 7.64 (d, $J = 8.5\text{ Hz}$, 2H), 7.18 (d, $J = 8.5\text{ Hz}$, 2H), 6.66 (d, $J = 3\text{ Hz}$, 1H), 6.60 (d, $J = 3\text{ Hz}$, 1H), 4.60 (s, 1H), 4.26 (s, 1H), 3.16-3.02 (m, 2H), 2.20-0.86 (m, 12H), 0.80 (s, 3H), 0.74 (s, 3H), 0.62 (s, 3H)
$^{13}\text{C NMR}$ (125 MHz, CDCl_3)	: 186.0, 141.8, 138.6, 132.7, 128.0, 123.9, 123.4, 122.4, 110.1, 107.3, 55.9, 55.6, 42.0,

40.0, 38.7, 38.0, 33.5, 33.4, 29.6, 24.3, 21.6,
20.9, 19.2, 14.0

HRMS (ESI) : m/z : $[M+Na]^+$ calcd for $C_{26}H_{32}BrNONa$ is
476.1565, found 476.1572

4.8.3.6. Synthesis of 1-(4-iodophenyl)-2-((5,5,8a-trimethyl-2-methylenedecahydronaphthalene-1-yl)methyl)-1H-pyrrole-3-carbaldehyde (3f)

The compound 3f was prepared by the reaction of (*E*)-labda-8(17),12-diene-15,16-dial (30 mg, 1equiv.) and 4-iodoaniline (32.61 mg, 1.5 equiv.) in THF (3 ml) as per the method described in section 4.8.2. Yield: 30% (15.5 mg).



FT-IR (NaCl, : 3325, 2964, 2920, 2851, 1946, 1658, 1589,
 v_{max} , cm^{-1}) 1494, 1442

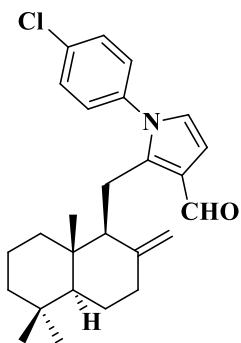
1H NMR (500 : 9.99 (s, 1H), 7.84 (d, $J = 8.5$ Hz, 2H), 7.04
MHz, $CDCl_3$) (d, $J = 9$ Hz, 2H), 6.66 (d, $J = 3.5$ Hz, 1H),
6.60 (s, 1H), 4.61 (s, 1H), 4.27 (s, 1H), 3.16-
3.01 (m, 2H), 2.20-0.86 (m, 12H), 0.80 (s,
3H), 0.74 (s, 3H), 0.62 (s, 3H)

^{13}C NMR (125 : 186.0, 147.8, 141.8, 139.2, 138.7, 128.2,
MHz, $CDCl_3$) 123.8, 123.4, 110.1, 107.3, 93.5, 55.9, 55.6,
42.0, 40.0, 38.6, 38.0, 33.6, 33.4, 29.7, 26.8,
24.2, 21.6, 20.9, 19.2, 14.1

HRMS (ESI) : m/z : $[M+Na]^+$ calcd for $C_{26}H_{32}INONa$ is
524.1426, found 524.1435

4.8.3.7. Synthesis of 1-(4-chlorophenyl)-2-((5,5,8a-trimethyl-2-methylenedecahydronaphthalen-1-yl)methyl)-1H-pyrrole-3-carbaldehyde (3g)

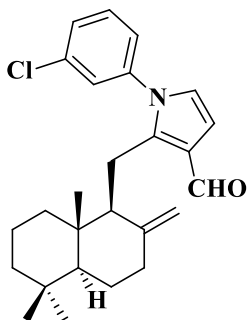
The compound 3g was prepared by the reaction of (*E*)-labda-8(17),12-diene-15,16-dial (30 mg, 1equiv.) and 4-chloroaniline (18.99 mg, 1.5 equiv.) in THF (3 ml) as per the method described in the section 4.8.2. Yield: 39% (17 mg).



FT-IR (NaCl, ν_{\max} , cm^{-1})	: 3420, 2939, 2101, 1652, 1536, 1494, 1439
^1H NMR (500 MHz, CDCl_3)	: 9.99 (s, 1H), 7.50 (d, $J = 8.5$ Hz, 2H), 7.24 (d, $J = 8.5$ Hz, 2H), 6.66 (d, $J = 3$ Hz, 1H), 6.60 (d, $J = 3$ Hz, 1H), 4.61 (s, 1H), 4.27 (s, 1H), 3.14 (dd, $J = 10$ Hz, 1H), 3.04 (dd, $J = 4.5$ Hz, 1H), 2.21-2.18 (m, 1H), 2.21-1.05 (m, 10H), 1.92-1.90 (m, 1H), 0.80 (s, 3H), 0.74 (s, 3H), 0.63 (s, 3H)
^{13}C NMR (125 MHz, CDCl_3)	: 185.0, 146.9, 140.9, 137.0, 133.4, 128.6, 126.7, 122.7, 122.4, 109.0, 106.3, 54.9, 54.6, 40.9, 39.0, 37.7, 37.0, 32.5, 32.4, 23.3, 20.6, 19.9, 18.2, 13.0
HRMS (ESI)	: m/z : $[\text{M}+\text{Na}]^+$ calcd for $\text{C}_{26}\text{H}_{32}\text{ClN}$ is 432.2070, found 432.2075

4.8.3.8. Synthesis of 1-(3-chlorophenyl)-2-((5,5,8a-trimethyl-2-methylenedecahydronaphthalen-1-yl)methyl)-1H-pyrrole-3-carbaldehyde (3h)

The compound 3h was prepared by the reaction of (*E*)-labda-8(17),12-diene-15,16-dial (30 mg, 1 equiv.) and 3-chloroaniline (18.99 mg, 1.5 equiv.) in THF (3 ml) as per the method described in section 4.8.2. Yield: 35% (15 mg).



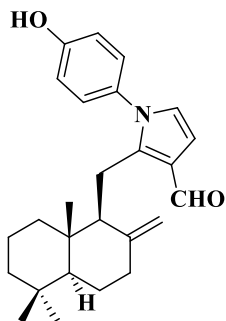
FT-IR (NaCl, ν_{\max} , cm^{-1})	: 3428, 2939, 2102, 1656, 1534, 1494, 1439
^1H NMR (500 MHz, CDCl_3)	: 9.99 (s, 1H), 7.46-7.19 (m, 4H), 6.66 (d, $J = 3$ Hz, 1H), 6.63 (d, $J = 3$ Hz, 1H), 4.62 (s, 1H), 4.32 (s, 1H), 3.24-3.19 (m, 1H), 3.06-3.02 (m, 1H), 2.20-0.84 (m, 12H), 0.79 (s, 3H), 0.74 (s, 3H), 0.64 (s, 3H)
^{13}C NMR (125 MHz, CDCl_3)	: 186.2, 147.7, 141.8, 140.6, 135.2, 130.5, 128.6, 126.9, 124.6, 123.4, 110.1, 107.4,

55.7, 55.6, 42.0, 40.0, 38.6, 38.0, 33.5, 33.4,
24.3, 21.6, 20.8, 20.8, 19.2, 14.0

HRMS (ESI) : m/z: $[M+Na]^+$ calcd for $C_{26}H_{32}ClNO_2Na$ is
432.2070, found 432.2079

4.8.3.9. Synthesis of 1-(4-hydroxyphenyl)-2-((5,5,8a-trimethyl-2-methylenedecahydronaphthalene-1-yl)methyl)-1H-pyrrole-3-carbaldehyde (3i)

The compound 3i was prepared by the reaction of (*E*)-labda-8(17),12-diene-15,16-dial (30 mg, 1 equiv.) and 4-hydroxyaniline (16.25 mg, 1.5 equiv.) in THF (3 ml) as per the method described in section 4.8.2. Yield: 32% (13 mg).



FT-IR (NaCl, : 3790, 3640, 3370, 2920, 2849, 2077, 1735,
 ν_{max}, cm^{-1}) 1643, 1597, 1540, 1520, 1459

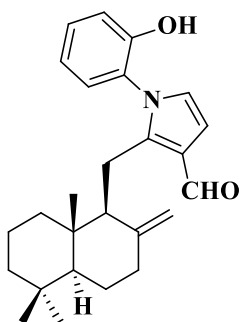
1H NMR (500 : 9.97 (s, 1H), 7.14 (d, $J = 8.5$ Hz, 2H), 6.96
MHz, $CDCl_3$) (d, $J = 9$ Hz, 2H), 6.64 (d, $J = 3$ Hz, 1H),
6.60 (d, $J = 3.5$ Hz, 1H), 5.72 (bs, 1H), 4.62
(s, 1H), 4.32 (s, 1H), 3.17-2.98 (m, 2H),
2.20-0.82 (m, 12H), 0.80 (s, 3H), 0.74 (s,
3H), 0.62 (s, 3H)

^{13}C NMR (125 : 186.2, 155.9, 148.0, 142.6, 132.4, 127.8,
MHz, $CDCl_3$) 123.9, 123.2, 116.0, 109.4, 107.4, 55.6, 55.5,
42.0, 40.0, 38.6, 38.1, 33.6, 33.4, 29.6, 24.3,
21.6, 21.0, 19.2, 14.0

HRMS (ESI) : m/z: $[M+Na]^+$ calcd for $C_{26}H_{33}NO_2Na$ is
414.2409, found 414.2415

4.8.3.10. Synthesis of 1-(2-hydroxyphenyl)-2-((5,5,8a-trimethyl-2-methylenedecahydro-naphthalen-1-yl)methyl)-1H-pyrrole-3-carbaldehyde (3j)

The compound 3j was prepared by the reaction of (*E*)-labda-8(17),12-diene-15,16-dial (30 mg, 1 equiv.) and 2-hydroxyaniline (16.25 mg, 1.5 equiv.) in THF (3 ml) as per the method described in section 4.8.2. Yield: 32% (13 mg).

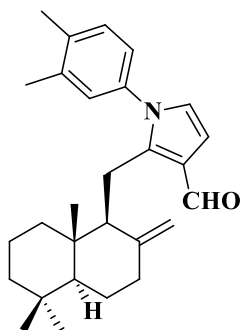


FT-IR (NaCl, ν_{\max} , cm^{-1})	: 3797, 3644, 3367, 2926, 2849, 2077, 1641, 1597, 1538, 1512, 1459
^1H NMR (500 MHz, CDCl_3)	: 9.98 (s, 1H), 7.39-7.36 (m, 1H), 7.19-7.10 (m, 3H), 7.04-7.02 (dt, $J_1 = 1$ Hz, $J_2 = 7.5$ Hz, 1H), 6.70 (s, 1H), 6.58 (d, $J = 3$ Hz, 1H), 4.67 (s, 1H), 4.52 (s, 1H), 2.87 (dd, $J_1 = 3.5$ Hz, $J_2 = 15.5$ Hz, 1H), 2.22-2.18 (m, 1H), 1.88-0.86 (m, 12H), 0.78 (s, 3H), 0.72 (s, 3H), 0.65 (s, 3H)
^{13}C NMR (125 MHz, CDCl_3)	: 186.1, 152.0, 148.4, 130.8, 129.3, 128.2, 123.6, 121.0, 117.2, 115.3, 110.9, 107.7, 55.5, 54.2, 41.9, 39.8, 38.4, 37.9, 33.5, 33.4, 24.3, 21.6, 20.53, 19.2, 13.9
HRMS (ESI)	: m/z : $[\text{M}+\text{Na}]^+$ calcd for $\text{C}_{26}\text{H}_{33}\text{NO}_2\text{Na}$ is 414.2409, found 414.2416

4.8.3.11. Synthesis of 1-(3,4-dimethylphenyl)-2-((5,5,8a-trimethyl-2-methylenedecahydro-naphthalen-1-yl)methyl)-1H-pyrrole-3-carbaldehyde (3k)

The compound 3k was prepared by the reaction of (*E*)-labda-8(17),12-diene-15,16-dial (30 mg, 1 equiv.) and 3,4-dimethylaniline (18.04 mg, 1.5 equiv.) in THF (3 ml) as per the method described in section 4.8.2. Yield: 50% (21 mg).

FT-IR (NaCl, ν_{\max} , cm^{-1})	: 3290, 2962, 1996, 1732, 1650, 1480
--	--------------------------------------



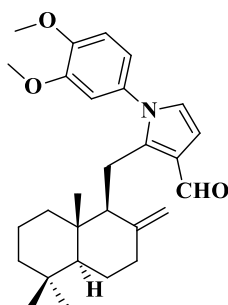
^1H NMR (500 MHz, CDCl_3) : 9.98 (s, 1H), 7.25 (d, $J = 8$ Hz, 1H), 7.04 (s, 1H), 7.01-6.99 (dd, $J_1 = 2$ Hz, $J_2 = 8$ Hz, 1H), 6.62-6.60 (m, 2H), 4.61 (s, 1H), 4.36 (s, 1H), 3.19-2.99 (m, 2H), 2.34 (s, 3H), 2.32 (s, 3H), 2.20-0.98 (m, 12H), 0.78 (s, 3H), 0.72 (s, 3H), 0.62 (s, 3H)

^{13}C NMR (125 MHz, CDCl_3) : 186.1, 147.9, 142.2, 137.9, 137.2, 137.1, 130.4, 127.6, 123.7, 123.6, 123.3, 109.4, 107.3, 55.6, 55.5, 42.1, 39.9, 38.4, 38.0, 33.6, 33.4, 24.3, 21.6, 20.8, 19.8, 19.4, 19.3, 14.0

HRMS (ESI) : m/z : $[\text{M}+\text{Na}]^+$ calcd for $\text{C}_{28}\text{H}_{37}\text{NONa}$ is 426.2773, found 426.2783

4.8.3.12. Synthesis of 1-(3,4-dimethoxyphenyl)-2-((5,5,8a-trimethyl-2-methylenedecahydronaphthalen-1-yl)methyl)-1H-pyrrole-3-carbaldehyde (3l)

The compound 3l was prepared by the reaction of (*E*)-labda-8(17),12-diene-15,16-dial (30 mg, 1 equiv.) and 3,4-dimethoxyaniline (22.81 mg, 1.5 equiv.) in THF (3 ml) as per the method described in section 4.8.2. Yield: 40% (18 mg).



FT-IR (NaCl, ν_{max} , cm^{-1}) : 3265, 2926, 1948, 1735, 1648, 1438

^1H NMR (500 MHz, CDCl_3) : 9.98 (s, 1H), 6.96-6.78 (m, 3H), 6.64-6.62 (m, 2H), 4.62 (s, 1H), 4.37 (s, 1H), 3.96 (s, 3H), 3.88 (s, 3H), 3.22-3.02 (m, 2H), 2.21-0.84 (m, 12H), 0.78 (s, 3H), 0.74 (s, 3H), 0.64 (s, 3H)

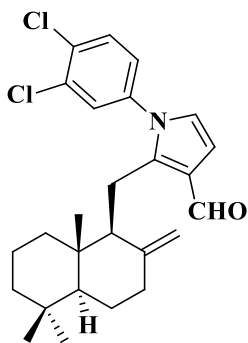
^{13}C NMR (125 MHz, CDCl_3) : 186.1, 149.4, 149.2, 148.0, 142.2, 132.5, 123.8, 123.2, 118.6, 111.2, 110.0, 109.5, 107.4, 56.3, 56.2, 55.6, 55.4, 42.0, 39.9,

38.6, 38.2, 33.6, 33.4, 24.3, 21.6, 21.0, 19.3,
14.0

HRMS (ESI) : m/z: $[M+Na]^+$ calcd for $C_{28}H_{37}NO_3Na$ is
458.2671, found 458.2673

4.8.3.13. Synthesis of 1-(3,4-dichlorophenyl)-2-((5,5,8a-trimethyl-2-methylenedecahydr-onaphthalene-1-yl)methyl)-1H-pyrrole-3-carbaldehyde (3m)

The compound 3m was prepared by the reaction of (*E*)-labda-8(17),12-diene-15,16-dial (30 mg, 1 equiv.) and 3,4-dichloroaniline (24.12 mg, 1.5 equiv.) in THF (3 ml) as per the method described in section 4.8.2. Yield: 39% (18 mg).



FT-IR (NaCl, : 3420, 2941, 1732, 1656, 1540, 1496, 1440
 v_{max}, cm^{-1})

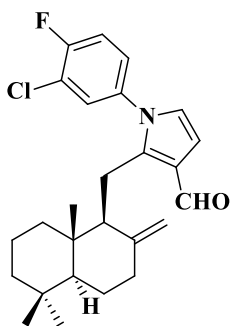
1H NMR (500 : 9.94 (s, 1H), 7.60 (d, $J = 8.5$ Hz, 1H), 7.43
MHz, $CDCl_3$) (s, 1H), 7.16 (d, $J = 8.5$ Hz, 1H), 6.66 (d, $J =$
2.5 Hz, 1H), 6.62 (s, 1H), 4.63 (s, 1H), 4.28
(s, 1H), 3.19-3.14 (m, 1H), 3.07-3.03 (m,
1H), 2.22-0.89 (m, 12H), 0.80 (s, 3H), 0.74
(s, 3H), 0.65 (s, 3H)

^{13}C NMR : 185.0, 146.8, 140.8, 137.8, 132.6, 131.9,
(125 MHz, 130.1, 127.5, 124.6, 122.9, 122.3, 109.4,
 $CDCl_3$) 106.4, 54.9, 54.7, 41.0, 39.1, 37.8, 37.0,
32.5, 32.4, 23.2, 20.6, 19.8, 18.2, 13.0

HRMS (ESI) : m/z: $[M+Na]^+$ calcd for $C_{26}H_{31}Cl_2NONa$ is
466.1680, found 466.1696

4.8.3.14. Synthesis of 1-(3-chloro-4-fluorophenyl)-2-((5,5,8a-trimethyl-2-methylenedecahydronaphthalen-1-yl)methyl)-1H-pyrrole-3-carbaldehyde (3n)

The compound 3n was prepared by the reaction of (*E*)-labda-8(17),12-diene-15,16-dial (30 mg, 1 equiv.) and 3-chloro-4-fluoroaniline (21.68 mg, 1.5 equiv.) in THF (3 ml) as per the method described in section 4.8.2. Yield: 31% (14 mg).

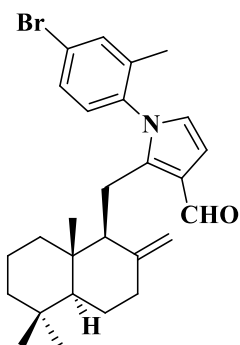


FT-IR (NaCl, ν_{\max} , cm^{-1})	: 3280, 2930, 1735, 1648, 1430
^1H NMR (500 MHz, CDCl_3)	: 9.99 (s, 1H), 7.39-7.18 (m, 3H), 6.66 (d, $J = 3$ Hz, 1H), 6.60 (d, $J = 3$ Hz, 1H), 4.63 (s, 1H), 4.30 (s, 1H), 3.32-3.01 (m, 2H), 2.22-0.88 (m, 12H), 0.80 (s, 3H), 0.74 (s, 3H), 0.65 (s, 3H)
^{13}C NMR (125 MHz, CDCl_3)	: 186.1, 158.9, 147.7, 141.9, 128.9, 126.3, 126.2, 123.7, 123.6, 117.4, 117.2, 110.2, 107.4, 55.8, 55.8, 41.9, 40.1, 38.8, 38.0, 33.5, 33.5, 24.3, 21.6, 20.2, 19.2, 14.0
HRMS (ESI)	: m/z : $[\text{M}+\text{Na}]^+$ calcd for $\text{C}_{26}\text{H}_{31}\text{ClFNONa}$ is 450.1976, found 450.1980

4.8.3.15. Synthesis of 1-(4-bromo-2-methylphenyl)-2-((5,5,8a-trimethyl-2-methylenedecahydronaphthalen-1-yl)methyl)-1H-pyrrole-3-carbaldehyde (3o)

The compound 3o was prepared by the reaction of (*E*)-labda-8(17),12-diene-15,16-dial (30 mg, 1 equiv.) and 4-bromo-2-methylaniline (27.70 mg, 1.5 equiv.) in THF (3 ml) as per the method described in section 4.8.2. Yield: 30% (14.5 mg).

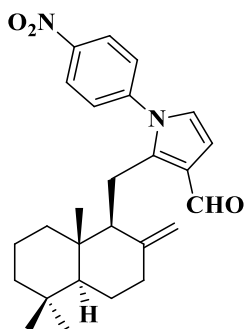
FT-IR (NaCl, ν_{\max} , cm^{-1})	: 3270, 2926, 1737, 1720, 1650, 1511
--	--------------------------------------



^1H NMR (500 MHz, CDCl_3)	: 9.98 (s, 1H), 7.54 (dd, $J_1 = 2$ Hz, $J_2 = 12$ Hz, 1H), 7.48-7.45 (m, 1H), 7.08 (dd, $J_1 = 3.5$ Hz, $J_2 = 8.5$ Hz, 1H), 6.67 (t, $J = 3$ Hz, 1H), 6.50 (d, $J = 3.5$ Hz, 1H), 4.68 (s, 1H), 4.44 (s, 1H), 3.23-2.66 (m, 2H), 2.18 (s, 3H), 2.03-0.89 (m, 12H), 0.81 (s, 3H), 0.74 (s, 3H), 0.65 (s, 3H)
^{13}C NMR (125 MHz, CDCl_3)	: 186.2, 147.4, 137.4, 134.0, 133.9, 129.6, 129.9, 129.8, 127.6, 123.2, 115.8, 108.0, 55.8, 54.4, 42.0, 39.8, 38.6, 38.0, 33.6, 33.5, 24.2, 21.6, 20.9, 20.4, 19.2, 14.0
HRMS (ESI)	: m/z : $[\text{M}+\text{H}]^+$ calcd for $\text{C}_{27}\text{H}_{35}\text{BrNO}$ is 468.1902, found 468.1906

4.8.3.16. Synthesis of 1-(4-nitrophenyl)-2-((5,5,8a-trimethyl-2-methylenedecahydronaphthalen-1-yl)methyl)-1H-pyrrole-3-carbaldehyde (3p)

The compound 3p was prepared by the reaction of (*E*)-labda-8(17),12-diene-15,16-dial (30 mg, 1 equiv.) and 4-nitroaniline (20.57 mg, 1.5 equiv.) in THF (3 ml) as per the method described in section 4.8.2. Yield: 30% (13 mg).



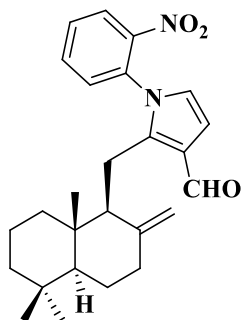
FT-IR (NaCl, ν_{max} , cm^{-1})	: 3371, 2922, 2850, 1737, 1667, 1596, 1526, 1501, 1460, 1439, 1400
^1H NMR (500 MHz, CDCl_3)	: 10.02 (s, 1H), 8.40 (d, $J = 9$ Hz, 2H), 7.50 (d, $J = 9$ Hz, 2H), 6.72 (d, $J = 3$ Hz, 1H), 6.67 (d, $J = 3$ Hz, 1H), 4.60 (s, 1H), 4.18 (s, 1H), 3.17 (s, 1H), 3.16 (d, $J = 2.5$ Hz, 1H), 2.19-0.86 (m, 12H), 0.786 (s, 3H), 0.736 (s, 3H), 0.631 (s, 3H)
^{13}C NMR (125 MHz, CDCl_3)	: 186.0, 147.9, 147.1, 144.8, 141.7, 126.9, 125.0, 124.4, 123.2, 110.9, 107.2, 56.5, 55.6

41.8, 40.2, 38.8, 38.0, 33.4, 29.7, 24.2, 21.6,
21.1, 19.2, 14.0

HRMS (ESI) : m/z: $[M+Na]^+$ calcd for $C_{26}H_{32}N_2O_3Na$ is
443.2311, found 443.2321

4.8.3.17. Synthesis of 1-(2-nitrophenyl)-2-((5,5,8a-trimethyl-2-methylenedecahydronaphthalen-1-yl)methyl)-1H-pyrrole-3-carbaldehyde (3q)

The compound 3q was prepared by the reaction of (*E*)-labda-8(17),12-diene-15,16-dial (30 mg, 1 equiv.) and 2-nitroaniline (20.57 mg, 1.5 equiv.) in THF (3 ml) as per the method described in section 4.8.2. Yield: 30% (13 mg).



FT-IR (NaCl, ν_{max}, cm^{-1}) : 3350, 2840, 1735, 1665, 1590, 1501

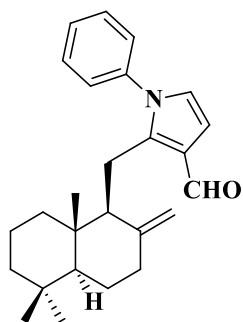
1H NMR (500 MHz, $CDCl_3$) : 9.99 (d, $J = 13$ Hz, 1H), 8.09 (d, $J = 7$ Hz, 1H), 7.76-7.68 (m, 2H), 7.45 (d, $J = 7$ Hz, 1H), 6.70 (s, 1H), 6.60 (s, 1H), 4.66 (s, 1H), 4.32 (s, 1H), 3.32-0.78 (m, 14H), 0.76 (s, 3H), 0.72 (s, 3H), 0.62 (s, 3H)

^{13}C NMR (125 MHz, $CDCl_3$) : 186.2, 147.4, 142.7, 133.7, 130.8, 130.6, 125.6, 125.4, 123.6, 110.6, 108.1, 107.2, 55.8, 54.9, 41.9, 40.1, 38.5, 37.9, 37.8, 33.6, 33.4, 29.7, 24.2, 21.6, 19.2, 13.8

HRMS (ESI) : m/z: $[M+Na]^+$ calcd for $C_{26}H_{32}N_2O_3Na$ is
443.2311, found 443.2315

4.8.3.18. Synthesis of 1-phenyl-2-((5,5,8a-trimethyl-2-methylenedecahydronaphthalen-1-yl)methyl)-1H-pyrrole-3-carbaldehyde (3r)

The compound 3r was prepared by the reaction of (*E*)-labda-8(17),12-diene-15,16-dial (30 mg, 1 equiv.) and aniline (13.86 mg, 1.5 equiv.) in THF (3 ml) as per the method described in section 4.8.2. Yield: 30% (12 mg).



FT-IR (NaCl, ν_{\max} , cm^{-1})	: 3644, 3582, 2962, 2920, 2849, 1946, 1732, 1718, 1666, 1598, 1538, 1501, 1459
^1H NMR (500 MHz, CDCl_3)	: 10.00 (s, 1H), 7.52-7.46 (m, 3H), 7.30-7.28 (m, 2H), 6.66-6.64 (m, 2H), 4.61 (s, 1H), 4.32 (s, 1H), 3.22-3.17 (m, 1H), 3.06-3.02 (m, 1H), 2.18-0.80 (m, 12H), 0.77 (s, 3H), 0.72 (s, 3H), 0.62 (s, 3H)
^{13}C NMR (125 MHz, CDCl_3)	: 186.1, 157.1, 148.8, 147.8, 145.3, 142.8, 129.4, 128.4, 126.4, 123.6, 109.5, 107.3, 55.5, 42.0, 39.9, 38.6, 38.0, 33.5, 30.8, 29.6, 24.3, 21.6, 20.9, 19.2, 14.0
HRMS (ESI)	: m/z: $[\text{M}+\text{Na}]^+$ calcd for $\text{C}_{26}\text{H}_{33}\text{NONa}$ is 398.2460, found 398.2449

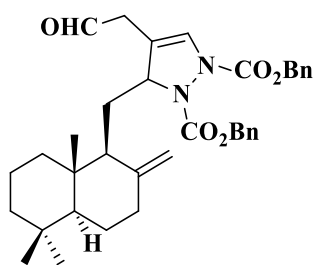
4.8.4. General procedure for synthesis of (*E*)-labda-8(17),12-diene-15,16-dial-pyrazole analogues (5a-5d)

To a stirred solution of (*E*)-labda-8(17),12-diene-15,16-dial (1 equiv.) and dialkyl azodicarboxylate (1.5 equiv.) in dichloromethane (DCM), triphenylphosphine (1.5 equiv.) was added and stirred for 2-3 hours at room temperature. The completion of the reaction was confirmed by TLC. The resulting solution was concentrated and purified by column chromatography using hexane and ethyl acetate as solvents.⁴⁴

4.8.4.1. Synthesis of dibenzyl 4-(2-oxoethyl)-3-((5,5,8a-trimethyl-2-methylenedecahydr-onaphthalen-1-yl)methyl)-1H-pyrazole-1,2(3H)-dicarboxylate (5a)

The compound 5a was prepared by the reaction of (*E*)-labda-8(17),12-diene-15,16-dial (30 mg, 1 equiv.) and dibenzyl azodicarboxylate (44.40 mg 1.5 equiv.) in DCM (3 ml) as per the method described in section 4.8.4. Yield: 30% (13.5 mg).

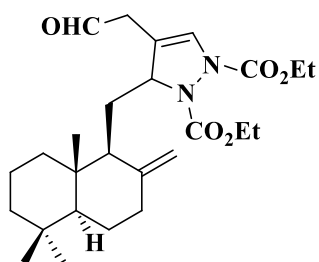
FT-IR (NaCl, ν_{\max} , cm^{-1})	: 2927, 2852, 1731, 1630, 1396, 1226
---	--------------------------------------



^1H NMR (500 MHz, CDCl_3)	: 9.35 (s, 1H), 8.20 (d, $J = 14$ Hz, 1H), 7.34 (m, 10H), 6.28 (s, 1H), 5.84 (d, $J = 14$ Hz, 1H), 5.24 (m, 4H), 4.81 (s, 1H), 4.32 (s, 1H), 2.56-1.14 (m, 15 H), 0.885 (s, 3H), 0.825 (s, 3H), 0.719 (s, 3H)
^{13}C NMR (125 MHz, CDCl_3)	: 194.0, 156.0, 153.6, 148.1, 135.6, 135.2, 130.8, 128.6, 128.1, 127.6, 107.9, 69.4, 67.6, 56.8, 55.4, 42.04, 39.6, 39.2, 37.8, 33.6, 31.8, 29.6, 24.0, 21.8, 19.4, 14.4
HRMS (ESI)	: m/z : $[\text{M}+\text{Na}]^+$ calcd for $\text{C}_{36}\text{H}_{44}\text{N}_2\text{O}_5\text{Na}$ is 607.3148, found 607.3131

4.8.4.2. Synthesis of diethyl 4-(2-oxoethyl)-3-((5,5,8a-trimethyl-2-methylenedecahydro-naphthalen-1-yl)methyl)-1H-pyrazole-1,2(3H)-dicarboxylate (5b)

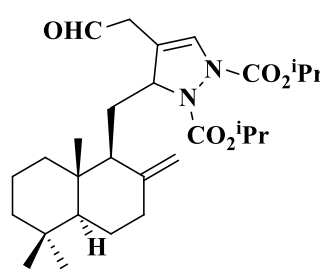
The compound 5b was prepared by the reaction of (*E*)-labda-8(17),12-diene-15,16-dial (30 mg, 1 equiv.) and diethyl azodicarboxylate (25.93 mg 1.5 equiv.) in DCM (3 ml) as per the method described in section 4.8.4. Yield: 30% (14 mg).



FT-IR (NaCl, ν_{max} , cm^{-1})	: 3297, 2935, 2725, 1728, 1647, 1461
^1H NMR (500 MHz, CDCl_3)	: 9.36 (s, 1H), 8.14 (s, 1H), 6.294 (t, $J = 6.5$ Hz, 1H), 5.84 (d, $J = 14$ Hz, 1H), 4.83 (s, 1H), 4.37 (s, 1H), 4.27 (m, 4H), 2.42-1.19 (m, 15 H), 1.33 (m, 6H), 0.89 (s, 3H), 0.83 (s, 3H), 0.76 (s, 3H)
^{13}C NMR (125 MHz, CDCl_3)	: 194.2, 169.3, 148.2, 135.9, 131.0, 107.9, 63.8, 62.5, 56.8, 55.4, 42.0, 39.6, 39.2, 37.8, 33.6, 31.6, 24.6, 24.2, 22.6, 21.7, 19.3, 14.4, 14.4, 14.0
HRMS (ESI)	: m/z : $[\text{M}+\text{Na}]^+$ calcd for $\text{C}_{26}\text{H}_{40}\text{N}_2\text{O}_5\text{Na}$ is 483.2835, found 483.2823

4.8.4.3. Synthesis of diisopropyl4-(2-oxoethyl)-3-((5,5,8a-trimethyl-2-methylenedecahydronaphthalen-1-yl)methyl)-1H-pyrazole-1,2(3H)-dicarboxylate (5c)

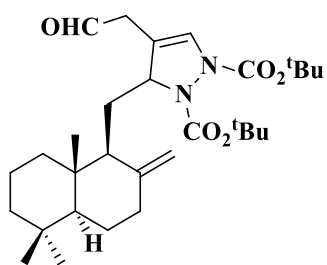
The compound 5c was prepared by the reaction of (*E*)-labda-8(17),12-diene-15,16-dial (30 mg, 1 equiv.) and diisopropyl azodicarboxylate (30.11 mg 1.5 equiv.) in DCM (3 ml) as per the method described in section 4.8.4. Yield: 40% (19 mg).

	FT-IR (NaCl, v_{\max} , cm^{-1})	: 3300, 2935, 1723, 1630, 1461
	^1H NMR (500 MHz, CDCl_3)	: 9.29 (s, 1H), 8.04 (d, $J = 14$ Hz, 1H), 6.20 (t, $J = 6.5$ Hz, 1H), 5.76 (d, $J = 13.5$ Hz, 1H), 4.98-4.94 (m, 2H), 4.76 (s, 1H), 4.28 (s, 1H), 1.21 (m, 12H, $-\text{CH}_3$ group of ^iPr), 2.53-1.06 (m, 15H), 0.82 (s, 3H), 0.76 (s, 3H), 0.68 (s, 3H)
	^{13}C NMR (125 MHz, CDCl_3)	: 194.4, 152.9, 148.2, 131.1, 107.9, 70.4, 56.8, 55.4, 42.0, 39.6, 39.30, 37.8, 33.6, 33.6, 29.7, 24.6, 24.1, 21.9, 21.8, 19.3, 14.4
HRMS (ESI)	: m/z : $[\text{M}+\text{Na}]^+$ calcd for $\text{C}_{28}\text{H}_{44}\text{N}_2\text{O}_5\text{Na}$ is 511.3148, found 511.3128	

4.8.4.4. Synthesis of di-ter-butyl4-(2-oxoethyl)-3-((5,5,8a-trimethyl-2-methylenedecahydronaphthalen-1-yl)methyl)-1H-pyrazole-1,2(3H)-dicarboxylate (5d)

The compound 5d was prepared by the reaction of (*E*)-labda-8(17),12-diene-15,16-dial (30 mg, 1 equiv.) and di-ter-butyl azodicarboxylate (34.27 mg 1.5 equiv.) in DCM (3 ml) as per the method described in section 4.8.4. Yield: 80% (41 mg).

	FT-IR (NaCl, v_{\max} , cm^{-1})	: 3420, 2978, 2931, 2848, 1730, 1665, 1645
--	--	--



^1H NMR (500 MHz, CDCl_3)	: 9.36 (s, 1H), 8.11 (d, $J = 14$ Hz, 1H), 6.23 (t, $J = 5.5$ Hz, 1H), 5.79 (d, $J = 14$ Hz, 1H), 4.82 (s, 1H), 4.36 (s, 1H), 1.43 (m, 18 H, - CH_3 of ^tBu), 2.59-1.10 (m, 15 H), 0.89 (s, 3H), 0.82 (s, 3H), 0.76 (s, 3H)
^{13}C NMR (125 MHz, CDCl_3)	: 194.4, 151.8, 148.2, 131.7, 108.0, 56.8, 55.4, 42.0, 39.6, 39.2, 37.8, 33.6, 33.6, 28.0, 24.6, 24.1, 21.8, 19.3, 14.4
HRMS (ESI)	: m/z: $[\text{M}+\text{Na}]^+$ calcd for $\text{C}_{30}\text{H}_{48}\text{N}_2\text{O}_5\text{Na}$ is 539.3461, found 539.3480

4.8.5. Biological screening

4.8.5.1. Cell cultures

Human hepatoma cells were obtained from the NCBS (National Centre for Biological Sciences, Pune). The cells were cultured in DMEM medium (containing 0.3 g/L L-glutamine and 2.0 g/L sodium bicarbonate) supplemented with 10% FBS, 1% penicillin-streptomycin mixture and maintained at 37 °C in a 5% CO_2 and 95% air atmosphere in a humidified incubator.⁴¹⁻⁴²

4.8.5.2. Cytotoxic evaluation of compounds by MTT assay

Cytotoxicity of the compounds was measured by means of MTT assay in HepG2 cell lines. For MTT assay, HepG2 cells were seeded at a density of 1×10^5 cells per well in 96-well plates and pre-incubated in DMEM containing 10% FBS and 1% penicillin-streptomycin. After 24 hours, incubated with the test compounds (1-100 μM) for 48 hrs, were washed and MTT (0.5 g/l) dissolved in PBS, was added to each well for the estimation of mitochondrial dehydrogenase activity as described previously by Mosmann (1983). After 4 hrs of incubation at 37 °C in a CO_2 incubator, 10% SDS in DMSO was added to each well and the absorbance of solubilised MTT formazan products were measured at 570 nm after 45 min, using a microplate reader (Bioteck, U.S.A). Results were expressed as a percentage of cell viability. Based on viability data 5 and 10 μM concentrations of test compounds have been

selected for analyzing their effect on triglyceride accumulation and total cholesterol synthesis in Hep G₂ cell lines.⁴¹⁻⁴²

4.8.5.3. HepG2 cell culture for the assessment of lipid synthesis and secretion

HepG2 cells were seeded in a 6 well plate (5×10^5 cells/well) and then grown in DMEM containing 10% FBS and 1% antibiotic solution. Medium was then discharged and supplemented with starving medium (DMEM + 1% antibiotic solution) then incubated for 24 hours. Starving medium then discharged and supplemented with high fatty acid rich medium (DMEM, 1:2 of 1 mM palmitic acid : 1 mM linoleic acid and BSA). Test compounds were treated in 10 μ M concentration for oil red O staining to assess lipid accumulation. 5 and 10 μ M concentration of test compounds were treated for testing triglyceride (TG) and cholesterol synthesis, as described above. Cells were then incubated for 24 hours in a 37 °C humidified atmosphere of 5% CO₂.⁴¹⁻⁴²

4.8.5.4. Oil red-O staining

After the incubation, the HepG2 cells were washed with PBS. The cells were then fixed for 30 minutes with 40% paraformaldehyde in PBS with 1% triton-X-100. Cells were washed with double distilled water and stained for 30 min by complete immersion in a 2:3 diluted working solution of oil red O (Sigma Aldrich, USA). Cells were then washed in PBS 3 times and are then observed under an inverted light Olympus microscope after the oil-red O staining to compare the lipid droplet formation of normal cells and treated cells.⁴¹⁻⁴²

4.8.5.5. Triglycerides assay

The TG levels were measured in cell lysate after the treatment with fatty acid rich medium and test compounds (5 and 10 μ M) for 24 hrs. Fenofibrate, a well-known drug used for treating high blood TG, at 10 μ M concentration was used as the positive control in this experiment. The concentration of triglyceride in the cell lysate was measured using the triglyceride quantification colorimetric assay kit as per the manufacturer's protocol and TG concentration was calculated as instructed. Briefly, 50 μ l test samples along with standards in triglyceride assay buffer were added to a 96-well plate. 2 μ l Lipase was added to each well and incubated for 20 min at room temperature. 50 μ l triglyceride reaction mixture was added

to each well and incubated at room temperature for 30-60 min. Absorbance was measured at 570 nm in a microtiter plate reader. The amount of TG was calculated from the standard curve.⁴¹⁻⁴² The percentage inhibition was calculated as follows.

$$\% \text{ inhibition} = \frac{\text{Abs}_{\text{control}} - \text{Abs}_{\text{sample}}}{\text{Abs}_{\text{control}}} \times 100$$

4.8.5.6. Total cholesterol assay

For analysing the effect of test compounds on the synthesis of cholesterol, HepG2 cells were treated as mentioned above and the medium was collected after 24 hr incubation. Total cholesterol assay kit was used for the quantitative determination of cholesterol levels in the medium treated by the compound. Atorvastatin, a well known hypocholesterolemic drug at 10 μM concentration was used as the positive control in this experiment. The concentration of total cholesterol in the supernatant was measured as per the kit's protocol and the concentrations were calculated following the manufacturer's instructions. Briefly, cells were lysed in chloroform/isopropanol/NP-40 (7:11:0.1) using a homogenizer and debris was removed by centrifugation at 15,000 x g for 10 minutes. The solvents were removed from samples by air drying at 50 °C for 1-2 hr followed by vacuum drying for 2 hr. The dried lipid content was dissolved in a 200 μl assay diluent. 40 U/ml superoxide dismutase was added to the samples to minimize the endogenous oxidation of the assay probe. 50 μl of the cholesterol reaction mixture with or without cholesterol esterase was mixed with 50 μl samples along with standards and incubated for 45 min at 37 °C. The amount of cholesterol was calculated by standard curve.⁴¹⁻⁴²

4.8.5.7. HMG CoA reductase activity assay

HMG CoA reductase activity was assessed based on the oxidation of NADPH by using a screening assay kit (Sigma Aldrich, USA) as per the manufacturer's instructions. Briefly, the reaction was started by the addition of HMG CoA reductase to the assay mixture containing buffer, NADPH, HMG CoA, test compounds and then the decreasing rate of absorbance was measured. Continuously determined for 20 min at 340 nm. The rate of reaction in the units of $\Delta\text{Abs}_{340}/\text{min}$ was then calculated for the enzyme specific activity.

4.8.5.8. Statistical analysis

All data represent the means \pm SD of at least five individual experiments unless otherwise indicated in the text. Data were analyzed using SPSS v9.0 software (SPSS Inc., Chicago, IL, U.S.A). Replicates were averaged before entry as a single data point. Statistical significance was determined using one way ANOVA with significance accepted at $P\leq 0.05$. If F reaches significance, Duncan's post hoc test was used to compare groups.

4.9. References

1. Asija, R.; Singh, C. A Comprehensive Review on Anti-hyperlipidemic Activity of Various Medicinal Plants. *Int. J. Curr. Pharm. Rev. Res.* **2016**, *7*, 407-41.
2. Goldstein, J. L.; Brown, M. S. A century of Cholesterol and Coronaries: from Plaques to Genes to Statins. *Cell* **2015**, *161*, 161-172.
3. Global Health Observatory (GHO) Data, http://www.who.int/gho/ncd/risk-factors/cholesterol_text/en/.
4. Shattat, G.F. A Review Article on Hyperlipidemia: Types, Treatments and New Drug Targets. *J. Biomed. Pharmacol.* **2014**, *7*, 399-409.
5. Jain, K. S.; Kathiravan, M. K.; Somani, R. S.; Shishoo, C. J. The Biology and Chemistry of Hyperlipidemia. *Bioorg. Med. Chem.* **2007**, *15*, 4674-4699.
6. Lodhi, I. J.; Yin, L.; Jensen-Urstad, A. P.; Funai, K.; Coleman, T.; Baird, J. H.; Ramahi, M. K.; Razani, B.; Song, H.; Fu-Hsu, F.; Turk, J.; Semenkovich, C. F. Inhibiting Adipose Tissue Lipogenesis Reprograms Thermogenesis and PPAR γ Activation to Decrease Diet-Induced Obesity. *Cell Metab.* **2012**, *16*, 189-201.
7. Ramasamy, I. Update on the Molecular Biology of Dyslipidemias. *Clin. Chim. Acta.* **2016**, *454*, 143-185.
8. Nordestgaard, B. G.; Langsted, A.; Freiberg, J. J. Nonfasting Hyperlipidemia and Cardiovascular Disease. *Curr. Drug Targets* **2009**, *10*, 328-335.
9. Hassan El-Gharib, N. E. Obesity and Clinical Riskiness Relationship: Therapeutic Management by Dietary Antioxidant Supplementation-A Review. *Appl. Biochem. Biotechnol.* **2015**, *176*, 647-69.

10. Yun, J. W. Possible Anti-obesity Therapeutics from Nature-A Review. *Phytochemistry* **2010**, *71*, 1625-41.
11. Ray, K.K.; Cannon, C.P. The Potential Relevance of the Multiple Lipid-independent (Pleiotropic) Effects of Statins in the Management of Acute Coronary Syndromes. *J. Am. Coll. Cardiol.* **2005**, *46*, 1425–1433.
12. Endo, A. A Gift from Nature: the Birth of the Statins. *Nat. Med.* **2008**, *14*, 1050-1052.
13. Alberts, W.; Chen, J.; Kuron, G.; Hunt, V.; Huff, J.; Hoffman, C.; Rothrock, J.; Lopez, M.; Joshua, H.; Harris, E.; Patchett, A.; Monaghan, R.; Currie, S.; Stapley, E.; Albers-Schonberg, G.; Hensens, O.; Hirshfield, J.; Hoogsteen, K.; Liescht, J.; Springer, J. Mevinolin: A Highly Potent Competitive Inhibitor of Hydroxymethylglutaryl-Coenzyme a Reductase and a Cholesterol-Lowering Agent. *Proc. Natl. Acad. Sci. USA*, **1980**, *77*, 3957-3961.
14. Endo, A. A Historical Perspective on the Discovery of Statins. *Proc. Jpn. Acad. Ser. B*, **2010**, *86*, 484-493.
15. Sirtori, C. R. The Pharmacology of Statins. *Pharmacol. Res.* **2014**, *88*, 3-11.
16. Srinivasan, M. R.; Chandrasekhara, N. Effect of Mango Ginger (*Curcuma amada* Roxb.) on Lipid Status in Normal and Hypertriglyceridemic Rats. *J. Food Sci. Technol.* **1992**, *29*, 130-132.
17. Srinivasan, M. R.; Chandrasekhara, N. Effect of Mango Ginger [*Curcuma amada* Roxb.] on Triton WR-1339 Induced-Hyperlipidemia and Plasma Lipases Activity in the Rat. *Nutr. Res.* **1993**, *13*, 1183-1190.
18. Srinivasan, M. R.; Chandrasekhara, N.; Srinivasan, K. Cholesterol Lowering Activity of Mango Ginger (*Curcuma amada* Roxb.) in Induced Hypercholesterolemic Rats. *Eur. Food Res. Technol.* **2008**, *227*, 1159-1163.
19. Estevez, V.; Villacampa, M.; Menendez, J. C. Recent Advances in the Synthesis of Pyrroles by Multicomponent Reactions. *Chem. Soc. Rev.* **2012**, 1-26. doi: 10.1039/x0xx00000x
20. Karrouchi, K.; Radi, S.; Ramli, Y.; Taoufik, J.; Mabkhot, Y. N. ; Al-aizari, F. A.; Ansar, M. Synthesis and Pharmacological Activities of Pyrazole Derivatives: A Review. *Molecules* **2018**, *23*, 1-86.

21. Alonso, M.; Serrano, A.; Vida, M.; Crespillo, A.; Hernandez-Folgado, L.; Jagerovic, N.; Goya, P.; Reyes-Cabello, C.; Perez-Valero, V.; Decara, J.; Macias-Gonzalez, M.; Bermúdez-Silva, F. J.; Suarez, J.; Fonseca, F. R.; Pavon, F. J. Anti-obesity Efficacy of LH-21, A Cannabinoid CB1 Receptor Antagonist with Poor Brain Penetration, in Diet-Induced Obese Rats. *Br. J. Pharmacol.* **2012**, *165*, 2274-2291.
22. Srivastava, B. K.; Joharapurkar, A.; Raval, S.; Patel, J. Z.; Soni, R.; Raval, P.; Gite, A.; Goswami, A.; Sadhwani, N.; Gandhi, N.; Patel, H.; Mishra, B.; Solanki, M.; Pandey, B.; Jain, M. R.; Patel, P. R. Diaryl Dihydropyrazole-3-carboxamides with Significant *In Vivo* Antiobesity Activity Related to CB1 Receptor Antagonism: Synthesis, Biological Evaluation, and Molecular Modeling in the Homology Model. *J. Med. Chem.* **2007**, *50*, 5951-5966.
23. Lee, S. H.; Seo, H. J.; Lee, S.; Jung, M. E.; Park, J.; Park, H.; Yoo, J.; Yun, H.; Na, J.; Kang, S. Y.; Song, K.; Kim, M.; Chang, C.; Kim, J.; Lee, J. Biarylpyrazolyl Oxadiazole as Potent, Selective, Orally Bioavailable Cannabinoid-1 Receptor Antagonists for the Treatment of Obesity. *J. Med. Chem.* **2008**, *51*, 7216-7233.
24. Jahromi, M. A.; Ray, A. B. Antihyperlipidemic Effect of Flavonoids from *Pterocarpus marsupium*. *J. Nat. Prod.* **1993**, *56*, 989-994.
25. Zhang, X.; Wu, C.; Wu, H.; Sheng, L.; Su, Y.; Zhang, X.; Luan, H.; Sun, G.; Sun, X.; Tian, Y.; Ji, Y.; Guo, P.; Xu, X. Antihyperlipidemic Effects and Potential Mechanisms of Action of the Caffeoylquinic Acid-Rich *Pandanus tectorius* Fruit Extract in Hamsters Fed a High Fat-Diet. *Plos One* **2013**, *8*, 1-12.
26. Rayalama, S.; Della-Feraa, M. A.; Baile, C. A. Phytochemicals and Regulation of the Adipocyte Life Cycle. *J. Nutr. Biochem.* **2008**, *19*, 717-726.
27. Nakayama, T.; Suzuki, S.; Kudo, H.; Sassa, S.; Nomura, M.; Sakamoto, S. Effects of Three Chinese Herbal Medicines on Plasma and Liver lipids in Mice Fed a High-Fat Diet. *J. Ethnopharmacol.* **2007**, *109*, 236-240.
28. Moro, C. O.; Basile, U. G. Obesity and Medicinal Plants. *Fitoterapia* **2000**, *71*, 73-82.
29. Mohammed Saghir, S. A.; Revadigar, V.; Murugaiyah, V. Natural Lipid-Lowering Agents and their Effects: An Update. *Eur. Food Res. Technol.* **2014**, *238*, 705-725.

30. Jalaja, R.; Leela, S. G.; Valmiki, P. K.; Salfeena, C. T. F.; Ashitha, K. T.; Nair, M. S.; Gopalan, R. K.; Krishna Rao, V. D.; Somappa, S. B. Discovery of Natural Product Derived Labdane Appended Triazoles as Potent Pancreatic Lipase Inhibitors. *ACS Med. Chem. Lett.* **2018**, *9*, 662-666.
31. Shilpa, G.; Renjitha, J.; Saranga, R.; Francis, S. K.; Nair, M. S.; Joy, B.; Somappa, S. B.; Priya, S.; Epoxyazadiradione Purified from the *Azadirachta indica* Seed Induced Mitochondrial Apoptosis and Inhibition of NF- κ B Nuclear Translocation in Human Cervical Cancer Cells. *Phytother. Res.* **2017**, *31*, 1892-1902.
32. Valmiki, P. K.; Salfeena, C. T. F.; Ashitha, K. T.; Varughese, S.; Somappa, S. B. Antibacterial and Anti-tubercular Evaluation of Dihydronaphthalenone-Indole Hybrid Analogues. *Chem. Biol. Drug Des.* **2017**, *90*, 703-708.
33. Salfeena, C. T. F.; Ashitha, K. T.; Somappa, S. B. $\text{BF}_3 \cdot \text{Et}_2\text{O}$ Mediated One-Step Synthesis of N-Substituted-1,2-dihydropyridines, Indenopyridines and 5,6-Dihydroisoquinolines. *Org. Biomol. Chem.* **2016**, *14*, 10165-10169.
34. Somappa, S. B.; Biradar, J. S.; Rajesab, P.; Rahber, S.; Sundar, M. One-Pot Synthesis of Indole Appended Heterocycles as Potent Anti-inflammatory, Analgesic, and CNS Depressant Agents. *Monatsh. Chem.* **2015**, *146*, 2067-2078.
35. Ashitha, K. T.; Valmiki, P. K.; Salfeena, C. T. F.; Somappa, S. B. $\text{BF}_3 \cdot \text{OEt}_2$ -Mediated Tandem Annulation: A Strategy To Construct Functionalized Chromeno- and Pyrano- Fused Pyridines. *J. Org. Chem.* **2018**, *83*, 113-124.
36. Ashitha, K. T.; Vinaya, P. P.; Krishna, A.; Vincent, D. C.; Jalaja, R.; Varughese, S.; Somappa, S. B. I_2/TBHP Mediated Diastereoselective Synthesis of Spiroaziridines. *Org. Biomol. Chem.* **2020**, *18*, 1588-1593.
37. Reddy, P. P.; Tiwari, A. K.; Rao, R. R.; Madhusudhana, K.; Rao, V. R. S.; Ali, A. Z.; Babu, K. S.; Rao, J. M. New Labdane Diterpenes as Intestinal α -Glucosidase Inhibitor from Antihyperglycemic Extract of *Hedychium spicatum* (Ham. Ex Smith) rhizomes. *Bioorg. Med. Chem. Lett.* **2009**, *19*, 2562-2565.
38. Lohray, B. B.; Lohray, V. Novel Pyrrole-Containing Hypoglycemic and Hypotriglyceridemic Compounds. *Pure Appl. Chem.* **2005**, *77*, 179-184.

39. Bellina, F.; Rossi, R. Synthesis and Biological Activity of Pyrrole, Pyrroline and Pyrrolidine Derivatives with Two Aryl Groups on Adjacent Positions. *Tetrahedron* **2006**, *62*, 7213-7256.
40. Alvarado, M.; Goya, P.; Macias-Gonzalez, M.; Pavon, F. J.; Serrano, A.; Jagerovic, N.; Elguero, J.; Gutierrez-Rodriguez, A.; Garcia-Granda, S.; Suardiaz, M.; Fonseca, F. R. Antiobesity Designed Multiple Ligands: Synthesis of Pyrazole Fatty Acid Amides and Evaluation as Hypophagic Agents. *Bioorg. Med. Chem.* **2008**, *16*, 10098-10105.
41. E. Leng, Y. Xiao, Z. Mo, Y. Li, Y. Zhang, X. Deng, M. Zhou, C. Zhou, Z. He, J. He, L. Xiao, J. Li, W. Li, Synergistic Effect of Phytochemicals on Cholesterol Metabolism and Lipid Accumulation in HepG2 Cells. *BMC Complement. Altern. Med.* **2018**, *18*, 1-10.
42. Budaiman, I.; Tjokropranoto, R.; Widowati, W.; Fauziah, N.; Erawijantari, P. P. Potency of Turmeric (*Curcuma longa L.*) Extract and Curcumin as Anti-obesity by Inhibiting the Cholesterol and Triglyceride Synthesis in HepG2 Cells. *Int. J. Res. Med. Sci.* **2015**, *3*, 1165-1171.
43. Kornienko, A.; La Clair, J. L. Covalent Modification of Biological Targets with Natural Products through Paal–Knorr Pyrrole Formation. *Nat. Prod. Rep.* **2017**, *34*, 1051-1060.
44. Nair, V.; Biju, A. T.; Mathew, S. C.; Babu, B. P.; Carbon-Nitrogen Bond-Forming Reactions of Dialkyl Azodicarboxylate: A Promising Synthetic Strategy. *Chem. Asian J.* **2008**, *3*, 810-820.

ABSTRACT

Name of the Student: **Mrs. Renjitha J.**

Faculty of Study: Chemical Sciences

AcSIR academic centre/CSIR Lab: CSIR-National

Institute for Interdisciplinary

Science and Technology (CSIR-NIIST)

Name of the Supervisors: Dr. Sasidhar B. S. and Dr. Mangalam S. Nair

Title of the thesis: **Design and Synthetic Studies on Plant Based Bioactives Against Metabolic Disorders**

Registration No.: 10CC16J39001

Year of Submission: 2022

Natural products are a rich source of human therapeutics. Different areas of natural product research have led to the development of the most commonly used drugs, worldwide. Plants produce secondary metabolites with different chemical diversity. Secondary metabolites are responsible for the particular therapeutic action. The **first chapter** deals with the importance of natural products in drug discovery and highlights FDA-approved natural product derived drugs and drug candidates for metabolic diseases. These contents also briefly outline the drug discovery process.

The **second chapter** deals with the isolation of various phytochemicals from three selected plants of the *Zingiberaceae* family viz. *Curcuma amada*, *Curcuma malabarica* and *Curcuma aromatica*. GC-MS analysis of essential oil of *C. amada* also has been carried out in this chapter. All the isolated phytochemicals were well characterized using ^1H NMR, ^{13}C NMR, 2D NMR and HRMS techniques. The isolated compounds are evaluated for their efficacy against pancreatic lipase and subjected for their toxicity studies.

The **third chapter** discusses the design strategy adopted for the semi-synthetic transformation of one of the isolated compound, viz., (*E*)-labda-8(17),12-diene-15,16-dial into novel labdane appended triazole derivatives to enhance its biological potential. After designing molecules, we have performed molecular docking studies to identify the potential ligands which can inhibit Human pancreatic lipase. Next, the designed molecules are synthesized through click chemistry and the pancreatic lipase inhibition potential is evaluated. From the enzyme inhibition study, we have identified two lead molecules.

In the **fourth chapter**, we have successfully synthesized natural product derived labdane-pyrroles and pyrazoles with anti-hyperlipidemic efficacy. The rationale for designing natural products appended pyrrole and pyrazole is based on their biological potential. Through a one-pot reaction, we have synthesized all the designed molecules. The synthesized analogues are evaluated against triglyceride synthesis, cholesterol synthesis and HMG CoA reductase inhibition properties. One of the synthesized compounds showed promising potential than standard drugs fenofibrate, atorvastatin and pravastatin.

LIST OF PUBLICATIONS

Related to thesis

- 1) **Renjitha Jalaja**, Shyni G. Leela, Praveen K. Valmiki, Mangalam S. Nair, Raghu K. Gopal, Sasidhar B. Somappa, Discovery of Natural Product Derived Labdane Appended Triazoles as Novel Pancreatic Lipase Inhibitors, *ACS Med. Chem. Lett.*, **2018**, 9, 662-666.
- 2) **Renjitha Jalaja**, Shyni G. Leela, Sangeetha Mohan, Mangalam S. Nair, Raghu K. Gopal, Sasidhar B. Somappa, Anti-hyperlipidemic potential of natural product based labdane-pyrroles via inhibition of cholesterol and triglycerides synthesis in HepG2 cells, *Bioorg. Chem.*, **2021**, 108, 1-10.
- 3) **Renjitha Jalaja**, Shyni G. Leela, Raghu K. Gopal, Sasidhar B. Somappa, Inhibitory effects of coronarin D from *Zingiberaceae* family on pancreatic lipase and Mouse 3T3 cells adipogenesis. [Manuscript under preparation]

Not related to thesis

- 4) G. Shilpa,[†] **J. Renjitha**,[†] R. Saranga, Francis K. Sajin, Mangalam S. Nair, Beena Joy, B.S. Sasidhar and S. Priya, Epoxyazadiradione purified from the *Azadirachta indica* seed induced mitochondrial apoptosis and inhibition of NFκB nuclear translocation in human cervical cancer cells, *Phytother. Res.*, **2017**, 31, 1892-1902.

[†]Equally contributed

- 5) Sreerenjini Lakshmi, **Jalaja Renjitha**, Somappa B. Sasidhar, Sulochana Priya, Epoxyazadiradione induced apoptosis/anoikis in triple-negative breast cancer cells, MDA-MB-231, by modulating diverse cellular effects, *J. Biochem. Mol. Toxicol.* **2021**, 1-17. doi: 10.1002/jbt.22756.
- 6) G. L. Shyni, **J. Renjitha**, Sasidhar B. Somappa, K. G. Raghu, Zerumin A attenuates the inflammatory responses in LPS-stimulated H9c2 cardiomyoblasts, *J. Biochem. Mol. Toxicol.*, **2021**, 35, 1-11.
- 7) Fardous F. El-Senduny, Miram Altouhamy, Gamal Zayed, Choudhary Harsha, **Renjitha Jalaja**, Sasidhar Balappa Somappa, Mangalam S. Nair, Ajaikumar B. Kunnumakkara, Fahd A. Badria., Azadiradione-loaded liposomes with improved bioavailability and

anticancer efficacy against triple negative breast cancer, *J. Drug Deliv. Sci. Technol.* **2021**, *65*, 1-7.

- 8) Praveen Kumar V, **Renjitha J**, Fathimath Salfeena C T, Ashitha K T, Rangappa S. Keri, Sunil Varughese, Sasidhar B S., Antibacterial and antitubercular evaluation of dihydronaphthalenone-indole hybrid analogs, *Chem. Biol. Drug Des.*, **2017**, *90*, 703-708.
- 9) Chettiyan Thodi F. Salfeena, **Renjitha Jalaja**, Rincy Davis, Eringathodi Suresh, and Sasidhar B. Somappa, Synthesis of 1,2,4-Trisubstituted-(1H)-imidazoles through Cu(OTf)₂-/ I₂-Catalyzed C–C Bond cleavage of chalcones and benzylamines, *ACS Omega*, **2018**, *3*, 8074-8082.
- 10) Kizhakkan Thiruthi Ashitha, Puthiya Purayil Vinaya, Ajay Krishna, Deepthy Cheeran Vincent, **Renjitha Jalaja**, Sunil Varughese, Sasidhar Balappa Somappa, I₂/TBHP Mediated diastereoselective synthesis of spiroaziridines, *Org. Biomol. Chem.*, **2020**, *18*, 1588-1593.

CONTRIBUTION TO ACADEMIC CONFERENCES

- 1) Design and Synthesis of Natural Product Based Labdane-pyrroles and their Anti-hyperlipidemic Potential via Inhibition of Cholesterol and Triglycerides Synthesis. **Renjitha Jalaja**, Shyni G. Leela, Sangeetha Mohan, Mangalam S. Nair, Raghu K. Gopalan and Sasidhar B. Somappa, *International Webinar on Phytochemistry-Impacts and Applications* organized by kerala academy of sciences at Thiruvananthapuram, Kerala. 27-28 September, 2021. [**Best paper presentation award**]
- 2) Natural product derived triazole hybrids as potent pancreatic lipase inhibitors. **Renjitha J.**, Shyni G. L., Raghu K. G. and Sasidhar B. S., *Current Trends in Drug Discovery Research (CTDDR-2019)* at CSIR-CDRI, Lucknow, Uttar Pradesh, India. 20-23 February, 2019. [**Poster presentation**]
- 3) Antibacterial evaluation of (*E*)-labda-8,(17),12-diene-15,16-dial isolated from the edible ginger *Curcuma amada* and its semi-synthetic derivatives. **Renjitha J.**, Dileep Kumar B. S. and Sasidhar B. S., *International seminar on Phytochemistry (ISP-2018)* organized

by Kerala academy of Sciences & Jawaharlal Nehru Tropical Botanic Garden and Research Institute, palode, India. 26-27 March, 2018. [**Poster presentation**]

- 4) Isolation and synthetic modifications of bioactive from nutraceutically important *Curcuma amada*. **Renjitha J.** and Sasidhar B. S., *2nd International Conference on “Nutraceuticals and Chronic Diseases”*, Goa, India. 01-03 September, 2017. [**Poster presentation**]
- 5) Discovery of potent pancreatic lipase inhibitors via natural product derived labdane appended triazole, **Renjitha J.**, Shyni G. L., Raghu K. G. and Sasidhar B. S., *32nd Kerala Science Congress*, Yuvakshetra Institute of Management Studies, Mundoor, Palakkad, kerala, India. 25-27 January 2020. [**Poster presentation**]

Discovery of Natural Product Derived Labdane Appended Triazoles as Potent Pancreatic Lipase Inhibitors

Renjitha Jalaja,^{†,||} Shyni G. Leela,[‡] Praveen K. Valmiki,^{†,||} Chettiyan Thodi F. Salfeena,^{†,||} Kizhakkann T. Ashitha,^{†,||} Venkata Rao D. Krishna Rao,[§] Mangalam S. Nair,[†] Raghu K. Gopalan,^{*,†,||} and Sasidhar B. Somappa^{*,†,||}

[†]Chemical Sciences and Technology Division, CSIR - National Institute for Interdisciplinary Science and Technology (CSIR-NIIST), Thiruvananthapuram - 695 019, Kerala, India

[‡]Agro-Processing and Technology Division, CSIR-NIIST, Thiruvananthapuram - 695 019, Kerala, India

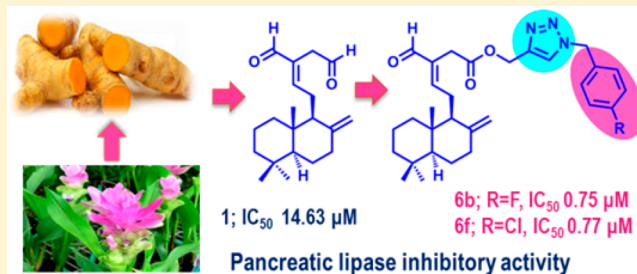
[§]CSIR - Central Institute of Medicinal and Aromatic Plants, Research Centre, Bangalore - 560065, Karnataka, India

^{||}Academy of Scientific and Innovative Research (AcSIR), CSIR-NIIST, Thiruvananthapuram - 695 019, Kerala, India

Supporting Information

ABSTRACT: Obesity contributes to the genesis of many metabolic disorders including dyslipidemia, coronary heart disease (CHD), nonalcoholic fatty liver, type 2 diabetes, etc. Pancreatic lipase plays a vital role in food fat digestion and absorption. Therefore, to control obesity, inhibition of pancreatic lipase is the active therapy. Thus, novel natural product derived labdane appended triazoles with pancreatic lipase inhibition potential were designed and synthesized. Among these hybrids, **6b** and **6f** exhibited excellent inhibitory activity (IC_{50} $0.75 \pm 0.02 \mu\text{M}$ and $0.77 \pm 0.01 \mu\text{M}$), slightly better than that of the positive control Orlistat (IC_{50} $0.8 \pm 0.03 \mu\text{M}$). Compounds **6c**, **6e**, and **6g–j** inhibited the PL comparable to that of positive control. Interestingly none of the compounds showed cytotoxicity (Hep G2) in the concentration range from 0.5 to 100 μM . Overall results reveal the potential of labdane appended triazoles as antiobesity agents.

KEYWORDS: Zingiberaceae, *curcuma amada*, triazoles, pancreatic lipase inhibition, obesity related disorders



Obesity is a medical condition with excess body fat accumulation to the extent which leads to serious health consequences. Obesity contributes to the genesis of many metabolic disorders, including dyslipidemia,¹ coronary heart disease (CHD),² nonalcoholic fatty liver,³ type 2 diabetes,⁴ etc. In 2017 WHO reported that global obesity has almost tripled since 1975.⁵ As per literature, more than 340 million children and adolescents between 5 and 19 aged are overweight or obese.⁵ As a result, physicians are prompted to take aggressive treatments in lifestyle changes, pharmacological interventions, and surgical therapies before a severe consequence becomes clinically apparent. Among these various treatments, pharmacotherapy is the most commonly used one.^{6,7}

Pancreatic lipase plays a vital role in food fat digestion and absorption.⁸ Therefore, to control obesity, inhibition of pancreatic lipase enzyme is the active therapy. Among the existing medicines, Orlistat is one such precise drug used for the inhibition of pancreatic lipase. In recent times, natural/herbal products have also been considered as an alternative medicine for the treatment of obesity and related disorders.^{9,10} Many plant-based extracts have been reported for the treatment of obesity and associated diseases. For instance, ethanolic extracts of *Terminalia paniculata* showed very good

antilipase and antiobesity activities.¹¹ Likewise, some terpenoid saponins from the leaves of *Acantho panaxsenticosus*,¹² the phenolic acids from fermented oats,¹³ apple polyphenols,¹⁴ and flavan-3-ol digalate esters of oolong tea are found to have substantial pancreatic lipase inhibitory properties.¹⁵

Based on the traditional applications and its large medicinal properties in a long history of Ayurvedic medicine, we have selected *Curcuma amada* Roxb. for the exploration of its inhibition properties against the pancreatic lipase. *C. amada*, an edible ginger is one of the rhizomatous species in the Zingiberaceae family. The rhizomes of *C. amada* are a rich source of essential oils, and more than 130 phytochemicals are isolated,¹⁶ which possess various biological properties, viz. antimicrobial, antioxidant, anti-inflammatory, anticancer, cardiovascular, and gastrointestinal disorders, etc.^{16–19}

Therefore, in continuation of our focused ongoing research interest in natural products and natural product based lead molecule^{20–22} identification for therapeutic applications, in the present work, we have isolated the major compound (E)-

Received: March 6, 2018

Accepted: June 18, 2018

Published: June 18, 2018



Labda-8(17),12-diene-15,16-dial. This was synthetically transformed to rationally designed triazole appended analogues and evaluated for their pancreatic lipase inhibitory potential. The rationale for the targeted synthesis of triazole appended analogues is based upon its broad spectrum of biological properties.^{23,24} Triazole and pyrazole based synthetic drugs are also well-known for the treatment of obesity and related disorders (Figure 1).^{25–27} To begin with, the fresh rhizomes of

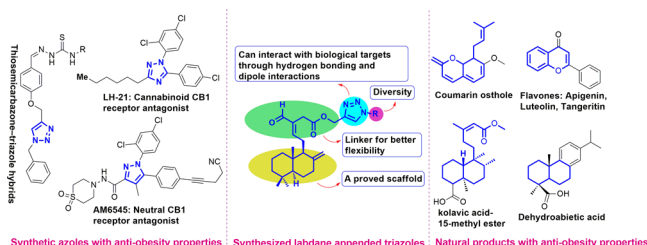
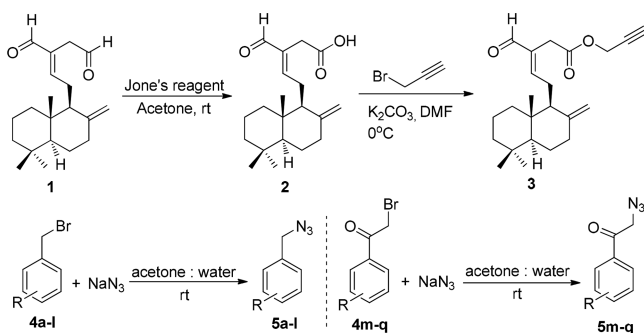


Figure 1. Rationale for the synthesis of labdane appended triazoles.

C. amada were collected from CTCRI, Thiruvananthapuram, India, in February 2017. By following a standard protocol (Supporting Information) compound **1** (*E*)-labda 8(17), 12-diene-15,16-dial was isolated from the chloroform extract as a colorless solid and confirmed by using various spectroscopic data: IR, ¹H NMR, ¹³C NMR, HRMS, etc.^{19,28} A series of variously substituted triazole appended labdane derivatives were prepared by a three-step protocol starting from compound **1**. When subjected to Jones's oxidation, one of the aldehydes of compound **1** is selectively oxidized into the acid derivative, Zerumin A (**2**). The alkyne intermediate (**3**) of Zerumin A is prepared in excellent yields by treating **2** with propargyl bromide (Scheme 1). The propargylated labdane

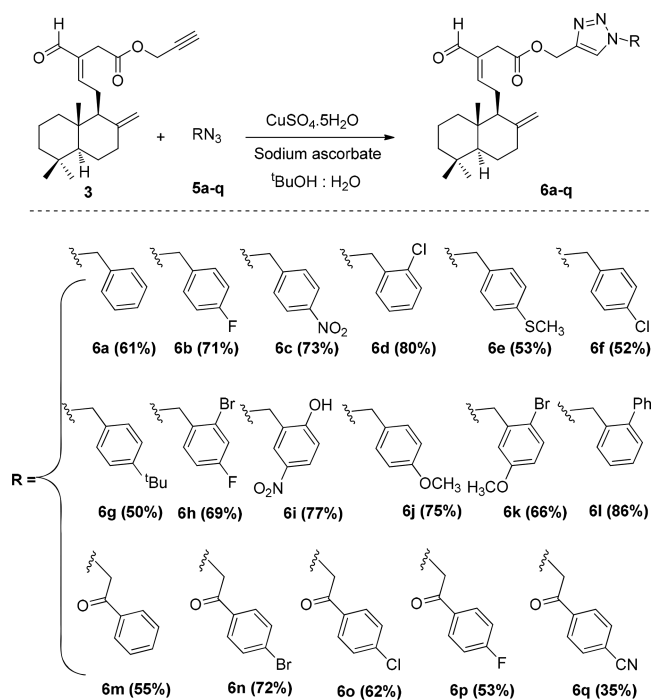
Scheme 1. Synthesis of Propargylated Labdane (**3**) and Substituted Benzyl and Phenacylazides (**5a–q**)



undergoes the click reaction with various substituted benzyl and phenacyl azides (**5**) at room temperature to provide 1,2,3-triazole appended labdane derivatives (**6a–q**) in good to excellent yields (Scheme 2). All the synthesized derivatives are fully characterized by IR, NMR, and HRMS spectral data (Supporting Information).

The isolated *E*-labda-8(17),12-diene-15,16-dial (**1**), semi-synthetic intermediates, and targeted triazole appendages were evaluated for the inhibitory activity against pancreatic lipase (PL) (Method A)²⁹ (Supporting Information). The parent molecule labdane dial exhibited moderate activity. Among those tested, the majority of the triazole hybrids showed strong PL inhibitory activity in the concentration ranging from 0.75 to 14.63 μ M. Initially, the percentage of enzyme inhibition of

Scheme 2. Synthesis of Labdane Appended Triazoles by Click Chemistry (**6a–q**)



compounds at various concentrations (1, 5, 10, and 20 μ M) was evaluated. At lower concentration of 1 μ M, compounds **6b** and **6f** showed inhibition of 75 to 80%. At 20 μ M concentration the derivatives **6b**, **6c**, **6e**, **6f**, **6g**, **6h**, and **6j** exhibited maximum inhibition percentage of 80 to 85 (Figure 2). The other compounds (**6a**, **6k**, **6l**, **6m**, and **6q**) also

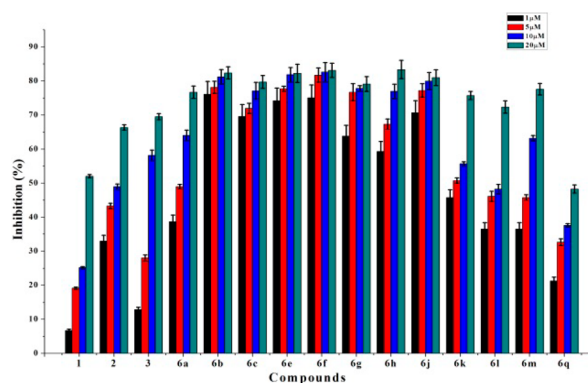


Figure 2. Percentage inhibition of isolates and synthetic derivatives against pancreatic lipase in various concentrations.

showed better tendency to inhibit the PL. In contrast, few derivatives (**6d**, **6i**, **6n**, **6o**, and **6p**) failed to show any significant effect on pancreatic lipase. Overall, the labdane-triazole hybrids inhibited the PL through a concentration dependent manner.

Isolates and synthetic derivatives are tested at concentrations 1–20 μ M. Each experiment was independently performed four times in duplicate and expressed as mean \pm SD ($n = 4$).

In an attempt to validate the potential of the compounds, the PL inhibitory activity was repeated using human pancreatic lipase (Method B)³⁰ (Supporting Information). As expected, the compounds followed the similar trend in exhibiting the

inhibitory potential with IC_{50} values in the range of 1.10–14.48 μM concentration. The derivatives **6b**, **6c**, **6g**, and **6h** presented maximum PL inhibition percentage of 80 to 85 at 15 μM concentration (Figure 3). Similarly, triazole analogues **6d**,

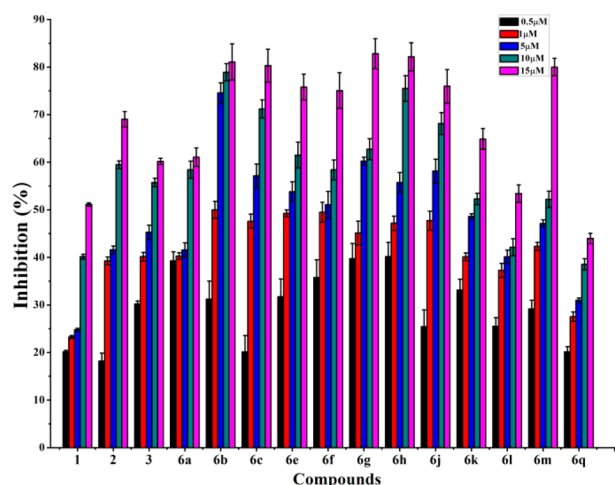


Figure 3. Percentage of isolates and synthetic derivatives against human pancreatic lipase in various concentrations.

6i, **6n**, **6o**, and **6p** have failed to inhibit the human pancreatic lipase. The IC_{50} values of active compounds with maximum inhibitory potential are calculated and summarized in Table 1.

Table 1. 50% Inhibitory Concentration (IC_{50}) Evaluation of Labdane Appended Triazoles

Compound	IC_{50} (μM) ^a	
	Method A	Method B
1	14.63 ± 0.11	14.48 ± 0.51
2	10.30 ± 2.71	11.75 ± 0.64
3	8.64 ± 3.13	7.38 ± 0.77
6a	5.35 ± 1.20	9.15 ± 0.27
6b	0.75 ± 0.02	1.1 ± 0.53
6c	0.85 ± 0.03	2.01 ± 0.73
6e	0.80 ± 0.05	1.65 ± 0.93
6f	0.77 ± 0.01	1.25 ± 0.78
6g	0.91 ± 0.02	2.28 ± 0.88
6h	0.95 ± 0.02	2.31 ± 0.62
6j	0.84 ± 0.07	1.87 ± 0.14
6k	4.43 ± 1.02	6.90 ± 0.73
6l	10.36 ± 2.20	13.48 ± 0.53
6m	6.22 ± 2.04	7.82 ± 0.48
Orlistat	0.80 ± 0.03	0.19 ± 0.62

^aThe IC_{50} values of PL inhibitory activity for selected compounds and the positive control Orlistat. Values are mean ± SD of four independent experiments performed in duplicates.

The IC_{50} results revealed (Method A) that the labdane triazole appendages **6b** and **6f** exhibited an excellent inhibitory activity with $0.75 \pm 0.02 \mu\text{M}$ and $0.77 \pm 0.01 \mu\text{M}$, respectively, which is slightly better than that of positive control Orlistat (IC_{50} $0.8 \pm 0.03 \mu\text{M}$). Compounds **6c**, **6e**, and **6g–j** inhibited the pancreatic lipase comparable to that of positive control in the range IC_{50} 0.8 to 0.9 μM , whereas, the parent molecule **1**, semisynthetic intermediates **2** and **3**, and labdane triazole derivatives **6a**, **6k**, **6l**, and **6m** showed moderate potency in the range of IC_{50} 5.35–14.63 μM . However, against the human

pancreatic lipase (Method B), labdane triazole appendages **6b** and **6f** being the more potent analogues exhibited the inhibitory activities with IC_{50} values $1.1 \pm 0.53 \mu\text{M}$ and $1.25 \pm 0.78 \mu\text{M}$, respectively. Compounds **6c**, **6e**, and **6g–j** also showed promising ability in inhibiting the PL with IC_{50} values in the range of 1.65 to 2.31 μM . The parent molecule and other derivatives showed moderate activity. The preliminary studies also revealed that the compounds are bound to the active site of PL and probably exhibited a covalent interaction with PL. Nevertheless, extended kinetics and crystallographic studies are to be conducted for further authentication of a mode of interaction. We believe this is the first report on the pancreatic lipase inhibitory activity of labdane dial and its semisynthetic triazole appendages.

Isolates and synthetic derivatives are tested at concentrations 0.5–15 μM . Each experiment was independently performed four times in duplicate and expressed as means ± SD ($n = 4$).

From a structure–activity relationship point of view, we observed that the labdane-triazole hybrids incorporating benzyl azides (**6a–l**) were more active than the phenacyl azides (**6m–q**). Most of the analogues synthesized from benzyl azides exhibited excellent inhibition properties, slightly better than or equal to that of Orlistat. In contrast, the triazole analogues synthesized from phenacyl azides (**6m–q**) did not show any significant inhibition potential except for compound **6m**. Precisely, among the triazoles incorporated from the variously substituted benzyl azides, all the para-substituted analogues showed the lowest IC_{50} . However, the unsubstituted (**6a**), ortho- and meta-substituted benzyl azide incorporated triazole appendages showed moderate activity. Interestingly, there was no clear trend followed by the nature of the para substitution, i.e., among the halogen, electron donating, and electron withdrawing groups. Overall, among the various substituted hybrids **6b** and **6f** with *p*-F and *p*-Cl substituted benzyl azide incorporated triazole appendages were found to be the most potent candidates of the series.

Molecular docking studies have also been performed³¹ in the present study to understand the basic knowledge on how these compounds have blocked human pancreatic lipase activity. There were 20 compounds docked on human pancreatic lipase to understand their possible binding site with respect to the binding energies of structure conformations of compounds (Figure 4; Figure S, Supporting Information). The top ranked stable structure conformations on protein have shown the least Gibb's free binding energies. The docking results have shown that all the triazole derivatives are able to interact with lipase at the possible predicted site with different binding energies (Table S; Supporting Information). However, further experimental studies (i.e., site directed mutagenesis) are much

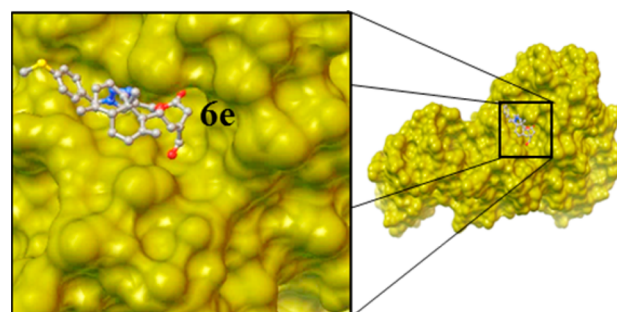


Figure 4. Representative molecular docking studies of compound **6e**.

needed to understand the precise mechanism of action of these compounds. This data provided us a vital clue about the interaction sites, which helps in our future in-depth studies toward lipase inhibition.

Further, *in vitro* toxicity of isolated and semisynthetic derivatives is carried out to analyze the effect of compounds on human liver cell lines. This method is primarily used to identify potentially hazardous compounds and their toxic effect in the early stage of development of therapeutic drugs. The cytotoxicity of compounds on Hep G2 human liver carcinoma-derived cell lines was measured by MTT assay.³² The cytotoxic effect of each compound was estimated by calculating the percentage of cell viability in a dose-dependent manner ranging from 0.5 μM to 100 μM (Figure 5). Based on

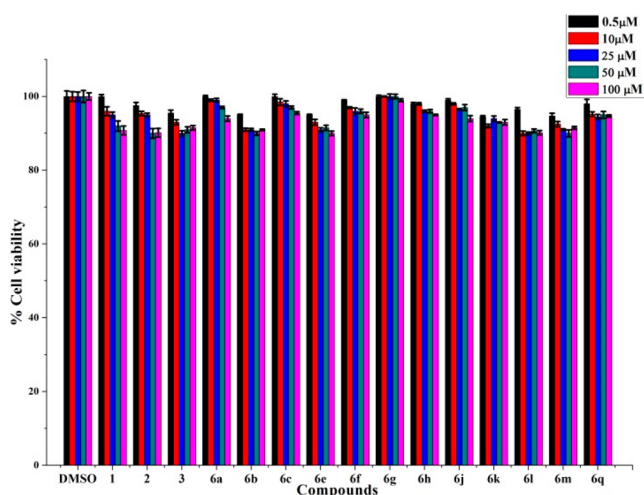


Figure 5. Cytotoxic study of isolates and selected semisynthetic derivatives by MTT assay.

the percentage of cell viability, compounds **6a**, **6c**, **6f**, **6g**, **6h**, **6j**, **6k**, and **6q** were found to be the least toxic on Hep G2 human liver cell lines, and none of the compounds showed any signs of toxicity at all the tested concentrations.

The cytotoxic effect of each compound is expressed as percentage of cell viability in a dose dependent manner. Values are mean \pm SD of four independent experiments performed in duplicates.

In summary, a new series of natural product derived labdane-triazole hybrids were designed, synthesized, and evaluated for pancreatic lipase inhibitory potential. Among the semisynthetic derivatives, **6b** and **6f** are the most active candidates of the series with excellent PL inhibitory activity slightly higher than that of the positive control Orlistat. Hybrids **6c**, **6e**, and **6g–j** inhibited the PL comparable to that of positive control. The structure–activity relationship studies suggested that the *p*-substitution on benzyl azides seems to be vital for improved PL inhibition. Cytotoxicity of the compounds on Hep G2 human liver carcinoma-derived cell line was measured by MTT assay. Based on the percentage of cell viability, none of the compounds showed any signs of toxicity at all the tested concentrations. This is the first report on the PL inhibitory activity of labdane dial and its semisynthetic triazole appendages. Our findings will provide useful insights for the design and synthesis of novel PL inhibitors. Presently, a detailed study to elucidate the molecular mechanistic action of an antiobesity effect of the

compounds **6b** and **6f** by using *in vitro* and *in vivo* experimental models and structural optimization is in progress in our laboratory.

■ ASSOCIATED CONTENT

§ Supporting Information

The Supporting Information is available free of charge on the ACS Publications website at DOI: 10.1021/acsmchemlett.8b00109.

Experimental details of synthesis, pancreatic lipase activity assay, MTT assay, molecular docking studies, characterization data, and copies of ^1H and ^{13}C NMR spectra of all the newly synthesized compounds (PDF)

■ AUTHOR INFORMATION

Corresponding Authors

*Raghu K. Gopalan E-mail: raghukgopal@niist.res.in.

*Sasidhar B. Somappa E-mail: drsasidharbs@niist.res.in.

ORCID

Sasidhar B. Somappa: 0000-0003-1546-2083

Notes

The authors declare no competing financial interest.

■ ACKNOWLEDGMENTS

Financial support from the DST-Science & Engineering Research Board (SERB), Government of India, New Delhi, India, (Grant no.EEQ/2016/000089) is gratefully acknowledged. R.J. and P.K.V. thank CSIR and UGC for research fellowships. S.G.L. acknowledges Young Scientist Fellowship from Department of Health Research (DHR-HRD).

■ REFERENCES

- (1) Barnes, A. Overweight versus Obese: Different Risk and Different Management. *Tex Heart Inst. J.* **2015**, *42*, 237–238.
- (2) Donahue, R. P.; Abbott, R. D.; Bloom, E.; Reed, D. M.; Yano, K. Central Obesity and Coronary Heart Disease in Men. *Lancet* **1987**, *329*, 821–824.
- (3) Fabbri, E.; Sullivan, S.; Klein, S. Obesity and nonalcoholic fatty liver disease: biochemical, metabolic, and clinical implications. *Hepatology* **2010**, *51*, 679–89.
- (4) Golay, A.; Ybarra, J. Link between obesity and type 2 diabetes. *Best Pract. Res. Clin. Endocrinol. Metab.* **2005**, *19*, 649–63.
- (5) Obesity facts from: <http://www.who.int/mediacentre/factsheets/fs311/en/index.html>.
- (6) Fu, C.; Jiang, Y.; Guo, J.; Su, Z. Natural Products with Anti-obesity Effects and Different Mechanisms of Action. *J. Agric. Food Chem.* **2016**, *64*, 9571–9585.
- (7) Cosentino, G.; Conrad, A. O.; Uwaifo, G. I. Phentermine and topiramate for the management of obesity: a review. *Drug Des., Dev. Ther.* **2013**, *7*, 267–278.
- (8) Wang, T. Y.; Liu, M.; Portincasa, P.; Wang, D. Q. New insights into the molecular mechanism of intestinal fatty acid absorption. *Eur. J. Clin. Invest.* **2013**, *43*, 1203–23.
- (9) Sun, N. N.; Wu, T. Y.; Chau, C. F. Natural Dietary and Herbal Products in Anti-Obesity Treatment. *Molecules* **2016**, *21*, 1351.
- (10) Fu, C.; Jiang, Y.; Guo, J.; Su, Z. Natural Products with Anti-obesity Effects and Different Mechanisms of Action. *J. Agric. Food Chem.* **2016**, *64*, 9571–9585.
- (11) Mopuri, R.; Meriga, B. Anti-Lipase and Anti-Obesity Activities of *Terminalia paniculata* Bark in High Calorie Diet-Induced Obese Rats. *Global J. Pharmacol.* **2014**, *8*, 114–119.
- (12) Jiang, W.; Li, W.; Han, L.; Liu, L.; Zhang, Q.; Zhang, S.; Nikaido, T.; Koike, K. Biologically Active Triterpenoid Saponins from *Acanthopanax senticosus*. *J. Nat. Prod.* **2006**, *69*, 1577–1581.

- (13) Cai, S.; Wang, O.; Wang, M.; He, J.; Wang, Y.; Zhang, D.; Zhou, F.; Ji, B. In Vitro Inhibitory Effect on Pancreatic Lipase Activity of Sub fractions from Ethanol Extracts of Fermented Oats (*Avena sativa* L.) and Synergistic Effect of Three Phenolic Acids. *J. Agric. Food Chem.* **2012**, *60*, 7245–7251.
- (14) Sugiyama, H.; Akazome, Y.; Shoji, T.; Yamaguchi, A.; Yasue, M.; Kanda, T.; Ohtake, Y. Oligomeric Procyanidins in Apple Polyphenol Are Main Active Components for Inhibition of Pancreatic Lipase and Triglyceride Absorption. *J. Agric. Food Chem.* **2007**, *55*, 4604–4609.
- (15) Nakai, M.; Fukui, Y.; Asami, S.; Toyoda-Ono, Y.; Iwashita, T.; Shibata, H.; Mitsunaga, T.; Hashimoto, F.; Kiso, Y. Inhibitory Effects of Oolong Tea Polyphenols on Pancreatic Lipase in Vitro. *J. Agric. Food Chem.* **2005**, *53*, 4593–4598.
- (16) Jatoi, S. A.; Kikuchi, A.; Gilani, S. A.; Watanabe, K. N. Phytochemical, Pharmacological and Ethnobotanical Studies in Mango Ginger. *Phytother. Res.* **2007**, *21*, 507–516.
- (17) Behera, K. K. Ethnomedicinal Plants used by the Tribals of Similipal Bio-reserve, Orissa, India: A Pilot Study. *Ethnobotanical Leaflets* **2006**, *10*, 149–173.
- (18) Ramachandran, C.; Quirin, K. W.; Escalon, E. A.; Lollett, I. V.; Melnick, S. J. Therapeutic Effect of Supercritical CO₂ Extracts of Curcuma Species with Cancer Drugs in Rhabdomyosarcoma Cell Lines. *Phytother. Res.* **2015**, *29*, 1152–1160.
- (19) Singh, S.; Kumar, J. K.; Saikia, D.; Shanker, K.; Thakur, J. P.; Negi, A. S.; Banerjee, S. A bioactive labdane diterpenoid from *Curcuma amada* and its semi-synthetic analogues as antitubercular agents. *Eur. J. Med. Chem.* **2010**, *45*, 4379–4382.
- (20) Shilpa, G.; Renjitha, J.; Saranga, R.; Sajin, K. F.; Nair, M. S.; Joy, B.; Sasidhar, B. S.; Priya, S. Epoxyzadiradione Purified from the *Azadirachta indica* Seed Induced Mitochondrial Apoptosis and Inhibition of NFκB Nuclear Translocation in Human Cervical Cancer Cells. *Phytother. Res.* **2017**, *31*, 1892–1902.
- (21) Kumar, V. P.; Renjitha, J.; Salfeena, C. T. F.; Ashitha, K. T.; Keri, R. S.; Varughese, S.; Sasidhar, B. S. Antibacterial and antitubercular evaluation of dihydronaphthalenone-indole hybrid analogs. *Chem. Biol. Drug Des.* **2017**, *90*, 703–708.
- (22) Ashitha, K. T.; Kumar, V. P.; Salfeena, C. T. F.; Sasidhar, B. S. BF₃·OEt₂-Mediated Tandem Annulation: A Strategy To Construct Functionalized Chromeno- and Pyrano-Fused Pyridines. *J. Org. Chem.* **2018**, *83*, 113–124.
- (23) Narsimha, S.; Battula, K. S.; Nukala, S. K.; Gondru, R.; Reddy, Y. N.; Nagavelli, V. R. One-pot synthesis of fused benzoxazino[1,2,3]triazolyl[4,5-c]quinolinone derivatives and their anticancer activity. *RSC Adv.* **2016**, *6*, 74332.
- (24) Tantray, M. A.; Khan, I.; Hamid, H.; Alam, M. S.; Umar, S.; Ali, Y.; Sharma, K.; Hussain, F. Synthesis of Novel Oxazolo[4,5-b]pyridine-2-one based 1,2,3-triazoles as Glycogen Synthase Kinase-3b Inhibitors with Anti-inflammatory Potential. *Chem. Biol. Drug Des.* **2016**, *87*, 918–926.
- (25) Kharb, R.; Sharma, P. C.; Yar, M. S. Pharmacological significance of triazole scaffold. *J. Enzyme Inhib. Med. Chem.* **2011**, *26*, 1–21.
- (26) Kinf, H. H.; Belay, Y. H.; Joseph, J. S.; Mukwevho, E. Evaluation of the Influence of thiosemicarbazone–triazole hybrids on genes implicated in lipid oxidation and accumulation as potential anti-obesity agents. *Bioorg. Med. Chem. Lett.* **2013**, *23*, 5275–5278.
- (27) Sharma, M. K.; Machhi, J.; Murumkar, P.; Yadav, M. R. New role of phenothiazine derivatives as peripherally acting CB1 receptor antagonizing anti-obesity agents. *Sci. Rep.* **2018**, *8*, 1650.
- (28) Sheeja, A. D. B.; Nair, M. S. Facile isolation of *E*-labda 8(17), 12-diene-15, 16-dial from curcuma amada and its conversion to other biologically active compounds. *Indian. J. Chem. Sect. B* **2014**, *53*, 319–324.
- (29) Bustanji, Y.; Issa, A.; Mohammad, M.; Hudaib, M.; Tawah, K. Inhibition of hormone sensitive lipase and pancreatic lipase by *Rosmarinus officinalis* extract and selected phenolic constituents. *J. Med. Plants Res.* **2010**, *4*, 2235–2242.
- (30) Kido, Y.; Hiramoto, S.; Murao, M.; Horio, Y.; Miyazaki, T.; Kodama, T.; Nakabou, Y. Epsilon-polylysine inhibits pancreatic lipase activity and suppresses postprandial hypertriglyceridemia in rats. *J. Nutr.* **2003**, *133*, 1887–91.
- (31) Morris, G. M.; Goodsell, D. S.; Halliday, R. S.; Huey, R.; Hart, W. E.; Belew, R. K.; Olson, A. J. Automated Docking Using a Lamarckian Genetic Algorithm and an Empirical Binding Free Energy Function. *J. Comput. Chem.* **1998**, *19*, 1639–1662.
- (32) Wilson, A. P. Cytotoxicity and viability assay. In *Animal cell culture: A practical approach*, 2nd ed.; Masters JRW, Oxford University Press: Oxford, 2000; pp 175–219.



Anti-hyperlipidemic potential of natural product based labdane-pyrroles via inhibition of cholesterol and triglycerides synthesis

Renjitha Jalaja^{a,c}, Shyni G. Leela^b, Sangeetha Mohan^{a,c}, Mangalam S. Nair^a,
Raghu K. Gopalan^b, Sasidhar B. Somappa^{a,c,*}

^a Chemical Sciences and Technology Division, CSIR-National Institute for Interdisciplinary Science and Technology (CSIR-NIIST), Thiruvananthapuram 695 019, Kerala, India

^b Agro-Processing and Technology Division, CSIR-NIIST, Thiruvananthapuram 695 019, Kerala, India

^c Academy of Scientific and Innovative Research (AcSIR), Ghaziabad 201002, India

ARTICLE INFO

Keywords:

Curcuma amada
Pyrrole conjugates
Lipid accumulation
HMG CoA reductase
Cholesterol
HepG2 cells
Anti-hyperlipidemia agents

ABSTRACT

Hyperlipidemia is the clinical condition where blood has an increased level of lipids, such as cholesterol and triglycerides. Therefore controlling hyperlipidemia is considered to be a protective strategy to treat many associated diseases. Thus, a novel natural product derived pyrrole, and pyrazole-(E)-Labda-8(17),12-diene-15,16-dial conjugates with cholesterol and triglycerides synthesis inhibition potential was designed through scaffold hopping approach and synthesized via one-pot selective cycloaddition. Amongst the tested hybrids, **3i** exhibited excellent activity against triglyceride and cholesterol synthesis with the percentage inhibition of 71.73 ± 0.78 and 68.61 ± 1.19 , which is comparable to the positive controls fenofibrate and atorvastatin, respectively. Compounds **3j** and **3k** also exhibited the considerable potential of promising leads. The HMG CoA reductase inhibitory activity of the compounds was consistent with that of inhibitory activity of cholesterol synthesis. Compound **3i** showed the highest inhibitory potential (78.61 ± 2.80) percentage of suppression, which was comparable to that of the positive control pravastatin (78.05 ± 5.4). Favourably, none of the compounds showed cytotoxicity (HepG2) in the concentration ranging from 0.5 to 100 μ M.

1. Introduction

Hyperlipidemia is a metabolic disorder characterized by higher levels of cholesterol, triglycerides (TG) or both in plasma [1], and it is a major known risk factor for atherosclerosis, coronary heart diseases (CHD), myocardial infarction, ischemic stroke, etc. [2]. The World Health Organization has reported that elevated levels of plasma cholesterol concentrations affect approximately 40% of the global population's health [3]. Therefore to control hyperlipidemia is one of the major challenges worldwide. It is well reported that a 10% drop in serum cholesterol level will reduce the risk of CHD by 30% [4,5]. Hyperlipidemia is most commonly associated with high-fat diets, a sedentary lifestyle, obesity and diabetes. The pathophysiology of obesity is closely allied with dyslipidemia, in particular the formation of excessive lipid deposits in non-adipose tissue, such as the liver [6–8]. Thus, controlling hyperlipidemia is considered to be a protective strategy to treat obesity [9,10]. Statins are the most widely used therapeutic agents to reduce hyperlipidemia by inhibiting cholesterol synthesis

(Fig. 1). Lovastatin is the first FDA approved drug for the treatment of high-level cholesterol [11]. Simvastatin, a semisynthetic derivative of lovastatin and many other semisynthetic and synthetic statins are also presently in practice. Amongst the currently available statins, atorvastatin is one of the most prescribed medications to treat abnormal lipid levels (Fig. 1) [11–14]. However; several unwarranted side effects are reported for the existing statins [15]. In light of these reports, the medicinal chemists are actively engaged in the development of new and safer therapeutic agents from natural-product based approaches.

In the past, few plant species are well documented for their anti-hyperlipidemic potential, this includes plant extracts, phytochemicals and semisynthetic derivatives of phytochemicals [16–20]. The families such as, Amaranthus, Lamiaceae, Asteraceae, Malvaceae, Myrtaceae, Fabaceae and Apiaceae contributes large number of lipid-lowering agents. The active phyto-constituents such as flavonoids, polyphenols, terpenoids, alkaloids, saponins, etc. are responsible for the therapeutic potential of these plant species [21]. A few reports reveal, anti-hyperlipidemic efficacy of *C. amada*, which belongs to the

* Corresponding author.

E-mail address: drsasidharbs@niist.res.in (S.B. Somappa).

<https://doi.org/10.1016/j.bioorg.2021.104664>

Received 11 October 2020; Received in revised form 4 December 2020; Accepted 5 January 2021

Available online 28 January 2021

0045-2068/© 2021 Elsevier Inc. All rights reserved.

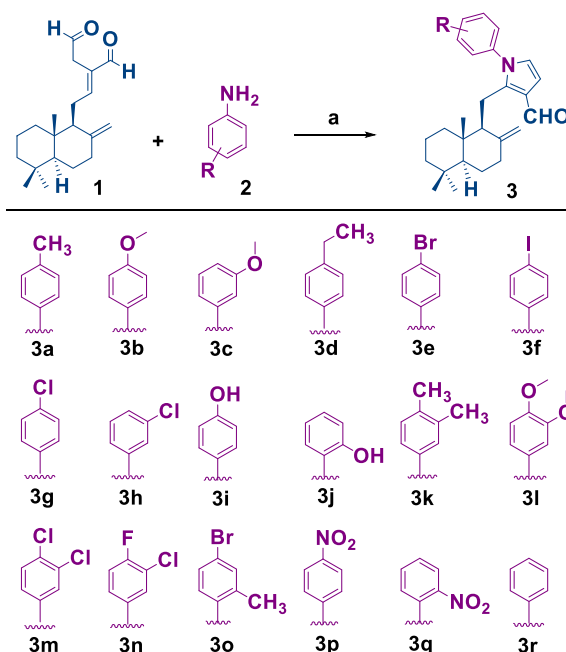
Zingiberaceae family. Srinivasan, *et al.* reported the hypotriglyceridemic activity of *C. amada* [22] and they also disclosed anti-hypercholesterolemic potential by treating hypercholesterolemic in rats [23]. Recently, we have identified promising anti-obesity leads of triazole appended - labdanes via pancreatic lipase inhibition studies [24]. In continuation of our discovery programme on natural products and bioactive heterocycles [25–30], herein, we isolated the potential and abundant bioactive molecule (E)-Labda-8(17),12-diene-15,16-dial from *C. amada* by following our previously reported process [24] and synthetically modified to (E)-Labda-8(17),12-diene-15,16-dial-pyrrole and (E)-Labda-8(17),12-diene-15,16-dial-pyrazoles. The efficacy of compounds on the inhibition of lipid droplet formation, inhibition of TG and cholesterol synthesis in the culture medium of human liver carcinoma cell lines, viz HepG2 cells successfully evaluated.

C. amada is a rhizomatic aromatic herb from the Zingiberaceae family, and it is commonly known as mango ginger because of raw mango-like flavor [31]. It has a long history from folk medicine to many culinary preparations. The rhizomes are rich in essential oil [32], and more than 130 biologically active compounds are isolated [33]. It exhibits full range of biological activities which includes anticancer [34], antibacterial, antifungal, hypotriglyceridemic, CNS depressant and analgesic activity etc. [35]. The rationale for the designed hybrids is schematically represented by the molecular hybridization approach in Fig. 1. As depicted in Fig. 1, labdane terpenes, pyrroles, and pyrazole constitute a crucial central core in many of the FDA approved statin drugs [11–14]. Besides, pyrrole and pyrazole represent as a vital scaffold in medicinal chemistry with their diverse pharmacological properties [36–39]. Therefore, we emphasize that the molecular hybridization of these pharmacophores in single entity will enrich the pharmacological properties in finding the potent “leads” as Anti-hyperlipidemic agents.

2. Results and discussion

2.1. Chemistry

To start with, fresh samples of *C. amada* rhizomes collected from CTCRI, Thiruvananthapuram, India during February 2019. By adopting our previous protocol [24], we have isolated the abundant (E)-labda 8 (17), 12-diene-15, 16-dial from the chloroform extract as a colourless solid and structure confirmed by using various spectroscopic characterization and analytical data. From the (E)-labda 8(17), 12-diene –15, 16-dial (1), a library of (E)-Labda-8(17),12-diene-15,16-dial appended pyrroles (Scheme 1) and pyrazoles (Scheme 2) synthesized via one-pot cascade protocol. (E)-labda 8(17), 12-diene-15, 16-dial (1) undergoes



Scheme 1. One-pot synthetic strategy for the (E)-Labda-8(17),12-diene-15,16-dial appended pyrroles^a. ^aReagents and conditions: (a) THF, AcOH, rt (1-2hrs).

metal-free, acid catalysed cyclocondensation with various substituted anilines (2) in THF at room temperature to produce (E)-Labda-8(17),12-diene-15,16-dial appended-1H-pyrrole-3-carbaldehydes (3) (Scheme 1). Similarly, a [3 + 2] cycloaddition of 1 and dialkyl azodicarboxylate (4) in DCM at room temperature has led to the 1H-pyrazole-1,2(3H)-dicarboxylate (E)-Labda-8(17),12-diene-15,16-dial appendages (5) (Scheme 2). All the semi-synthetic derivatives are well characterized by IR, ¹H, ¹³C NMR and HRMS analysis (Supporting information).

2.2. Biology

As we know, the synthesis of TG and cholesterol is essential for the normal physiological function of the body. But if the integration exceeds its breakdown, that will deposit on adipose tissue as well as non-adipose tissue which leads to hyperlipidemia and related consequences. It has reported that the inhibitions of lipid accumulation, inhibition of TG and cholesterol synthesis are an effective strategy to control hyperlipidemia

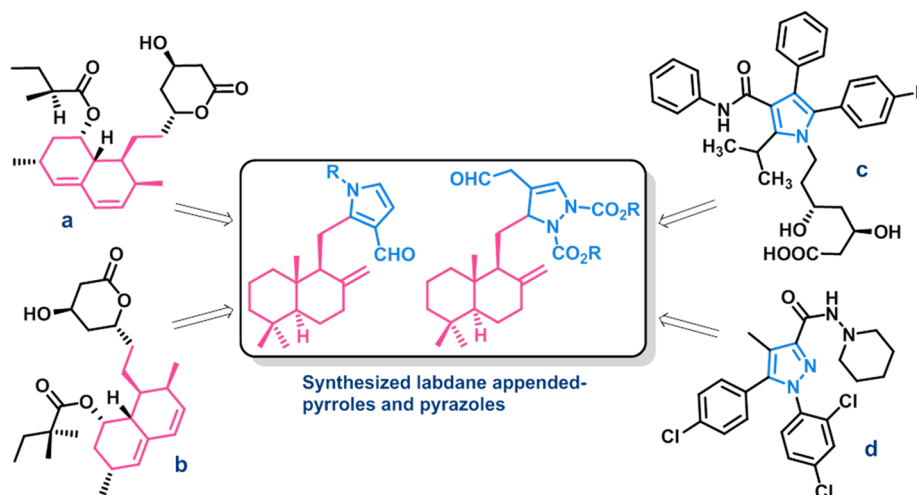
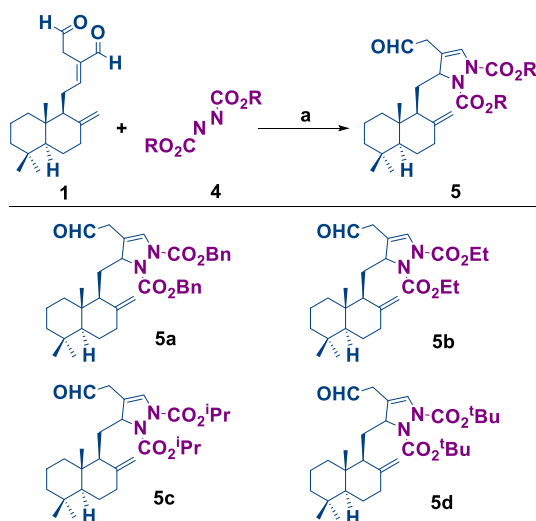


Fig. 1. Molecular hybridization approach led to the discovery of novel (E)-Labda-8(17),12-diene-15,16-dial hybrids (a: lovastatin, b: simvastatin, c: atorvastatin, d: rimonabant).



Scheme 2. One-pot access for the (E)-Labda-8(17),12-diene-15,16-dial appended pyrazoles. Reagents and conditions: (a) DCM, PPh₃, rt (2-3hrs).

and related complications. Many researchers demonstrated that natural compounds from medicinal plants are capable of controlling hyperlipidemia. In order to develop alternative therapeutic entities from natural products, we have isolated the compound **1** from *C. amada* [24] and synthesized a series of (E)-Labda-8(17),12-diene-15,16-dial appended pyrrole and pyrazole targets. Therefore we examined the efficacy of compounds on the inhibition of lipid droplet formation, inhibition of TG and cholesterol synthesis in the culture medium of human liver carcinoma cell lines, viz HepG2 cells. The HMG CoA reductase inhibitory activity of the compounds further confirms the inhibitory potential of cholesterol synthesis.

2.2.1. MTT assay

To begin with, the toxicity of the compounds was tested in HepG2 cell lines by MTT assay (Fig. 2) [40,41]. Cytotoxic effect of each compound expressed as a percentage of cell viability in a dose-dependent manner. Values are mean \pm SD of four independent experiments performed in duplicates. The results of the study displayed that none of the compounds caused any toxicity at all the tested concentrations. More than 91 percent of cell viability observed when cells pretreated with 100 μ M levels of test compounds for 48 hrs.

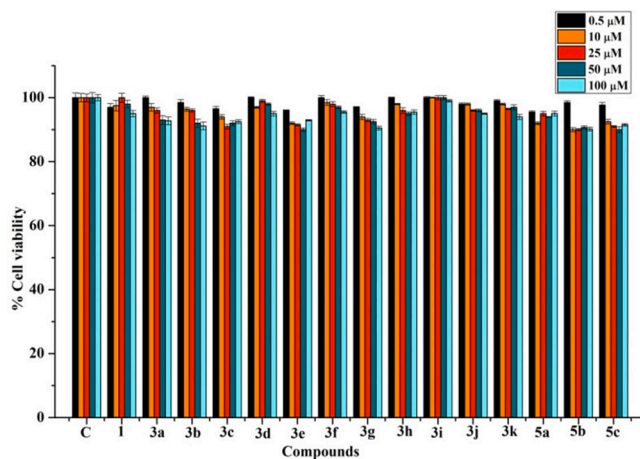


Fig. 2. Cytotoxic study of isolates and selected semi-synthetic derivatives by MTT assay.

2.2.2. The effect of compounds on lipid droplet accumulation in HFA treated HepG2 cells

Next, to see the effect of compounds on lipid droplet accumulation in high fatty acid rich (HFA) medium treated HepG2 cells, oil red O staining assay was performed (Figs. 3 & 4) [40,41]. Initially, we have conducted a preliminary screening of the compounds with concentration ranging from 0.5 μ M to 100 μ M on HFA medium treated HepG2 cells to identify the most potent concentration with a maximum inhibition of lipid accumulation. It was observed that most of the compounds showed maximum efficacy at 10 μ M concentration (data not included). Hence, all the comparative studies were performed at 10 μ M concentration. The relative intensity of lipid accumulation was also analyzed (Fig. 4). The results showed that the number of lipid droplets formation in HepG2 cells treated with the compounds were less than the control groups. As depicted in Fig. 4, compound **3i** showed highest lipid accumulation inhibitory activity, which was comparable to that of the positive control fenofibrate (FF). Compounds **3j** and **3k** also showed significant activity when compared to other derivatives. The labdane appended pyrazole molecules **5a**, **5b** and **5c** exhibited the lowest activity. However, **3i-3r** failed to show any effect on lipid accumulation.

2.2.3. Effect of compounds on the inhibition of triglyceride synthesis in HepG2 cells

Subsequently, we investigated whether the synthesized derivatives could inhibit triglyceride (TG) accumulation in HepG2 cells [40,41]. The TG levels were analyzed in HepG2 cells in HFA induced medium and test compounds for 24 hrs (Table 1) at two different concentrations viz. 5 and 10 μ M. The findings reveal that the synthesis of TG has significantly decreased in a dose-dependent manner in compound treated HepG2 cells. The percentage inhibition of TG synthesis at 10 μ M varies from 71.73 ± 0.78 to 37.25 ± 1.13 (Table 1). All the compounds except **3a**, **3c**, **5a**, **5b** and **5c** showed significant efficacy than the parent molecule **1**. One of the derivative **3i** exhibited the highest percentage of the inhibitory potential of TG synthesis with 71.73 ± 0.78 , which is comparable to that of the positive control FF (74.01 ± 0.33). Also, the compounds **3j**, **3k**, **3f** and **3g** showed a considerable TG synthesis inhibitory potential of 64.22 ± 0.61 , 62.30 ± 0.38 , 53.94 ± 1.32 and 51.51 ± 1.21 percent respectively. Surprisingly, pyrazole derivatives **5a**, **5b** and **5c** exhibited weak inhibition of TG synthesis.

2.2.4. Evaluation of effect of compounds on the inhibition of cholesterol synthesis in HepG2 cells

We further examined the effect of test compounds on the inhibition of cholesterol synthesis in HFA rich medium treated HepG2 cells (Table 2) [40,41]. The results revealed that the inhibition of cholesterol synthesis showed a concentration-dependent effect. The percentage inhibition of cholesterol synthesis at 10 μ M varies from 68.61 ± 1.19 to 46.32 ± 1.34 . All the compounds except **3a**, **5a**, **5b** and **5c** showed a marked increase in the inhibition of cholesterol synthesis. As anticipated, compound **3i** showed a consistent activity in the inhibition of cholesterol synthesis with the highest (68.61 ± 1.19) percentage of suppression, which was comparable to that of the positive control atorvastatin (AS) (70.19 ± 0.64). Compounds **3j**, **3k**, **3h**, **3f** and **3g** also showed a substantial percentage of inhibition with 65.81 ± 0.85 , 63.51 ± 0.04 , 62.07 ± 1.65 , 60.48 ± 1.09 and 57.65 ± 1.92 respectively at 10 μ M concentration. In line with other assays, here also the pyrazole derivatives showed the lowest efficiency among the tested compounds.

2.2.5. Evaluation of effect of compounds on the inhibition of HMG CoA reductase enzyme

We further examined the effect of test compounds on the inhibition of HMG CoA reductase enzyme, a rate limiting enzyme in the cholesterol synthesis pathway (Fig. 5). We used an *in vitro* HMG CoA reductase detection assay kit, which is designed to screen for different inhibitors/activators of the purified catalytic subunit of the enzyme. Since, most of the compounds showed maximum efficacy at 10 μ M concentration, we

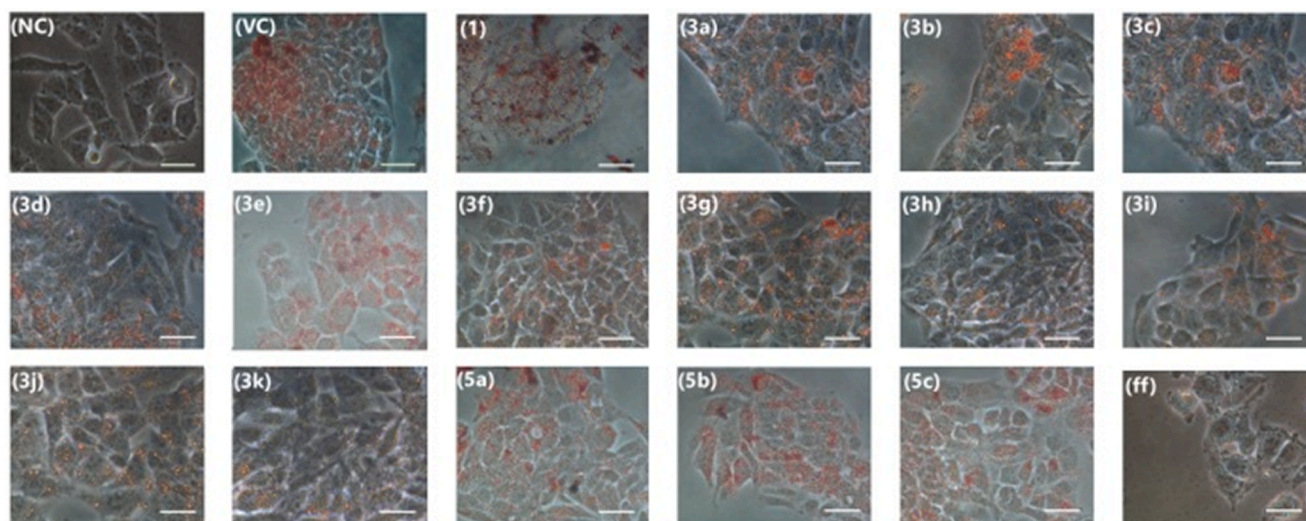


Fig. 3. The effect of compounds and standard drug FF (Fenofibrate) on lipid droplet accumulation in HepG2 cells by oil red O staining: Representative microscopic images of oil red O stained HepG2 cells treated with compounds or FF (10 μ M). NC (normal control), without any treatment; VC (vehicle control) –0.1% DMSO treated cells cultured in high fatty acid rich medium. (For interpretation of the references to colour in this figure legend, the reader is referred to the web version of this article.)

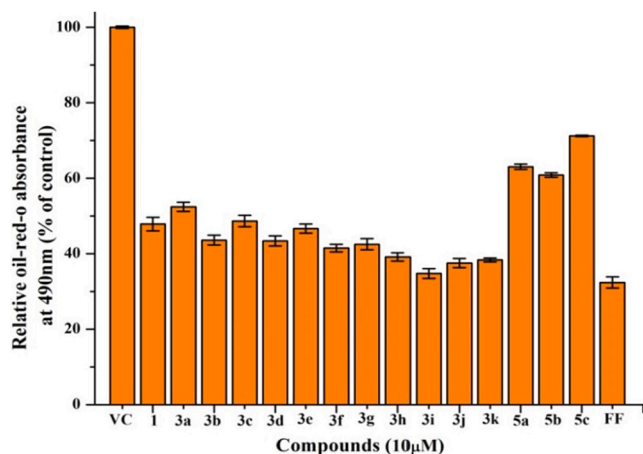


Fig. 4. The effect of compounds and standard drug FF (Fenofibrate) on lipid droplet accumulation in HepG2 cells by oil red O staining: Absorbance measured at 490 nm after oil-red-O staining and data is presented as % of control. Results are mean \pm SD, (n = 4). VC (vehicle control) –0.1% DMSO treated cells cultured in high fatty acid rich medium. (For interpretation of the references to colour in this figure legend, the reader is referred to the web version of this article.)

evaluated the % of HMG CoA reductase enzyme inhibition at 10 μ M concentration and presented the data for the same. The percentage inhibition of cholesterol synthesis at 10 μ M varies from 78.51 ± 2.80 to 45.87 ± 2.50 . The HMG CoA reductase inhibitory activity of the compounds was consistent with that of inhibitory activity of cholesterol synthesis. All the compounds except **3a**, **5a**, **5b** and **5c** exhibited significant inhibition of HMG CoA reductase enzyme. Consistent with the results of cholesterol synthesis, compound **3i** showed the highest percentage of inhibitory potential (78.61 ± 2.80), which is comparable to that of the positive control pravastatin (**PS**) (78.05 ± 5.4). Compounds **3j**, **3k**, **3h**, **3f** and **3g** also showed a considerable percentage of inhibition with 77.59 ± 6.9 , 74.94 ± 8.27 , 71.81 ± 1.84 , 68.47 ± 9.42 and 65.47 ± 6.03 respectively at 10 μ M concentration. Similar to cholesterol synthesis, the pyrazole derivatives (**5a-c**) displayed the lowest activity among the tested compounds.

Table 1

The effect of compounds on percentage inhibition of TG synthesis in high fatty acid treated HepG2 cells.^a

Compounds	TG level (mg/dl) 5 μ M	TG level (mg/dl) 10 μ M	% Inhibition (10 μ M)
NC	15.00 \pm 0.15		
VC	90.50 \pm 0.49		
1	55.00 \pm 1.41	49.50 \pm 0.70	45.51 \pm 0.71
3a	66.00 \pm 1.21	54.05 \pm 0.91	40.51 \pm 1.02
3b	50.00 \pm 0.70	49.50 \pm 1.41	45.51 \pm 0.68
3c	64.60 \pm 1.06	51.65 \pm 2.33	43.15 \pm 1.17
3d	50.00 \pm 1.41	46.75 \pm 2.19	48.54 \pm 0.85
3e	50.10 \pm 1.97	46.00 \pm 0.42	49.37 \pm 0.46
3f	45.00 \pm 1.41	41.85 \pm 1.41	53.94 \pm 1.32
3g	49.30 \pm 1.83	44.05 \pm 3.11	51.51 \pm 1.21
3h	42.00 \pm 2.82	38.70 \pm 1.90	46.96 \pm 0.24
3i	39.00 \pm 2.12	27.50 \pm 0.70	71.73 \pm 0.78
3j	42.50 \pm 1.76	32.50 \pm 0.60	64.22 \pm 0.61
3k	45.00 \pm 0.70	34.25 \pm 2.12	62.30 \pm 0.38
5a	64.00 \pm 2.12	55.85 \pm 1.41	38.52 \pm 0.23
5b	60.00 \pm 2.12	55.00 \pm 1.41	39.46 \pm 0.52
5c	68.00 \pm 0.70	57.00 \pm 1.41	37.25 \pm 1.13
FF(10 μ M)	–	23.00 \pm 2.12	74.01 \pm 0.33

^a Data is presented as mean \pm SD of five different experiments at $P \leq 0.05$. % inhibition of TG synthesis in HepG2 cells were calculated at 10 μ M concentration. FF (Fenofibrate) at 10 μ M concentration is used as positive control. NC (normal control), without any treatment, VC (vehicle control) –0.1% DMSO treated cells cultured in high fatty acid rich medium.

2.3. Structure activity relationship (SAR) studies

From the Structure-activity relationship (SAR) studies, amongst the novel pyrrole and pyrazole conjugated (E)-Labda-8(17),12-diene-15,16-dial, the pyrroles (**3a-k**) are more potent than pyrazole derivatives (**5a-c**). In pyrrole series, 1-(4-hydroxyphenyl)-2-((5,5,8a-trimethyl-2-methylenedecahydronaphthalen-1-yl)methyl)-1H-pyrrole-3 carbaldehyde (**3i**) exhibited highest efficacy, which is more potent than the parent molecule (E)-labda 8(17), 12-diene-15, 16-dial (**1**) and comparable to that of positive controls. Analogues **3j** and **3k** with *m*-OH and *m*, *p*-disubstituted-CH₃ functionality respectively also exhibited excellent efficacy. However, the analogues **3l-r** did not show any significant inhibition potential. The potency of these molecules may be attributed to the synergistic interaction of the (E)-Labda-8(17),12-diene-15,16-dial

Table 2

The effect of compounds on inhibition of cholesterol synthesis in high fatty acid treated HepG2 cells.^a

Compounds	Total cholesterol (mg/dl) 5 μ M	Total cholesterol (mg/dl) 10 μ M	% Inhibition (10 μ M)
NC	26.58 \pm 1.73		
VC	71.36 \pm 0.08		
1	41.01 \pm 0.68	33.56 \pm 1.07	52.98 \pm 1.57
3a	43.74 \pm 0.71	35.32 \pm 0.98	50.51 \pm 1.45
3b	40.82 \pm 0.98	32.66 \pm 0.64	54.23 \pm 0.83
3c	48.14 \pm 0.30	33.69 \pm 1.32	52.79 \pm 1.78
3d	37.98 \pm 0.79	31.50 \pm 1.24	55.86 \pm 1.80
3e	40.00 \pm 0.21	33.13 \pm 0.96	53.57 \pm 1.41
3f	40.03 \pm 0.14	28.19 \pm 0.82	60.48 \pm 1.09
3g	35.71 \pm 1.01	30.22 \pm 1.32	57.65 \pm 1.92
3h	37.32 \pm 0.76	27.07 \pm 1.21	62.07 \pm 1.65
3i	29.75 \pm 1.06	22.40 \pm 0.82	68.61 \pm 1.19
3j	32.43 \pm 1.31	24.39 \pm 0.64	65.81 \pm 0.85
3k	32.27 \pm 1.37	26.04 \pm 0.07	63.51 \pm 0.04
5a	45.68 \pm 0.64	36.95 \pm 1.16	48.22 \pm 1.71
5b	43.23 \pm 0.12	36.03 \pm 0.70	49.50 \pm 1.05
5c	46.71 \pm 1.05	38.31 \pm 0.90	46.32 \pm 1.34
AS (10 μ M)	–	21.27 \pm 0.48	70.19 \pm 0.64

^a Data is presented as mean \pm SD at $P \leq 0.05$ of five different experiments. % inhibition of cholesterol synthesis in HepG2 cells were calculated at 10 μ M concentration. AS (atorvastatin) at 10 μ M concentration is used as positive control. NC (normal control), without any treatment, VC (vehicle control) –0.1% DMSO treated cells cultured in high fatty acid rich medium.

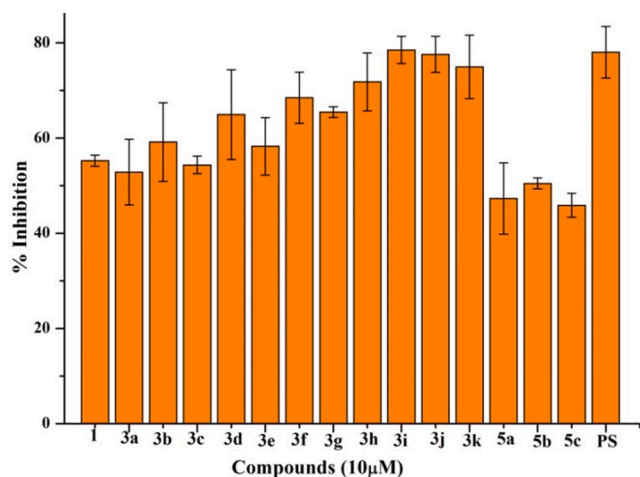


Fig. 5. The effect of compounds on the inhibition of HMG CoA reductase enzyme. PS (positive control pravastatin).

core, pyrrole ring, and aromatic ring linked to the nitrogen atom on the pyrrole ring. Even though, all the molecules possess these scaffolds, precisely the improved activity of some molecules amongst others may be due to the electronic properties of an aromatic ring which comes from various substitutions. In molecule **3i**, there is an electron-withdrawing –OH group present in the para position of the aromatic ring. Here the *p*-OH group may play an important role in the inhibition of TG and cholesterol synthesis through hydrogen bonding interactions. The molecules **3j** and **3k** with *m*-OH and *m, p*-disubstituted-CH₃ functionality also showed better activity. Compound **3a** with electron-donating *p*-CH₃ substitution on the aromatic ring possesses least activity among the other tested derivatives of pyrroles. However, there is no significant trend in the activity of the molecules followed by the nature of electron-donating and electron-withdrawing groups on the aromatic ring. Overall, among the variously substituted pyrrole conjugated (E)-Labda-8(17),12-diene-15,16-dial, **3i** with *p*-OH substituted aromatic ring was found to be the most potent molecule. These findings established that the synthesized hybrids could be utilized as effective lead candidates in

the treatment of dyslipidemia and related complications. However, further detailed molecular biology studies are required to confirm its mechanism of action and other pharmacological properties to promote as a safe clinical candidate.

3. Conclusion

In conclusion, the design of tailor-made analogues conceived from the structural features of known ligands has paved the way for the discovery of promising pyrrole appended (E)-Labda-8(17),12-diene-15,16-dial synthesized via semi-synthetic strategy. The study reveals (E)-Labda-8(17),12-diene-15,16-dial derived pyrroles play a significant role in controlling hyperlipidemia by inhibiting TG and cholesterol synthesis in HepG2 cells. The HMG CoA reductase inhibitory activity of the compounds was consistent with that of inhibitory activity of cholesterol synthesis. Amongst, synthesized pyrrole derivatives, **3i** possess the highest efficacy, which is comparable to the positive control Fenofibrate, Atorvastatin and Pravastatin. To the best of our knowledge this is the first report on the natural product derived (E)-Labda-8(17),12-diene-15,16-dial appended pyrrole and pyrazole analogues as anti-hyperlipidemic agents. Nonetheless, further detailed investigations are in progress to explore the lead analogue **3i** as a potent and safe therapeutic clinical candidate

4. Experimental

All the reagents used for the isolation, pyrrole and pyrazole synthesis were purchased from sigma-Aldrich and Spectrochem. Dulbecco's Modified Eagle's Medium (DMEM-high glucose), trypsin-EDTA and 100 U/L/ml penicillin-streptomycin (100 μ g/ml) mix, were purchased from Himedia Pvt Ltd (Mumbai, India). Fetal bovine serum (FBS) was from Gibco (Grand Island, NY). 3-[4,5-dimethylthiazol-2-yl]-2,5-diphenyl tetrazolium bromide (MTT), linoleic acid, palmitic acid, BSA, para-formaldehyde, oil red O, fenofibrate and atorvastatin were purchased from Sigma-Aldrich (U.S.A). Total cholesterol assay kit was purchased from Cell Biolabs, Inc (CA, U.S.A) and triglyceride quantification colorimetric assay kit was purchased from Biovision (CA, U.S.A). Human hepatoma cells were obtained from the NCBS (National Centre for Biological Sciences, Pune). HMG CoA reductase activity was assessed based on the oxidation of NADPH by using screening assay kit assay (Sigma Aldrich, USA) as per the manufacturer's instructions. Solvents were purchased from Merck and were distilled before use. TLC plates (silica gel 60 F₂₅₄) used for monitoring the purity of the isolated compounds and the reaction progress. Column chromatographic techniques were used for the isolation of natural compounds and its analogues. Heidolph rotary evaporator was used for the removal of solvents. The absorbance was recorded at 540 nm by the Elisa reader. The IR spectra were recorded on Bruker Alpha-T FT-IR spectrophotometer. The ¹H and ¹³C NMR spectra were recorded at 500 MHz and 125 MHz respectively on Bruker AMX 500 MHz FT NMR and 125 MHz spectrometer. Tetramethylsilane (TMS) was used as an internal standard, chemical shifts are expressed in δ scale and coupling constant in Hertz. Mass spectra were recorded under HRMS (ESI) using Thermo Scientific Exactive Orbitrap mass spectrometer.

4.1. Chemistry

4.1.1. Isolation of E-labda 8(17),12-diene-15,16-dial (1)

One kilogram of the dried powdered rhizomes of *C. amada* was extracted four times with chloroform. After the removal of solvent, 45 g of the crude extract was obtained. 30 g of the crude extract was chromatographed on silica gel (100–200 mesh). The column was eluted with mixture of ethylacetate-hexane of increasing polarity. The fraction obtained from 5% ethylacetate-hexane on subjected to crystallization using hexane to yield pure compound **1** (E-labda 8(17), 12-diene –15, 16-dial, 10 g) as colorless solid. The structure of the compound was

confirmed by various spectroscopic and analytical techniques such as IR, ^1H NMR, ^{13}C NMR, HRMS and comparison with the reported literature [42,43].

4.1.2. General procedure for the synthesis of (*E*)-Labda-8(17),12-diene-15,16-dial-pyrrole analogues (3a-3r)

To a solution of *E*-labda 8(17),12-diene -15,16-dial (1equiv.), various substituted aniline (1.5 equiv.) in THF solvent, acetic acid (6 equiv.) was added drop wise. The resulting mixture was stirred at room temperature for 1–2 h and the progress of the reaction was monitored by TLC. After completion of the reaction, the content was extracted with ethylacetate, washed with brine and the compound was dried over anhydrous Na_2SO_4 and the solvent was removed under reduced pressure. The product was purified by column chromatography using ethylacetate and hexane as solvents [44].

4.1.2.1. Synthesis of 1-(*p*-tolyl)-2-((5,5,8a-trimethyl-2-methylenedecahydronaphthalen-1-yl)methyl)-1*H*-pyrrole-3-carbaldehyde (3a). The compound **3a** was prepared by the reaction of *E*-labda 8(17),12-diene -15,16-dial (30 mg, 1equiv.) and 4-methylaniline (15.96 mg, 1.5 equiv.) in THF (3 ml) as per the method described in the section 4.1.2. Yield: 31% (12 mg); IR (NaCl, ν_{max} , cm^{-1}): 3308, 2960, 2848, 1944, 1732, 1666, 1530, 1495; ^1H NMR (500 MHz, CDCl_3) δ : 9.98(s, 1H), 7.30(d, $J = 8$ Hz, 2H), 7.16(d, $J = 8.5$ Hz, 2H), 6.64(d, $J = 3$ Hz, 1H), 6.62(d, $J = 3$ Hz, 1H), 4.60(s, 1H), 4.32(s, 1H), 3.07(m, 2H), 2.44(s, 3H), 2.20–1.01(m, 12H), 0.78(s, 3H), 0.73(s, 3H), 0.61(s, 3H); ^{13}C NMR (125 MHz, CDCl_3) δ : 186.06, 147.98, 142.17, 138.52, 136.97, 129.97, 126.26, 123.69, 123.40, 109.54, 107.30, 55.66, 55.50, 42.04, 39.94, 38.52, 38.07, 33.56, 33.45, 24.30, 21.59, 21.10, 20.94, 19.25, 14.04; HRMS (ESI) m/z : $[\text{M}+\text{H}]^+$ calcd for $\text{C}_{27}\text{H}_{35}\text{NO}$ is 390.2797, found 390.2809.

4.1.2.2. Synthesis of 1-(4-methoxyphenyl)-2-((5,5,8a-trimethyl-2-methylenedecahydronaphthalen-1-yl)methyl)-1*H*-pyrrole-3-carbaldehyde (3b). The compound **3b** was prepared by the reaction of *E*-labda 8(17),12-diene -15,16-dial (30 mg, 1equiv.) and 4-methoxyaniline (18.34 mg, 1.5 equiv.) in THF (3 ml) as per the method described in the section 4.1.2. Yield: 42% (18 mg); IR (NaCl, ν_{max} , cm^{-1}): 3642, 3273, 2924, 2851, 1870, 1896, 1737, 1718, 1701, 1652, 1591, 1543, 1513, 1460; ^1H NMR (500 MHz, CDCl_3) δ : 9.98(s, 1H), 7.20(d, $J = 9$ Hz, 2H), 7.00(d, $J = 9$ Hz, 2H), 6.63(d, $J = 3.5$ Hz, 1H), 6.60(d, $J = 3$ Hz, 1H), 4.62(s, 1H), 4.33(s, 1H), 3.88(s, 3H), 3.16–2.98(m, 2H), 2.21–0.84(m, 12H), 0.79(s, 3H), 0.74(s, 3H), 0.62(s, 3H); ^{13}C NMR (125 MHz, CDCl_3) δ : 186.03, 159.60, 147.99, 147.58, 142.28, 132.43, 127.66, 123.84, 123.32, 114.58, 109.52, 107.36, 55.70, 55.56, 42.06, 39.98, 38.61, 38.12, 33.56, 33.48, 24.32, 21.62, 20.98, 19.28, 14.04; HRMS (ESI) m/z : $[\text{M}+\text{Na}]^+$ calcd for $\text{C}_{27}\text{H}_{35}\text{NO}_2$ is 428.2565, found 428.2571.

4.1.2.3. Synthesis of 1-(3-methoxyphenyl)-2-((5,5,8a-trimethyl-2-methylenedecahydronaphthalen-1-yl)methyl)-1*H*-pyrrole-3-carbaldehyde (3c). The compound **3c** was prepared by the reaction of *E*-labda 8(17),12-diene -15,16-dial (30 mg, 1equiv.) and 3-methoxyaniline (18.34 mg, 1.5 equiv.) in THF (3 ml) as per the method described in the section 4.1.2. Yield: 35% (15 mg); IR (NaCl, ν_{max} , cm^{-1}): 3428, 2934, 2841, 2101, 1663, 1607, 1533, 1495, 1459, 1438; ^1H NMR (500 MHz, CDCl_3) δ : 9.99(s, 1H), 7.40(t, $J = 8$ Hz, 1H), 7.00(dd, $J_1 = 2$ Hz, $J_2 = 8$ Hz, 1H), 6.88(d, $J = 7.5$ Hz, 1H), 6.81(t, $J = 2$ Hz, 1H), 6.64(s, 2H), 4.62(s, 1H), 4.36(s, 1H), 3.84(s, 3H), 3.22–3.04(m, 2H), 2.20–0.88(m, 12H), 0.78(s, 3H), 0.73(s, 3H), 0.64(s, 3H); ^{13}C NMR (125 MHz, CDCl_3) δ : 186.12, 160.40, 147.97, 141.96, 140.60, 130.22, 123.60, 118.65, 114.25, 112.25, 109.70, 107.34, 55.60, 55.47, 42.08, 39.98, 38.59, 38.14, 33.56, 33.48, 24.33, 21.62, 20.96, 19.30, 14.06; HRMS (ESI) m/z : $[\text{M}+\text{Na}]^+$ calcd for $\text{C}_{27}\text{H}_{35}\text{NO}_2$ is 428.2565, found 428.2565.

4.1.2.4. Synthesis of 1-(4-ethylphenyl)-2-((5,5,8a-trimethyl-2-methylenedecahydronaphthalen-1-yl)methyl)-1*H*-pyrrole-3-carbaldehyde (3d). The compound **3d** was prepared by the reaction of *E*-labda 8(17),12-diene -15,16-dial (30 mg, 1equiv.) and 4-ethylaniline (18.04 mg, 1.5 equiv.) in THF (3 ml) as per the method described in the section 4.1.2. Yield: 31% (13 mg); IR (NaCl, ν_{max} , cm^{-1}): 3283, 2934, 2852, 1737, 1665, 1538, 1439; ^1H NMR (500 MHz, CDCl_3) δ : 9.98 (s, 1H), 7.32 (d, $J = 7.5$ Hz, 2H), 7.20 (d, $J = 8$ Hz, 2H), 6.62 (s, 2H), 4.62 (s, 1H), 4.38 (s, 1H), 3.21 (dd, $J = 10.5$ Hz, 1H), 2.99 (dd, $J = 3.5$ Hz, 1H), 2.74 (q, $J_1 = 7.5$ Hz, $J_2 = 15$ Hz, 2H), 2.17 (br d, $J = 12.5$ Hz, 1H), 1.82 (br d, $J = 9$ Hz, 1H), 1.66–0.87 (m, 10H), 1.30 (d, 7.5 Hz, 3H), 0.76 (s, 3H), 0.72 (s, 3H), 0.62 (s, 3H); ^{13}C NMR (125 MHz, CDCl_3) δ : 186.12, 147.76, 145.07, 142.06, 137.22, 128.82, 126.44, 123.70, 123.45, 109.56, 107.44, 55.56, 55.22, 42.06, 39.86, 38.48, 38.09, 33.54, 33.45, 28.61, 24.32, 21.58, 20.78, 19.26, 15.92, 14.03; HRMS (ESI) m/z : $[\text{M}+\text{Na}]^+$ calcd for $\text{C}_{28}\text{H}_{37}\text{NO}$ is 426.2773, found 426.2775.

4.1.2.5. Synthesis of 1-(4-bromophenyl)-2-((5,5,8a-trimethyl-2-methylenedecahydronaphthalen-1-yl)methyl)-1*H*-pyrrole-3-carbaldehyde (3e). The compound **3e** was prepared by the reaction of *E*-labda 8(17),12-diene -15,16-dial (30 mg, 1equiv.) and 4-bromoaniline (25.62 mg, 1.5 equiv.) in THF (3 ml) as per the method described in the section 4.1.2. Yield: 29% (13.5 mg); IR (NaCl, ν_{max} , cm^{-1}): 3339, 2942, 2848, 1666, 1593, 1533, 1496, 1460, 1439; ^1H NMR (500 MHz, CDCl_3) δ : 9.99 (s, 1H), 7.64(d, $J = 8.5$ Hz, 2H), 7.18(d, $J = 8.5$ Hz, 2H), 6.66(d, $J = 3$ Hz, 1H), 6.60(d, $J = 3$ Hz, 1H), 4.60(s, 1H), 4.26(s, 1H), 3.16–3.02(m, 2H), 2.20–0.86(m, 12H), 0.80(s, 3H), 0.74(s, 3H), 0.62(s, 3H); ^{13}C NMR (125 MHz, CDCl_3) δ : 186.04, 141.86, 138.69, 132.70, 128.06, 123.95, 123.40, 122.44, 110.14, 107.34, 55.93, 55.60, 42.00, 40.09, 38.70, 38.08, 33.53, 33.48, 29.68, 24.30, 21.62, 20.98, 19.24, 14.07; HRMS (ESI) m/z : $[\text{M}+\text{Na}]^+$ calcd for $\text{C}_{26}\text{H}_{32}\text{BrNO}$ is 476.1565, found 476.1572.

4.1.2.6. Synthesis of 1-(4-iodophenyl)-2-((5,5,8a-trimethyl-2-methylenedecahydronaphthalen-1-yl)methyl)-1*H*-pyrrole-3-carbaldehyde (3f). The compound **3f** was prepared by the reaction of *E*-labda 8(17),12-diene -15,16-dial (30 mg, 1equiv.) and 4-iodoaniline (32.61 mg, 1.5 equiv.) in THF (3 ml) as per the method described in the section 4.1.2. Yield: 30% (15.5 mg); IR (NaCl, ν_{max} , cm^{-1}): 3325, 2964, 2920, 2851, 1946, 1658, 1589, 1494, 1442; ^1H NMR (500 MHz, CDCl_3) δ : 9.99(s, 1H), 7.84(d, $J = 8.5$ Hz, 2H), 7.04(d, $J = 9$ Hz, 2H), 6.66(d, $J = 3.5$ Hz, 1H), 6.60(s, 1H), 4.61(s, 1H), 4.27(s, 1H), 3.16–3.01(m, 2H), 2.20–0.86(m, 12H), 0.80(s, 3H), 0.74(s, 3H), 0.62(s, 3H); ^{13}C NMR (125 MHz, CDCl_3) δ : 186.08, 147.89, 141.87, 139.22, 138.72, 128.28, 123.76, 123.36, 110.12, 107.34, 93.54, 55.96, 55.58, 42.00, 40.06, 38.66, 38.08, 33.56, 33.49, 29.74, 26.86, 24.29, 21.63, 20.90, 19.26, 14.10; HRMS (ESI) m/z : $[\text{M}+\text{Na}]^+$ calcd for $\text{C}_{26}\text{H}_{32}\text{INO}$ is 524.1426, found 524.1435.

4.1.2.7. Synthesis of 1-(4-chlorophenyl)-2-((5,5,8a-trimethyl-2-methylenedecahydronaphthalen-1-yl)methyl)-1*H*-pyrrole-3-carbaldehyde (3g). The compound **3g** was prepared by the reaction of *E*-labda 8(17),12-diene -15,16-dial (30 mg, 1equiv.) and 4-chloroaniline (18.99 mg, 1.5 equiv.) in THF (3 ml) as per the method described in the section 4.1.2. Yield: 39% (17 mg); IR (NaCl, ν_{max} , cm^{-1}): 3420, 2939, 2101, 1652, 1536, 1494, 1439; ^1H NMR (500 MHz, CDCl_3) δ : 9.99 (s, 1H), 7.50 (d, $J = 8.5$ Hz, 2H), 7.24 (d, $J = 8.5$ Hz, 2H), 6.66 (d, $J = 3$ Hz, 1H), 6.60 (d, $J = 3$ Hz, 1H), 4.61 (s, 1H), 4.27 (s, 1H), 3.14 (dd, $J = 10$ Hz, 1H), 3.04 (dd, $J = 4.5$ Hz, 1H), 2.21–2.18 (m, 1H), 2.21–1.05 (m, 10H), 1.92–1.90 (m, 1H), 0.80(s, 3H), 0.74(s, 3H), 0.63 (s, 3H); ^{13}C NMR (125 MHz, CDCl_3) δ : 185.04, 146.94, 140.91, 137.04, 133.48, 128.68, 126.73, 122.72, 122.47, 109.09, 106.34, 54.90, 54.59, 40.98, 39.08, 37.70, 37.07, 32.52, 32.47, 23.30, 20.62, 19.98, 18.24, 13.06; HRMS (ESI) m/z : $[\text{M}+\text{Na}]^+$ calcd for $\text{C}_{26}\text{H}_{32}\text{ClNO}$ is 432.2070, found 432.2075.

4.1.2.8. Synthesis of 1-(3-chlorophenyl)-2-((5,5,8a-trimethyl-2-methylenedecahydronaphthalen-1-yl)methyl)-1H-pyrrole-3-carbaldehyde (**3h**).

The compound **3h** was prepared by the reaction of *E*-labda 8(17),12-diene –15,16-dial (30 mg, 1equiv.) and 3-chloroaniline (18.99 mg, 1.5 equiv.) in THF (3 ml) as per the method described in the section 4.1.2. Yield: 35% (15 mg); IR (NaCl, ν_{\max} , cm^{-1}): 3428, 2939, 2102, 1656, 1534, 1494, 1439; ^1H NMR (500 MHz, CDCl_3) δ : 9.99(s, 1H), 7.46–7.19(m, 4H), 6.66(d, $J = 3$ Hz, 1H), 6.63(d, $J = 3$ Hz, 1H), 4.62(s, 1H), 4.32(s, 1H), 3.24–3.19(m, 1H), 3.06–3.02(m, 1H), 2.20–0.84(m, 12H), 0.79(s, 3H), 0.74(s, 3H), 0.64(s, 3H); ^{13}C NMR (125 MHz, CDCl_3) δ : 186.15, 147.74, 141.81, 140.68, 135.20, 130.52, 128.66, 126.90, 124.62, 123.44, 110.14, 107.40, 55.70, 55.68, 42.04, 40.04, 38.69, 38.06, 33.54, 33.48, 24.30, 21.60, 20.82, 20.78, 19.29, 14.05; HRMS (ESI) m/z : $[\text{M}+\text{Na}]^+$ calcd for $\text{C}_{26}\text{H}_{32}\text{ClNO}$ is 432.2070, found 432.2079.

4.1.2.9. Synthesis of 1-(4-hydroxyphenyl)-2-((5,5,8a-trimethyl-2-methylenedecahydronaphthalen-1-yl)methyl)-1H-pyrrole-3-carbaldehyde (**3i**).

The compound **3i** was prepared by the reaction of *E*-labda 8(17),12-diene –15,16-dial (30 mg, 1equiv.) and 4-hydroxyaniline (16.25 mg, 1.5 equiv.) in THF (3 ml) as per the method described in the section 4.1.2. Yield: 32% (13 mg); IR (NaCl, ν_{\max} , cm^{-1}): 3790, 3640, 3370, 2920, 2849, 2077, 1735, 1643, 1597, 1540, 1520, 1459; ^1H NMR (500 MHz, CDCl_3) δ : 9.97(s, 1H), 7.14(d, $J = 8.5$ Hz, 2H), 6.96(d, $J = 9$ Hz, 2H), 6.64(d, $J = 3$ Hz, 1H), 6.60(d, $J = 3.5$ Hz, 1H), 5.72(bs, 1H), 4.62(s, 1H), 4.32(s, 1H), 3.17–2.98(m, 2H), 2.20–0.82(m, 12H), 0.80(s, 3H), 0.74(s, 3H), 0.62(s, 3H); ^{13}C NMR (125 MHz, CDCl_3) δ : 186.22, 155.92, 148.02, 142.60, 132.36, 127.80, 123.99, 123.24, 116.07, 109.49, 107.39, 55.62, 55.54, 42.02, 40.02, 38.64, 38.12, 33.56, 33.49, 29.65, 24.32, 21.66, 21.00, 19.28, 14.04; HRMS (ESI) m/z : $[\text{M}+\text{Na}]^+$ calcd for $\text{C}_{26}\text{H}_{33}\text{NO}_2$ is 414.2409, found 414.2415.

4.1.2.10. Synthesis of 1-(2-hydroxyphenyl)-2-((5,5,8a-trimethyl-2-methylenedecahydronaphthalen-1-yl)methyl)-1H-pyrrole-3-carbaldehyde (**3j**).

The compound **3j** was prepared by the reaction of *E*-labda 8(17),12-diene –15,16-dial (30 mg, 1equiv.) and 2-hydroxyaniline (16.25 mg, 1.5 equiv.) in THF (3 ml) as per the method described in the section 4.1.2. Yield: 32% (13 mg); IR (NaCl, ν_{\max} , cm^{-1}): 3797, 3644, 3367, 2926, 2849, 2077, 1641, 1597, 1538, 1512, 1459; ^1H NMR (500 MHz, CDCl_3) δ : 9.98(s, 1H), 7.39–7.36(m, 1H), 7.19–7.10(m, 3H), 7.04–7.02(dt, $J_1 = 1$ Hz, $J_2 = 7.5$ Hz, 1H), 6.70(s, 1H), 6.58(d, $J = 3$ Hz, 1H), 4.67(s, 1H), 4.52(s, 1H), 2.87(dd, $J_1 = 3.5$ Hz, $J_2 = 15.5$ Hz, 1H), 2.22–2.18(m, 1H), 1.88–0.86(m, 12H), 0.78(s, 3H), 0.72(s, 3H), 0.65(s, 3H); ^{13}C NMR (125 MHz, CDCl_3) δ : 186.12, 152.05, 148.42, 130.83, 129.33, 128.28, 123.62, 121.04, 117.25, 115.30, 110.96, 107.70, 55.54, 54.19, 41.99, 39.82, 38.42, 37.96, 33.54, 33.46, 24.32, 21.58, 20.53, 19.22, 13.92; HRMS (ESI) m/z : $[\text{M}+\text{Na}]^+$ calcd for $\text{C}_{26}\text{H}_{33}\text{NO}_2$ is 414.2409, found 414.2416.

4.1.2.11. Synthesis of 1-(3,4-dimethylphenyl)-2-((5,5,8a-trimethyl-2-methylenedecahydronaphthalen-1-yl)methyl)-1H-pyrrole-3-carbaldehyde (**3k**).

The compound **3k** was prepared by the reaction of *E*-labda 8(17),12-diene –15,16-dial (30 mg, 1equiv.) and 3,4-dimethylaniline (18.04 mg, 1.5 equiv.) in THF (3 ml) as per the method described in the section 4.1.2. Yield: 50% (21 mg); IR (NaCl, ν_{\max} , cm^{-1}): 3290, 2962, 1996, 1732, 1650, 1480; ^1H NMR (500 MHz, CDCl_3) δ : 9.98(s, 1H), 7.24(d, $J = 8$ Hz, 1H), 7.04(s, 1H), 7.01–6.99(dd, $J_1 = 2$ Hz, $J_2 = 8$ Hz, 1H), 6.62–6.60(m, 2H), 4.61(s, 1H), 4.36(s, 1H), 3.19–2.99(m, 2H), 2.34(s, 3H), 2.32(s, 3H), 2.20–0.98(m, 12H), 0.78(s, 3H), 0.72(s, 3H), 0.62(s, 3H); ^{13}C NMR (125 MHz, CDCl_3) δ : 186.12, 147.90, 142.20, 137.95, 137.19, 137.12, 130.42, 127.55, 123.72, 123.68, 123.32, 109.42, 107.30, 55.58, 55.52, 42.12, 39.90, 38.46, 38.08, 33.61, 33.46, 24.30, 21.58, 20.82, 19.78, 19.46, 19.32, 14.08; HRMS (ESI) m/z : $[\text{M}+\text{Na}]^+$ calcd for $\text{C}_{28}\text{H}_{37}\text{NO}$ is 426.2773, found 426.2783.

4.1.2.12. Synthesis of 1-(3,4-dimethoxyphenyl)-2-((5,5,8a-trimethyl-2-methylenedecahydronaphthalen-1-yl)methyl)-1H-pyrrole-3-carbaldehyde (**3l**).

The compound **3l** was prepared by the reaction of *E*-labda 8(17),12-diene –15,16-dial (30 mg, 1equiv.) and 3,4-dimethoxyaniline (22.81 mg, 1.5 equiv.) in THF (3 ml) as per the method described in the section 4.1.2. Yield: 40% (18 mg); IR (NaCl, ν_{\max} , cm^{-1}): 3265, 2926, 1948, 1735, 1648, 1438; ^1H NMR (500 MHz, CDCl_3) δ : 9.98(s, 1H), 6.96–6.78(m, 3H), 6.64–6.62(m, 2H), 4.62(s, 1H), 4.37(s, 1H), 3.96(s, 3H), 3.88(s, 3H), 3.22–3.02(m, 2H), 2.21–0.84(m, 12H), 0.78(s, 3H), 0.74(s, 3H), 0.64(s, 3H); ^{13}C NMR (125 MHz, CDCl_3) δ : 186.12, 149.44, 149.18, 148.06, 142.28, 132.52, 123.88, 123.29, 118.68, 111.18, 110.08, 109.52, 107.40, 56.31, 56.20, 55.65, 55.40, 42.06, 39.99, 38.68, 38.19, 33.58, 33.48, 24.32, 21.63, 21.04, 19.30, 14.05; HRMS (ESI) m/z : $[\text{M}+\text{Na}]^+$ calcd for $\text{C}_{28}\text{H}_{37}\text{NO}_3$ is 458.2671, found 458.2673.

4.1.2.13. Synthesis of 1-(3,4-dichlorophenyl)-2-((5,5,8a-trimethyl-2-methylenedecahydronaphthalen-1-yl)methyl)-1H-pyrrole-3-carbaldehyde (**3m**).

The compound **3m** was prepared by the reaction of *E*-labda 8(17),12-diene –15,16-dial (30 mg, 1equiv.) and 3,4-dichloroaniline (24.12 mg, 1.5 equiv.) in THF (3 ml) as per the method described in the section 4.1.2. Yield: 39% (18 mg); IR (NaCl, ν_{\max} , cm^{-1}): 3420, 2941, 1732, 1656, 1540, 1496, 1440; ^1H NMR (500 MHz, CDCl_3) δ : 9.94(s, 1H), 7.60(d, $J = 8.5$ Hz, 1H), 7.43(s, 1H), 7.16(d, $J = 8.5$ Hz, 1H), 6.66(d, $J = 2.5$ Hz, 1H), 6.62(s, 1H), 4.63(s, 1H), 4.28(s, 1H), 3.19–3.14(m, 1H), 3.07–3.03(m, 1H), 2.22–0.89(m, 12H), 0.80(s, 3H), 0.74(s, 3H), 0.65(s, 3H); ^{13}C NMR (125 MHz, CDCl_3) δ : 185.04, 146.76, 140.76, 137.81, 132.60, 131.95, 130.13, 127.52, 124.68, 122.91, 122.31, 109.40, 106.38, 54.99, 54.73, 41.00, 39.14, 37.80, 37.04, 32.52, 32.48, 23.28, 20.60, 19.86, 18.27, 13.09; HRMS (ESI) m/z : $[\text{M}+\text{Na}]^+$ calcd for $\text{C}_{26}\text{H}_{31}\text{Cl}_2\text{NO}$ is 466.1680, found 466.1696.

4.1.2.14. Synthesis of 1-(3-chloro-4-fluorophenyl)-2-((5,5,8a-trimethyl-2-methylenedecahydronaphthalen-1-yl)methyl)-1H-pyrrole-3-carbaldehyde (**3n**).

The compound **3n** was prepared by the reaction of *E*-labda 8(17),12-diene –15,16-dial (30 mg, 1equiv.) and 3-chloro-4-fluoroaniline (21.68 mg, 1.5 equiv.) in THF (3 ml) as per the method described in the section 4.1.2. Yield: 31% (14 mg); IR (NaCl, ν_{\max} , cm^{-1}): 3280, 2930, 1735, 1648, 1430; ^1H NMR (500 MHz, CDCl_3) δ : 9.99(s, 1H), 7.39–7.18(m, 3H), 6.66(d, $J = 3$ Hz, 1H), 6.60(d, $J = 3$ Hz, 1H), 4.63(s, 1H), 4.30(s, 1H), 3.32–3.01(m, 2H), 2.22–0.88(m, 12H), 0.80(s, 3H), 0.74(s, 3H), 0.65(s, 3H); ^{13}C NMR (125 MHz, CDCl_3) δ : 186.12, 158.96, 147.74, 141.93, 128.98, 126.32, 126.26, 123.73, 123.56, 117.40, 117.22, 110.22, 107.44, 55.88, 55.75, 41.99, 40.14, 38.80, 38.08, 33.54, 33.50, 24.30, 21.63, 20.82, 19.28, 14.07; HRMS (ESI) m/z : $[\text{M}+\text{Na}]^+$ calcd for $\text{C}_{26}\text{H}_{31}\text{ClFNO}$ is 450.1976, found 450.1980.

4.1.2.15. Synthesis of 1-(4-bromo-2-methylphenyl)-2-((5,5,8a-trimethyl-2-methylenedecahydronaphthalen-1-yl)methyl)-1H-pyrrole-3-carbaldehyde (**3o**).

The compound **3o** was prepared by the reaction of *E*-labda 8(17),12-diene –15,16-dial (30 mg, 1equiv.) and 4-bromo-2-methylaniline (27.70 mg, 1.5 equiv.) in THF (3 ml) as per the method described in the section 4.1.2. Yield: 30% (14.5 mg); IR (NaCl, ν_{\max} , cm^{-1}): 3270, 2926, 1737, 1720, 1650, 1511; ^1H NMR (500 MHz, CDCl_3) δ : 9.98(s, 1H), 7.54(dd, $J_1 = 2$ Hz, $J_2 = 12$ Hz, 1H), 7.48–7.45(m, 1H), 7.08(dd, $J_1 = 3.5$ Hz, $J_2 = 8.5$ Hz, 1H), 6.67(t, $J = 3$ Hz, 1H), 6.50(d, $J = 3.5$ Hz, 1H), 4.68(s, 1H), 4.44(s, 1H), 3.23–2.66(m, 2H), 2.18(s, 3H), 2.03–0.89(m, 12H), 0.81(s, 3H), 0.74(s, 3H), 0.65(s, 3H); ^{13}C NMR (125 MHz, CDCl_3) δ : 186.22, 147.38, 137.45, 134.09, 133.99, 129.57, 129.98, 129.88, 127.55, 123.20, 115.86, 108.08, 55.81, 54.42, 42.08, 39.80, 38.64, 38.04, 33.62, 33.50, 24.24, 21.61, 20.96, 20.42, 19.27, 14.01; HRMS (ESI) m/z : $[\text{M}+\text{H}]^+$ calcd for $\text{C}_{27}\text{H}_{34}\text{BrNO}$ is 468.1902, found 468.1906.

4.1.2.16. Synthesis of 1-(4-nitrophenyl)-2-((5,5,8a-trimethyl-2-methylenedecahydronaphthalen-1-yl)methyl)-1H-pyrrole-3-carbaldehyde (**3p**).

The compound **3p** was prepared by the reaction of *E*-labda 8(17),12-

diene –15,16-dial (30 mg, 1equiv.) and 4-nitroaniline (20.57 mg, 1.5 equiv.) in THF (3 ml) as per the method described in the section 4.1.2. Yield: 30% (13 mg); IR (NaCl, ν_{\max} , cm^{-1}): 3371, 2922, 2850, 1737, 1667, 1596, 1526, 1501, 1460, 1439, 1400; ^1H NMR (500 MHz, CDCl_3) δ : 10.02(s, 1H), 8.40(d, $J = 9$ Hz, 2H), 7.50(d, $J = 9$ Hz, 2H), 6.72(d, $J = 3$ Hz, 1H), 6.67(d, $J = 3$ Hz, 1H), 4.60(s, 1H), 4.18(s, 1H), 3.17(s, 1H), 3.16(d, $J = 2.5$ Hz, 1H), 2.19–0.86(m, 12H), 0.786(s, 3H), 0.736(s, 3H), 0.631(s, 3H); ^{13}C NMR (125 MHz, CDCl_3) δ : 186.07, 147.99, 147.11, 144.85, 141.72, 126.94, 125.06, 124.44, 123.22, 110.98, 107.25, 56.50, 55.62, 41.89, 40.29, 38.81, 38.05, 33.48, 29.74, 24.26, 21.64, 21.14, 19.22, 14.09; HRMS (ESI) m/z : $[\text{M}+\text{Na}]^+$ calcd for $\text{C}_{26}\text{H}_{32}\text{N}_2\text{O}_3$ is 443.2311, found 443.2321.

4.1.2.17. Synthesis of 1-(2-nitrophenyl)-2-((5,5,8a-trimethyl-2-methylenedecahydronaphthalen-1-yl)methyl)-1H-pyrrole-3-carbaldehyde (3q). The compound **3q** was prepared by the reaction of *E*-labda 8(17),12-diene –15,16-dial (30 mg, 1equiv.) and 2-nitroaniline (20.57 mg, 1.5 equiv.) in THF (3 ml) as per the method described in the section 4.1.2. Yield: 30% (13 mg); IR (NaCl, ν_{\max} , cm^{-1}): 3350, 2840, 1735, 1665, 1590, 1501; ^1H NMR (500 MHz, CDCl_3) δ : 9.99(d, $J = 13$ Hz, 1H), 8.09(d, $J = 7$ Hz, 1H), 7.76–7.68(m, 2H), 7.45(d, $J = 7$ Hz, 1H), 6.70(s, 1H), 6.60(s, 1H), 4.66(s, 1H), 4.32(s, 1H), 3.32–0.78(m, 14H), 0.76(s, 3H), 0.72(s, 3H), 0.62(s, 3H); ^{13}C NMR (125 MHz, CDCl_3) δ : 186.22, 147.45, 142.72, 133.74, 130.78, 130.56, 125.56, 125.42, 123.63, 110.60, 108.10, 107.26, 55.81, 54.98, 41.97, 40.12, 38.53, 37.97, 37.85, 33.55, 33.44, 29.71, 24.20, 21.60, 19.16, 13.86; HRMS (ESI) m/z : $[\text{M}+\text{Na}]^+$ calcd for $\text{C}_{26}\text{H}_{32}\text{N}_2\text{O}_3$ is 443.2311, found 443.2315.

4.1.2.18. Synthesis of 1-phenyl-2-((5,5,8a-trimethyl-2-methylenedecahydronaphthalen-1-yl) methyl)-1H-pyrrole-3-carbaldehyde (3r). The compound **3r** was prepared by the reaction of *E*-labda 8(17),12-diene –15,16-dial (30 mg, 1equiv.) and aniline (13.86 mg, 1.5 equiv.) in THF (3 ml) as per the method described in the section 4.1.2. Yield: 30% (12 mg); IR (NaCl, ν_{\max} , cm^{-1}): 3644, 3582, 2962, 2920, 2849, 1946, 1732, 1718, 1666, 1598, 1538, 1501, 1459; ^1H NMR (500 MHz, CDCl_3) δ : 10.00(s, 1H), 7.52–7.46(m, 3H), 7.30–7.28(m, 2H), 6.66–6.64(m, 2H), 4.61(s, 1H), 4.32(s, 1H), 3.22–3.17(m, 1H), 3.06–3.02(m, 1H), 2.18–0.80(m, 12H), 0.77(s, 3H), 0.72(s, 3H), 0.62(s, 3H); ^{13}C NMR (125 MHz, CDCl_3) δ : 186.12, 157.10, 148.87, 147.83, 145.30, 142.80, 129.47, 128.46, 126.47, 123.66, 109.52, 107.34, 55.53, 42.02, 39.96, 38.56, 38.08, 33.52, 30.89, 29.68, 24.31, 21.61, 20.93, 19.25, 14.02; HRMS (ESI) m/z : $[\text{M}+\text{Na}]^+$ calcd for $\text{C}_{26}\text{H}_{33}\text{NO}$ is 398.2460, found 398.2449.

4.1.3. General procedure for synthesis of (*E*)-Labda-8(17),12-diene-15,16-dial-pyrazole analogues (5a-5d)

To a stirred solution of (*E*)-labda-8(17),12-diene-15,16-dial (1equiv.) and dialkyl azodicarboxylate (1.5equiv.) in dichloromethane (DCM), triphenyl phosphine (1.5equiv.) was added and stirred for 2–3 h at room temperature. The completion of the reaction was confirmed by TLC. The resulting solution was concentrated and purified by column chromatography using Hexane and Ethyl acetate as solvents [45].

4.1.3.1. Synthesis of dibenzyl 4-(2-oxoethyl)-3-((5,5,8a-trimethyl-2-methylenedecahydronaphthalen-1-yl)methyl)-1H-pyrazole-1,2(3H)-dicarboxylate (5a). The compound **5a** was prepared by the reaction of *E*-labda 8(17),12-diene –15,16-dial (30 mg, 1equiv.) and dibenzyl azodicarboxylate (44.40 mg 1.5equiv.) in DCM (3 ml) as per the method described in the section 4.1.3. Yield: 30% (13.5 mg); IR (NaCl, ν_{\max} , cm^{-1}): 2927, 2852, 1731, 1630, 1396, 1226; ^1H NMR (500 MHz, CDCl_3): 9.35 (s, 1H), 8.20 (d, $J = 14$ Hz, 1H), 7.34 (m, 10H), 6.28 (s, 1H), 5.84 (d, $J = 14$ Hz, 1H), 5.24 (m, 4H), 4.81 (s, 1H), 4.32 (s, 1H), 2.56–1.14 (m, 15H), 0.885 (s, 3H), 0.825 (s, 3H), 0.719 (s, 3H); ^{13}C NMR (125 MHz, CDCl_3): 194.05, 156.05, 153.68, 148.14, 135.62, 135.15, 130.86, 128.63, 128.12, 127.58, 107.96, 69.46, 67.63, 56.87, 55.39, 42.04, 39.61, 39.25, 37.86,

33.58, 31.88, 29.69, 24.09, 21.75, 19.36, 14.48; HRMS (ESI) m/z : $[\text{M}+\text{Na}]^+$ calcd for $\text{C}_{36}\text{H}_{44}\text{N}_2\text{O}_5$ is 607.3148, found 607.3131.

4.1.3.2. Synthesis of diethyl 4-(2-oxoethyl)-3-((5,5,8a-trimethyl-2-methylenedecahydro-naphthalen-1-yl)methyl)-1H-pyrazole-1,2(3H)-dicarboxylate (5b). The compound **5b** was prepared by the reaction of *E*-labda 8(17),12-diene –15,16-dial (30 mg, 1equiv.) and diethyl azodicarboxylate (25.93 mg 1.5equiv.) in DCM (3 ml) as per the method described in the section 4.1.3. Yield: 30% (14 mg); IR (NaCl, ν_{\max} , cm^{-1}): 3297, 2935, 2725, 1728, 1647, 1461; ^1H NMR (500 MHz, CDCl_3): 9.36 (s, 1H), 8.14 (s, 1H), 6.294 (t, $J = 6.5$ Hz, 1H), 5.84 (d, $J = 14$ Hz, 1H), 4.83 (s, 1H), 4.37 (s, 1H), 4.27 (m, 4H), 1.33 (m, 6H), 2.42–1.19 (m, 12H), 0.89 (s, 3H), 0.83 (s, 3H), 0.76 (s, 3H); ^{13}C NMR (125 MHz, CDCl_3): 194.24, 169.34, 148.16, 135.96, 131.02, 107.92, 99.40, 63.86, 62.54, 56.82, 55.39, 42.04, 39.62, 39.29, 37.86, 33.58, 31.56, 24.61, 24.16, 22.63, 21.74, 19.34, 14.44, 14.38, 14.08; HRMS (ESI) m/z : $[\text{M}+\text{Na}]^+$ calcd for $\text{C}_{26}\text{H}_{40}\text{N}_2\text{O}_5$ is 483.2835, found 483.2823.

4.1.3.3. Synthesis of diisopropyl 4-(2-oxoethyl)-3-((5,5,8a-trimethyl-2-methylenedecahydro-naphthalen-1-yl)methyl)-1H-pyrazole-1,2(3H)-dicarboxylate (5c). The compound **5c** was prepared by the reaction of *E*-labda 8(17),12-diene –15,16-dial (30 mg, 1equiv.) and diisopropyl azodicarboxylate (30.11 mg 1.5equiv.) in DCM (3 ml) as per the method described in the section 4.1.3. Yield: 40% (19 mg); IR (NaCl, ν_{\max} , cm^{-1}): 3300, 2935, 1723, 1630, 1461; ^1H NMR (500 MHz, CDCl_3): 9.36 (s, 1H), 8.12 (d, $J = 13.5$ Hz, 1H), 6.27 (t, $J = 6$ Hz, 1H), 5.82 (d, $J = 13.5$ Hz, 1H), 5.03 (t, $J = 6$ Hz, 2H), 4.83 (s, 1H), 4.36 (s, 1H), 1.30 (m, 12H, –CH₃ group of ¹Pr), 2.60–1.13 (m, 15H), 0.893 (s, 3H), 0.829 (s, 3H), 0.756 (s, 3H); ^{13}C NMR (125 MHz, CDCl_3): 194.02, 156.19, 152.53, 148.16, 131.16, 107.97, 98.06, 72.20, 70.40, 56.78, 55.39, 42.04, 39.59, 39.31, 37.87, 33.58, 27.00, 24.68, 24.11, 21.91, 21.74, 19.32, 14.44; HRMS (ESI) m/z : $[\text{M}+\text{Na}]^+$ calcd for $\text{C}_{28}\text{H}_{44}\text{N}_2\text{O}_5$ is 511.3148, found 511.3128.

4.1.3.4. Synthesis of di-ter-butyl 4-(2-oxoethyl)-3-((5,5,8a-trimethyl-2-methylenedecahydro-naphthalen-1-yl)methyl)-1H-pyrazole-1,2(3H)-dicarboxylate (5d). The compound **5d** was prepared by the reaction of *E*-labda 8(17),12-diene –15,16-dial (30 mg, 1equiv.) and di-ter-butyl azodicarboxylate (34.27 mg 1.5equiv.) in DCM (3 ml) as per the method described in the section 4.1.3. Yield: 80% (41 mg); IR (NaCl, ν_{\max} , cm^{-1}): 3420, 2978, 2931, 2848, 1730, 1665, 1645; ^1H NMR (500 MHz, CDCl_3): 9.36 (s, 1H), 8.11 (d, $J = 14$ Hz, 1H), 6.23 (t, $J = 5.5$ Hz, 1), 5.79 (d, $J = 14$ Hz, 1H), 4.82 (s, 1H), 4.36 (s, 1H), 1.34 (m, 18H, –CH₃ of ^tBu), 2.59–1.10 (m, 15H), 0.89 (s, 3H), 0.82 (s, 3H), 0.76 (s, 3H); ^{13}C NMR (125 MHz, CDCl_3): 194.94, 151.80, 148.14, 136.79, 131.26, 107.99, 103.58, 98.94, 82.40, 56.54, 55.39, 42.04, 39.58, 39.29, 37.88, 33.59, 33.58, 28.11, 28.07, 24.64, 24.11, 21.75, 19.32, 14.45; HRMS (ESI) m/z : $[\text{M}+\text{Na}]^+$ calcd for $\text{C}_{30}\text{H}_{48}\text{N}_2\text{O}_5$ is 539.3461, found 539.3480.

4.2. Biological screening

4.2.1. Cell cultures

Human hepatoma cells were obtained from the NCBS (National Centre for Biological Sciences, Pune). The cells were cultured in DMEM medium (containing 0.3 g/L L-glutamine and 2.0 g/L sodium bicarbonate) supplemented with 10% FBS, 1% penicillin-streptomycin mixture and maintained at 37 °C in a 5% CO₂ and 95% air atmosphere in a humidified incubator [40–41].

4.2.2. Cytotoxic evaluation of compounds by MTT assay

Cytotoxicity of compounds was measured by means of MTT assay in HepG2 cell lines. For MTT assay, HepG2 cells were seeded at a density of 1×10^5 cells per well in 96-well plates and pre-incubated in DMEM containing 10% FBS and 1% penicillin-streptomycin. After 24 h,

incubated with the test compounds (1–100 μM) for 48 h, were washed and MTT (0.5 g/l), dissolved in PBS, was added to each well for the estimation of mitochondrial dehydrogenase activity as described previously by Mosmann (1983). After 4 h of incubation at 37 °C in a CO₂ incubator, 10% SDS in DMSO was added to each well and the absorbance of solubilised MTT formazan products were measured at 570 nm after 45 min, using a microplate reader (Bioteck, U.S.A). Results were expressed as percentage of cell viability. Based on viability data 5 and 10 μM concentrations of test compounds have been selected for analyzing its effect on triglyceride accumulation and total cholesterol synthesis in HepG₂ cell lines [40–41].

4.2.3. HepG₂ cell culture for the assessment of lipid synthesis and secretion

HepG₂ cells were seeded in a 6 well plate (5x10⁵ cells/well) and then grown in DMEM containing 10% FBS and 1% antibiotic solution. Medium then discharged and supplemented with starving medium (DMEM + 1% antibiotic solution) then incubated for 24 h. Starving medium then discharged and supplemented with highfatty acid rich medium (DMEM, 1:2 of 1 mM palmitic acid: 1 mM linoleic acid and BSA). Test compounds were treated in 10 μM concentration for oil red O staining to assess lipid accumulation. 5 and 10 μM concentration of test compounds were treated for testing triglyceride (TG) and cholesterol synthesis, as described above. Cells then incubated for 24 h in 37 °C humidified atmosphere of 5% CO₂ [40–41].

4.2.4. Oil red-O staining

After the incubation, the HepG₂ cells were washed with PBS. The cells then fixed for 30 min with 40% paraformaldehyde in PBS with 1% triton-X-100. Cells were washed with double distilled water and stained for 30 min by complete immersion in a 2:3 diluted working solution of Oil red O (Sigma Aldrich, USA). Cells were then washed in PBS for 3 times Cell then observed under an inverted light Olympus microscope after the Oil-red O staining to compare the lipid droplet formation of normal cells and treated cells [40–41].

4.2.5. Triglycerides assay

The TG levels were measured in cell lysate after the treatment with fatty acid rich medium and test compounds (5 and 10 μM) for 24 hrs. Fenofibrate, a well-known drug used for treating high blood TG, at 10 μM concentration was used as the positive control in this experiment. The concentration of triglyceride in the cell lysate was measured using the triglyceride quantification colorimetric assay kit as per the manufacturer's protocol and TG concentration was calculated as instructed. Briefly, 50 μl test samples along with standards in triglyceride assay buffer were added to a 96-well plate. 2 μl Lipase was added to each well and incubated for 20 min at room temperature. 50 μl triglyceride reaction mixture was added to each well and incubated at room temperature for 30–60 min. Measure absorbance at 570 nm in a microtiter plate reader. The amount of TG was calculated from the standard curve [40–41].

4.2.6. Total cholesterol assay

For analysing the effect of test compounds on the synthesis of cholesterol, HepG₂ cells are treated as mentioned above and the medium was collected after 24 hr incubation. Total cholesterol assay kit was used for the quantitative determination of cholesterol level in medium treated by the compound. Atorvastatin, a well known hypocholesterolemic drug at 10 μM concentration was used as the positive control in this experiment. The concentration of total cholesterol in the supernatant was measured as per the kit's protocol and the concentrations were calculated following the manufacturer's instructions. Briefly, cells were lysed in chloroform/isopropanol/NP-40 (7:11:0.1) using a homogenizer and debris was removed by centrifugation at 15,000g for 10 min. The solvents were removed from samples by air drying at 50 °C for 1–2 h followed by vacuum drying for 2 h. The dried lipid content was dissolved in 200 μl assay diluent. 40 U/ml super oxide dismutase was

added to the samples to minimize the endogenous oxidation of assay probe. 50 μl of cholesterol reaction mixture with or without cholesterol esterase was mixed with 50 μl samples along with standards and incubated for 45 min at 37 °C. The amount of cholesterol was calculated by standard curve [40–41].

4.2.7. HMG CoA reductase activity assay

HMG CoA reductase activity was assessed based on the oxidation of NADPH by using screening assay kit (Sigma Aldrich, USA) as per the manufacturer's instructions. Briefly, the reaction was started by the addition of HMG CoA reductase to the assay mixture containing buffer, NADPH, HMG CoA, and test compounds and then decreasing rate of absorbance was measured. Continuously determined for 20 min at 340 nm. The rate of reaction in the units of $\Delta\text{Abs } 340/\text{min}$ was then calculated for the enzyme specific activity.

4.2.8. Statistical analysis

All data represent the means \pm SD of at least five individual experiments unless otherwise indicated in the text. Data were analyzed using SPSS v9.0 software (SPSS Inc., Chicago, IL, U.S.A). Replicates were averaged before entry as a single data point. Statistical significance was determined using one way ANOVA with significance accepted at $P \leq 0.05$. If F reaches significance, the Duncan's post hoc test was used to compare groups.

Declaration of Competing Interest

The authors declare that they have no known competing financial interests or personal relationships that could have appeared to influence the work reported in this paper.

Acknowledgements

Financial support from the DST-Science & Engineering Research Board (SERB), Government of India, New Delhi, India, (Grant no. EEQ/2016/000089) and CSIR Young Scientist Award Research Grant (HRDG/YSA-19/02/33(0045)/2020) from Council of Scientific and Industrial Research (CSIR), Government of India, New Delhi, is gratefully acknowledged. RJ thanks CSIR for research fellowship. SGL acknowledges DHR-HRD, Government of India, New Delhi, for Young Scientist Fellowship.

Appendix A. Supplementary material

Supplementary data to this article can be found online at <https://doi.org/10.1016/j.bioorg.2021.104664>.

References

- [1] R. Asija, C. Singh, A comprehensive review on anti-hyperlipidemic activity of various medicinal plants, *Int. J. Curr. Pharm. Rev. Res.* 7 (2016) 407–441.
- [2] J.L. Goldstein, M.S. Brown, A century of cholesterol and coronaries: from plaques to genes to statins, *Cell* 161 (2015) 161–172, <https://doi.org/10.1016/j.cell.2015.01.036>.
- [3] Global Health Observatory (GHO) Data, http://www.who.int/gho/ncd/risk_factors/cholesterol_text/en/.
- [4] G.F. Shattat, A review article on hyperlipidemia: types, treatments and new drug targets, *Biomed. Pharmacol. J.* 7 (2014) 399–409, <https://doi.org/10.13005/bpj/504>.
- [5] K.S. Jain, M.K. Kathiravan, R.S. Somani, C.J. Shishoo, The biology and chemistry of hyperlipidemia, *Bioorg. Med. Chem.* 15 (2007) 4674–4699, <https://doi.org/10.1016/j.bmc.2007.04.031>.
- [6] I.J. Lodhi, L. Yin, A.P. Jensen-Urstad, K. Funai, T. Coleman, J.H. Baird, M. K. Ramahi, B. Razani, H. Song, F. Fu-Hsu, J. Turk, C.F. Semenkovich, Inhibiting adipose tissue lipogenesis reprograms thermogenesis and PPAR γ activation to decrease diet-induced obesity, *Cell Metab.* 16 (2012) 189–201, <https://doi.org/10.1016/j.cmet.2012.06.013>.
- [7] I. Ramasamy, Update on the molecular biology of dyslipidemias, *Clin. Chim. Acta.* 454 (2016) 143–185, <https://doi.org/10.1016/j.cca.2015.10.033>.

- [8] B.G. Nordestgaard, A. Langsted, J.J. Freiberg, Non fasting hyperlipidemia and cardiovascular disease, *Curr. Drug Targets* 10 (2009) 328–335, <https://doi.org/10.2174/138945009787846434>.
- [9] N.E. Hassan El-Gharib, Obesity and clinical riskiness relationship: therapeutic management by dietary antioxidant supplementation—a review, *Appl. Biochem. Biotechnol.* 176 (2015) 647–669, <https://doi.org/10.1007/s12010-015-1602-6>.
- [10] J.W. Yun, Possible anti-obesity therapeutics from nature—A review, *Phytochemistry* 71 (2010) 1625–1641, <https://doi.org/10.1016/j.phytochem.2010.07.011>.
- [11] A. Endo, A gift from nature: the birth of the statins, *Nat. Med.* 14 (2008) 1050–1052, <https://doi.org/10.1038/nm1008-1050>.
- [12] A.W. Alberts, J. Chen, G. Kuron, V. Hunt, J. Huff, C. Hoffman, J. Rothrock, M. Lopez, H. Joshua, E. Harris, A. Patchett, R. Monaghan, S. Currie, E. Stapley, G. Albers-Schonberg, O. Hensens, J. Hirshfield, K. Hoogsteen, J. Liescht, J. Springer, Mevinolin: a highly potent competitive inhibitor of hydroxymethylglutaryl-coenzyme a reductase and a cholesterol-lowering agent, *Proc. Natl. Acad. Sci. USA* 77 (1980) 3957–3961, <https://doi.org/10.1073/pnas.77.7.3957>.
- [13] A. Endo, A historical perspective on the discovery of statins, *Proc. Jpn. Acad.*, Ser. B 86 (2010) 484–493, <https://doi.org/10.2183/pjab.86.484>.
- [14] K.K. Ray, C.P. Cannon, The potential relevance of the multiple lipid-independent (pleiotropic) effects of statins in the management of acute coronary syndromes, *J. Am. Coll. Cardiol.* 46 (2005) 1425–1433, <https://doi.org/10.1016/j.jacc.2005.05.086>.
- [15] C.R. Sirtori, The pharmacology of statin, *Pharmacol. Res.* 88 (2014) 3–11, <https://doi.org/10.1016/j.phrs.2014.03.002>.
- [16] M.A. Jahromi, A.B. Ray, Antihyperlipidemic effect of flavonoids from *Pterocarpus marsupium*, *J. Nat. Prod.* 56 (1993) 989–994, <https://doi.org/10.1021/np50097a001>.
- [17] X. Zhang, C. Wu, H. Wu, L. Sheng, Y. Su, X. Zhang, H. Luan, G. Sun, X. Sun, Y. Tian, Y. Ji, P. Guo, X. Xu, Anti-hyperlipidemic effects and potential mechanisms of action of the caffeoylquinic acid-rich *Pandanus tectorius* fruit extract in hamsters fed a high fat-diet, *PLoS ONE* 8 (2013) 1–12, <https://doi.org/10.1371/journal.pone.0061922>.
- [18] S. Rayalama, M.A. Della-Feraa, C. Baile, Phytochemicals and regulation of the adipocyte life cycle, *J. Nutr. Biochem.* 19 (2008) 717–726, <https://doi.org/10.1016/j.jnutbio.2007.12.007>.
- [19] T. Nakayama, S. Suzuki, H. Kudo, S. Sassa, M. Nomura, S. Sakamoto, Effects of three Chinese herbal medicines on plasma and liver lipids in mice fed a high-fat diet, *J. Ethnopharmacol.* 109 (2007) 236–240, <https://doi.org/10.1016/j.jep.2006.07.041>.
- [20] C.O. Moro, U.G. Basile, Obesity and medicinal plants, *Fitoterapia* 71 (2000) 73–82, [https://doi.org/10.1016/S0367-326X\(00\)00177-5](https://doi.org/10.1016/S0367-326X(00)00177-5).
- [21] S.A. Mohammed Saghir, V. Revadigar, V. Murugaiyah, Natural lipid-lowering agents and their effects: an update, *Eur. Food Res. Technol.* 238 (2014) 705–725, <https://doi.org/10.1007/s00217-014-2194-z>.
- [22] M.R. Srinivasan, N. Chandrasekhara, Effect of mango ginger on lipid status in normal and hypertriglyceridemic rats, *J. Food Sci. Technol.* 29 (1992) 130–132.
- [23] M.R. Srinivasan, N. Chandrasekhara, K. Srinivasan, Cholesterol lowering activity of mango ginger (*Curcuma amada* Roxb.) in induced hypercholesterolemic rats, *Eur. Food Res. Technol.* 227 (2008) 1159–1163, <https://doi.org/10.1007/s00217-008-0831-0>.
- [24] R. Jalaja, S.G. Leela, P.K. Valmiki, C.T.F. Salfeena, K.T. Ashitha, M.S. Nair, R. K. Gopalan, V.D. Krishna Rao, S.B. Somappa, Discovery of natural product derived labdane appended triazoles as potent pancreatic lipase inhibitors, *ACS Med. Chem. Lett.* 9 (2018) 662–666, <https://doi.org/10.1021/acsmchemlett.8b00109>.
- [25] G. Shilpa, J. Renjitha, R. Saranga, S.K. Francis, M.S. Nair, B. Joy, S.B. Somappa, S. Priya, Epoxyazadiradione purified from the *Azadirachta indica* seed induced mitochondrial apoptosis and inhibition of NF- κ B nuclear translocation in human cervical cancer cells, *Phytother. Res.* 31 (2017) 1892–1902, <https://doi.org/10.1002/ptr.5932>.
- [26] P.K. Valmiki, C.T.F. Salfeena, K.T. Ashitha, S. Varughese, S.B. Somappa, Antibacterial and anti-tubercular evaluation of dihydronaphthalene-indole hybrid analogues, *Chem. Biol. Drug Des.* 90 (2017) 703–708, <https://doi.org/10.1111/cbdd.12990>.
- [27] C.T.F. Salfeena, K.T. Ashitha, S.B. Somappa, BF₃•Et₂O mediated one-step synthesis of N-substituted-1,2-dihydropyridines, indenopyridines and 5,6-dihydroisoquinolines, *Org. Biomol. Chem.* 14 (2016) 10165–10169, <https://doi.org/10.1039/c6ob02133f>.
- [28] S.B. Somappa, J.S. Biradar, P. Rajesab, S. Rahber, M. Sundar, One-pot synthesis of indole appended heterocycles as potent anti-inflammatory, analgesic, and CNS depressant agents, *Monatsh. Chem.* 146 (2015) 2067–2078, <https://doi.org/10.1007/s00706-015-1476-x>.
- [29] K.T. Ashitha, P.K. Valmiki, C.T.F. Salfeena, S.B. Somappa, BF₃•OEt₂ Mediated Tandem Annulation: A Strategy to Construct Functionalized Chromeno-, and Pyrano- Fused Pyridines, *J. Org. Chem.* 83 (2018) 113–124, <https://doi.org/10.1021/acs.joc.7b02463>.
- [30] K.T. Ashitha, P.P. Vinaya, A. Krishna, D.C. Vincent, R. Jalaja, S. Varughese, S. B. Somappa, I₂/TBHP Mediated Diastereoselective Synthesis of Spiroaziridines, *Org. Biomol. Chem.* 18 (2020) 1588–1593, <https://doi.org/10.1039/c9ob02711d>.
- [31] A.S. Rao, B. Rajanikanth, R. Seshadri, Volatile aroma components of *Curcuma amada* Roxb., *J. Agric. Food Chem.* 37 (1989) 740–743, <https://doi.org/10.1021/jf00087a036>.
- [32] N.S. Dosoky, W.N. Setzer, Chemical composition and biological activities of essential oils of *Curcuma* species, *Nutrients* 10 (2018) 1–42, <https://doi.org/10.3390/nu10091196>.
- [33] S.A. Jatoti, A. Kikuchi, S.A. Gilani, K.N. Watanabe, Phytochemical, pharmacological and ethnobotanical studies in mango ginger (*Curcuma amada* Roxb.; Zingiberaceae), *Phytother. Res.* 21 (2007) 507–516, <https://doi.org/10.1002/ptr.2137>.
- [34] C. Ramachandran, K. Quirin, E.A. Escalon, I.V. Lollett, S.J. Melnick, Therapeutic effect of supercritical CO₂ extracts of *Curcuma* species with cancer drugs in rhabdomyosarcoma cell lines, *Phytother. Res.* 29 (2015) 1152–1160, <https://doi.org/10.1002/ptr.5360>.
- [35] R.S. Policegoudra, S.M. Aradhya, L. Singh, Mango ginger (*Curcuma amada* Roxb.) - A promising spice for phytochemicals and biological activities, *J. Biosci.* 36 (2011) 738–748, <https://doi.org/10.1007/s12038-011-9106-1>.
- [36] P.P. Reddy, A.K. Tiwari, R.R. Rao, K. Madhusudhana, V.R.S. Rao, A.Z. Ali, K. S. Babu, J.M. Rao, New labdane diterpenes as intestinal α -glucosidase inhibitor from antihyperglycemic extract of *Hedychium spicatum* (Ham. Ex Smith) rhizomes, *Bioorg. Med. Chem. Lett.* 19 (2009) 2562–2565, <https://doi.org/10.1016/j.bmcl.2009.03.045>.
- [37] B.B. Lohray, V. Lohray, Novel pyrrole-containing hypoglycemic and hypotriglyceridemic compounds, *Pure Appl. Chem.* 77 (2005) 179–184, <https://doi.org/10.1351/pac200577010179>.
- [38] F. Bellina, R. Rossi, Synthesis and biological activity of pyrrole, pyrrolidine and pyrrolidone derivatives with two aryl groups on adjacent positions, *Tetrahedron* 62 (2006) 7213–7256, <https://doi.org/10.1016/j.tet.2006.05.024>.
- [39] M. Alvarado, P. Goya, M. Macias-Gonzalez, F.J. Pavon, A. Serrano, N. Jagerovic, J. Elguero, A. Gutierrez-Rodriguez, S. Garcia-Granda, M. Suardiaz, F.R. Fonseca, Antiobesity designed multiple ligands: synthesis of pyrazole fatty acid amides and evaluation as hypophagic agents, *Bioorg. Med. Chem.* 16 (2008) 10098–10105, <https://doi.org/10.1016/j.bmc.2008.10.023>.
- [40] E. Leng, Y. Xiao, Z. Mo, Y. Li, Y. Zhang, X. Deng, M. Zhou, C. Zhou, Z. He, J. He, L. Xiao, J. Li, W. Li, Synergistic effect of phytochemicals on cholesterol metabolism and lipid accumulation in HepG2 cells, *BMC Complement. Altern. Med.* 18 (2018) 1–10, <https://doi.org/10.1186/s12906-018-2189-6>.
- [41] I. Budaiman, R. Tjokropranoto, W. Widowati, N. Fauziah, P.P. Erawijantari, Potency of turmeric (*Curcuma longa* L.) extract and curcumin as anti-obesity by inhibiting the cholesterol and triglyceride synthesis in HepG2 cells, *Int. J. Res. Med. Sci.* 3 (2015) 1165–1171, <https://doi.org/10.5455/2320-6012.ijrms20150525>.
- [42] S. Singh, J.K. Kumar, D. Saikia, K. Shanker, J.P. Thakur, A.S. Negi, S. Banerjee, A bioactive labdane diterpenoid from *Curcuma amada* and its semisynthetic analogues as antitubercular agents, *Eur. J. Med. Chem.* 45 (2010) 4379–4382, <https://doi.org/10.1016/j.ejmech.2010.06.006>.
- [43] A.D.B. Sheeja, M.S. Nair, Facile isolation of *E*-labda 8(17), 12-diene-15, 16-dial from *curcuma amada* and its conversion to other biologically active compounds, *Indian. J. Chem. Sect. B* 53 (2014) 319–324.
- [44] A. Kornienko, J.L. La Clair, Covalent modification of biological targets with natural products through Paal-Knorr pyrrole formation, *Nat. Prod. Rep.* 34 (2017) 1051–1060, <https://doi.org/10.1039/C7np00024C>.
- [45] V. Nair, A.T. Biju, S.C. Mathew, B.P. Babu, Carbon-nitrogen bond-forming reactions of dialkyl azodicarboxylate: a promising synthetic strategy, *Chem. Asian J.* 3 (2008) 810–820, <https://doi.org/10.1002/asia.200700341>.